Using Modern Synthetic Techniques to Conduct Difficult Transformations Relating to the Agrochemical Industry

MALLIA, CARL,JAMES

Durham University

Using Modern Synthetic Techniques to Conduct Difficult Transformations Relating to the Agrochemical Industry

Carl James Mallia

Doctor of Philosophy Thesis

Ustinov College

Department of Chemistry

2016

Declaration

Durham, June 2016

This dissertation is submitted for the degree of Doctor of Philosophy and is the result of my own work and includes nothing which is the outcome of work done in collaboration except where specifically indicated in the text.

Carl James Mallia

Statement of Copyright

Abstract

The work described in this dissertation is divided into three chapters each discussing independent projects where either gas-liquid flow technology or microwave reactor technology was applied to organic synthesis.

The **first chapter** describes the flow hydroxy-carbonylation of ortho-substituted iodo arenes. It was found that through the use of a “tube-in-tube” reactor to introduce the carbon monoxide gas to the reaction mixture, a number of ortho-substituted carboxylic acids could be prepared. The second part of this chapter deals with the synthesis of a herbicidal intermediate which was prepared through the carboxylation reaction with carbon dioxide (dry ice). A parallel flow process for the preparation of this herbicidal intermediate was also developed. This work was reported in one publication.

In the **second chapter** another gas; oxygen, was used in continuous flow as an oxidant in the Chan-Lam reaction. The first part of this chapter demonstrates how a continuous process for the synthesis of a herbicidal intermediate was developed through an optimised catalytic Chan-Lam reaction which was also shown to consistently work at different scales. In the second part a more generalised catalytic Chan-Lam reaction was optimised and this lead to a small collection of C-N coupled products. This work was published in one publication.

The use of 1,4-dithain-2,5-diol as a precursor for 2-mercaptoacetaldehyde was used as a building block for the synthesis of thiazoles in the **third chapter**. Using microwave reactor technology the optimised reaction conditions for this novel transformation was quickly achieved. A bifurcation pathway was discovered where either 2-aminothiophens or 2-substiuted thiazoles were prepared, which was demonstrated through the synthesis of a small library of compounds. This work was disclosed in two separate publications.

Publications Included in This Thesis

1. "Catalytic Chan–Lam coupling using a 'tube-in-tube' reactor to deliver molecular oxygen as an oxidant."
   Mallia, C. J.; Burton P. M.; Smith A. M. R.; Walter G. C.; Baxendale, I. R., *Beilstein J. Org. Chem.* **2016**, *12*, 1598-1607.

2. "Flow carbonylation of sterically hindered ortho-substituted iodoarenes."
   Mallia, C. J.; Walter G. C.; Baxendale, I. R. *Beilstein J. Org. Chem.* **2016**, *12*, 1501-1511.

3. "The use of gases in flow synthesis."
   Mallia, C. J.; Baxendale, I. R. *Org. Process. Res. Dev*. **2016**, *20* (2), 327-360. (DOI: 10.1021/acs.oprd.5b00222)

4. "Ethyl 2-hydroxy-2-phenyl-2-(thiazol-2-yl)acetate."
   Mallia, C. J.; Englert, L.; Walter G. C.; Baxendale, I. R. *Molbank* **2015**, *2015*, M857. (DOI:10.3390/M857)

5. "Thiazole formation through a modified Gewald reaction."
   Mallia, C. J.; Englert, L.; Walter G. C.; Baxendale, I. R. *Beilstein J. Org. Chem*. **2015**, *11*, 875-883. (DOI:10.3762/bjoc.11.98)

6. "Flow chemistry approaches directed at improving chemical synthesis."
   Baxendale, I. R.; Brocken, L.; Mallia, C. J. *Green Process. Synth.* **2013**, *2*, 211-230. (DOI 10.1515/gps-2013-0029)

Acknowledgments

I would like to thank my supervisor, Prof. Ian R. Baxendale, for his constant encouragement throughout my studies. I would like to show gratitude towards all your patience, your tenacity and your encouragement. I also really appreciate all the possibilities you gave me to learn new things, for your open-door policy and for all those times you dropped whatever you were doing to offer help or advice.

I am very grateful to Syngenta, especially Dr Gary Walter, for providing me with the financial support and for the development of ideas. I am particularly grateful to Dr Marcus Baumann whom I learnt a lot form and Dr Christian Stanetty who not only became a great friend but also provided great support. Special thanks go to all the people in the Baxendale's group past and present who made my PhD days both memorable and bearable. In particular, Laurens for his constant moral support and just for being always there, James for being my gym buddy, Laura for the word of the day and Lukas for his invaluable contribution to the thiazole project.

I would also like to thank all the academic and technical staff at the Department of Chemistry. The Sandford group has been another constant throughout my time in Durham who provided me with both equipment/chemicals and friendship. Tony deserves a special thanks, who in this process also became a great friend.

Special thanks go to my family for their constant encouragement and for their never ending support. Last but not least, my wife Emma deserves a special mention for all her never ending support, patience, and encouragement and simply for being my partner in crime.

Dedication

“To Emma”

Abbreviations

a interfacial area

Ac acetyl group

Ar undefined aryl substituent

atm atmosphere (unit)

BMIM 1-butyl-3-methylimidazolium

Boc *tert*-butyloxycarbonyl

BPO benzoyl peroxide

BPR back pressure regulator

br. broad peak/signal

***n*-Bu** *n*-butyl group

***t*-Bu** *tert*-butyl group

Bn benzyl group

°C degree Celsius

^{13}C carbon-13 (NMR spectroscopy)

CDI 1,1'-carbonyl diimidazole

CIF crystallographic information file

COSY 1H correlation spectroscopy

δ chemical shift (NMR spectroscopy)

d days, or doublet signal

DABSO 1,4-diazabicyclo[2.2.2]octane *bis*(sulfur dioxide) adduct

DAST diethylamino sulfurtrifluoride

DBU 1,8-diazabicycloundec-7-ene

DCC *N*,*N'*-dicyclohexylcarbodiimide

DCM dichloromethane

DEPT distortionless enhancement by polarisation transfer (NMR spectroscopy)

DIPEA *N*,*N*-diisopropylethyl amine

DMAc *N*,*N*-Dimethylacetamide

DMC dimethyl carbonate

DME dimethoxyethane

DMEDA *N*,*N'*-Dimethyl-1,2-ethanediamine

DMF *N*,*N*-dimethylformamide

DMSO dimethyl sulfoxide

Doe (*s*)-delphinine

DOE design of experiment

DPEPhos (oxydi-2,1 phenylene)-*bis*(diphenylphosphine)

dppb 1,4-*bis*(diphenylphosphino)butane

dppm 1,1-*bis*(diphenylphosphino)methane

dppf 1,1′-ferrocenediyl-*bis*(diphenylphosphine)

d.r. diastereomeric ratio

ee enantiomeric excess

equiv. equivalence

EPR electron paramagnetic resonance

ESI electronspray ionisation

Et ethyl group

^{19}F fluorine (NMR spectroscopy)

FEP fluorinated ethylene propylene

FFMR falling film micro-reactor

FT-IR Fourier transform infrared

g grams

GC gas chromatography

h hours

^{1}H proton (NMR spectroscopy)

HbpA 2-hydroxybiphenyl 3-monooxygenase

HMBC heteronuclear multiple bond connectivity (NMR spectroscopy)

HMDS *bis*(trimethylsilyl)amine

HMQC heteronuclear multiple quantum coherence (NMR spectroscopy)

HPL high pressure lab

HRMS high-resolution mass spectrometry

Hz Hertz

id inner diametre

***i*-Pr** *iso*-propyl group

IR infrared

J coupling constant

LC-MS liquid chromatography mass spectrometry

LED light emitting diode

LDA lithium diisopropylamide

mL millilitre

m multiplet, or medium

M molarity, or metal atom

Me methyl group

mg milligrams

min minutes

mL millilitre

MHz megahertz

mmol millimole

mol mole

mol% mole percentage

mp melting point

Ms mesyl group

MS mass spectrometry/molecular sieves

MW microwave

m/z mass to charge ratio

NBS *N*-bromosuccinimide

NMP *N*-methyl-2-pyrrolidone

NMR nuclear magnetic resonance

nOe nuclear Overhauser effect

NOESY nuclear Overhauser effect spectroscopy

NucH nucleophile

N/D not determined

PDMS poly(dimethylsiloxane)

Ph phenyl

PFA perfluoro alkoxy

ppm parts per million

PS-BEMP polymer-supported 2-(*tert*-butylimino)-2-diethylamino-1,3-dimethyl-perhydro-1,3,2-diazaphosphorine

PTFE polytetrafluoroethylene

PVP poly(*N*-vinyl-2-pyrrolidone)

PVSZ polyvinylsilazane

Py pyridine

q quartet signal (NMR spectroscopy)

QP-DMA Quadrapure dimethylamine resin

QP-SA Quadrapure sulfonic acid resin

QP-TU Quadrapure thiourea resin

R alkyl substituent

R dextrorotary enantiomer

r radius

rt room temperature

Rt retention time

s singlet signal, or strong absorbance

S levorotary enantiomer

scCO2 supercritical carbon dioxide

sccm standard cubic centimetre per minute

SYNPhos [(5,6),(5′,6′)-*bis*(ethylenedioxy)biphenyl-2,2′-diyl]*bis*(diphenylphosphine)

S-Phos 2-dicyclohexylphosphino-2′,6′-dimethoxybiphenyl

t triplet signal (NMR spectroscopy)

TBAF tetra-*n*-butylammonium fluoride

TEMPO (2,2,6,6-tetramethylpiperidin-1-yl)oxyl

Tf triflate group

tlc thin layer chromatography

THF tetrahydrofuran

TMEDA tetramethylethylenediamine

TMG *N*,*N*,*N*‘‘,*N*‘‘-tetramethyl guanidine

TMS trimethylsilane

TOF turnover frequency

TPFPP 5,10,15,20-tetrakis-(pentafluorophenyl)porphyrin

TPP tetraphenylporphyrin

Ts tosyl group

UV ultraviolet

ν wavenumber (IR spectroscopy)

v/v volume/volume

µW microwave

W watts

w weak absorbance

w/w weight/weight

X leaving group

Xantphos 4,5-*bis*(diphenylphosphino)-9,9-dimethylxanthene

X-Phos 2-dicyclohexylphosphino-2′,4′,6′-triisopropylbiphenyl

Table of Contents

1 Introduction

"Enabling technologies"[1] is a broad term used to refer to techniques that either increase the productivity of reactions through a more efficient process or offer an improved setup through the use of modern equipment. This includes intuitive programs such as Design of Experiment (DOE) programs and equipment that can be integrated with robotic modules such as microwave reactors, meso/micro-flow reactors and automated liquid handlers. These have all found a number of high-throughput applications, especially in library generation and fast optimisation of reaction conditions.

The use of enabling techniques in contemporary laboratory setups allow for a more efficient workforce by improving the overall process at different levels. Although there has been an immense improvement in the general chemistry knowledge over the last decades, allowing today's chemists to perform almost any transformation needed to build highly complex molecules, the techniques employed to build the structures did not change at the same rate. Due to the conservative nature of chemists, and the initial high costs associated with new techniques/equipment, the idea of substituting well known chemistry techniques with new and improved ones is still a challenge. Unlike in other sciences, chemists still use the same equipment associated with chemical synthesis (such as round bottom flasks, separator funnels and Schlenk lines) that were used over six decades ago. However, chemists have started to gain an appreciation that in order to overcome additional bottlenecks, there is a requirement to change of mind set and the application of novel enabling techniques.

The use of microwave reactor technology is one such example which has been used extensively in high throughput experiments due to the potential for automation.[2] Some researchers have reported the so called "microwave effect" which was used early on to explain the superior results obtained through microwave heating when compared to conventional heating. Loupy *et al*.[3] have suggested that these differences may be due to a number of reasons such as the formation of "hot spots" in the microwave vial. However, it is not easy to verify such proposals due to the difficulty to accurately measure the inside local temperatures without changing the environment of the reaction. Nevertheless, microwave reactors have found many uses in chemistry and are now found in most

modern research facilities. The holding capacity of most microwave vials is however a limiting factor when considering scaling up reactions.

Design of Experiments (DOE) is a method by which a designed experiment is performed to aid in explaining the variation of information obtained under the conditions used. When just one factor influences the output, it is relatively easy to vary that factor and monitor the response. However, when more than one factor is affecting the response, as is the case, in most real-life situations, changing just one factor at a time is inefficient. The use of DOE allows for the investigation of how factors jointly affect the response. This is generally done through the use of dedicated software (such as JMP) to analyse data obtained and model the pattern of responses to identify active factors, which can then be used to predict trends. Although, such analysis can be used to achieve well optimised systems, it is generally accepted that this comes with a considerable expenditure of resources and time. For some industries such optimised conditions may offer a cheaper, more efficient way of producing a product/intermediate, which on large scales offer a significant savings. However, for chemists that do not need to scale up reactions, the effort required to optimise a reaction through DOE might not be sufficiently beneficial when considering the resources and time required.

In this thesis, emphasis is given to gas-liquid chemistry, an area that still has several bottlenecks associated with both safe use and scale up. This thesis mainly aims to investigate classes of reactions that use toxic and/or dangerous gases to produce useful intermediates, using flow methodology to overcome the aforementioned bottlenecks. The next section will thus be dedicated to illustrating examples of gas-liquid flow chemistry from the literature, covering carbon monoxide, carbon dioxide and oxygen. There are other gases that are used in flow chemistry that will not be covered in this thesis, however, a comprehensive review detailing these can be found in our publication.[4]

1.1 The Use of Flow Chemistry in Aiding Gas-Liquid Chemistry

The use of toxic and dangerous gases is highly restricted and controlled in modern synthetic laboratories. Increased safety considerations, including precautionary limitations on their use at scale, are often mandated for gas processing operations. Understandably, for something as ethereal as a gas, which cannot be easily contained, leakages are very difficult to prevent when conventional synthetic equipment is used. Consequently, dedicated high pressure facility rooms are normally built specifically to enable access to gas based transformations. Pressurised gas reactions are normally continually monitored for leakage using specialised gas and/or pressure detectors, with personnel using such facilities having to undergo specialised training. Furthermore, restrictions on the scales of high pressure reactions are also put in place to mitigate risks, making the scale up of these reactions challenging.

1.1.1 Alternative Approaches

The use of gas surrogates has been developed to circumvent the direct use of certain gases, with the *in situ* liberation of the required gas being the most common method. Several carbon monoxide precursors exists such as those derived from aldehydes,[5] formyl saccharine[6] and various metal carbonyls, such as $Ni(CO)_4$,[7] $W(CO)_6$[8] and $Mo(CO)_6$.[9] Similarly, the use of transfer hydrogenation is often applied as a substitute for gaseous hydrogen, which can be delivered through a donor such as formic acid via a metal complex (e.g. Ru),[10] often in association with diamine or phosphine ligands. It is also possible to use metal free hydrogen gas substitutes such as Hantzsch esters often promoted by the addition of an auxiliary organocatalyst.[11] Additional gas substitutes for less common species have also been developed such as Selectfluor® (which acts as a F donor)[12] and DABSO as a gaseous sulfur dioxide substitute.[13] Even though these gas substitutes are useful for small scale chemistry, they often tend to be either too toxic,[14] atom inefficient or too expensive to be used at larger scales.

1.1.2 Application of Gases

One of the main limiting factors when pursuing a transformation using a gaseous component is establishing the required stoichiometry by solubilising sufficient quantities of the gas into the reaction media. The low solubility of certain gases like carbon monoxide (Table 1),[15] often deems that high pressures are required, with the concentration of the dissolved gas also showing a rapid decrease with an increase in

temperature, especially when the boiling point of the solvent is approached. Thus, following Henry's law, when the reaction temperature is elevated, an increase in pressure is required to maintain the same concentration of dissolved gas.

Table 1: Solubility of carbon monoxide in selected solvents at 25 °C.[15]

Solvent	Molar Volume	Solubility
		***C*[a]**
n-Heptane	146.46	11.71×10^{-3}
Cyclohexane	108.75	9.12×10^{-3}
Methylcyclohexane	128.35	9.68×10^{-3}
Toluene	106.86	7.59×10^{-3}
Perfluoroheptane	227.33	17.11×10^{-3}
Perfluorobenzene	115.79	1.35×10^{-3}
Chloroform	80.94	7.94×10^{-3}
Acetone	74.01	10.44×10^{-3}
MeOH	40.73	9.24×10^{-3}
EtOH	58.68	8.26×10^{-3}
n-Propanol[b]	74.79	7.36×10^{-3}
i-Propanol	76.55	7.89×10^{-3}
i-butanol	92.88	7.03×10^{-3}
Dimethylformamide[b]	77.04	1.82×10^{-3}
Water	18.07	0.95×10^{-3}

[a] Concentration in moles per litre at 1 atm. partial pressure of carbon monoxide.
[b] Measurements taken at 20 °C.

Continuous flow technology can provide many advantages over traditional batch synthesis.[16] Firstly, the high heat and mass transfer rates which are possible when using small channelled fluidic systems enable reactions to be performed under a wider range of conditions, many of which are not accessible within conventional batch reactors. In the case of gas-liquid reactions a high interfacial area (*a*) is essential for an efficient mass transfer rate. Batch reactions performed in a traditional round bottom flask have much lower interfacial areas and this decreases with an increase in the size of the flask, Figure 1. *Note: when the reaction is stirred, the vortex formed increases the interfacial area which also depends on the speed of mixing.* Table 2 shows some published interfacial areas for different reactors, showing much larger values for certain reactor types

especially microchannel reactors (a = 3400-18000 m^2m^{-3}), with a maximum interfacial value of 18000 m^2m^{-3} for a 300 µm x 100 µm microchannel.[17]

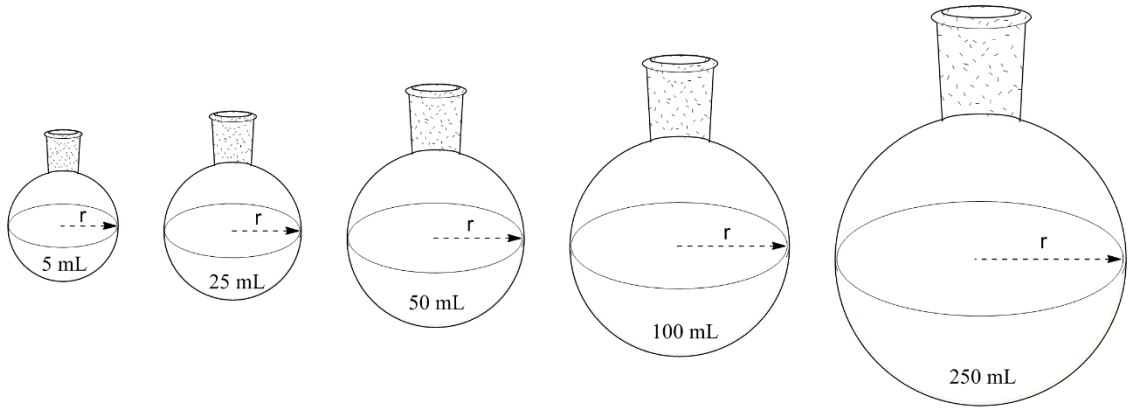

Radius r (m)				
0.014	0.021	0.025	0.033	0.043
Interfacial area a (m^2m^{-3})				
107	71	60	46	35

Figure 1: Qualitative measure of interfacial area (a) for typical round bottom flasks when the liquid is static.

Table 2: Published interfacial area for different gas liquid contactors.[17]

Type of contactor	***a* (m^2m^{-3})**
Bubble columns	50-600
Couette-Tylor flow reactor	200-1200
Impinging jet absorbers	90-2050
Packed columns, concurrent	10-1700
Packed columns, counter current	10-350
Spray column	75-170
Static mixers	100-1000
Stirred tank	100-2000
Tube reactors, horizontal and coiled	50-700
Tube reactors, vertical	100-2000
Gas-liquid microchannel contactor	3400-18000

A significant increase in the interfacial contact area can permit reactions that are not normally feasible under conventional batch synthesis conditions to be promoted in flow. In general, gases are easier to use in flow as their delivery can be regulated by dosing controlled flow volumes and using the higher internal pressures within the flow system to aid dissolution. Since flow technology also allows for coupling multiple connected

reactors, the storing of chemicals is reduced together with shipping costs as intermediates needed for the desired product can potentially be synthesised and used directly in the next step without the need of isolation. Also hazardous chemicals, such as pyrophoric or air sensitive chemicals are much easier to use without the need for complicated precautions. Scale-up to production levels is potentially easily achieved by replicating the same reactor used for pilot plant experiments via a numbering-up approach or through prolonged running of the same reactor in a continuous manufacture scenario without any redesign in the set-up. Both approaches drastically reduce the transition time moving to scale and are thus financially beneficial.

1.1.3 Approaches Used in Micro and Meso Gas-Liquid Flow Reactions

Microchannel reactors have been extensively used employing a biphasic flow regime most commonly segmented flow, where bubbles of a gas are separated by slugs of a liquid (Figure 2). The toroidal currents formed in both the liquid and gas segments enhance the mixing and increase mass transfer.[18] Another approach, which also involves a gas and a liquid stream concurrently flowing together, is created by the introduction of a fast flowing gas stream injected at high pressures into a slower liquid flow (Figure 2). The velocity of the gas creates an annular flow (pipe flow) with the liquid being pushed against the boundary walls of the microchannels. The thin liquid layer again allows for a high interfacial contact area, with a decrease in the diffusion length.

A further reactor design based upon this same principle is the falling film microreactor, in which the liquid phase flows through microchannels under gravity to form a thin liquid layer.[19] The gas input then flows co-currently or counter-currently to the liquid (Figure 3).

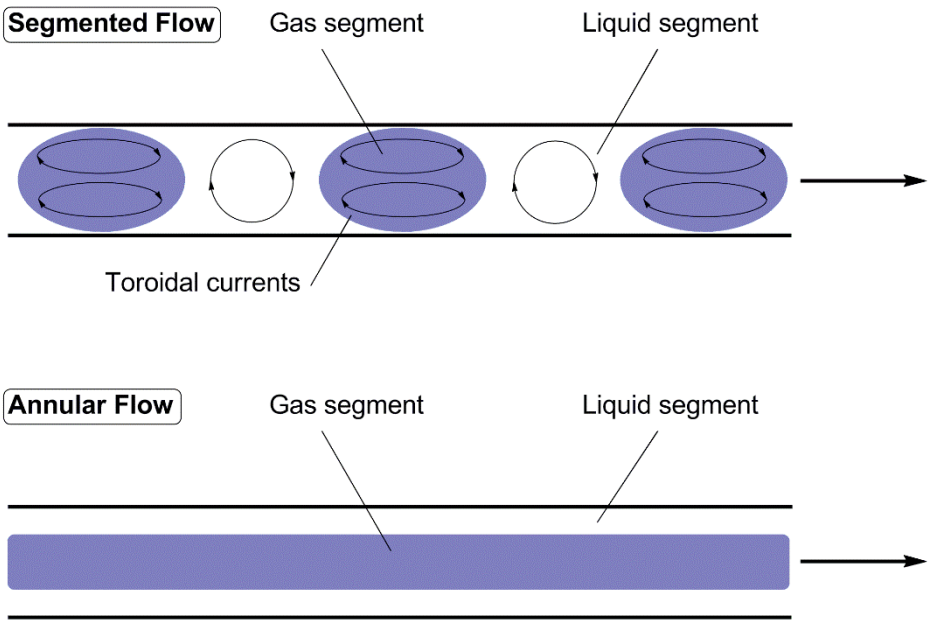

Figure 2: Gas-Liquid flow regimes: Segmented Flow and Annular Flow.

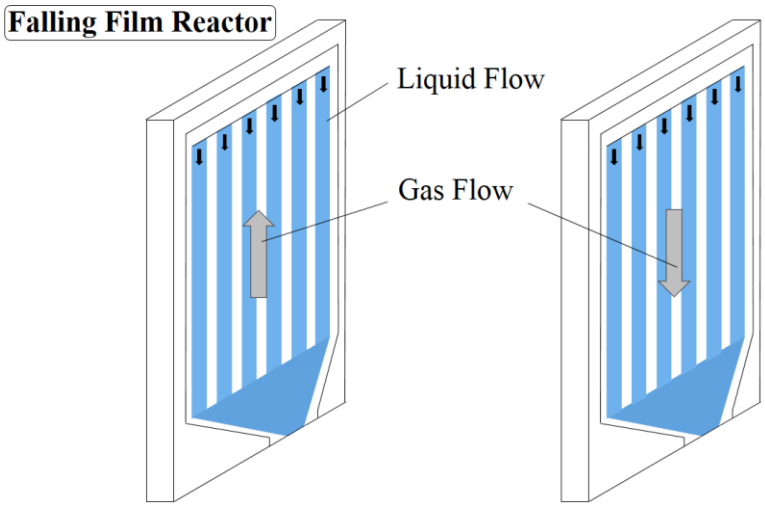

Figure 3: Falling film reactor with liquid flow falling downwards and gas flowing either upwards (left) or downwards (right) above the liquid flow.

Mesh microreactors have also used for gas-liquid flow reactions. This design makes use of a fine metal or ceramic mesh separating the liquid flow in the microchannels. The gas component is passed into the reactor and flows through the mesh to enter the liquid stream.[20] The fine openings in the mesh (average pore size of 76 µm) allows for an increase in the gas-liquid interfacial contact area and the small gap separating the mesh and the microchannel allows for a very short diffusion length.

A related approach involves the use of a gas-permeable membrane system which spatially separates the liquid and the gas flows by creating a mono-directional barrier. Several such systems have been constructed making use of this reactor format, employing gas porous interleafed sheets, wafers or tubing. As an example the conventional 'tube-in-tube' design reported by the Ley group[21] makes use of an amorphous fluoropolymer Teflon AF-2400 membrane which has high permeability for gases but not liquids.[22] The design enables the formation of micro-bubbles around the outer walls of the membrane tubing which are quickly dissolved into the traversing liquid flow (Figure 4). As a consequence of the large surface area and small cross sectional diameter of the Teflon AF-2400 tubing, gas diffusion across the membrane and into the inertia flow stream is extremely rapid. The Jensen group studied the diffusion phenomenon of several different configurations of the 'tube-in-tube' design involving the 'conventional' and reengineered 'reverse' designs (Figure 4).[23] The reverse 'tube-in-tube' design, also known as the 'on-demand' design, is capable of being additionally heated to warm the liquid flow whilst also supplying the gas, whereas the conventional 'tube-in-tube' design can only be used to saturate the liquid flow with a gas at ambient temperature. Despite this limitation the simple assembly of the conventional 'tube-in-tube' design still make the set-up attractive. It can be easily constructed from commercially available amorphous fluoropolymer Teflon AF-2400 membrane tubing simply inserted into a length of wider bore PTFE tube and connected by the appropriate Swagelock® unions. The corresponding reverse 'tube-in-tube' design is now available as a ready-made unit from several leading flow equipment suppliers.

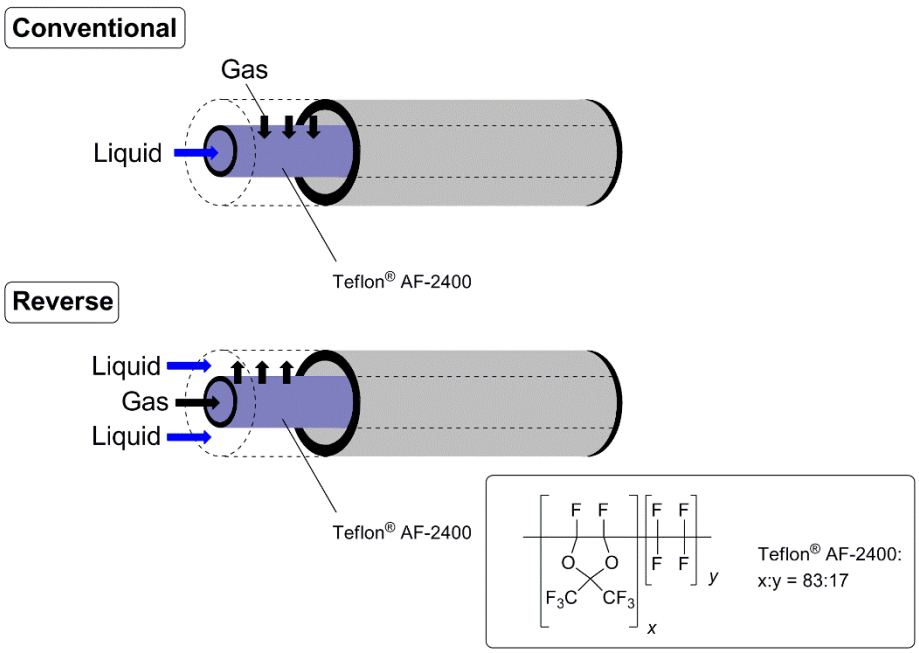

Figure 4: 'Tube-in-tube' reactors. Conventional design with liquid flowing through the inner tube (Top). Reverse design with gas flowing through the inner tube (Bottom).

1.1.4 Different Gases Used in Flow

As a consequence of all the new techniques developed for the easier introduction of gases to flow systems the area of gas-liquid reactions has become an increasing popular research topic. Several groups have made substantial progress in overcoming problems normally encountered when gases are used in batch as will be illustrated in the next sections. Carbon monoxide, carbon dioxide and oxygen will be covered in detail, other gases are covered in the full review we authored about the use of gases in flow chemistry.[4]

1.1.4.1 Carbon monoxide

Carbon monoxide is a toxic (poisoning symptoms occur above 50 ppm concentration in air)[14] and highly flammable gas that due to its limited solubility in most organic solvents (Table 1), reactions employing it are most commonly carried out at elevated pressure. This makes the use of carbon monoxide a risk, especially in standard labs or when large quantities are needed. However, because it is a synthetically versatile and low cost building block, chemists have continued using it despite its associated hazards.[24] Indeed, carbon monoxide is perhaps one of the most used gases and as such it is used in several industrial process such as the Fischer-Tropsch process,[25] and alcohol formation through hydroformylation.[26] Carbon monoxide is also routinely used for the conversion of aryl halides and pseudo-halides to higher oxidation level groups such as amides, esters, aldehydes and carboxylic acids.

The Long group reported one of the first flow-carbonylation in 2006 as a safe and scalable way to make simple amides from iodobenzene (**1a**), 4-iodoanisole (**1b**) and 2-bromopyridine (**1c**) with benzyl amine as the substrate. A microfluidic reactor was used to combine the reactants and a base and the carbon monoxide were delivered in an annular flow regime.[27] The reactions were compared with existing batch protocols and although the yields from the micro-flow system were only moderate (12-58% yields of amide formed), were an improvement on those obtained in batch (11-25% yields, Table 3). Of note was the α-ketoamide by-product, formed through over-carbonylation, which was also observed in some of the flow reaction conditions.

Table 3: Amino-carbonylation in micro-flow with benzylamine as the nucleophile.

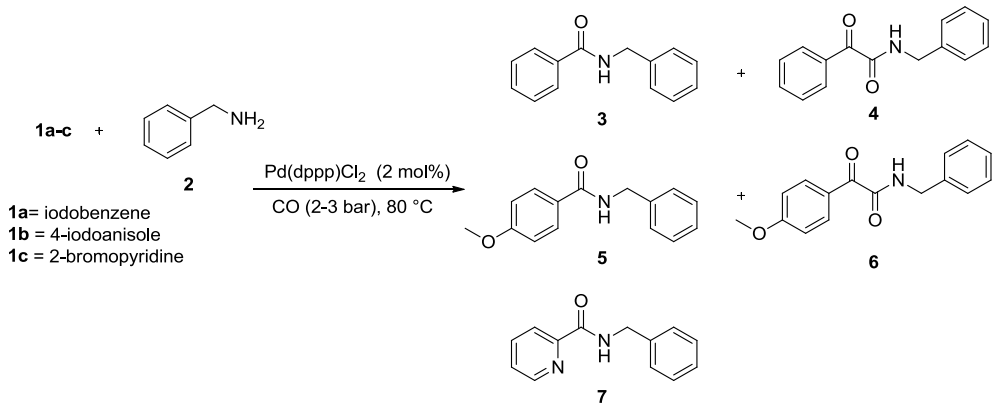

Substrate	Residence time	Yield of amide (%)	Yield of α-ketoamide (%)	Total yield (%)
1a	3.75 min	31	18	49
1a	7.5 min	37	17	54
1a	15 min	46	9	55
Batch	-	25	0	25
1b	3.75 min	10	20	30
1b	7.5 min	10	19	29
1b	15 min	12	28	40
Batch	-	11	0	11
1c	3.75 min	46	0	46
1c	7.5 min	51	0	51
1c	15 min	58	0	58
Batch	-	18	0	18

Ryu *et. al.* later published a flow carbonylation protocol for aryl iodides and phenylacetylene in ionic liquids such as [BMIm]PF_6 which can function as a recyclable reaction media and catalyst support. The results were again compared to the analogous batch reactions, and demonstrated higher yields when performed in flow (Scheme 1).[28] Furthermore, the palladium-catalysed carbonylative Sonogashira coupling yielded only the acetylenic ketone when performed in micro-flow but also formed the Sonogashira coupled by-product when run under batch conditions. When diethylamine was used as the nucleophilic partner, the micro-flow procedure gave a mixture of the amide (**14**) and the *α*-ketoamide (**15**) the latter being the main product (95:6 – 87:13, **15**:**14**). This was in drastic contrast to what was observed by the Long group who instead obtained the amide as the main product.[27] This was probably due to the higher pressures used in the Ryu plug

flow system (15-20 atm) which allows for a greater concentration of dissolved carbon monoxide in the solvent giving a higher proportion of the double addition α-ketoamide product.

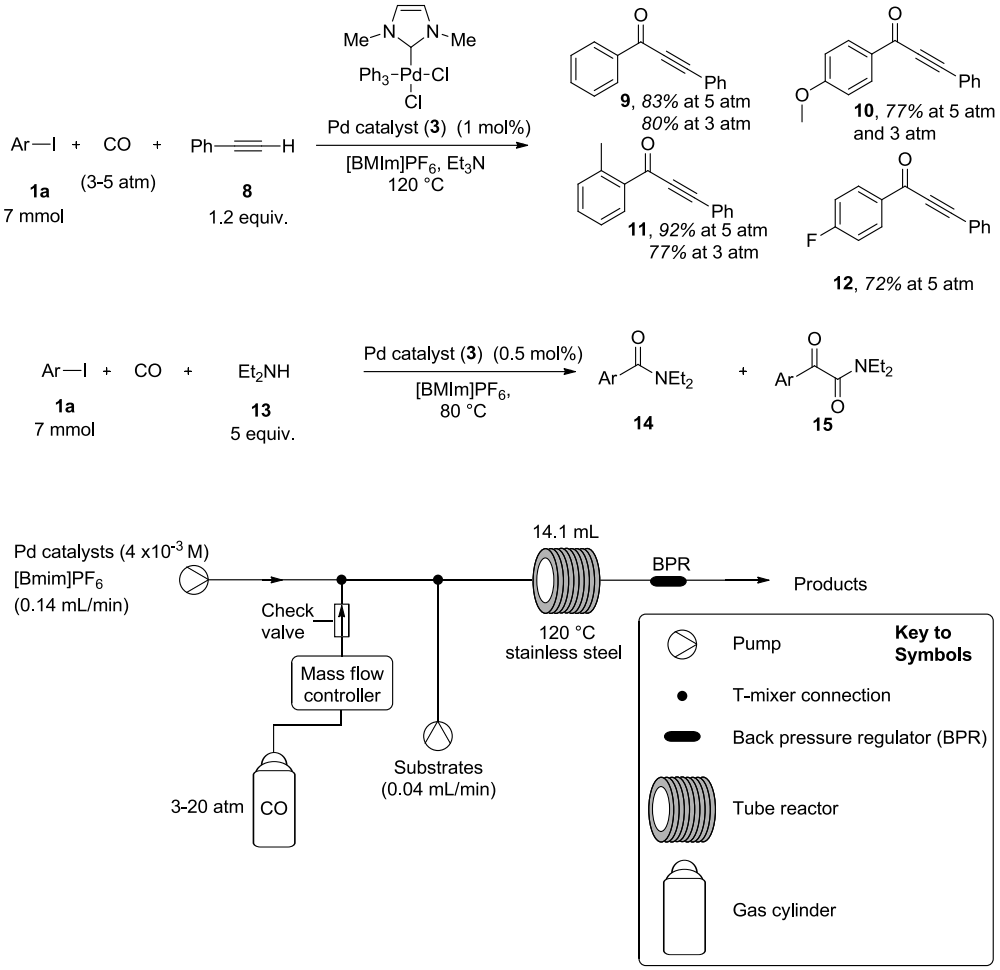

Scheme 1: Palladium-catalysed carbonylative coupling of aryl iodides and phenylacetylene in flow.

The specific conditions leading to the formation of the α-ketoamides was studied by the Buchwald group in an attempt to avoid its generation.[29] As would be expected it was concluded that in a micro-flow reactor either elevating the temperature or decreasing the pressure increases the selectivity for the formation of the amide with carbon monoxide added in an annular flow manner.

The Long group additionally reported on the use of flow carbonylation for the synthesis of amides comprising radiolabelled ^{11}CO.[30] In this reaction, a triphasic reaction system utilising a silica-supported palladium diphosphine catalyst was employed as a packed bed reactor, produced by loading the catalysts into a length of Teflon tubing. Very good yields were achieved for electron deficient bromo-arenes (99% yield, 3 examples) but much

lower yields were obtained for the more challenging electron rich systems (23-26%, 2 examples). This would correlate well with the need for longer reaction times for electron rich systems which would be difficult to achieve in the low residence time reactor assembled for this study.

Miller *et al.* showed that the use of a chip based microfluidic system with an annular CO flow profile could be used to rapidly screen for ligand activity in amino-carbonylations. A simple coupling between iodobenzene **1a** and benzylamine **2** was used as a standard test reaction.[31] A total of eight different catalysts were screened across a range of temperatures varying from 75 °C to 150 °C using very short residence times (2 min). Generally catalysts performed better as the temperature was increased, with $PdCl_2$(dppf), $PdCl_2$(dppp), $PdCl_2$(Biphenphos), $PdCl_2$(DPEphos), $PdCl_2$(Synphos) and $Pd(PPh_3)_4$ giving good GC yields (>75%) at 150 °C whereas $PdCl_2$(BINAP) still only gave 45% GC yield even at the highest temperature of 150 °C. The best pre-catalyst was found to be $PdCl_2$(Xantphos) which gave 94% GC yield at the higher temperature range and was found to give an 85% GC yield even at 75 °C.

The Ryu group described their continuing studies of carbonylation chemistry expanding into radical carbonylation of aliphatic halides.[32] They employed a microfluidic flow system with the carbon monoxide delivered through a simple T-piece connector (Table 4). It was shown that using the radical initiator V-65 [(2,2′-azobis(2,4-dimethylvaleronitrile), half-life time: 12 min at 80 °C] in the presence of 1-bromododecane (**16**), tributyltin hydride and carbon monoxide at 80 °C, full conversion of the 1-bromododecane was achieved in 12 min, with a 77% isolated yield of tridecanal (**17**). The same continuous micro-flow system was also used with silicon-based hydride donors delivering various aldehydes, unsymmetrical ketones and a δ-lactam all in good to excellent yields.

Table 4: Radical carbonylation in micro-flow system.

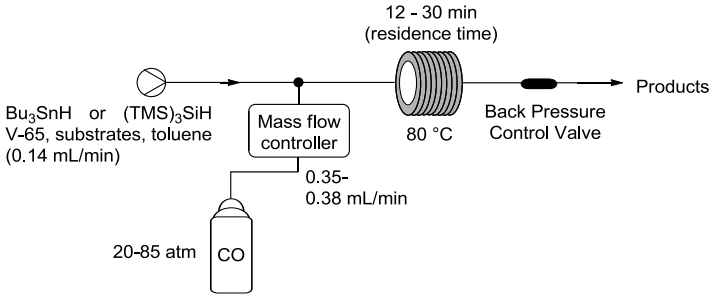

Entry	Substrate	Conditions	Substrate/Yield (%)
1	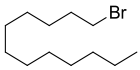 **16**	0.02 M in toluene, Bu_3SnH (1.2 equiv.), V-65 (10 mol%), CO 83 atm, 12 min	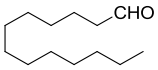 **17**, *77%*
2	 **18**	0.02 M in toluene, Bu_3SnH (1.2 equiv.), V-65 (10 mol%), CO 85 atm, 12 min	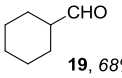 **19**, *68%*
3	 **20**	0.02 M in toluene, Bu_3SnH (1.2 equiv.), V-65 (10 mol%), CO 85 atm, 12 min	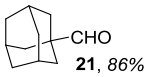 **21**, *86%*
4	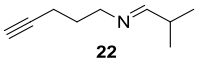 **22**	0.05 M in toluene, Bu_3SnH (1.1 equiv.), V-65 (10 mol%), CO 79 atm, 27 min	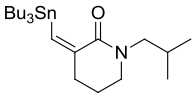 **23**, *85% (E/Z = 0/100)*
5	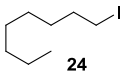 **24**	0.017 M in toluene, Bu_3SnH (1.5 equiv.), $H_2C{=}CH{-}COCH_3$ (4 equiv.) V-65 (10 mol%), CO 85 atm, 29 min	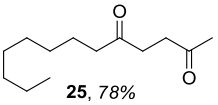 **25**, *78%*
6	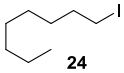 **24**	0.02 M in toluene, $(TMS)_3SiH$ (1.5 equiv.), $H_2C{=}CH{-}COCH_3$ (1.2 equiv.) V-65 (30 mol%), CO 20 atm, 30 min	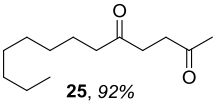 **25**, *92%*
7	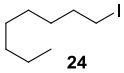 **24**	0.02 M in toluene, $(TMS)_3SiH$ (1.5 equiv.), $H_2C{=}CH{-}CN$ (1.2 equiv.) V-65 (30 mol%), CO 20 atm, 30 min	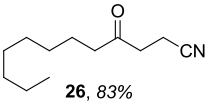 **26**, *83%*

The de Mello group and collaborators reported a comparison between the use of annular flow and plug flow for amino-carbonylation reactions (Scheme 2).[33] Even though the annular flow method was shown to be efficient, it was limited to short residence times (2-5 min). The plug flow method could enable longer residence times and had a reduced tendency to block the reactor due to formation of Pd black particulates during carbonylation. It was reported that the use of the Pd dimer $[Pd_2(\mu\text{-}I)_2(P^tBu_3)_2]$ served as an excellent pre-catalyst for aminocarbonylation being far superior to many other previously reported catalysts.

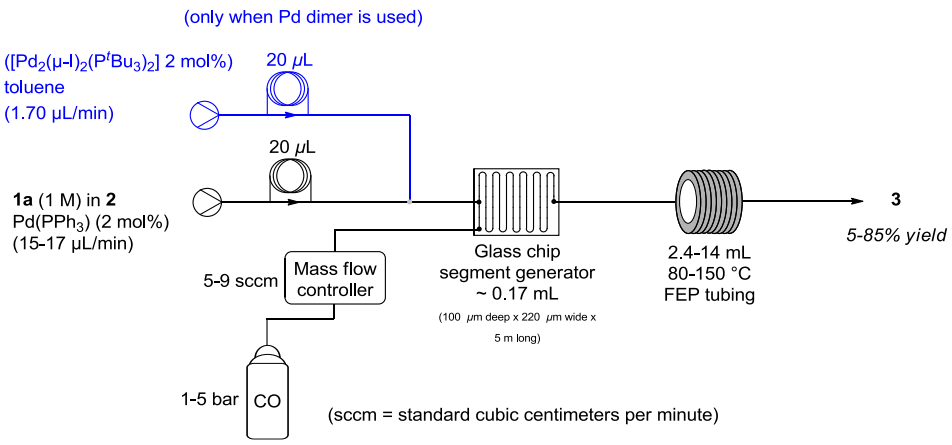

Scheme 2: Comparison between annular and segmented flow in amino-carbonylation system**.**

The amino-carbonylation of halogenated aryl carboxylic acids with various amines has also been reported by Csajági *et al*. using a commercial pressurised continuous flow reactor (Scheme 3).[34] The substrates were passed through a phosphine immobilised version of $Pd(PPh_3)_4$ to generate moderate to good yields of a variety of amide products (**27-39**) which were prepared in very short residence times (~2 min).

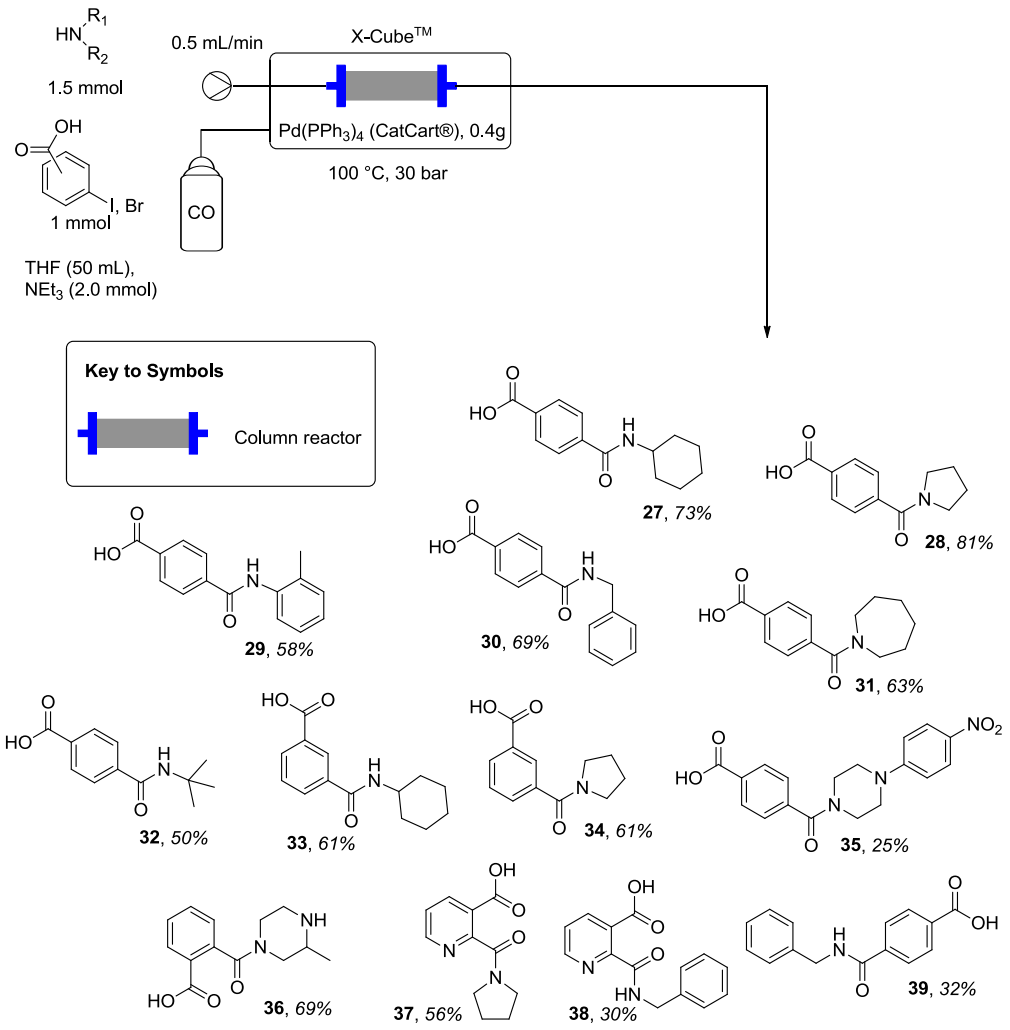

Scheme 3: Amino-carbonylation of halogenated aryl carboxylic acids in flow using the X-cube™.

The use of a conventional 'tube-in-tube' configuration for carbonylation reactions was reported by the Ley group (Scheme 4).[35] In this publication a selection of aryl iodides, bromides and vinyl iodides were tested, with most of the substrates giving good to excellent yields (62-93% yields, 14 examples). A solvent mixture of toluene, MeOH and dimethylformamide was used. The MeOH was utilised as the nucleophilic partner and the dimethylformamide was found to be beneficial for stabilising the palladium catalyst and thus preventing the formation of palladium black. An in-line scavenger cartridge packed with polymer-bound thiourea resin was used to remove the palladium from the reaction mixture making the purification of the crude material easier. Furthermore a ReactIR detector was deployed in-line to monitor the carbon monoxide concentration in the flow stream. This was used to find the optimum pressure to give the highest carbon monoxide concentration in the liquid stream. The use of a second 'tube-in-tube' system

under vacuum to remove the excess dissolved carbon monoxide as an in-line process was also described. The removal of residual carbon monoxide was also monitored using ReactIR. This is especially relevant for industrial processes that make use of carbonylation reactions facilitating detection and possible recycling of the excess gas.

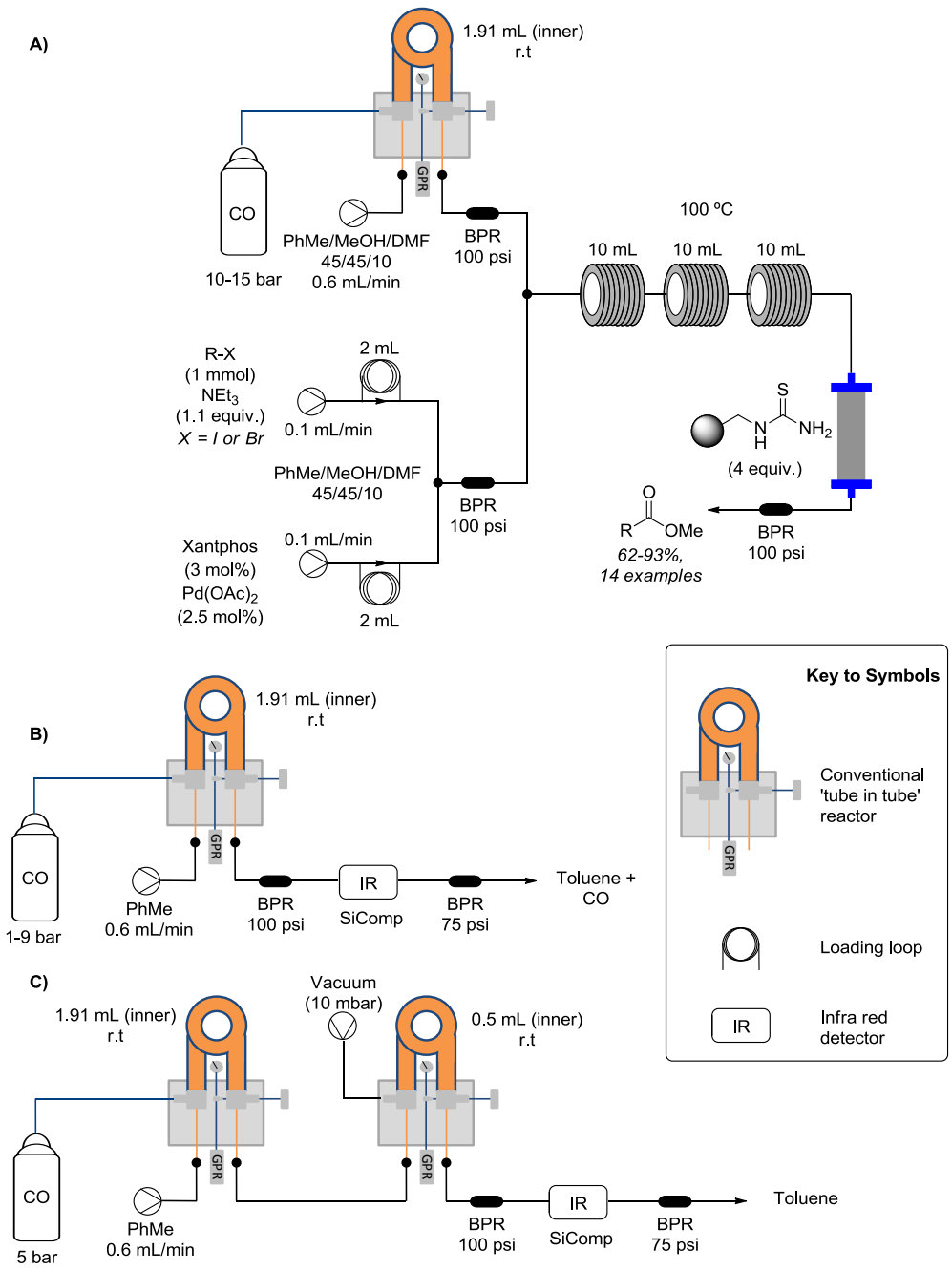

Scheme 4: A) Methoxy carbonylation in flow using the 'tube-in-tube' reactor design. B) Use of in-line IR monitoring to determine concentration of dissolved carbon monoxide in solvent. C) Use of a second 'tube-in-tube' under vacuum to remove the dissolved carbon monoxide.

The use of a reverse 'tube-in-tube' configuration was exemplified by Leadbeater and co-workers for the carbonylation of several aryl iodides to give the alkoxy carbonylative products in excellent conversions (91-99%, 8 examples) (Scheme 5).[36] The same group also published a carbonylative system where a plug flow system was used, and although it showed superior yields to the batch systems, it was still not as efficient as the reverse 'tube-in-tube' system.[37]

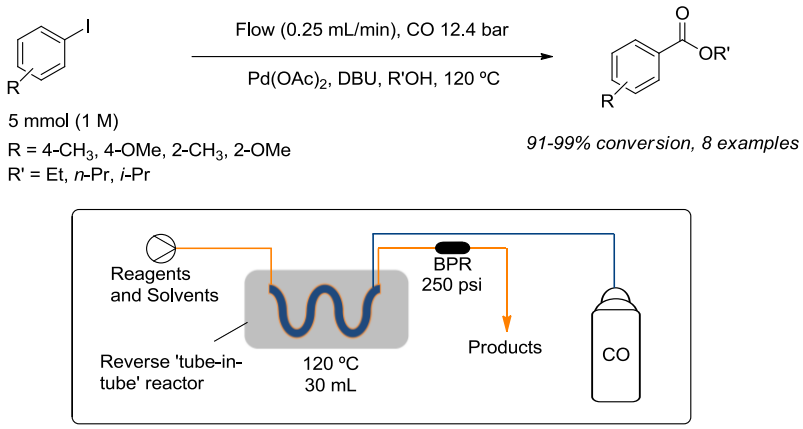

Scheme 5: Alkoxycarbonylation of aryl iodides in flow using the reverse 'tube-in-tube' reactor.

The Ryu group devised an innovative use of the 'tube-in-tube' system (Scheme 6).[38] Instead of directly dosing carbon monoxide to the inner gas-permeable tube, a mixture of concentrated sulfuric acid and formic acid was mixed to form carbon monoxide *in situ* (Morgan reaction), which was then shown to be available for Heck aminocarbonylation. Two flow streams were directed in a co-current flow configuration for the work described, however, no specific mention was made to acknowledge if the counter flow system was also trialled.

The same group published a similar protocol for the carbonylation of alcohols through the Koch-Haaf reaction.[39] Again, concentrated sulfuric acid and formic acid were directly mixed with the substrate in a Hastelloy-made micromixer. The acid mixture forms carbon monoxide *in situ* through the Morgan reaction which in turn reacts with the carbocation formed after the elimination of the hydroxyl group. The authors showed that there were selectivity limitations and the reaction in flow gave little improvement compared to batch protocols (Table 5). Additionally they also showed a multigram scale-up version for the synthesis of 1-adamantanecarboxylic acid **43** (Scheme 7).

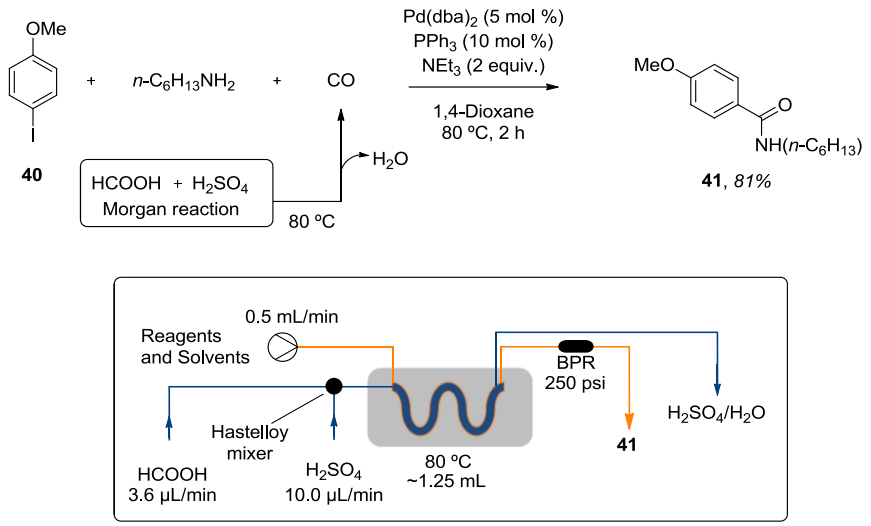

Scheme 6: Aminocarbonylation of **40** in flow using the Morgan reaction in the reverse 'tube-in-tube' reactor.

Table 5: Comparison of Koch-Haaf reactions of adamantanols in microflow and batch.[a]

Entry	Substrate	Reactor	Conditions	Product (yield)[b]
1	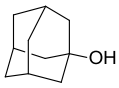 **42**	microflow	Temperature: 20 °C Flow rate (**42**/HCO_2H): 0.30 mL/min Flow rate (H_2SO_4): 0.88 mL/min Residence time: 2 min[c] Residence time: 1.5 min[d]	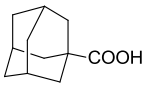 **43**, 89%
2	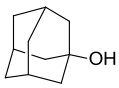 **42**	batch	Temperature: 15-20 °C Addition time: 5 min Reaction time: 2 min	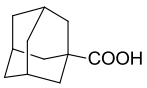 **43**, 92%
3	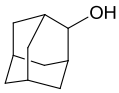 **44**	microflow	Temperature: 20 °C Flow rate (**44**/HCO_2H): 0.30 mL/min Flow rate (H_2SO_4): 0.88 mL/min Residence time: 2 min[c] Residence time: 1 min[d]	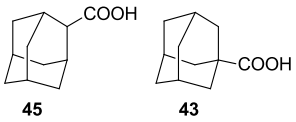 **45** **43** 82% (58:42)
4	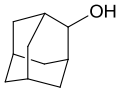 **44**	batch	Temperature: 17-20 °C Addition time: 5 min Reaction time: 1 min	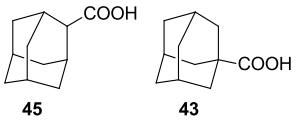 **45** **43** 65% (14:86)

5	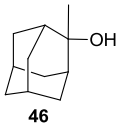 **46**	microflow	Temperature: 20 °C Flow rate (**46**/HCO_2H): 0.01 mL/min Flow rate (H_2SO_4): 0.3 mL/min Residence time: 20 min[c] Residence time: 2.5 min[d]	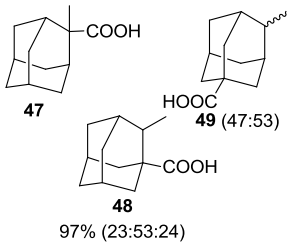 **47** **49** (47:53) **48** 97% (23:53:24)
6	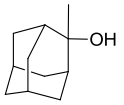 **46**	batch	Temperature: 17-20 °C Addition time: 3 min Reaction time: 10 min	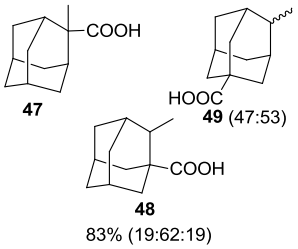 **47** **49** (47:53) **48** 83% (19:62:19)

[a]Substrate (4 mmol), HCO_2H (6 equiv.), H_2SO_4 (20 equiv.); [b]isolated yield after column chromatography on SiO_2; [c]calculated; [d]observed

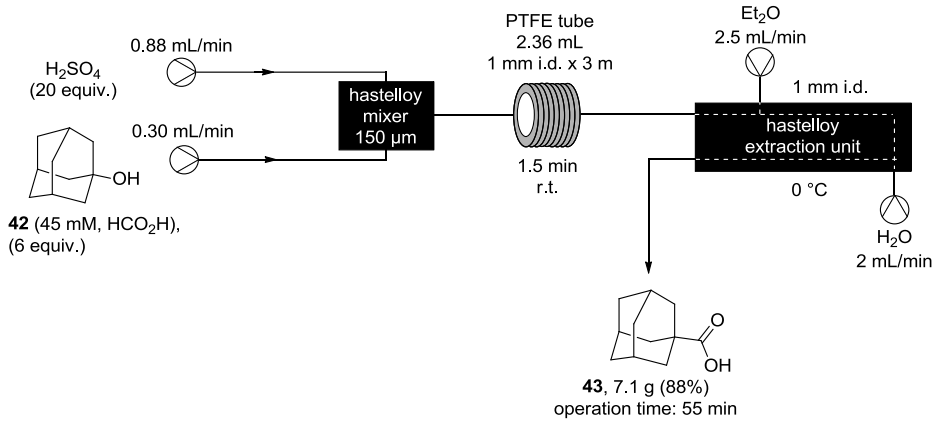

Scheme 7: Multigram scale flow synthesis of 1-adamantanecarboxylic acid (**43**).

Recently, a conventional 'tube-in-tube' system was used to expand the scope of carbonylation reaction in flow such as aminocarbonylations (79-93%, 5 examples), alkoxycarbonylations (60-95%, 9 examples) and hydroxycarbonylations (58-100%, 5 examples) including some intra-molecular examples to form two lactams and a lactone (95%, 3 examples).[40] An interesting addition was the use of a gaseous amine (dimethyl amine) in the hydrazine-promoted amino-carbonylation process, achieved by coupling two conventional 'tube-in-tube' systems in series (Scheme 8). In the initial screening, a higher concentration of substrates was investigated but this gave low conversions, indicating that the reaction was limiting in at least one of the gases used. An alternative set-up, where the substrates were directly passed through the 'tube-in-tube' reactors to saturate the streams was also tested but this showed low conversions. Eventually the

system set-up shown in Scheme 8 was used. This required the use of several back-pressure regulators positioned at different locations within the set-up to stabilise the flow and to maintain the required system pressure. Additionally, a small column packed with glass wool was employed after the reactor to filter off any precipitate formed during the reaction, mainly palladium black, which could lead to blocking of the final back pressure regulator.

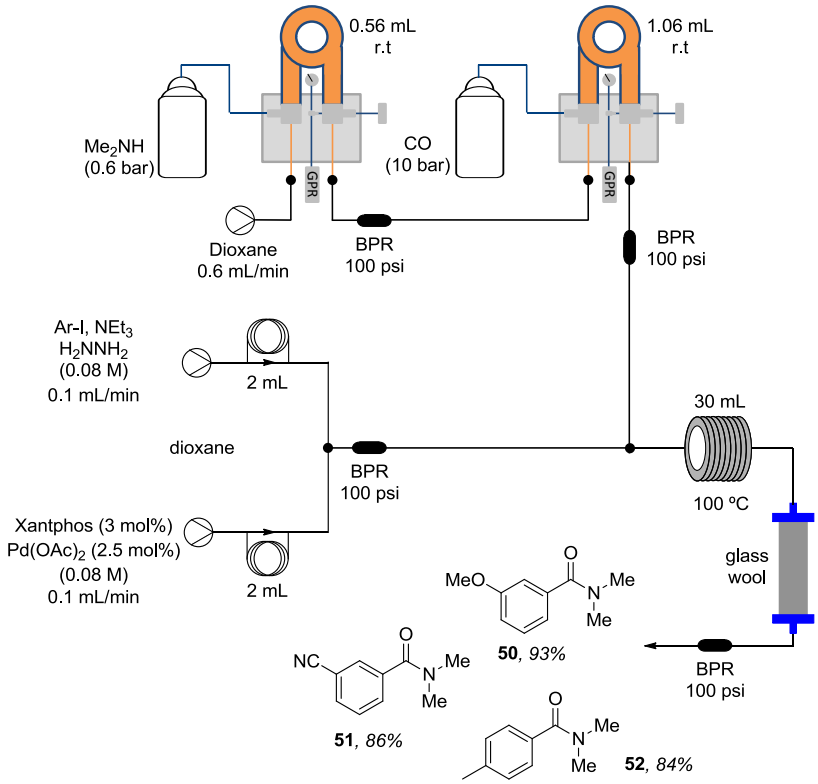

Scheme 8: Aminocarbonylation in flow using two gases via conventional 'tube-in-tube' reactors.

A near stoichiometric (1.2 equiv.) amount of carbon monoxide was shown to be effective for the continuous flow Heck-carbonylation of 1-bromo-3,5-*bis*(trifluoromethyl)benzene (**53**). The reaction was promoted by $PdCl_2(PPh_3)_2$ as the catalyst with 1,4-*bis*(diphenylphosphino)butane (dppb) as the supporting ligand.[41] A kilogram-scale production of product **54** was successful when using a large tubular reactor ~900 mL (10.7 mm i.d. x 10 m) at 0.65 M concentration to produce a throughput of 1.86 kg/day while still maintaining the 99% yield originally obtained for the smaller scale reaction (Scheme 9). In addition, the flow deprotonation of allylsilane (**55**) to form a 1-silylallyllithium intermediate which was then carbonylated and quickly quenched with trimethylsilane chloride to furnish a dienol silyl ether **56** in excellent yield and *E*/*Z* ratio: (93%, 97:3) was reported.[42] A comparison with the batch protocol indicated that the flow

process was more efficient and very straightforward to run (Scheme 10). The flow protocol was subsequently expanded to a wider selection of alkylsilanes and electrophiles all of which gave good to excellent yields and selectivities (77-88% yields, 91:9-97:3 (*E*/*Z*), 5 examples).

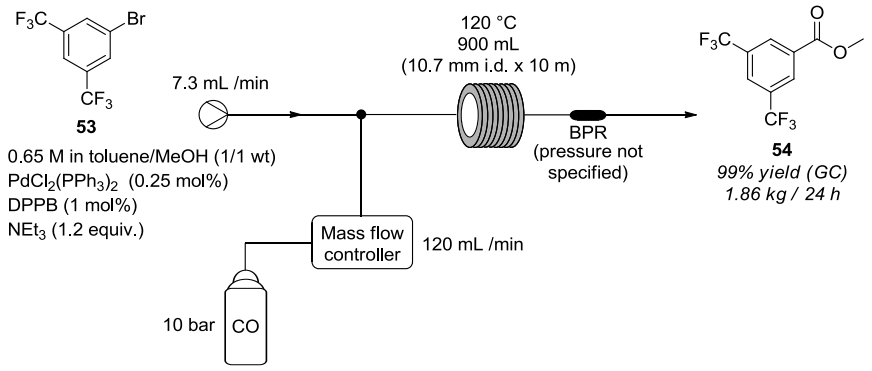

Scheme 9: Heck-carbonylation of bromide **45** in continuous flow.

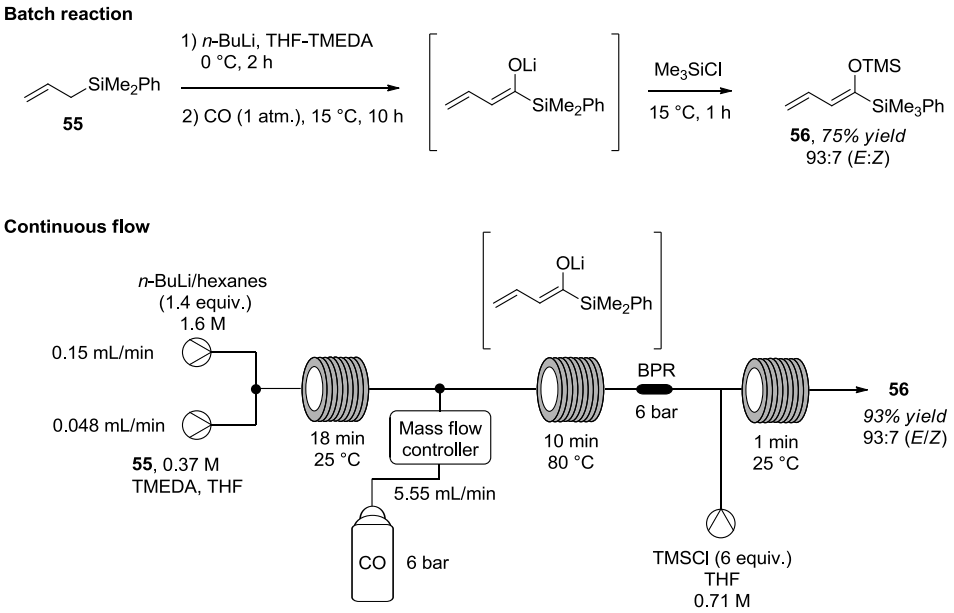

Scheme 10: Formation, carbonylation and quenching of 1-silylallyllithium intermediate to give the dienol silyl ether in flow, also showing the comparison with the batch protocol.

A synthesis of a phenyl isocyanate starting from nitrobenzene (**57**) in flow was reported by Takebayashi and co-workers using carbon monoxide as a reductant (Scheme 11).[43] The carbon monoxide was delivered at a 90° angle to the liquid flow through a T-piece connector, resulting in a segmented flow system, which was directed into a tubular reactor heated at 220 °C. The direct comparison of the corresponding batch protocol demonstrated that the flow procedure gave a higher yield, although the authors did not

quantify the yield or how it was measured. It was shown that changing the inner diameter (i.d.) of the tubular reactor had a significant impact on the reaction efficiency. The use of a 1.0 mm i.d. tube reactor gave a lower yield than using a 0.5 mm i.d. tube reactor. This was explained as being due to a higher surface to volume ratio of the carbon monoxide within the liquid plug, thus a smaller inner diameter tube will maintain a higher concentration of dissolved carbon monoxide in the reaction mixture.

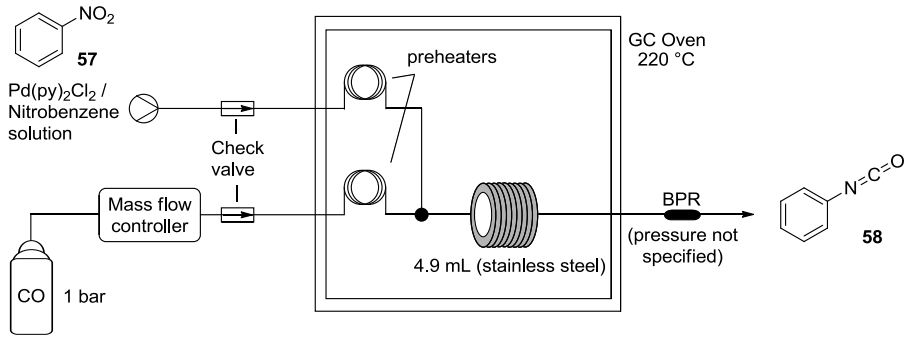

Scheme 11: Flow carbonylation of nitrobenzene to give phenylisocyanate **58**.

1.1.4.2 Carbon dioxide

Carbon dioxide is normally used as a building block in synthesis by making use of its weak electrophilic characteristic. A flow procedure to trap carbon dioxide in the formation of carboxylate group has been developed. Grignard substrates were passed through a conventional 'tube-in-tube' reactor to deliver the carbon dioxide (Scheme 17).[44] Optimum conditions were determined at 4 bar of carbon dioxide enabling near quantitative conversions even at moderate flow rates (0.4 mL/min, residence time = 42 s). A set of ten different carboxylic acids were prepared in good to excellent yields (75-100% yields), unfortunately, no examples using electron-withdrawing substituents were reported. An efficient 'catch-and-release' protocol was used to facilitate in-line purification of the carboxylic acid using a cartridge containing a polymer supported ammonium hydroxide species (A-900). Following trapping of the carboxylic acid, the cartridge was washed with THF to remove any unwanted organic impurities, then 'released' by treatment with a solution of formic acid in THF (1:9) to yield the pure carboxylic acid. Similarly, the Rutjes group reported on the formation of benzoic acid through the hydroxycarbonylation of phenylmagnesium bromide in flow delivering a throughput of 0.52 g/h using a commercial (FlowStart *Evo*, Future Chemistry) pumping system.[45]

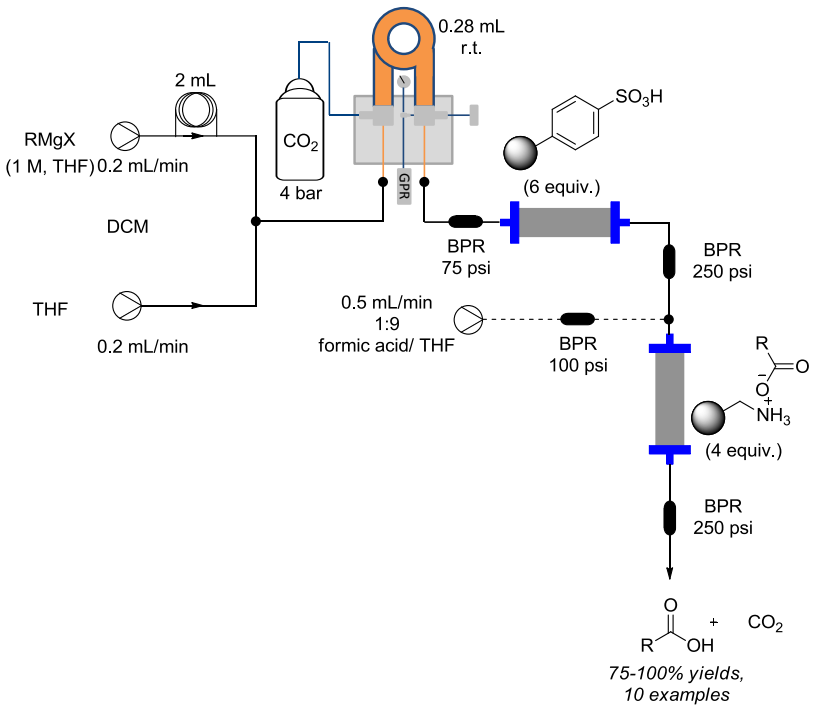

Scheme 12: Flow carboxylation of Grignard substrates using carbon dioxide.

The flow synthesis of Amitriptyline (**60**) using carbon dioxide in flow was reported by the Kirschning group.[46] As part of the process development it was noted that excess carbon dioxide was possibly reacting with the *n*-BuLi required for the second stage Parham cyclisation (Scheme 13). Ultimately, the excess carbon dioxide was removed by passing the liquid stream through a Teflon AF-2400 tube acting to degas the pressurised flow stream prior to adding the *n*-BuLi and yielding the product in an isolated yield of 76%.

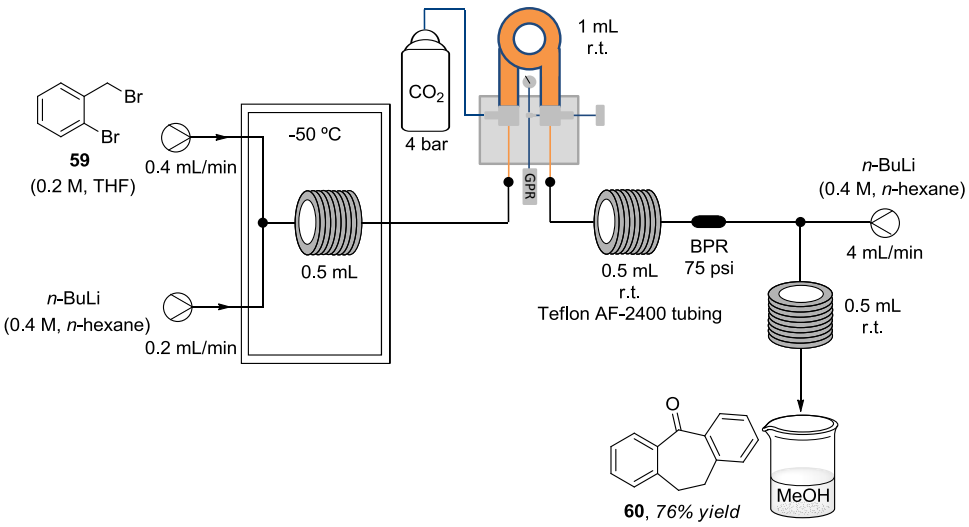

Scheme 13: The synthesis of Amitriptyline using carbon dioxide in flow.

A related transformation was performed by the Yoshida group, using *in situ* generated organilithium species (Scheme 14).[47] The organolithium intermediate formed by lithium halogen exchange was immediately trapped with carbon dioxide in an annular flow set-up. A stream of MeOH quenched the excess *n*-BuLi prior to collection of the product into a saturated sodium bicarbonate solution. Beneficially, the flow protocol did not yield any benzophenone or triphenyl MeOH derivatives which are normally observed in the corresponding batch reactions. Using this set-up (Scheme 14), a selection of carboxylic acids were synthesised in good yields (59-89% yield, 13 examples) representing a range of different electronics which appear not to influence the carboxylic acid yield.

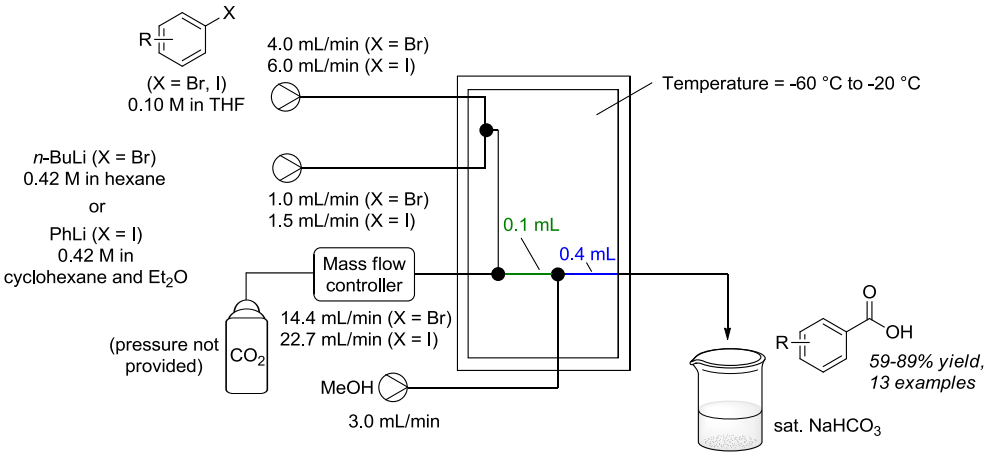

Scheme 14: Flow carbonylation of organolithiums using carbon dioxide.

A similar concept was later demonstrated by the Kappe group using lithium *bis*(trimethylsilyl)amide (LiHMDS) or lithium diisopropylamide (LDA) solutions to achieve the lithiation of terminal alkynes or heterocycles.[48] The lithiation was shown to happen very rapidly (~0.5 seconds at room temperature) but they opted for a ~3 second residence time after which the lithiated substrate was carboxylated with carbon dioxide through a T-mixer. In order to stabilize the CO_2 flow, the gas was preheated at 65 °C before going through the mass flow controller (Scheme 15). Additionally a water quench was introduced before the back pressure regulator to dissolve any small amounts of precipitate formed during the reaction. Using the optimised conditions a number of alkynes were carboxylated generally giving very good yields (66-90% yields, 8 examples). A couple of examples gave no results due to problems encountered with the reactor clogging. The carboxylation of some additional heterocycle substrates was also demonstrated using the same set-up with LDA giving moderate to good yields (43-86%

yields, 6 examples). Clogging issues were also observed despite the water quench but were overcome by changing to a dilution mixture of water and acetic acid (10:1).

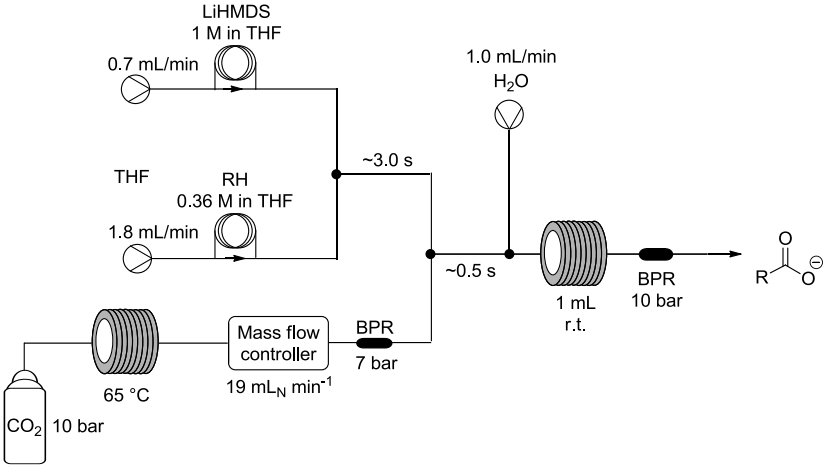

Scheme 15: Flow set-up for the carboxylation of lithiated species using CO_2 gas.

The Jamison group have taken this approach a step further and shown the feasibility of quenching the intermediate lithium carboxylate with another organolithium to form unsymmetric ketones (Scheme 16).[49] Peristaltic pumps were used to pump the organolithium species (kept between 0 and 20 °C due to their instability) at a low concentration (0.1 M in THF) to prevent issues of precipitation and potential reactor clogging. For some substrates, a degasser was used to remove the excess CO_2 before the organolithium quench to prevent symmetric ketone by-product formation. The sequence was shown to be general for most substrates giving good to excellent yields (40-92% yields, 18 examples).

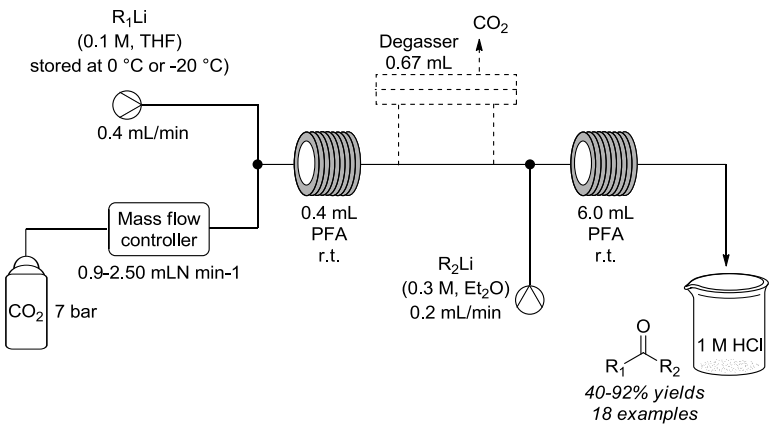

Scheme 16: Flow set-up for the synthesis of unsymmetric ketones using CO_2 gas.

Another interesting transformation reported by the Jamison group involves the synthesis of cyclic carbonates through a bromine-catalysed conversion of CO_2 and epoxides in continuous annular flow (Scheme 17).[50] A mixture of *N*-bromosuccinimide (NBS) and benzoyl peroxide (BPO) was used to form bromine, which activates the epoxide to nucleophilic attack. Substrates with aliphatic and aromatic substituents generally resulted in good to excellent yields (72-90% yields, 7 examples) with moderate yields being achieved for substrates with olefinic substituents (51-58% yields, 3 examples). Even though the authors postulate that the pendant alkene group might be interfering with the active catalyst, they do not report any bromination occurring on the alkene.

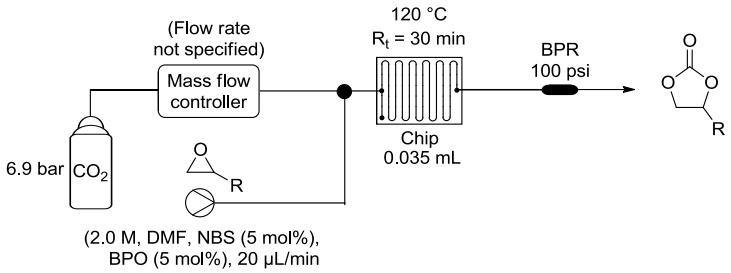

Scheme 17: Micro-flow synthesis of cyclic carbonates through bromine-catalysed conversion of CO_2 and epoxides.

Recently the continuous flow synthesis of 2,4,5-trifluorobenzoic acid (**62**) was reported through the Grignard reaction of 2,4,5-trifluorobromobenzene (**61**) and subsequent CO_2 trapping (Scheme 18) using a falling film microreactor (FFMR) (Figure 3).[51] The use of ethylmagnesium bromide as a Grignard exchange reagent was used due to the stability of the reagent, allowing the authors to conduct the reaction at 30 °C. As part of the study, the size of the T-mixer was investigated to avoid blockage of the system due to precipitation. An inner diameter of 1200 µm was found to be optimal which prevents clogging and still allows for efficient mixing. Although the authors describe an efficient way of forming the carboxylic acid through this set-up, the FFMR used has one drawback; the maximum flow rate was 0.83 mL/min and thus achieving high space-time yields was challenging.

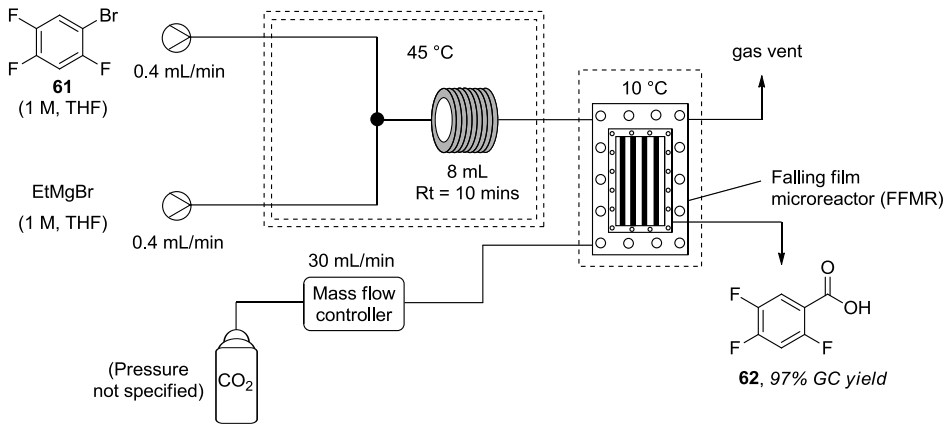

Scheme 18: Use of a FFMR for the synthesis of 2,4,5-trifluorobenzoic acid (**62**) as a continuous process.

1.1.4.3 The use of oxygen gas in flow

With the recent move towards even more environmentally friendly and sustainable oxidation chemistry, metal oxidants like permanganate and chromium(VI) compounds are receiving less attention. Oxygen is however considered to be a good alternative either alone or in conjunction with various promoting catalysts.

As an early example, the Glaser-Hay coupling in continuous flow was reported by the Ley group, with oxygen being used to re-oxidise the copper catalyst.[52] A conventional 'tube-in-tube' module was used to pre-saturate the solvent with oxygen which was then mixed with an additional liquid substrate stream containing the copper(I) complex and the terminal alkyne (Scheme 19). A polymer-supported thiourea scavenger cartridge was used post reaction to remove the copper catalyst from the flow stream with an additional polymer-supported sulfonic acid cartridge to sequester the *N*,*N*,*N′*,*N′*-tetramethylethane-1,2-diamine (TMEDA) base facilitating direct in-line purification. A range of aromatic and aliphatic terminal alkynes gave 1,3-butadiynes in moderate to excellent yields (49-100% yields, 11 examples).

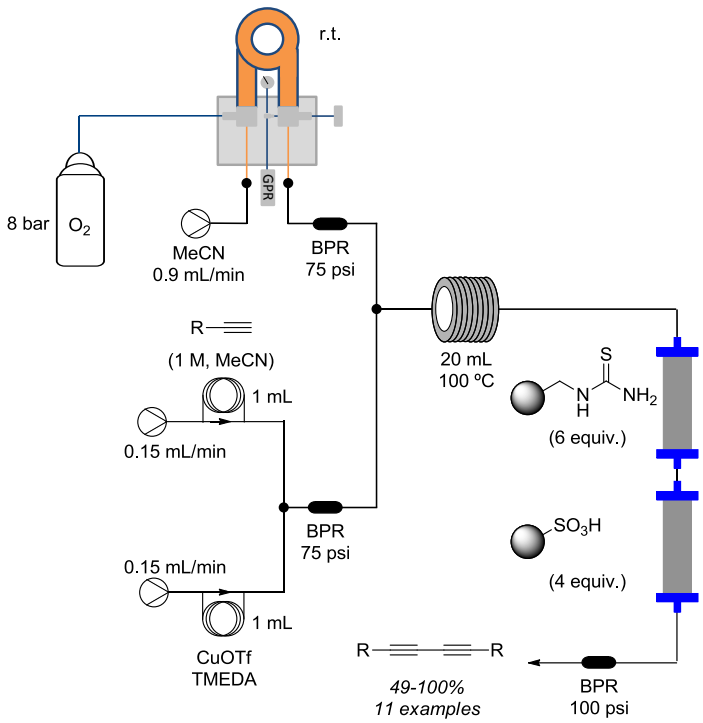

Scheme 19: Glaser-Hay coupling in continuous flow using oxygen to reoxidise the copper catalyst.

Oxygen has also used in continuous flow aerobic anti-Markovnikov Wacker oxidation.[53] Optimisation of the reaction temperature, oxygen pressure and water content was performed to achieve a good conversion and selectivity towards the desired aldehyde product. The reaction was successfully performed on a selection of styrenes possessing both electron withdrawing as well as electron donating groups, in good yield (56-80%, 12 examples) and good to excellent selectivities (from 77:2:14 to 92:2:3 [A:B:C – Scheme 20]). Some further optimisation on the set-up was performed to demonstrate a scale-up of the reaction (96 mmol over 6 h) with the addition of an extra 'tube-in-tube' reactor placed in series to achieve better oxidation of the copper catalyst (Scheme 20).

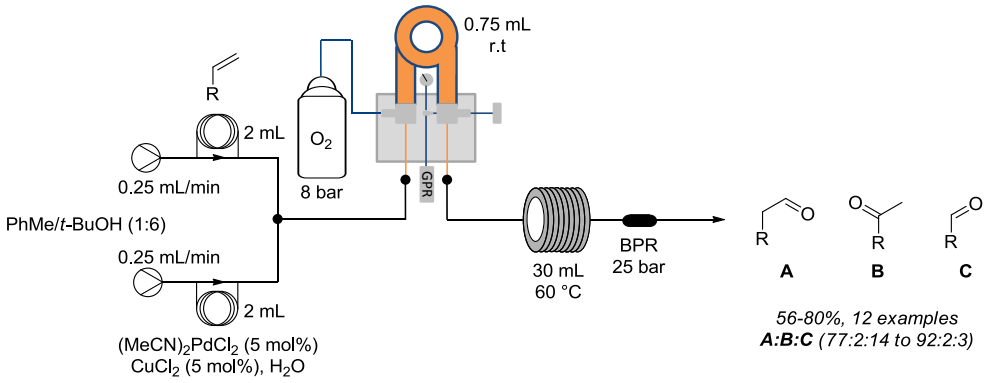

Scheme 20: The anti-Markovnikov Wacker oxidation of alkenes using oxygen in flow.

The air-promoted oxidation of 2-benzylpyridine derivatives (**63a-c**) to their corresponding 2-benzoylpyridines (**64a-c**) has been reported by the Kappe group employing propylene carbonate as a solvent (Scheme 21).[54] A microreactor was used with oxygen (delivered as atmospheric air) added through a T-mixer to give plug flow with the gas addition being supplied through a mass-flow controller. A high temperature (200 °C) and low residence time (13 min) combination was used to give the oxidation products in good yields (69-83% yields, 3 examples).

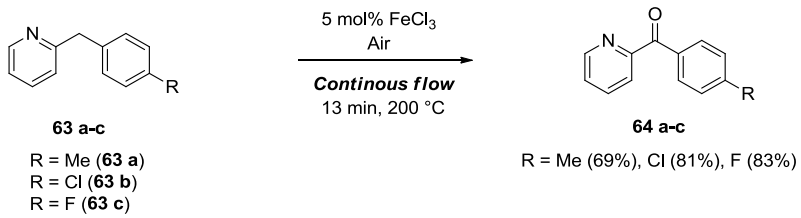

Scheme 21: Aerobic oxidation of the 2-benzylpyridine derivatives to their corresponding 2-benzoylpyridines in flow.

The Kocsis group have made use of the X-Cube^{TM} to deliver oxygen for a number of industrial relevant oxidations and *N*-alkylation reactions (Scheme 22).[55] The oxidation of indoline and 1-phenylethanol were used for the optimisation reactions in continuous flow with a range of catalysts, oxidants, solvents, temperatures and flow rates being evaluated. Subsequently the derived conditions were used to convert a small collection of alcohol substrates to the corresponding ketones or aldehydes in good yields (80-92%, 8 examples). The optimisation of the *N*-alkylation reaction using alcohols was performed in moderate yields (47-64% yields, 6 examples) employing activated Raney nickel as a catalyst for the oxidation of the alcohol in a 'borrowing hydrogen' process. The intermediate imine formed, through the condensation of the amine and aldehyde, was then reduced by the 'borrowed' hydrogen.

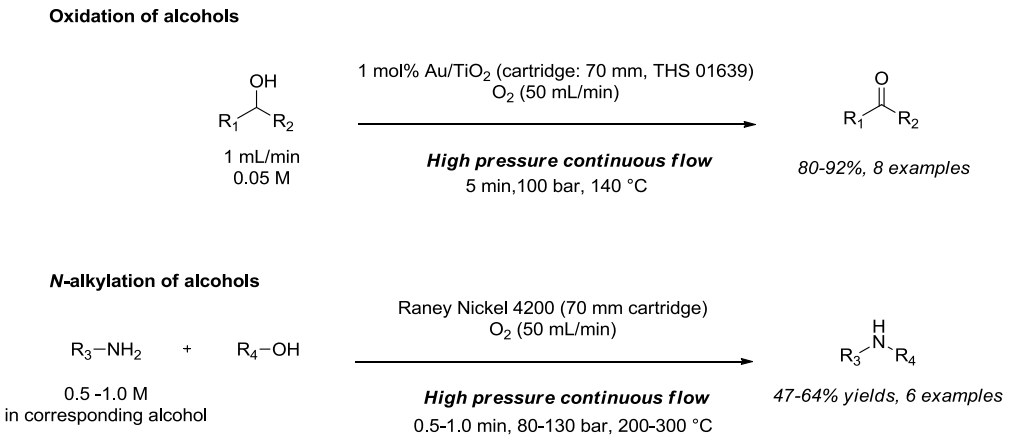

Scheme 22: Oxidation of alcohols using oxygen in flow (top) and *N*-alkylation of alcohols using oxygen in continuous flow (bottom).

The Kirschning group have used oxygen gas delivered through a conventional 'tube-in-tube' reactor to oxidise allylic and benzylic alcohols using gold-doped superparamagnetic nanostructured particles as the catalyst (Scheme 23).[56] The gold catalyst was immobilised on MAGSILICA® which facilitates inductive heating at medium frequency induction (25 KHz). Using this set-up no over-oxidation was observed which is encountered when the same process is conducted in batch.[57] Unfortunately, this set-up worked best with benzene as the solvent as other solvents such as MeOH, EtOAc, MeCN and DCM did not give full conversion. Toluene gave full conversions but produced by-products derived from the oxidation of the methyl group, making the purification more difficult.

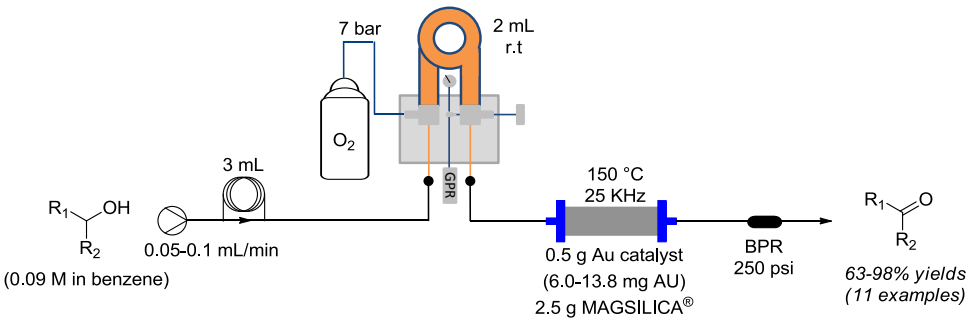

Scheme 23: Oxidation of allylic and benzylic alcohols using oxygen as the oxidant and gold-doped superparamagnetic nanostructured particles as catalysts under inductively-heated flow conditions.

The continuous flow synthesis of carboxylic acids through the aerobic oxidation of aldehydes was reported by the Favre-Réguillon group using a plug flow approach (Scheme 24).[58] The process was run at ambient temperature with 5 bar of oxygen pressure without any added metal catalysts. This was claimed to cleanly (98% purity) generate the carboxylic acids in high yields (61-91% yields, 4 examples). The aerobic oxidation of the

aldehydes goes through a free radical chain reaction to form the corresponding peracid which reacts with the remaining aldehyde to produce a tetrahedral adduct (similar to the Criegee intermediate in the Baeyer-Villiger reaction). The tetrahedral adduct then rearranges, through a migration of hydrogen or alkyl group from the aldehyde to give the corresponding carboxylate. The authors also described how through the use of EPR spectroscopy and spin trap methodology,[59] they could show that their process goes through a free radical auto-oxidation pathway which was initiated by a trace amount of carboxylic acid present in the starting materials at ppm levels.

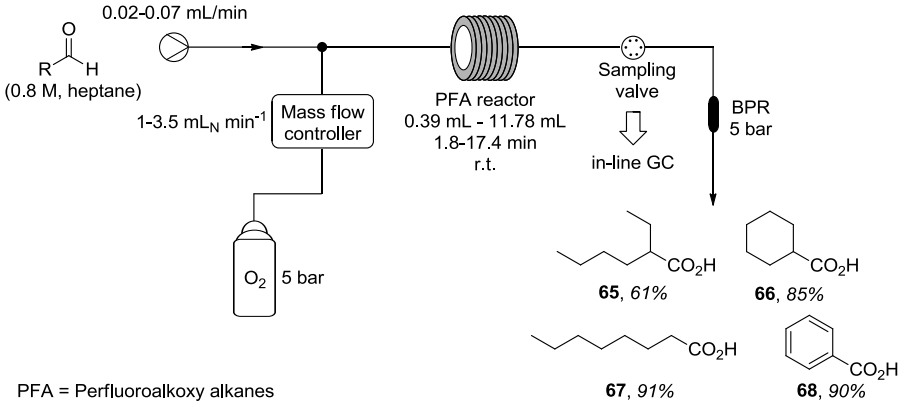

Scheme 24: Metal free oxidation of aldehydes to form carboxylic acids using oxygen in flow.

The synthesis of functionalised phenols using aerobic oxidation of Grignard substrates has been reported as a continuous flow procedure again using a plug flow system to deliver the oxygen.[60] The effect of temperature and system pressure were studied for the oxidation of phenylmagnesium bromide. Ultimately, a combination of 14 bar pressure and -25 °C was used to deliver a near quantitative conversion to the corresponding phenol in 3.4 min. These conditions were then applied to a wider range of Grignard reagents with electron-rich systems forming the corresponding phenols in moderate to good yields (57-87%, 13 examples). The corresponding electron-deficient substrates required elevated temperatures (-10 °C to 25 °C) but also gave comparable yields (53-81%). Some heteroaryl magnesium reagents were also tested, with thiophene and benzothiophene giving the ketone derivatives (24% and 32% yields respectively). Other heteroaryl magnesium reagents gave the expected phenol products (47-86% yields, 3 examples). This transformation was also utilised for the preparation of *ortho*-functionalised phenols in an integrated three-step continuous process using compressed air instead of pure oxygen (Scheme 25). A number of substrates were prepared within a residence time of 14 min in overall yields of 33-55% for the 8 examples studied.

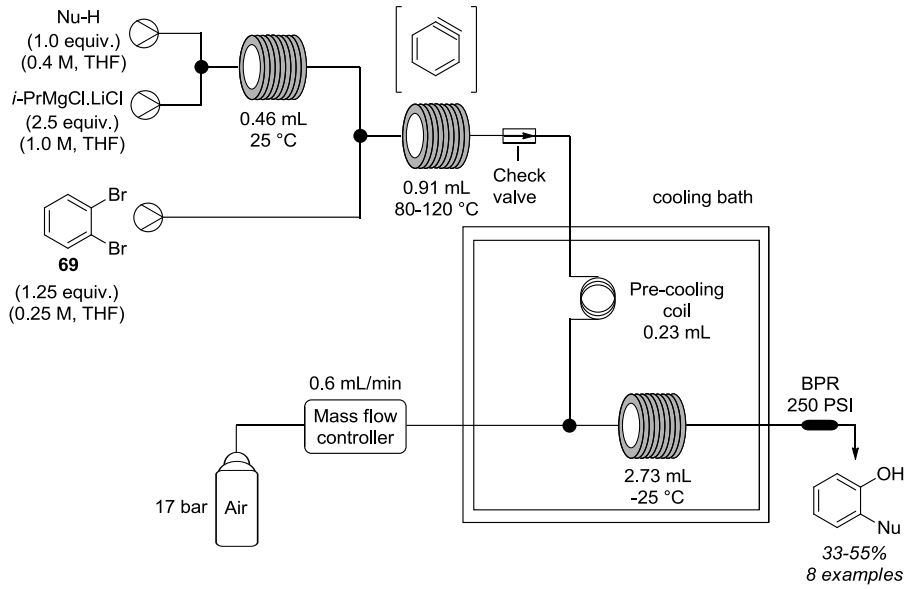

Scheme 25: Integrated flow system for the synthesis of *ortho*-functionalised phenols using air in flow.

The C-H activation of indoles via a cross-dehydrogenative coupling was reported in a segmented flow reactor (Scheme 26).[61] The oxygen has a similar role as in the earlier example of the oxidative Heck reaction reported in a dual-channel microreactor.[62] During the optimisation phase the authors reported that better conversions were obtained when the reactor size was doubled and the flow rate was maintained rather increasing the residence time by decreasing the flow rates. This was highlighted as being due to better mixing in the segmented flow path when higher flow rates were applied, ensuring efficient palladium reoxidation. Using optimised conditions a number of vinyl indoles were synthesised in moderate to excellent yields (27-92%, 15 examples). The choice of solvent, DMSO, was based on the solubility of the palladium catalyst and its propensity to decrease palladium black formation which could ultimately block the tubular reactor. Although practical at these small lab scales the use of DMSO is not ideal for scale-up due to the difficulty of its removal and so this process would require reaction reengineering before being more widely applicable. Additionally, the authors did not mention any use of back pressure regulators/pressure control, which would be essential to maintain a stabilised flow when scale up is required.

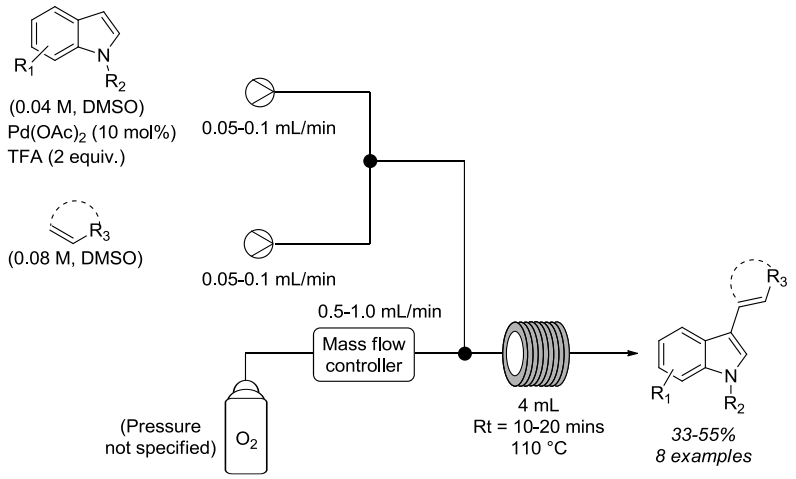

Scheme 26: Pd(II)-catalysed cross-dehydrogenative Heck reaction using oxygen gas in flow as an oxidant to reoxidise the palladium catalyst.

An iron-catalysed aerobic nitro-Mannich reaction was published by the CSIRO which affords a direct α-C(sp^3)-H functionalisation of *N*-aryl tetrahydroisoquinolines.[63] The oxygen was delivered through a conventional 'tube-in-tube' reactor with a stainless steel tube reactor being used as a residence time unit and to heat the flow stream (Scheme 27). A back pressure regulator was placed just after the 'tube-in-tube' reactor which precludes in-line degassing. The reaction was quenched by dropping the liquid output stream onto 2 equivalents of triethylamine which enabled isolation of the products in moderate to good yields after conventional purification (31-77%, 15 examples).

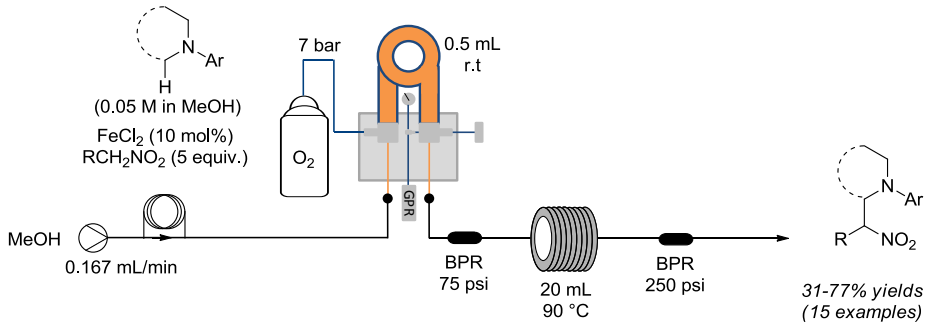

Scheme 27: Iron-catalysed aerobic nitro-Mannich reaction with oxygen gas as an oxidant in flow.

The biocatalytic production of catechols was demonstrated through a 2-hydroxybiphenyl 3-monooxygenase (HbpA) catalysed conversion of 2-hydroxybiphenyl to 3-phenylcatechol using a conventional 'tube-in-tube' to deliver an oxygen feed.[64] Although the authors showed a number of optimisation steps to increase the gas transport into the solution, when the transformation was carried on an 80 mmol scale, only a 5% isolated yield was obtained, indicating that the enzyme catalyst employed was the limiting aspect of the process.

The use of oxygen in flow photochemistry has also been extensively reported.[65] The addition of singlet oxygen to α-terpinene (**70**) to yield anthelmintic ascaridole (**71**) was realised using Rose Bengal as the sensitiser in a micro-chip reactor equipped with a 20 W tungsten lamp. The oxygen stream was introduced as a laminar flow (Scheme 28).[66] A direct comparison of the flow process with the batch process using a 500 W tungsten lamp shows a higher yield obtained for the flow process (85% *vs* 67%) but a lower productivity for the flow reactor (1.5 mg/h *vs* 175 mg/h). On the other hand, as the flow process should have a linear scalability, higher productivities could be achieved by multiple reactors in parallel rather than direct reactor scaling.

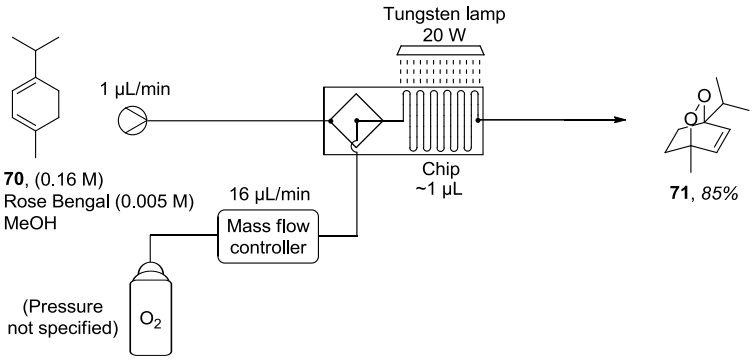

Scheme 28: Micro-flow preparation of anthelmintic ascaridole **71**.

Recently, the photo-oxidation of 4-substituted toluene derivatives was described using a microchip reactor and oxygen delivered as a segmented flow using 2-*tert*-butylanthraquinone (**72**) as a photosensitiser (Scheme 29).[67] Even though the yields obtained in flow were comparable to batch (30-83% yields) much shorter reaction times were needed - between 12 and 36 h were needed to achieve similar yields in batch.

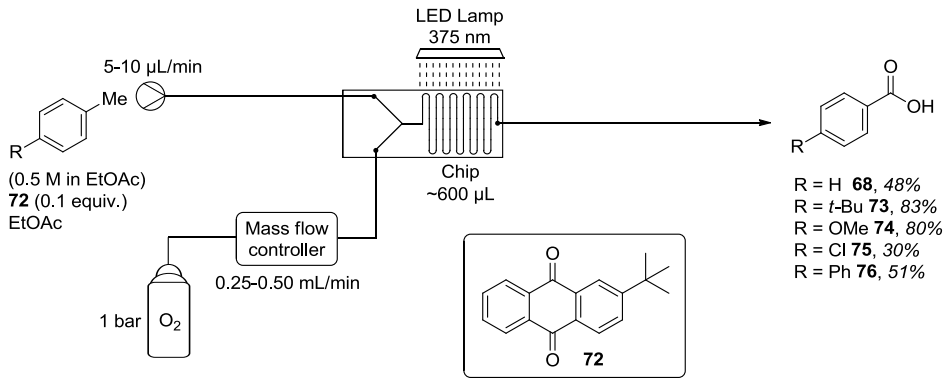

Scheme 29: Photo-oxidation of 4-substituted toluene derivatives using oxygen in micro-flow.

The oxidation of (-)-β-citronellol, using a borosilicate glass-loop microreactor with a diode array as a light source, was demonstrated in the synthesis of the fragrance rose

oxide, with Rose Bengal as an oxygen sensitiser. However, the reaction time needed for reasonable conversion on a 1 mmol scale (400 min) was deemed too long for the reactor to be used for efficient scale up.[68]

The use of a TiO_2 deposited photocatalyst within the channels of a flow microreactor has received attention for the oxidative degradation of *para*-chlorophenol,[69] toluene,[69] phenol[70] and methylene blue.[70] Other synthetically useful transformations were also reported such as the oxidation of α-terpinene (**70**) to yield ascaridole (**71**),[71] oxidation of L-methionine to the corresponding sulfoxide,[71] for the oxidation of β-citronellol[72] and the oxidation of allylic alcohols for the synthesis of the antimalarial artemisinin (Scheme 30).[73] The concept of this reactor is similar to that of the 'tube-in-tube' reactors but employing a poly(dimethylsiloxane) (PDMS) membrane separating the two channels allowing oxygen to permeate through the membrane and saturate the reaction mixture (Figure 5).

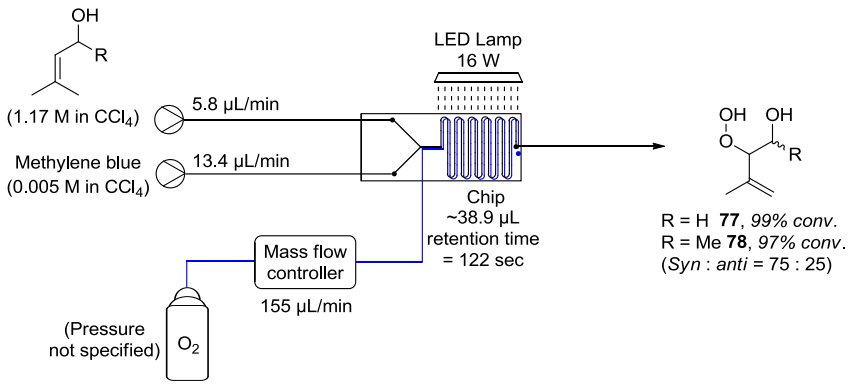

Scheme 30: Flow photo-oxidation of allylic alcohols for the synthesis of artemisinin using a PDMS membrane reactor.

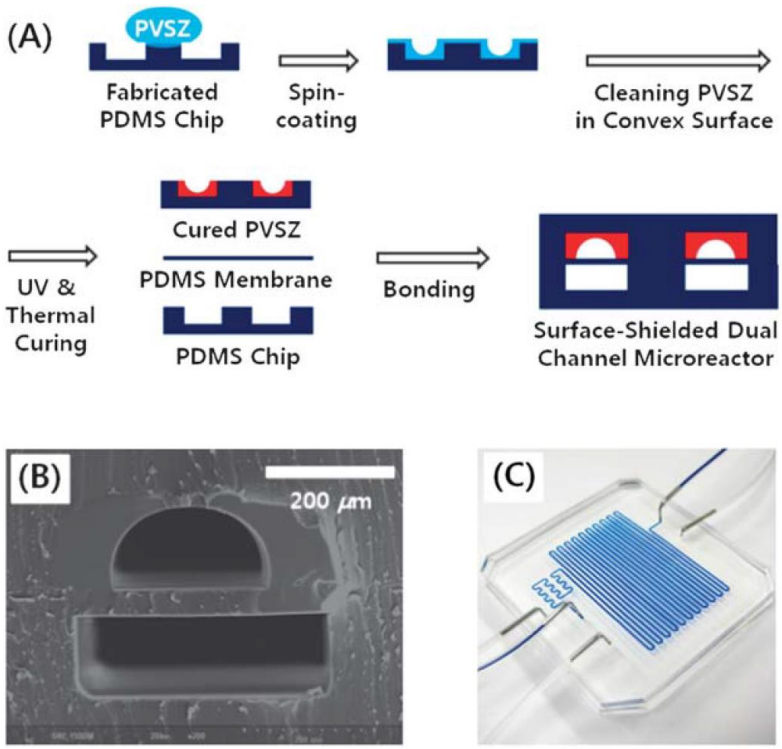

Figure 5: (A) Schematic illustration for the fabrication of a dual-channel microreactor with polyvinylsilazane (PVSZ) shielded upper channel. (B) Cross-sectional view of dual microchannel with the PVSZ shielded upper channel. (C) The PVSZ shielded dual-channel microreactor filled with O_2, methylene blue (photosensitizer), and α-terpinene (reagent).

Reproduced with permission from reference 73. Copyright 2011 The Royal Society of Chemistry.

The photochemical rearrangements of an *N*-oxide moiety has been used for the synthesis of 4-substituted quinolone derivatives (Scheme 31).[74] Oxygen was used as a triplet quench to suppress the [2+2]-dimerisation of the quinolones. This gave the desired quinolones (**79-82**) in good to excellent yields (72-99% yield, 4 examples), which were superior to the equivalent batch reactions. The flow reactor was built from a double coiled tubular reactor (Duran tube 7 mm, coil outer diameter: 75 mm, height: 200 mm, internal volume: 150 mL) placed in the middle of a Rayonet (RPR-100) photoreactor equipped with 16 lamps of fixed wavelength. The oxygen was bubbled through the solvent to pre-saturate the solution. The authors claimed this approach could be used to deliver gram scale quantities of products. They also used the same set-up for the synthesis of quinolones with tethered alkenes at the 4-position which enabled subsequent intramolecular [2+2] cycloadditions.[75]

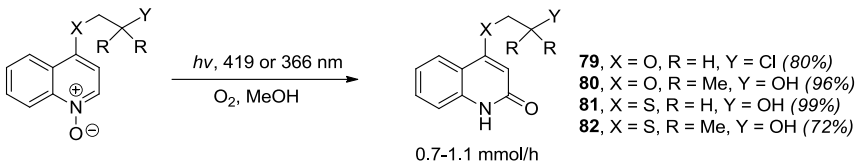

Scheme 31: Photochemical rearrangement of *N*-oxides to quinolones.

The high solubility of molecular oxygen in supercritical carbon dioxide ($scCO_2$) has been exploited in the oxidation of citronellol (**83**) using 5,10,15,20-tetrakis(pentafluorophenyl)porphyrin (TPFPP, **84**) as a photosensitiser (Scheme 32).[76] Oxygen was delivered through a Rheodyne dosing unit and combined with the $scCO_2$ before mixing with a solution of **83** in dimethyl carbonate (DMC) (1:1 *v*:*v*). The combined stream was then passed through a second micro-mixer before it was transferred into a sapphire cell equipped with four LEDs (1000 lumen). Complete consumption of **83** was achieved with 52% selectivity for **85** and 48% for **86** at a flow rate of 0.1 mL/min (1:1 *v*:*v* DMC:**83**), 1.0 mL/min of $scCO_2$ and 2 equivalents of oxygen at 180 bar. Although $scCO_2$ was completely miscible with oxygen in all proportions used,[77] it is not an ideal solvent for most organic compounds which can limit its use as a solvent in flow chemistry.[78]

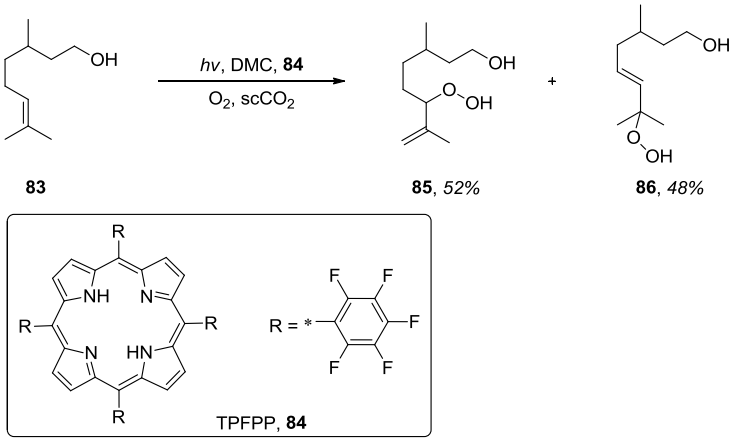

Scheme 32: Photo-oxidation of citronellol in flow using $scCO_2$.

The oxidation of citronellol (**83**) has also been reported by the Seeberger group using oxygen in a segmented flow regime with tetraphenylporphyrin (TPP) as the photosensitiser.[79] In their set-up (Scheme 33), the system could deliver up to 2.5 mmol/min of product. The same set-up was also used for the photo-oxidation of other substrates to show the scope of the method developed including the flow synthesis of the anti-malaria drug artemisinin.[80] A modified version of this set-up using 420 nm LED lamps was subsequently applied to the transformation of amines to *α*-cyanoepoxides

through an oxygen based oxidation (Scheme 34)[81] and the photo-oxidative cyanation of secondary amines to give **89-91** and primary amines to give **92-95** using singlet oxygen (Scheme 35).[82]

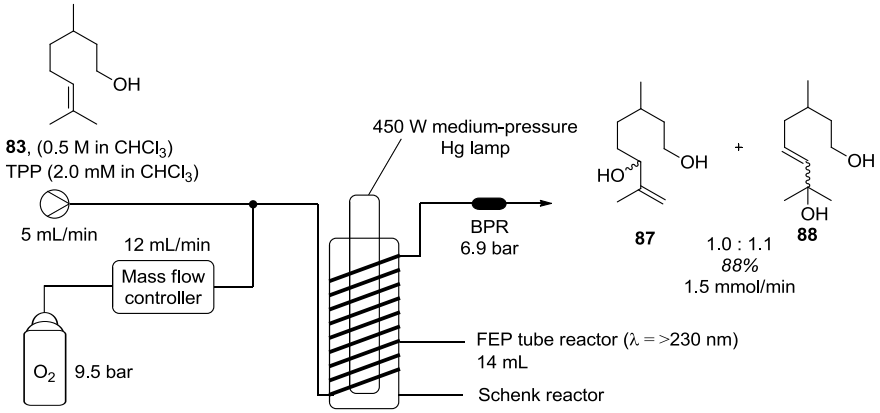

Scheme 33: Photo-oxidation of citronellol using oxygen in a segmented flow regime.

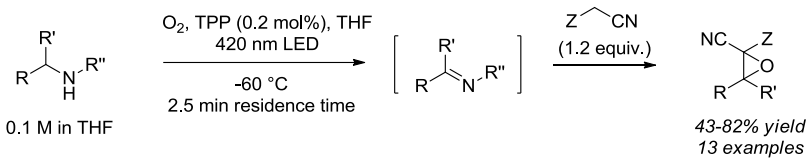

Scheme 34: Photo-oxidation of amines for the synthesis of α-cyanoepoxides.

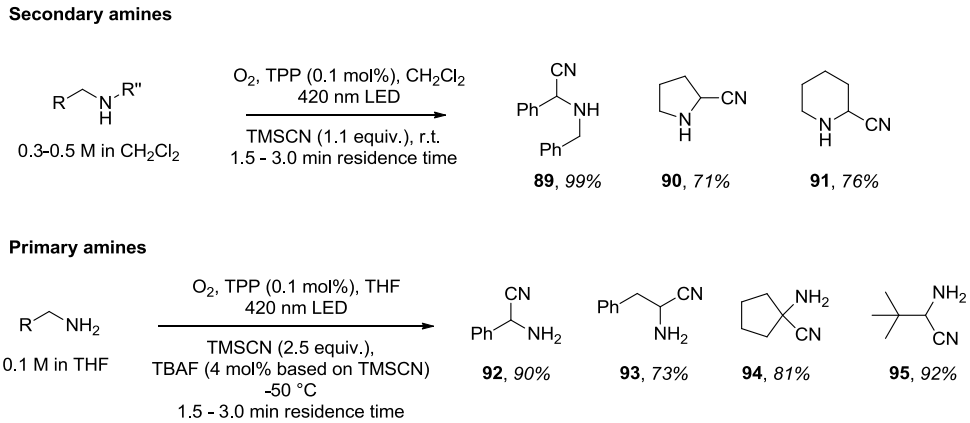

Scheme 35: Photo-oxidative cyanation of primary and secondary amines using singlet oxygen.

1.2 Perspectives on the Future of Flow Chemistry

With many different transformations already having been demonstrated using continuous flow processes, the next major challenge is to illustrate other advantageous aspects of flow chemistry. Some researchers have already demonstrated the feasibility of scale-up in flow rather than just inferring that their processes can be scaled up. Understandably, academic groups with no connection to industries find little use for actual scaling up of reactions in flow. However, with a considerable amount of academic funding nowadays coming from industrial partners, interest within academia is also changing, with a preference for both discovery chemistry as well as scale up chemistry.

In-line analysis is another technique that may be used in conjunction with continuous processes. Some of the examples shown above (Schemes 4 and 24) illustrate how analytical instruments such as IR, UV, Raman, NMR and MS spectrometers can be integrated into continuous flow streams to collect analytical data such as conversion, while the process is ongoing. This ultimately provides a way of enabling fast optimisation of conditions which can also be integrated with intuitive programmes which perform self-optimisation of reactions.[83] Although in theory this sounds excellent, the initial input from the researcher to "teach" the programme to become "intuitive" provides a barrier to most researchers. Consequently, groups or industries that are not interested in allocating a considerable amount of resources for the optimisation of one particular reaction prefer to perform manual optimisation, which, although most probably does not achieve the absolute optimum conditions, requires much less effort and time to achieve.

In the following chapters, the thesis will focus on innovative gas-liquid flow chemistry (CO, CO_2 and O_2) that was performed during this project as well as the development of a novel synthetic methodology for the synthesis of thiazoles using microwave reactors.

2 Results and Discussions

2.1 Carbonylation of Ortho-Substituted Substrates: Using Flow to Enhance and Facilitate Difficult Transformations

2.1.1 Introduction

As highlighted in the introduction section, the issues associated with the use of carbon monoxide (CO) as a reagent (such as toxicity and low solubility in solvents) has prompted some chemists to avoid CO, substituting it for other gases or changing the chemistry where needed. However, the use of flow chemistry has introduced a safer way of using toxic gases such as CO at variable scales (mg-kg). Heck-carbonylation reactions have received a lot of attention both in batch as well as in flow and generally produce the desired products in good yields. Carbonylation of ortho-substituted substrates can, however, still be challenging as highlighted by the limited literature precedence.[84]

The low yields associated with such transformations indicate that the CO attack on the intermediate aryl complex is being inhibited by the sterics present.[84a] This can be explained by considering an associative mechanism for the CO substitution where one ligand is substituted before a migratory insertion takes place. The initial CO coordination takes place on the axial coordination site of the square planar complex, with the aryl group oriented perpendicularly to minimise the steric interactions and placing the ortho-substituent straight over the axial position (Figure 6). The ortho-substituent imposes steric restrictions to the incoming CO thus slowing down the rate of the reaction. An X-ray structure of *trans*-bromo(*o*-tolyl)bis(triphenylphosphine)palladium(II) complex was reported by Cross *et al* (Figure 7).[85] The molecular structure of **96** comprises of a Pd atom with near perfect square planar geometry with a slight out of plane displacement of Br and C(1) where Br-Pd-C(1) angle is 170.9º. As a whole, the molecule has approximate C_s symmetry with the PPh_3 ligands almost eclipsing each other if viewed along the P-Pd-P axis and with the tolyl group sandwiched in-between two phenyl groups (Figure 7 structure B). Focusing on the tolyl group only, structure C (Figure 7) shows how the methyl of the tolyl group is placed straight over the axial position of the palladium. Structure D (Figure 7) is a top view of the crystal structure illustrating how the methyl

group is positioned directly over the axial position of the palladium which would introduce steric hindrance with regards to the CO attack on the intermediate aryl complex.

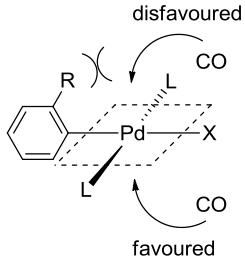

Figure 6: Steric interactions of the CO coordination to the aryl complex intermediate.

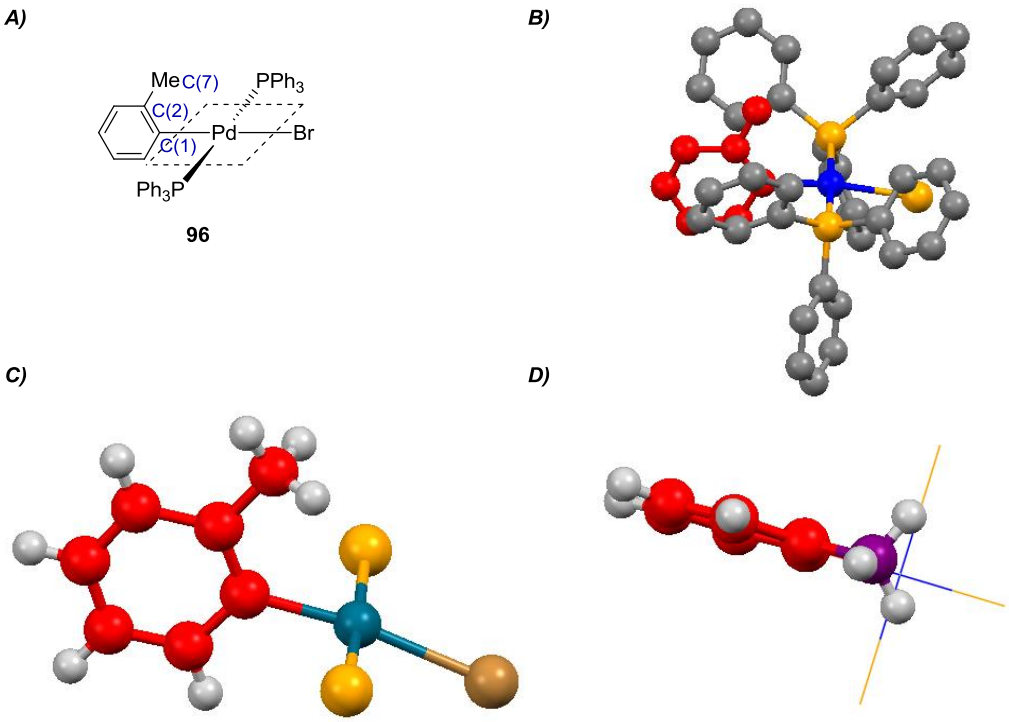

Figure 7: A) molecular structure of complex **96**; B) ball and stick representation of X-ray structure; C) ball and stick representation of X-ray structure showing the tolyl group only; D) topside view of X-ray structure.[85]

If the carbonylation step is indeed slow, the dehalogenation pathway becomes dominant, giving low yields of the carbonylated product. By increasing the CO concentration (by increasing the CO pressure) together with an increase in temperature an increase in the amount of the carbonylated product should be seen. However, an increase in carbon monoxide concentration can also decrease the amount of active Pd^0 catalyst in the catalytic cycle (Scheme 36) due to the π-acidic nature of CO as a ligand, thus slowing

down the reaction. Increasing the temperature will also increase the rate of side product formation.

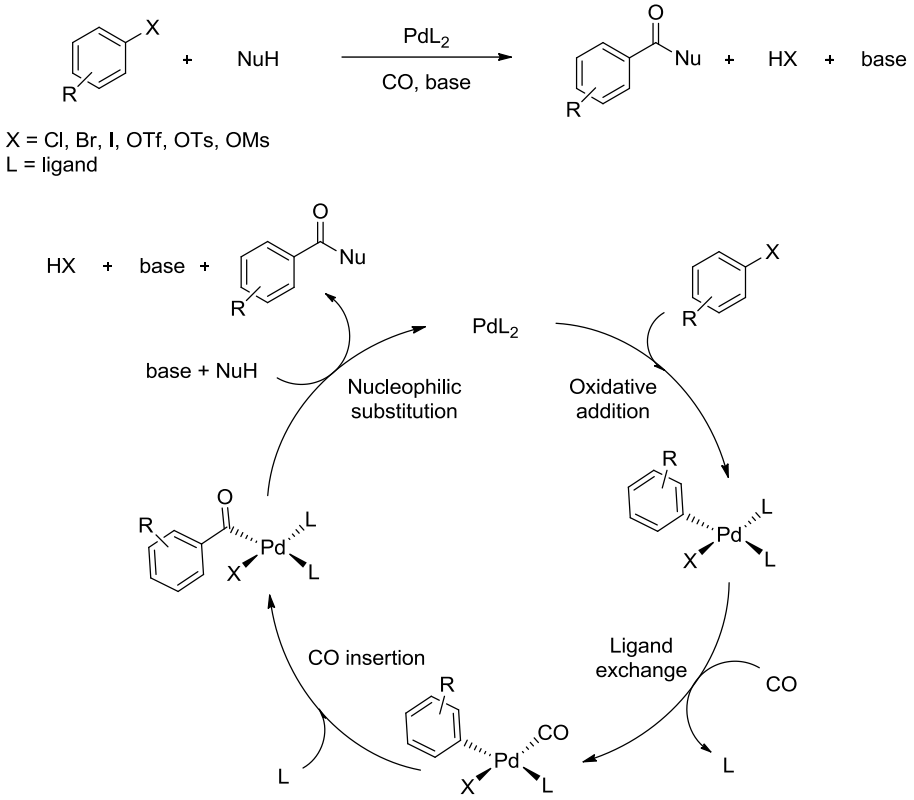

Scheme 36: General catalytic cycle for carbonylation mechanism.

Due to the low yields associated with the carbonylation of ortho-substituted substrates, such transformations are typically avoided. For example the simple compound, 2-chloro-6-methylbenzoic acid (**99**), has proved to be a challenging structure to synthesise on a large scale at high purity.[84b] This compound was required in multi-kilogram quantities for a programme at Roche which was previously obtained through three known routes (Scheme 37).[86] However, the Sandmeyer route is not suitable for large scale synthesis due to the low yields, tar formation, high dilution needed and the safety concerns associated with diazonium chemistry.[86a] The ortho-methylation *via* α-amino-alkoxide **101** route requires more than three equivalents of methyl iodide and butyllithium and the final product contains an impurity profile that was difficult to purify.[86b] Finally, the direct ortho-methylation method requires very low temperatures (-90 ºC) and is not very reproducible.[86c]

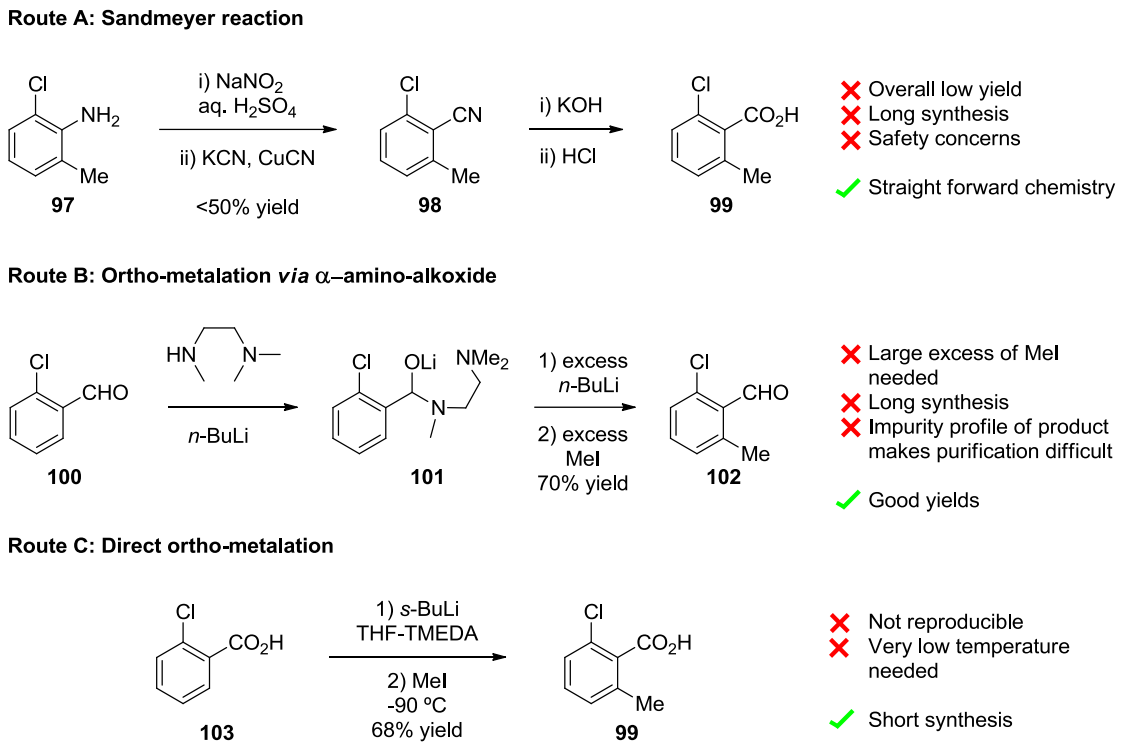

Scheme 37: Previously used routes for the synthesis of 2-chloro-6-methylbenzoic acid **99**.

The team at Roche decided to explore on two new routes targeting high quality **99** in an economical manner. Route one involved the use of direct nucleophilic aromatic substitution and the other made use of a carbonylation reaction (Scheme 38). The nucleophilic aromatic substitution route starts from the cheap starting material **104** giving the desired product in 81% overall yield with a very high purity. The second route, involving the carbonylation step on four *m*-chlorotoluene derivatives (**106a-d**), could not be directly executed as attempts to prepare the hydroxy-carbonylation with water as the nucleophile proved to be problematic, with the undesired 3-chlorotoluene obtained as the main product (50-80%). Also, the metalation of **106a** (*via* Grignard or lithiation) followed by trapping with CO_2 did not give any product, possibly due to benzyne formation (route E, Scheme 38). Product formation was only achieved when very high pressures of CO were used and water was replaced by MeOH to give the methylester which had to be hydrolysed in a separate step (route F, Scheme 38).

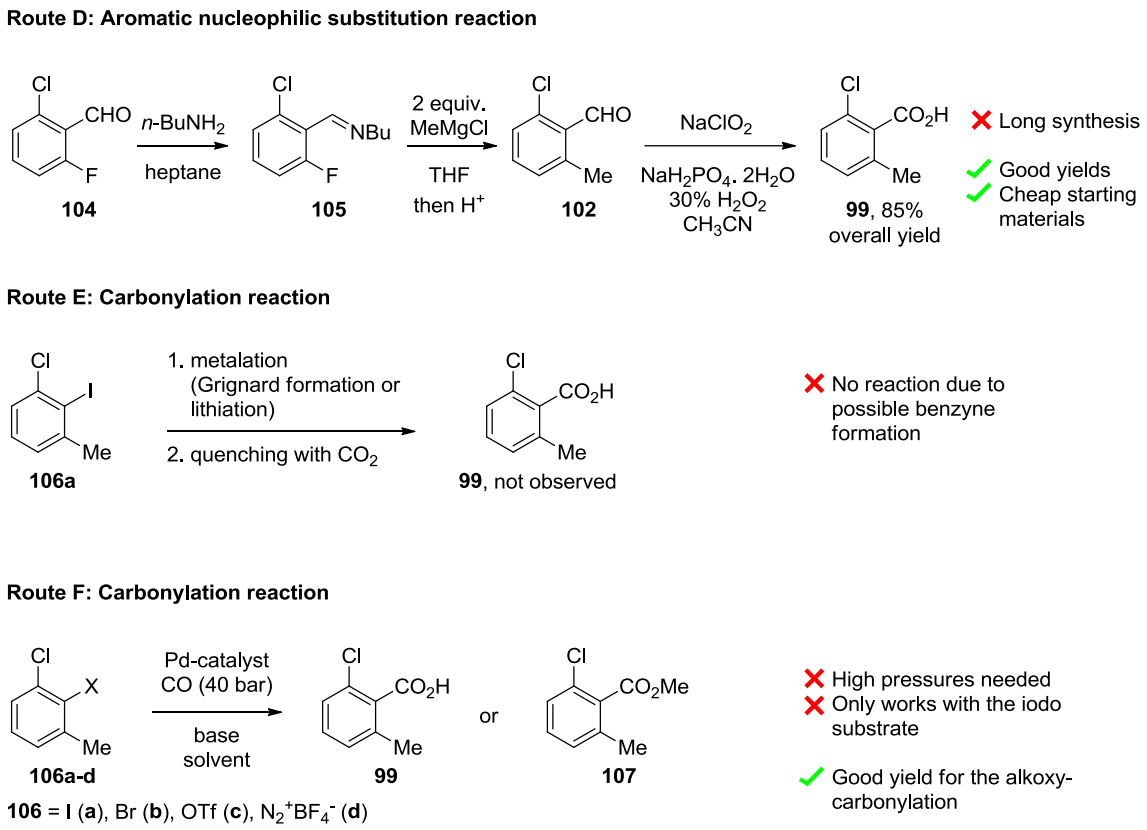

Scheme 38: Attempted routes for the synthesis of 2-chloro-6-methylbenzoic acid **99**.

In addition to the intermediate **99**, other important intermediates/products can be prepared using this method (carbonylation of ortho-substituted substrates). One such intermediate is 2,4,5-trifluorobenzoic acid **62** which serves as a starting material to several antibacterial drugs such as ciprofloxacin (Cipro™), norfloxacin (Noroxin™) and pefloxacin (Peflacine™).[51] A number of different approaches have been described for the synthesis of 2,4,5-trifluorobenzoic acid including the use of highly toxic CuCN,[87] $AlCl_3$-promoted Friedel-Craft acylation,[88] multi-step procedures including fluorination followed by decarboxylation[89] and metalation followed by carboxylation (Scheme 39).[51] The effort put into the syntheses of both 2-chloro-6-methylbenzoic acid and 2,4,5-trifluorobenzoic acid show the difficulty such a simple looking transformation can present and highlights the need for more research into a safe and scalable procedure for the carbonylation of ortho-substituted substrates, in particular when water is used as a nucleophile.

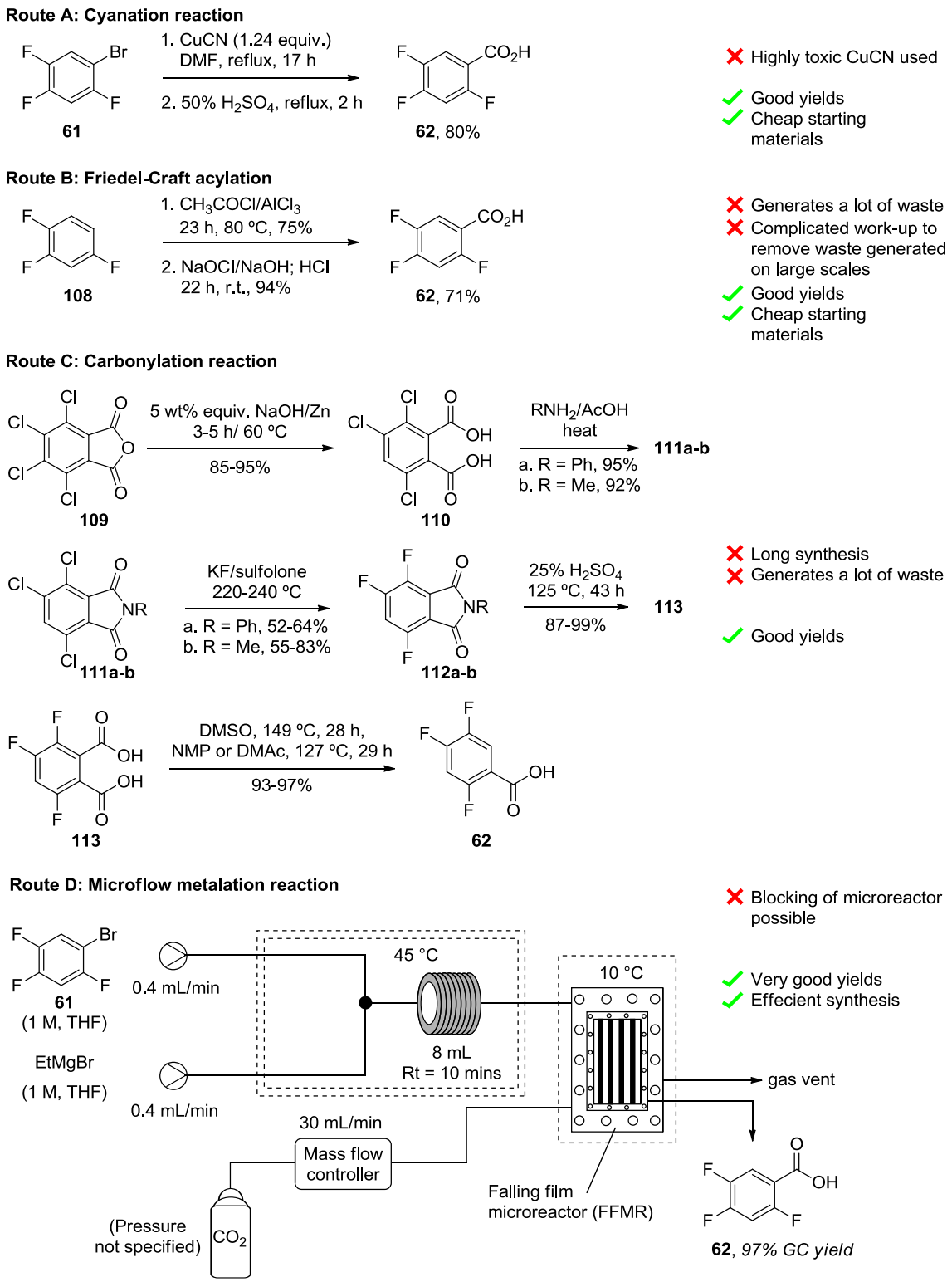

Scheme 39: Attempted routes for the synthesis of 2,4,5-trifluorobenzoic acid **62**.

2.1.2 Results

2.1.2.1 Flow hydroxy-carbonylation of ortho-substituted substrates

As part of a collaboration with Syngenta, an efficient carbonylation of ortho-substituted aromatic was required with specific interest in 2-chloro substituted aromatics. Similar to the above described 2,4,5-trifluorobenzoic acid (**62**) and 2-chloro-6-methylbenzoic acid (**99**), the carboxylic acid derivatives would be an ideal intermediate for several important agrochemicals. Unfortunately, using water as a nucleophile can be challenging due to its weaker nucleophilic nature when compared with alcohols, as illustrated through the synthesis of **99**.

The use of flow chemistry has already been shown to be beneficial for carbonylation reactions (See Section 1.1.4.1). For this reason we decided to investigate a flow protocol to provide a safer and scalable way of obtaining various ortho carbonylated products such as 2-chloro benzoic acids. Two types of reactors were considered for the carbonylation transformation, the reverse "tube-in-tube" reactor and a plug flow reactor. Iodobenzene (**1a**) was selected as a test substrate for evaluation (Scheme 40). The reverse "tube-in-tube" reactor[i] provided a more efficient means of delivering the CO gas to the liquid phase for carbonylation of **1a**. This was due to the higher surface area to volume ratio of CO gas provided by the "tube-in-tube" reactor, as described in section 1.1.3. The "tube-in-tube" reactor should deliver sufficient CO for coordination to the square planar aryl complex intermediate of ortho-substituted iodoarenes, in accordance with the standard associative mechanism explained above.

The gas-liquid unit was attached to a commercial flow system; a Vapourtec R2+ Series along with an R4 heating unit. It was decided that all the reactions would be conducted using 5 mol% of $Pd(OAc)_2$ and 10 mol% of the different phosphine ligands, which could be reduced further,[24b] this would allow for an efficient catalytic cycle and short reaction times in the region of two hours.[38]

[i] A commercially available reverse "tube-in-tube" reactor form Vapourtec was used throughout.

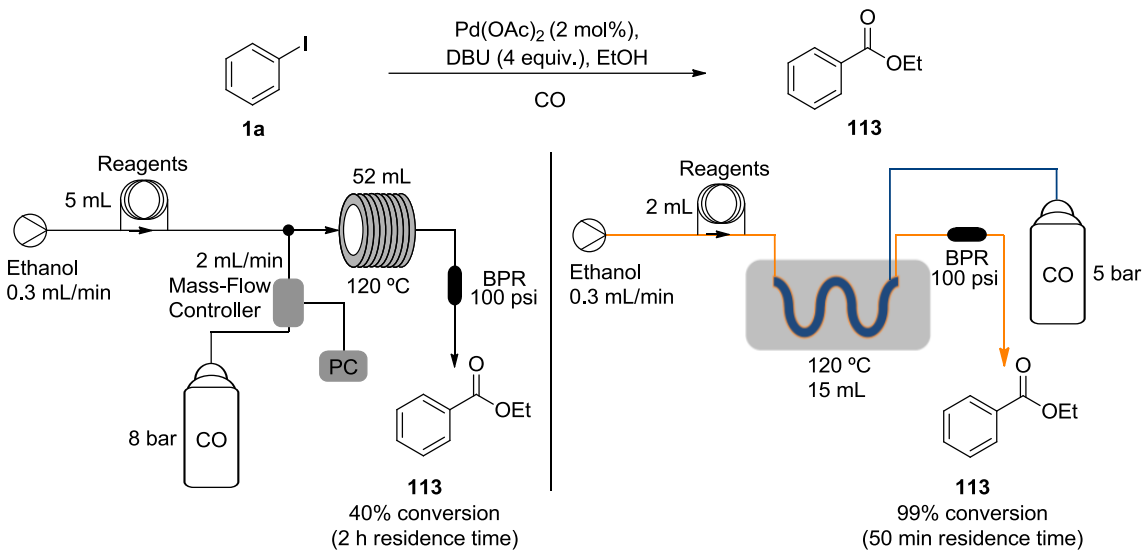

Scheme 40: Comparison of plug flow reactor carbonylation (left) and "tube-in-tube" reactor carbonylation (right).

2.1.2.2 Optimisation of the hydroxyl-carbonylation of ortho-substitution substrates in flow

As a test substrate, 2-chloro iodobenzene (**103**) was used for the initial screening to devise a set of general reaction conditions (Scheme 41). Five different phosphine ligands were tested, three of which were monodentate with a variable cone angle (**115-117**; 145-265°)[90] with the other two 1,4-*bis*(diphenylphosphino)butane (DPPB) and Xantphos (**118-119**, bite angles 98° and 111° respectively)[91] representing bidentate phosphine ligands (Figure 8).

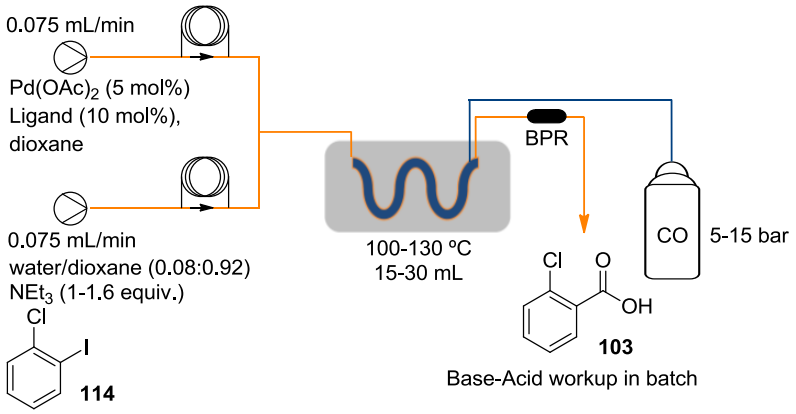

Scheme 41: Schematic diagram of the flow process for the carbonylation of ortho-substituted substrates.

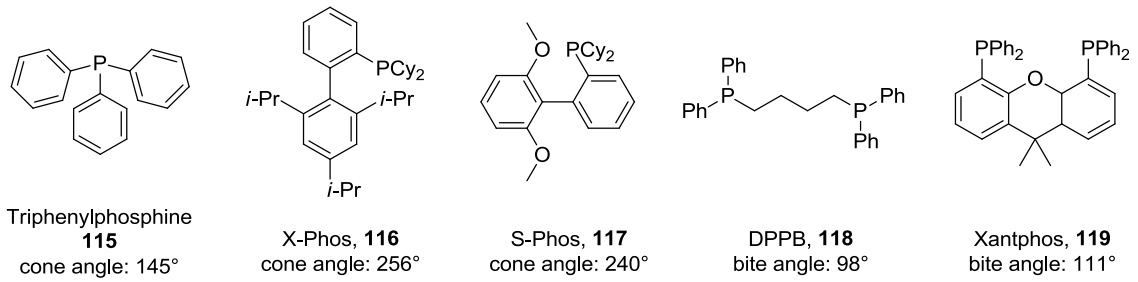

Figure 8: Phosphine ligands used for the carbonylation reaction.

Initially, using 5 bar of carbon monoxide and a temperature of 110 °C, the five ligands gave similar yields with DPPB (**118**) giving the highest yield and X-Phos (**116**) the lowest. However, the highest selectivity for the desired product was obtained with S-Phos (**117**) and triphenylphosphine (**115**) (Table 6, entries 2 and 5), with the difference between the conversion and the isolated yield due mainly to the formation of the dehalogenated product, chlorobenzene.

Table 6: Optimisation for the carbonylation of ortho-substituted substrates in flow.

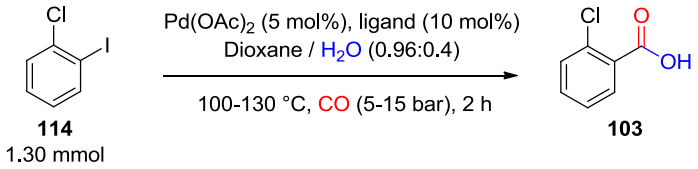

Entry	Ligand	Temperature (ºC)	CO pressure (bar)	Conversion (%)	Isolated Yield of 103 (%)
1	X-Phos	110	5	68	31
2	S-Phos	110	5	43	36
3	DPPB	110	5	90	38
4	Xantphos	110	5	57	36
5	PPh_3	110	5	44	36
6[a]	PPh_3	110	5	59	36
7[b]	PPh_3	110	5	80	33
8[c]	PPh_3	110	5	N/D	18
9	PPh_3	100	5	41	31
10	PPh_3	120	5	60	37
11	PPh_3	130	5	N/D	33
12[d]	PPh_3	110	10	67	46
13[d]	PPh_3	110	15	74	62
14[d,e]	PPh_3	110	15	N/D	31
15[f]	PPh_3	110	15	N/D	68
16[f,a]	PPh_3	110	15	99	90
17[f,b]	PPh_3	110	15	99	73

[a] 1.6 equiv. of base instead of 1.1 equiv. [b] 2.0 equiv. of base used. [c] 1.1 equiv. of DBU used instead of NEt_3. [d] 10 mL reactor was not "tube-in-tube". [e] 20 mol% DMF added. [f] 2 x 15 mL "tube-in-tube" reactors used.
N/D: not determined.

Changing the amount of triethylamine used to 1.6 equiv. and 2.0 equiv., did not significantly change the isolated yield of **103**. However, after changing to a stronger base such as DBU (pK_a in water at 25 ºC = 13.5)[92] the isolated yield dropped by half when compared to that obtained with 1.1 equiv. of triethylamine (Table 6, entry 8). A wider temperature range was then investigated utilising ligand **115** (Table 6, entries 9-11). However, only a small increase in the yield on going from 100 °C to 120 °C was achieved and a marginal decrease when the temperature was further raised to 130 °C. As there was no significant difference between 110 °C and 120 °C (Table 6, entries 5 and 10), the lower temperature was selected for the use in the next set of experiments. As anticipated, an increase in carbon monoxide pressure dramatically increased the product yield up to 62% (Table 6, entries 12-13). The addition of 20 mol% of dimethylformamide (DMF) as an additive did not improve the yield as suggested by its use in similar reactions in the literature.[35, 40] The effect of gas contact time was also evaluated by using two "tube-in-tube" reactors linked in series; this resulted in a modest improvement in yield, indicating that the carbon monoxide concentration was still limited (Table 6, entry 15). A further increase in product yield was observed when a larger excess of the triethylamine base (1.6 equiv.) was used (Table 6, entry 16), but the isolated yield dropped with a higher ratio of triethylamine (2.0 equiv.) (Table 6, entry 17). This indicated that the reaction was being inhibited by the low pH generated at higher conversions when insufficient base was present to neutralise the carboxylic acid being formed. The requirement for a higher excess of base during initial screening (Table 6, entries 6-7) had been masked due to the initial low conversions achieved.

For comparison, two additional batch carbonylation reactions were performed. The first of these batch reactions (conducted in a conventional lab) was set up using triphenylphosphine as the ligand under refluxing conditions with a double-walled balloon used to deliver the carbon monoxide (Scheme 42). This would constitute a normal set up used by many laboratory chemists when reactions involving gases are attempted if no specialised equipment is available. For further evaluation, one reaction was quenched after 2 hours and after purification it yielded 5% of product **103**, while an additional reaction was quenched after 24 h yielding 9% of purified **103**. The difference in the yields obtained in batch when compared to the reactions conducted in flow, most probably arises from the fact that not enough carbon monoxide is being delivered to the reaction mixture.

The dehalogenation pathway is then preferred, yielding chlorobenzene as the main product (9% of **103** and 65% chlorobenzene).

The second batch reaction, conducted in the departmental high pressure lab (HPL), was set up in a Parr autoclave using carbon monoxide at 15 bar and 110 °C for 2 hours. After purification, a yield of 87% for product **103** was obtained. This compares well with the flow protocol yield, however, the reaction "processing" time is in reality much longer due to the long cooling and heating times (4 h 15 min "processing" time, see experimental section for more details). Also, the time required due to the extra precaution measures needed when using high pressure facilities, means that the turnaround time is much longer. This makes the flow reactor more efficient in terms of processing time compared to the batch reactions conducted in the HPL. Additionally, the added safety and potential for scale up associated with the flow reactor makes it highly favourable.

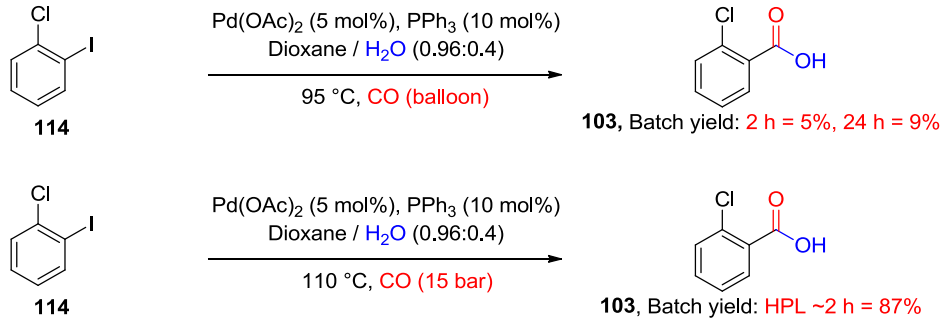

Scheme 42: The batch carbonylation of 2-chloro-iodobenzene in conventional lab conditions (top) and using a Parr autoclave in high pressure lab (bottom).

Having identified a set of standard conditions for this process, a number of additional substrates were assessed to determine the generality of the flow reaction. Substrates **122** and **128** were synthesised through known literature procedures (Scheme 43). Substrate **122** was obtained through the sodium borohydride reduction of **120** followed by metalation with iodoethane to give **122**. Substrate **128** was obtained from the formation of imine **124** followed by its dipolar-cycloaddition with *tert*-butyl methacrylate (**125**) to give the pyrrolidine **126**. Acylation of **126** with pivolyl chloride (**127**) gave substrate **128** as a racemate with the indicated relative stereochemistry.

A) Synthesis of 1-bromo-4-(ethoxymethyl)-2-iodobenzene 122

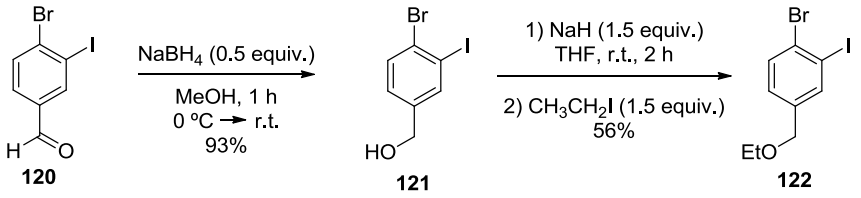

B) Synthesis of pyrrolidine 128

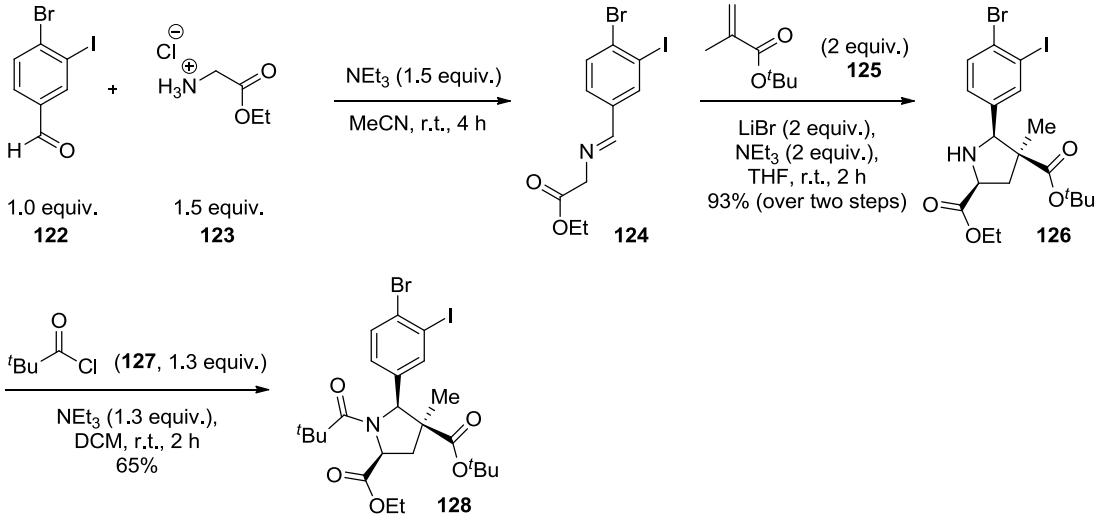

Scheme 43: Synthesis of substrates **122** and **128**.

2.1.2.3 Library formation

No significant change to the yield was observed upon altering the ortho-substituent to a bromo, fluoro or trifluoromethyl group. However, a slight decrease occurred with the bromo and trifluoromethyl groups due to their larger sizes (Scheme 44, **129**-**131**). A more pronounced decrease in yield was obtained for **132** and **133** (Scheme 44, 63% and 60% respectively) probably due to the larger size associated with these groups as well as electronic effects. Indeed, the more electron withdrawing trifluoromethyl group of **131** gave a better yield (71% yield) than both **132** and **133**. For comparisons of the sizes of the ortho-substituents used, A-values can be used as a guide (Cl: 0.43 kcal/mol, Br: 0.38 kcal/mol, F: 0.15 kcal/mol, OMe: 0.60 kcal/mol, CF_3: 2.10 kcal/mol and Me: 1.70 kcal/mol).[93]

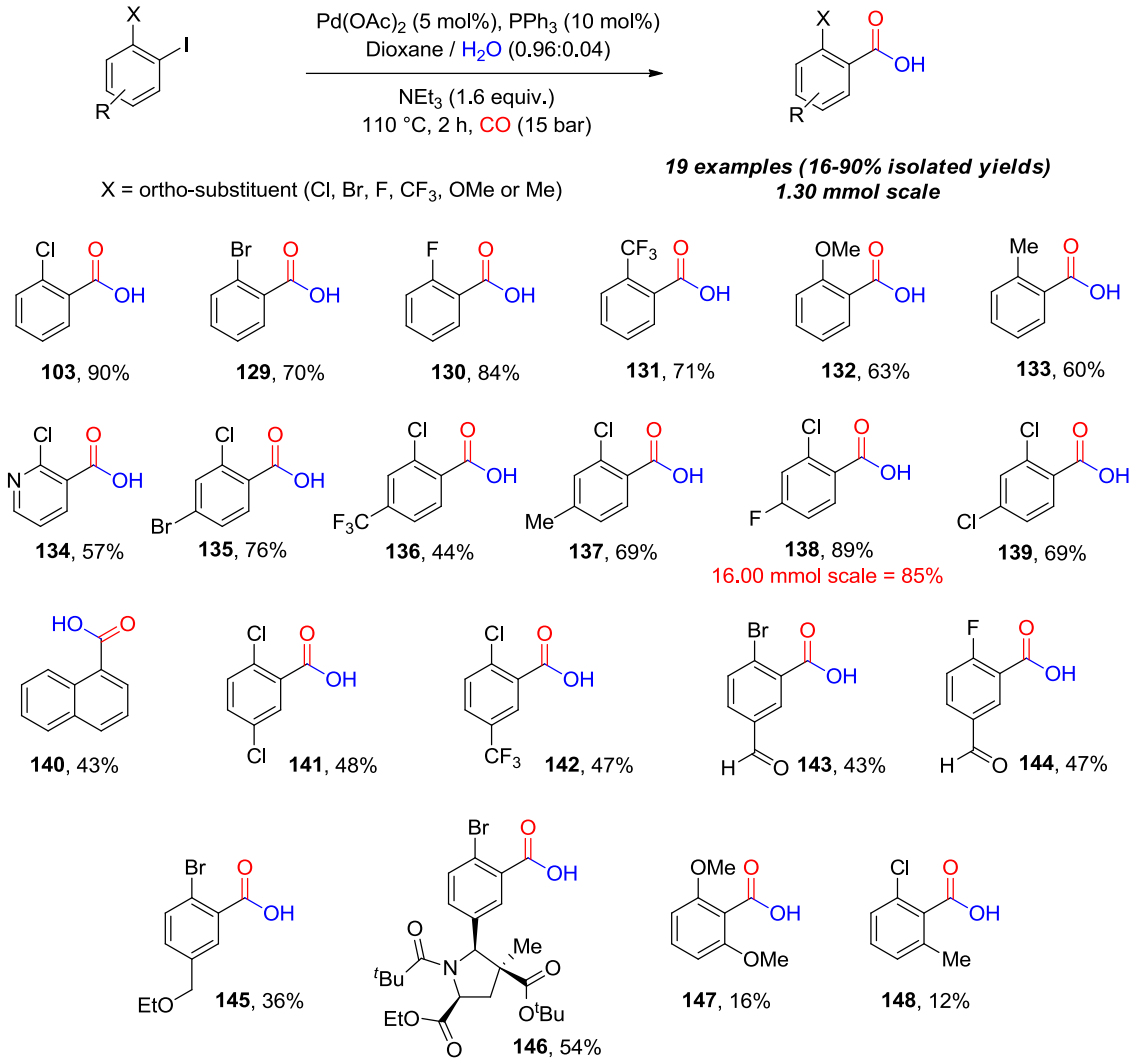

Scheme 44: Structures of ortho-substituted carboxylic acids prepared *via* a continuous flow hydroxy-carbonylation method.

Using pyridine as a heteroaromatic substrate also gave an acceptable yield of **134** but lower than the phenyl equivalent (**103**). Substitution at the 4-position of the aryl gave moderate to good yields (Scheme 44, **135-139**) with weakly electron withdrawing substituents or electron donating groups giving better yields (Scheme 44, compounds **135**, **137-139**) than the more electro-withdrawing CF_3 group (Scheme 44, compound **136**). In the case of **140** the attached aromatic ring introduces both the ortho substituted sterics and the electronic effects from the additional aromatic ring attached. For comparison 2-iodonaphthalene (**149**) was carboxylated under the same conditions to give 2-naphthoic acid (**150**) showing that reducing the steric encumbrance at the ortho position improves the yield by 10% for this substrate (Scheme 45).

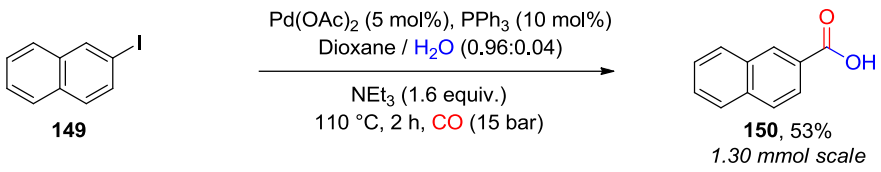

Scheme 45: Flow carbonylation of 2-iodonaphtalene.

Moderate yields were obtained with 5-substituted substrates (Scheme 44, compounds **141-146**). Both electron withdrawing groups (Scheme 44, compounds **141-144**) and electron donating groups gave similar yields (Scheme 44, compounds **145-146**) indicating that inductive effects were not affecting the yield. Comparing the yield obtained for **145-146** also indicates that sterics at the 5-position do not have an influence including the large group at the 5-position of substrate **146** (see X-ray structure of substrate **128**, Figure 9).

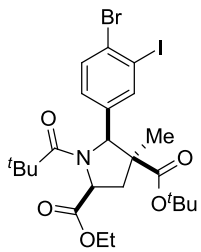

128

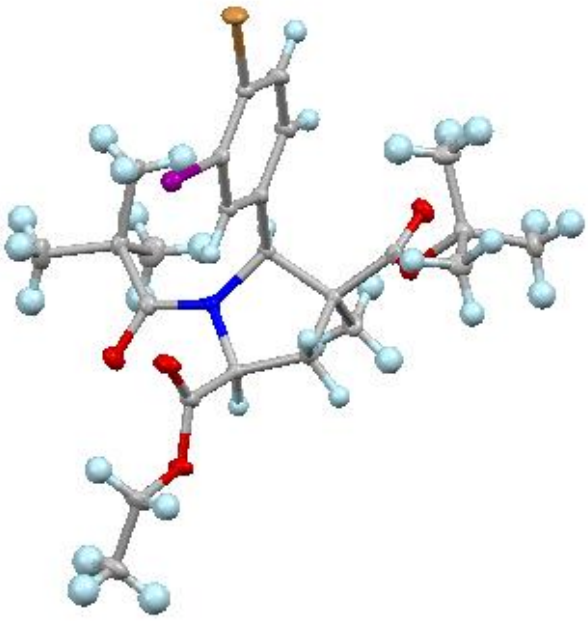

X-ray structure

Figure 9: X-ray structure of substrate **128**.

The lowest yields of the array were obtained for compounds **147** and **148**, demonstrating the importance of sterics and electronics adjacent to the leaving group. In both cases, the carbon monoxide insertion is assumed to be slow as both axial positions of the aryl complex would be hindered, meaning the competing proton-dehalogenation pathway becomes preferred, giving 1,3-dimethoxybenzene as the main product, which was isolated in 31% yield in the case of **147** and 3-chlorotoluene in the case of **148** which was isolated in 52% yield (Scheme 44).

To exemplify the scalability of the reaction conditions, the synthesis of **138** was repeated at 16 mmol scale, a factor of twelve times the original 1.3 mmol test scale (Scheme 46). The yield obtained for the larger scale was 85% which is consistent with the original 89% obtained at the 1.30 mmol scale, indicating that the processes is robust and reliable delivering 1.19 g h^{-1} of **138** at 85% isolated yield.

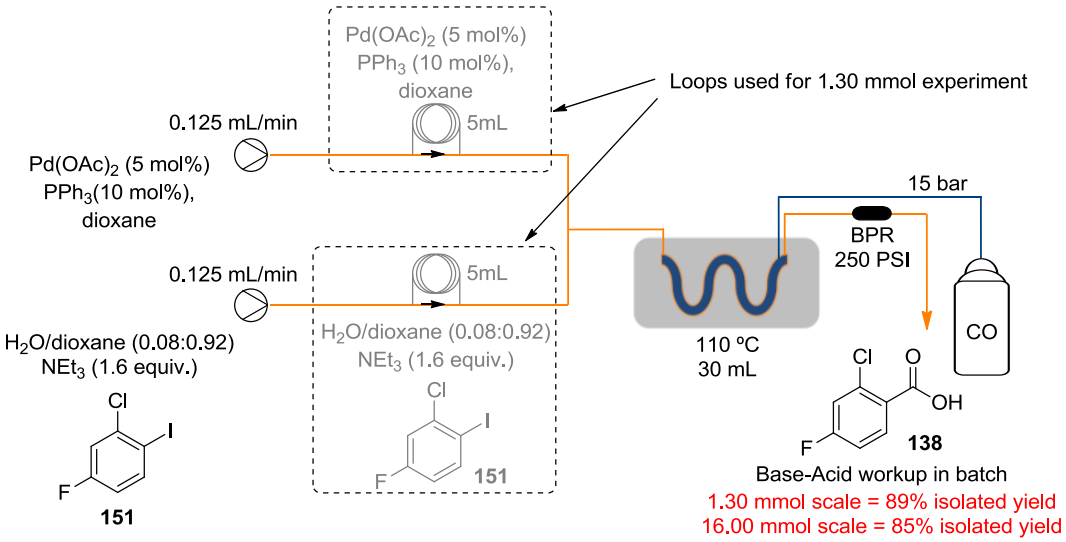

Scheme 46: Scale up synthesis of 2-chloro-4-fluorobenzoic acid (**138**).

2.1.2.2 Synthesis of 2-(methylthio)-4-(trifluoromethyl)benzoic acid intermediate

The synthesis of a range of 2,4-disubstituted aromatic amides was the focus of an extended evaluation being explored by our collaborative partner, Syngenta. This array relates to a biologically active set of 2-cyano-1,3-diones, possessing a 2-(methylthio)-4-(trifluoromethyl)benzene scaffold, that protect maize as a surface active herbicide.[94] Prior to this work, researchers at Syngenta attempted to use a CO surrogate as part of a Heck-aminocarbonylation reaction from the starting material **152** for their synthesis (Scheme 47).

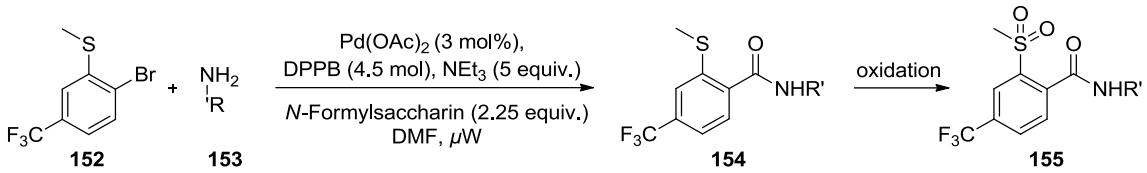

Scheme 47: Initial synthetic approach of 2,4-disubstituted aromatic amides.

The process involved manually loading the starting material **152** in a 2-5 mL microwave tube, then carefully layering DMF on top of the starting material making sure the two liquids did not mix. This was followed by the careful addition of palladium acetate, 1,4-*bis*(diphenylphosphino)butane (DPPB), *N*-formylsaccharin and the required amine (**153**). The vial would then be quickly sealed to avoid loss of CO. The need for carefully layering of the different liquids was to prevent premature CO release from the *N*-formylsaccharin CO surrogate. In the original publication, Mannabe reported that the *in situ* formation of CO ensues in a few min.[6] The reaction would then be heated using a microwave for the appropriate time and worked up to obtain the desired amides (**155**). As a large set of amides were needed and therefore an automated system would ideally be used (Chemspeed® Technologies). However, automation was not possible here due to the careful manual addition of the different components. Additionally, the reactions gave very low yields (not specified by the company). A more efficient approach was thus needed for the amide formation.

In an effort to find an alternative, efficient synthetic route for this amide collection, we decided to avoid the use of carbon monoxide in the amide formation step. Instead, it was decided that the benzoic acid intermediate **157** would be synthesised and subjected to thioether group oxidation to give the air stable compound **156**. This intermediate could then be fed into an automated system (such as the Chemspeed® Technologies used at Syngenta) to form the amides needed in a fast and efficient way (Scheme 48).

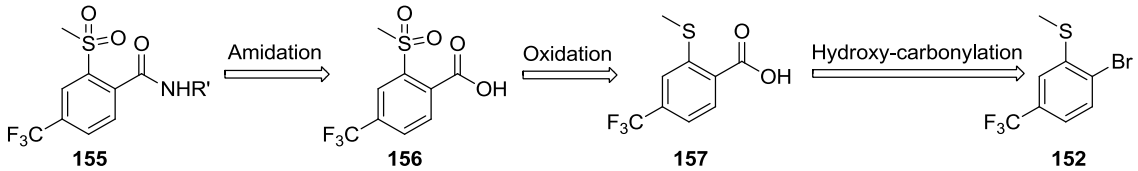

Scheme 48: Retrosynthetic approach for the synthesis of the amide library.

Using the optimised conditions for the hydroxy-carbonylation of ortho-substituted iodo arenes in flow (Table 6), **152** did not yield any of the desired product **157** (Scheme 49). This was ascribed to a slow rate of the oxidative addition as observed with bromo arenes

when compared to the iodo arenes. In a second flow experiment, MeOH was used as the solvent and Xantphos (**119**) as the ligand, with the methyl ester **158** obtained in 22% yield (Scheme 49). The use of Xantphos as the ligand increases the rate of the oxidative addition while the use of MeOH as the nucleophile increases the rate of the reductive elimination step, making the overall catalytic cycle more efficient. However, as both the direct hydroxy-carbonylation and the more efficient alkoxy-carbonylation did not give the desired product in a high enough yield, other approaches were considered.

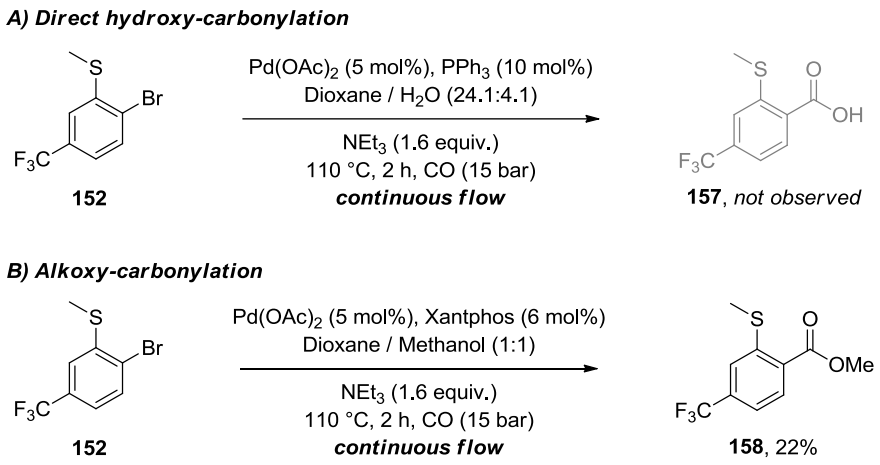

Scheme 49: Direct hydroxy-carbonylation of **152** (top) and alkoxy-carbonylation of **152** (bottom)

A metalation of the bromoarene **152** followed by trapping with carbon dioxide and a subsequent acid quench, was also explored as an alternative route (Scheme 50).

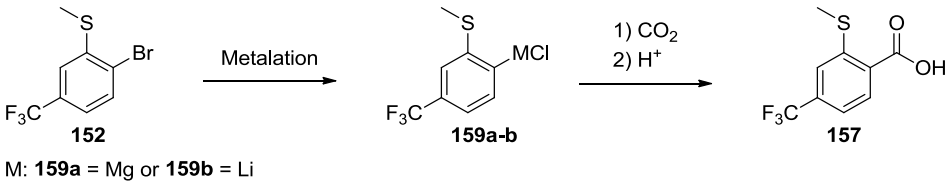

Scheme 50: Metalation of **152** followed by trapping with carbon dioxide and a subsequent acid quench to obtain **157**.

Isopropylmagnesium chloride lithium chloride complex solution (so called "turbo-Grignard") was used to form the exchanged Grignard salt **159a** which was then trapped with carbon dioxide followed by an acid quench. In batch, the first step required 2 hours mixing in THF prior to the addition of carbon dioxide and quenching with a dilute solution (1 M) of HCl. This gave the product in 34% overall yield (Scheme 51).

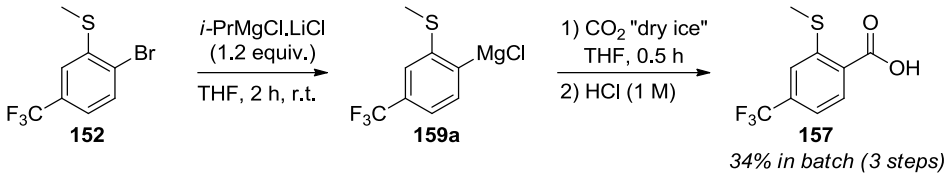

Scheme 51: Formation of target intermediate **157** through batch formation of Grignard salt.

In an effort to transfer the three step reaction to a continuous flow process, bromobenzene (**160**) was used as a test substrate with the "turbo-Grignard" to form the corresponding magnesium intermediate. Initially the carbon dioxide was loaded through a conventional "tube-in-tube" reactor as shown in Table 7. The metalation step was attempted at -40 ºC, -5 ºC and room temperature but none of these conditions gave any conversion (Table 7). Heating to 70 ºC gave 10% yield of the desired product **68**, along with some additional unidentified products also being observed.

Table 7: Grignard formation of bromobenzene followed by trapping of carbon dioxide and acid quench in collecting flask.

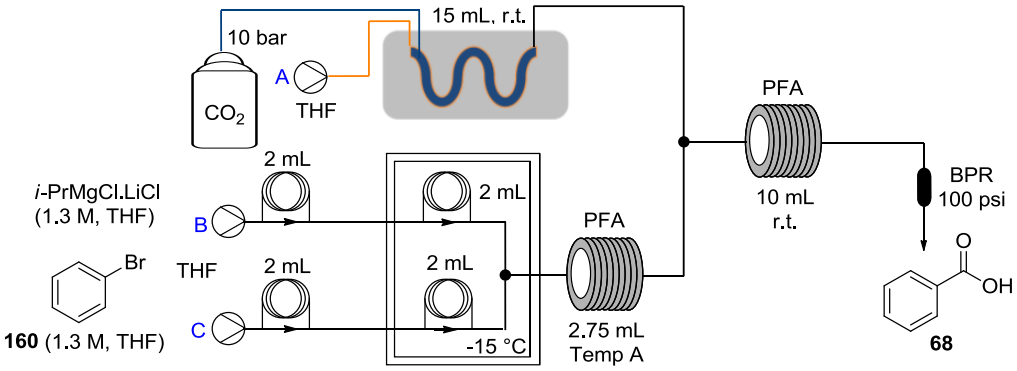

Entry	Pump A (mL/min)	Pump B (mL/min)	Pump C (mL/min)	Temperature (°C)	Yield (%)
1	0.5	0.5	0.5	-40	0
2	0.2	0.2	0.4	-5	0
3	0.3	0.3	0.6	18	0
4	0.3	0.3	0.6	70	10

Altering the delivery of the carbon dioxide loading to a reverse "tube-in-tube" reactor design in order to increase the carbon dioxide concentration and ensure it was not limiting, did not change the outcome, with still only 10% yield being obtained (Scheme 52). The same set up was eventually also used with **152** as a substrate but gave yields of **157** similar to those obtained for the test compound (8% yield, Scheme 52).

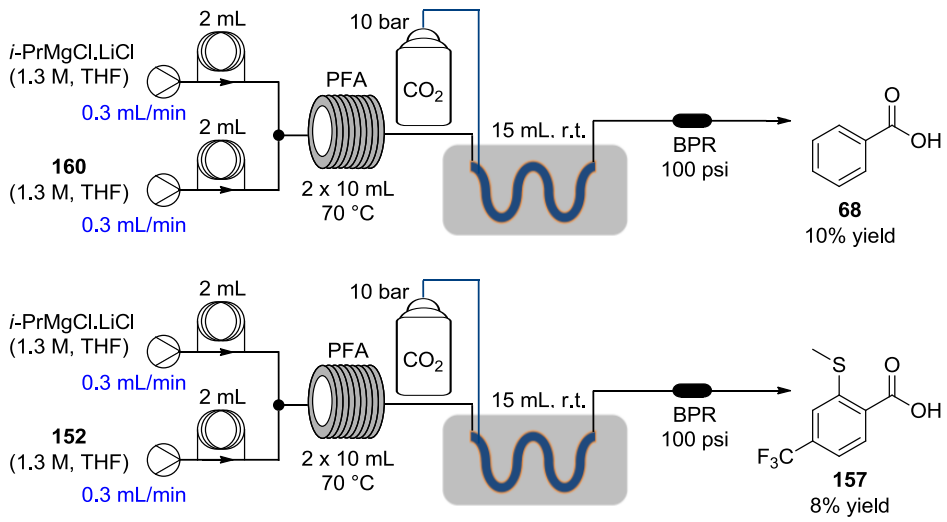

Scheme 52: Grignard hydroxy-carboxylation of bromobenzene (top) and **152** (bottom) using the reverse "tube-in-tube" reactor (Bottom).

Inspired by the work of the Yoshida group, the use of a lithium-halogen exchange process was explored.[47] It was possible to lithiate **152** using *n*-BuLi to form **158b**, which was then trapped by carbon dioxide (dry ice) in batch followed by acidification using 1 M HCl solution to give **157** in 83% yield. A flow protocol was also attempted but a lower yield of 60% was obtained (Scheme 53). The lower yield is probably due to the specific reactor set up used which could be improved by using mixing chips for the lithiation step. Additionally, due to solubility issues, a different concentration of *n*-BuLi in hexane had to be used in the flow procedure, which could also account for the lower yield obtained. Changing to an annular flow reactor, it was observed that the T-piece where the CO_2 gas was introduced, repeatedly blocked, making this process unreliable (Scheme 53). The batch process was thus used for this step.

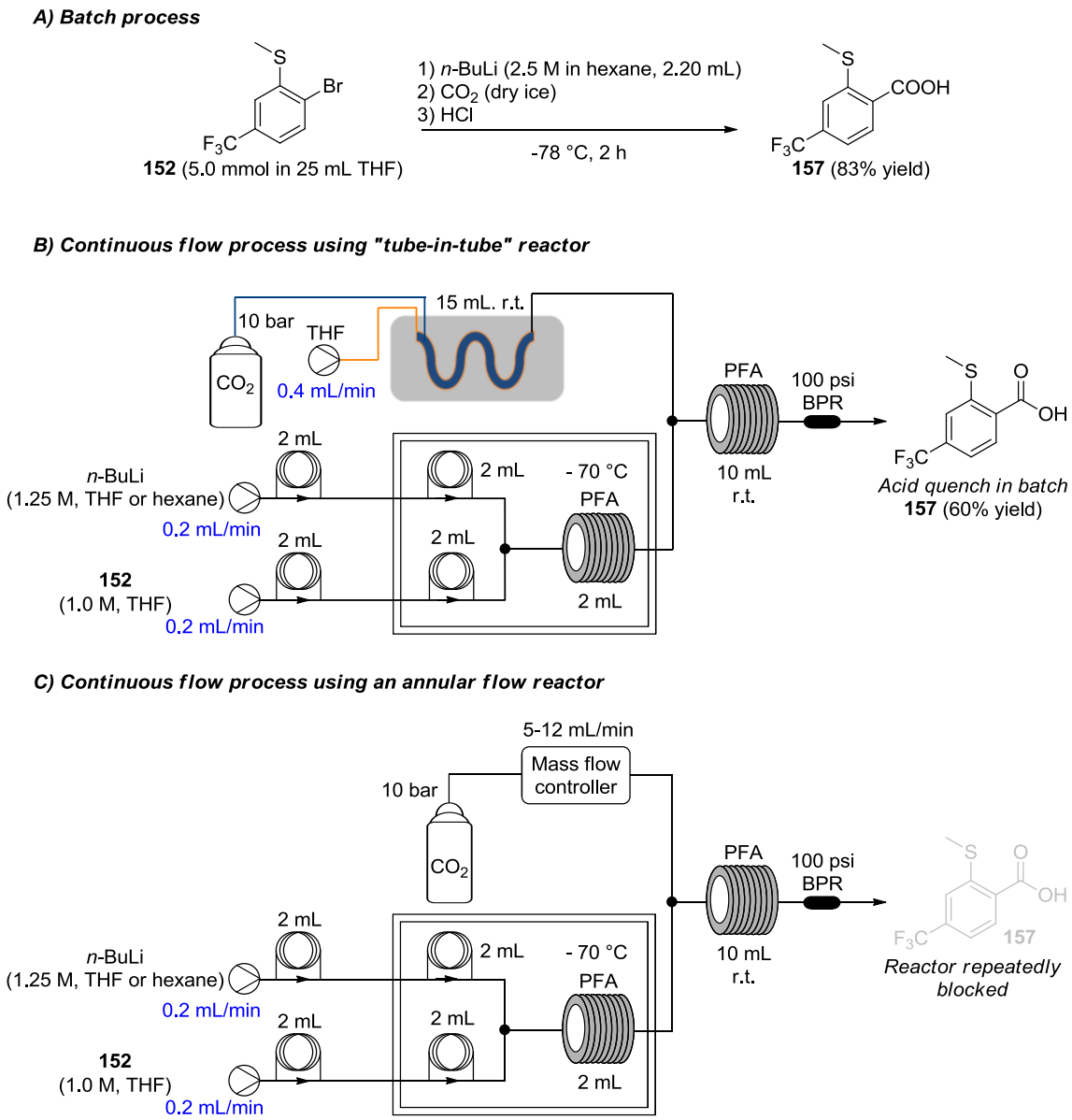

Scheme 53: Lithiation of **152** followed by hydroxy-carbonylation in batch (top) and in continuous flow (bottom).

The subsequent oxidation of the thioether product **157** to the desired sulfone **156** has been reported for similar thioether products using different oxidants such as Oxone®,[95] hydrogen peroxide[94] and HOF-MeCN solution.[96] Using Oxone®, the sulfoxide **161** was obtained as the main product (71%) with only minor amounts (5%) of the desired sulfone **156** (Scheme 54). The work up (involving dilution with brine and extracting with EtOAc) of this reaction was also prone to forming persistent emulsions. Using hydrogen peroxide (27%) with acetic anhydride (Ac_2O) in acetic acid, formed the desired sulfone **156** in 63% yield with no sulfoxide intermediate present (Scheme 54).

Using sub-stoichiometric amounts of sulfonic acid bound reagent (QP-SA) as an acid catalyst with hydrogen peroxide in acetic acid gave 55% yield in batch and when the

same method was used in flow (using a packed column of QP-SA), an 85% yield was realised (Scheme 54). The improved yields obtained in flow being most likely due to the "local" excess of acid catalyst. As the acid resin was packed in a column through which the substrates would flow, the dissolved substrates are always in contact with a large excess of acid at any one time, which increases the rate of reaction. The use of a variable back pressure regulator (BPR), was employed as some precipitate was formed during the reaction and this type of BPR was resistant to small amounts of precipitates avoiding potential blockages.

The use of HOF-MeCN as an oxidant gave a 90% yield in batch (Scheme 54), however as HOF-MeCN oxidation is normally very fast (seconds),[96] the flow protocol was not attempted as large amounts of substrate would be needed to operate the available flow fluorination set up in the Chemistry Department (Durham).

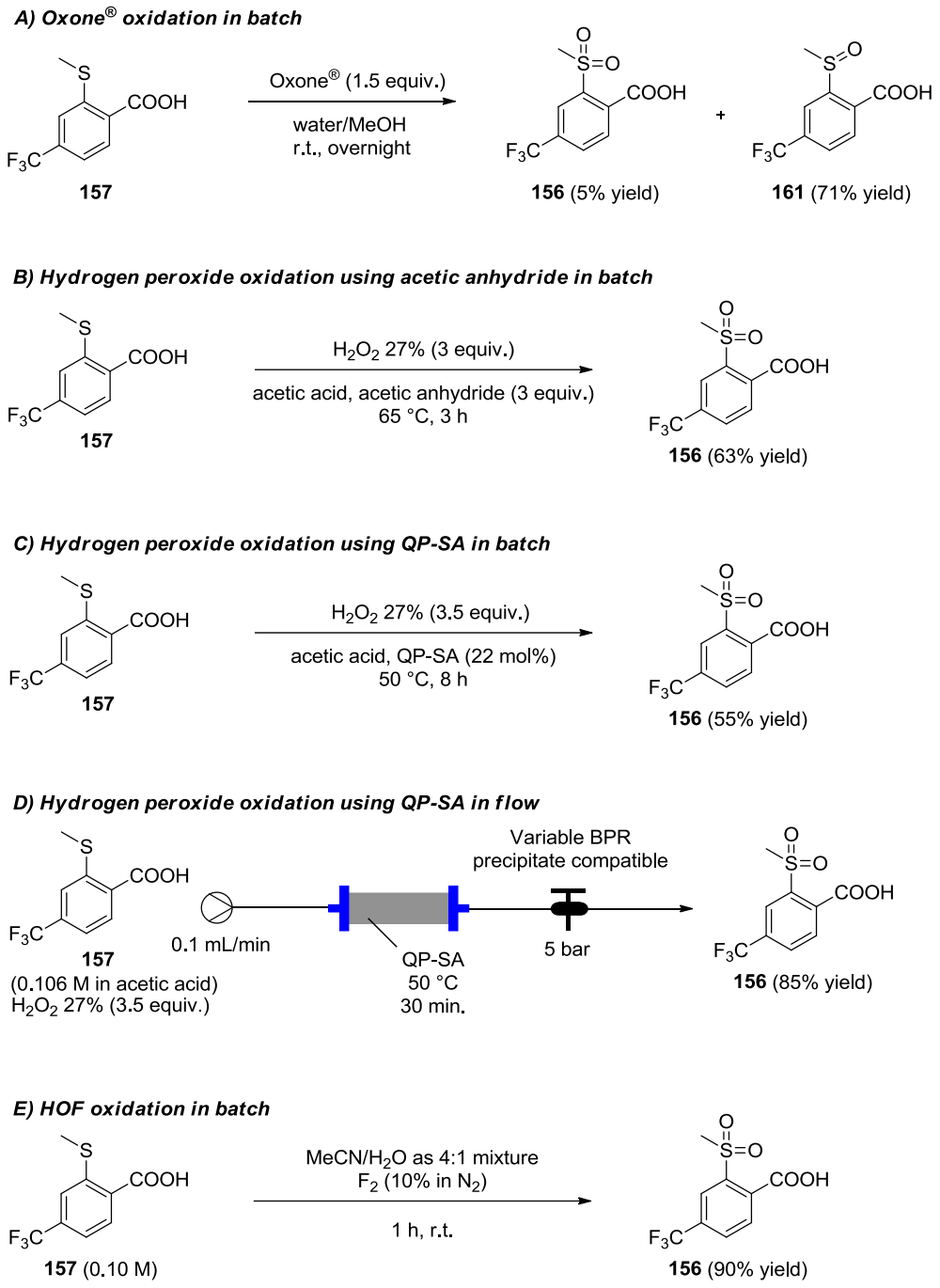

Scheme 54: Different methods explored for the oxidation of **157** to obtain the desired sulfone **156**.

Having explored a number of different ways to form the intermediate **157**, the batch lithiation procedure was the most promising for this step (Scheme 53) followed by either hydrogen peroxide oxidation with acetic anhydride in batch or hydrogen peroxide with QP-SA in flow. The latter, although it gave better yields, needed careful monitoring to avoid blockage of the system. The batch sequence was used to produce 20 g of the

intermediate **156** as an air stable solid to be used by Syngenta for the array generation through amide synthesis using the Chemspeed® Technologies equipment (Scheme 55).

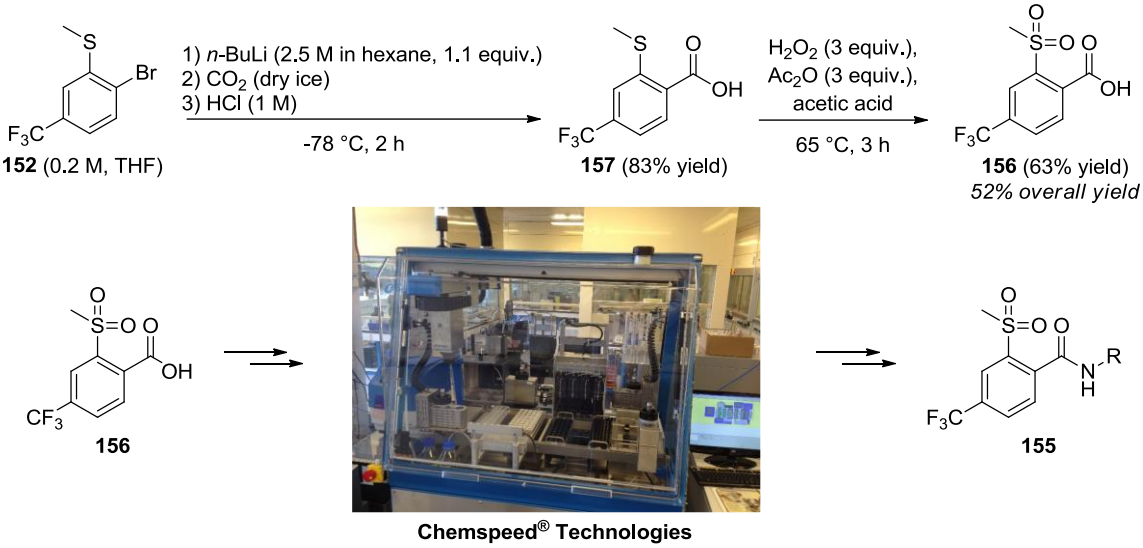

Scheme 55: Synthesis of **159** intermediate in batch.

There are several amide coupling strategies that are routinely used,[97] such as the use of 1,1′-carbonyldiimidazole (CDI),[98] diphenylphosphonic azide (DPPA)[99] and dicyclohexyl carbodiimide (DCC)[100] as coupling agents (Scheme 56). A one-pot procedure using CDI as a coupling reagent is normally preferred for scale up reactions. Initially the acyl carboxy imidazole (**166**) and imidazole (**165**) are formed which readily react together yielding the activated species as the acylimidazole **167** (Scheme 56). Upon complete conversion to the acylimidazole, the amine is added to give the amide product. As this reaction generates imidazole *in situ*, no additional base is needed meaning this technique is also compatible with HCl salts of the amines. The use of DPPA involves a convenient one-pot process which normally is not used for scale up due to possible formation of the highly toxic hydrazoic acid. DCC is used to form the activated intermediate (**174**) which reacts with an amine to form the amide product (**168**) and urea by-product (**175**) in a mild and efficient way. The main side reaction is that where the activated intermediate reacts with another carboxylate forming the anhydride (**176**) which then reacts with an amine to form the amide product and urea by-product (**175**). The milder version of this coupling reaction involves the use of two equivalents of the carboxylic acid for every DCC which unfortunately favours the anhydride formation and wastes half the carboxylic acid starting material proving problematic if the carboxylic acid is a valuable material.

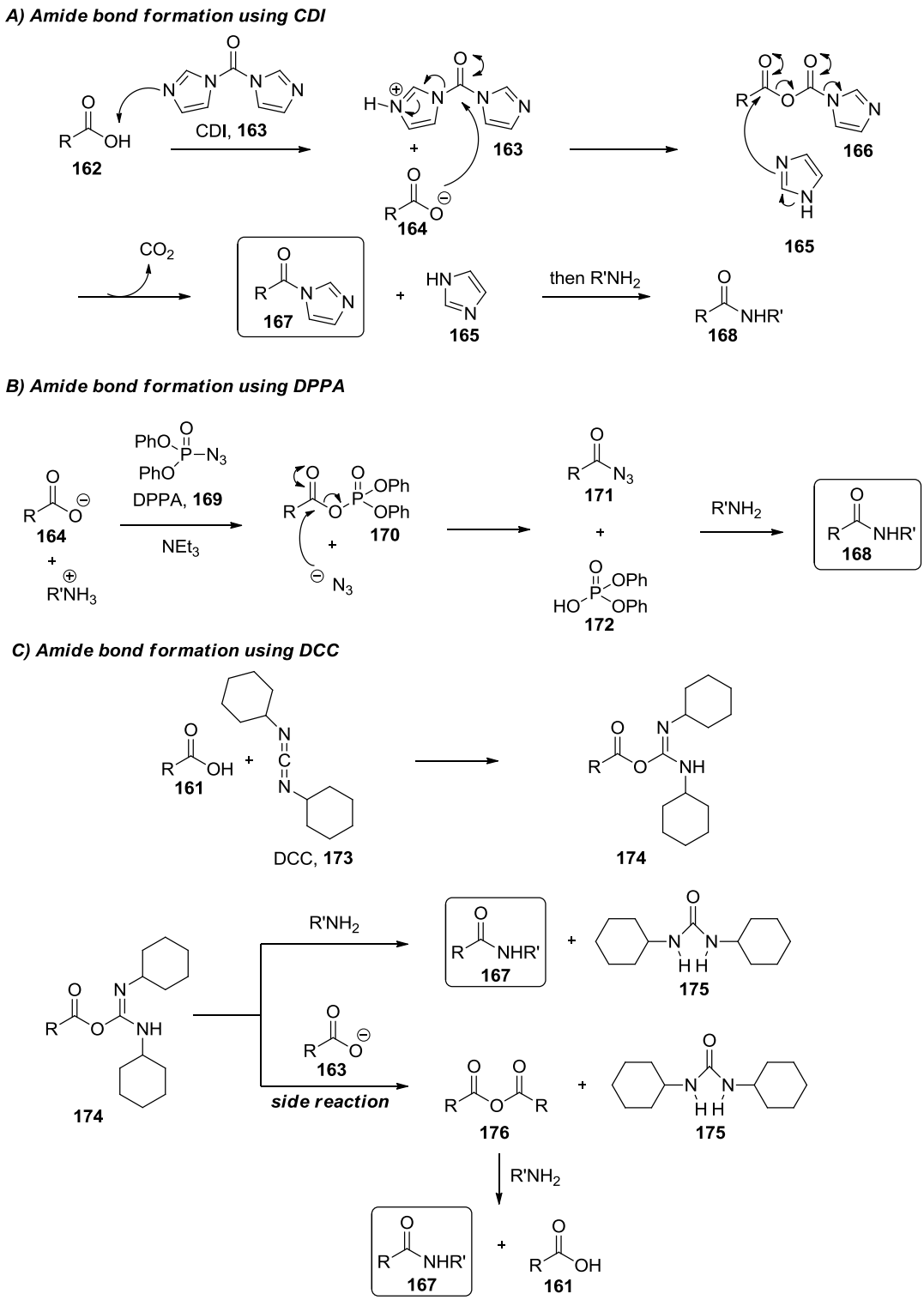

Scheme 56: Amide formation through different coupling routes.

2.1.3 Conclusions

The use of flow chemistry as a safe and scalable way of delivering carbon monoxide was demonstrated to be useful for the carbonylation of ortho-substituted substrates. Furthermore, the use of water as a nucleophile to directly obtain the carboxylic acid was also achieved, giving a number of different ortho-substituted carboxylic acids. Comparison of **140** with **150** also showed that the steric encumbrance on the ortho position has an effect on the yield even when other electronic effects are in place such as those coming from the additional aromatic ring attached. A scale-up of the reaction conditions was performed providing comparable yields to those obtained from the initial smaller test scale. This method could thus be an efficient and scalable approach to synthesising important intermediates containing ortho-substituted carboxylic acids. Two batch processes were also performed as a direct comparison with the flow method developed. It was clear that the carbonylation reaction in a round bottom flask equipped with a CO balloon is much less effective than the flow carbonylation due to the mass transfer limitations of CO. On the other hand, the batch carbonylation performed in the Parr reactor gave a similar yield to flow. The Parr reactor, however, has to be used in dedicated high pressure facilitates due to additional safety requirements. Furthermore, the Parr reactor carbonylation has a longer processing time due to the extra time required to reach the necessary temperature and the additional long cooling time after the reaction has finished. Limitations in terms of the size of the reaction vessel can also become an issue at large scale. One advantage with regards to carrying out carbonylations in Parr reactors is that, at the present time, they are simply more frequently encountered in a University environment than the “tube-in-tube” reactor.

A number of different approaches have been studied for the synthesis the air stable intermediate **157** as an alternative to the direct amide synthesis using a CO surrogate. Of the different approaches trialled, the best results were achieved through the lithiation of the starting material (**152**) followed by carbon dioxide trapping and subsequently quenching with dilute aqueous acid. The thioether intermediate (**157**) was then oxidised using hydrogen peroxide with acetic anhydride in acetic acid to give the final intermediate **156** in an overall isolated yield of 52%. The different flow procedures developed were not as efficient as the batch procedures. For the first step (hydroxy-carbonylation through a lithiation step and subsequent CO_2 trapping), the batch reaction gave superior yields to the flow process. As only small quantities of the material were needed the batch reaction

was preferred. If larger quantitates had been required, the batch process would suffer from scalability issues, however, for larger quantities the transformation itself would probably be avoided due to the low temperatures needed. The oxidation of the thioether intermediate worked best in flow although it was prone to precipitation, which if left unsupervised, could lead to blockage of the back pressure regulator. Better engineering of the flow system should make this process more favourable than the batch oxidation, however, the batch process was again chosen as it was more viable with regards to producing the required amount of material under the given time constraints.

2.2 Catalytic Chan-Lam Coupling Reactions in a Continuous Flow Reactor Using the "Tube-in-Tube" Approach to Deliver the Oxygen

2.2.1 Introduction

The functionalisation of aromatic and aliphatic amines has received considerable attention due to the number of biologically active compounds represented by these classes. For this reason many different synthetic methods for C−N bond formation have been developed over the years.

In 1901 Fritz Ullmann observed the Cu catalysed biaryl formation through coupling of two aryl halides, this is now referred to as the "classical Ullmann reaction".[101] The generally accepted mechanism for this transformation involves the formation of an organocuprate intermediate (**177**) from the aryl halide followed by its reaction with a second aryl halide through an oxidative addition. A reductive elimination process yields the biaryl product (**179**, Scheme 57).

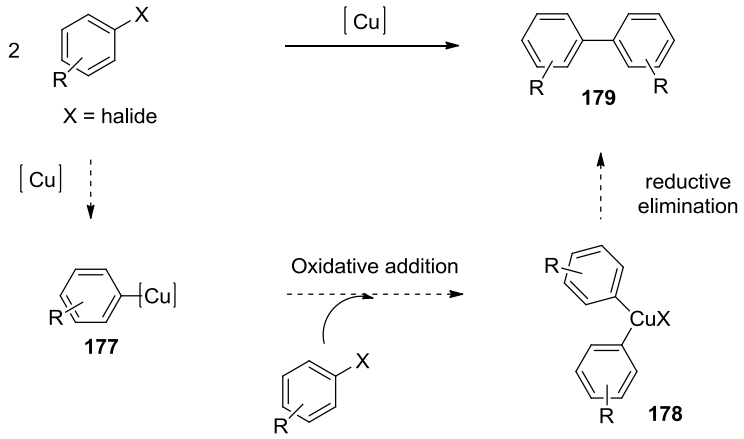

Scheme 57: General mechanism for the "classical Ullmann reaction".

Ullmann subsequently reported upon the use of these conditions to synthesise *N*-aryl amines (using stoichiometric Cu) and ethers in 1903 and 1905 respectively (Scheme 58).[102] Shortly after, in 1906 the first Cu-catalysed synthesis of aryl amides was reported by Irma Goldberg.[103] Almost 25 years later, in 1929, William Hurtley reported the coupling between *o*-bromobenzoic acid and *β*-dicarbonyls mediated by Cu bronze or $Cu(OAc)_2$.[104]

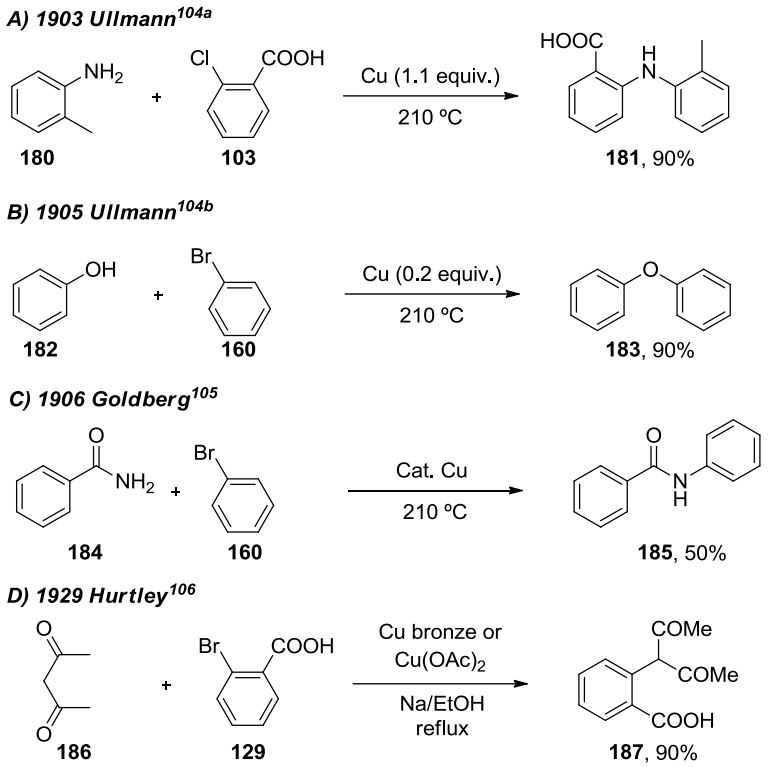

Scheme 58: Early methods of C–N/C–O bond formation.

These early coupling reactions, generally required harsh conditions (high temperature, strong bases, long reaction time and stoichiometric amounts of the copper reagent). Electron-poor aromatic substrates and high-boiling polar solvents were also often necessary. Moreover, problems related to the solubility of many Cu compounds were evident, hence, excess Cu often had to be used. Over the years, variations upon the Ullmann coupling have been reported which utilise milder conditions, this is especially the case when considering the use of bidendate ligands (Scheme 59).[105]

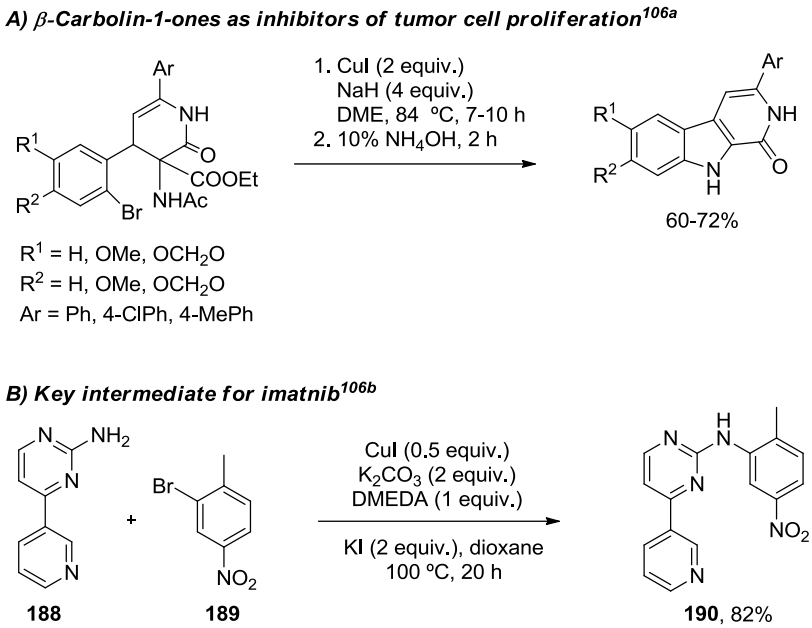

Scheme 59: Examples for modified variations of the Ullmann reaction.

In 1983 Mitiga reported the use of palladium as a catalyst with tinamines and arylbromides.[106] Ten years later, Hartwig took a closer look at the mechanism and proposed a catalytic cycle in which transmetallation is the rate limiting step (Scheme 60).[107]

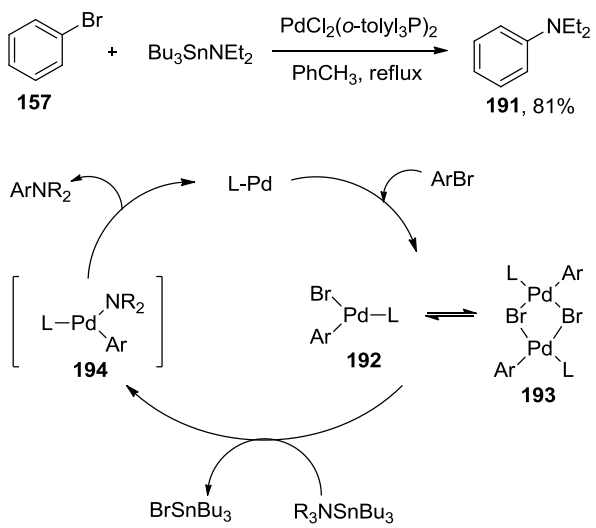

Scheme 60: Proposed mechanism for the palladium catalysed C–N coupling.

In quick succession, Buchwald and Hartwig published methods for a tin-free aryl-amine coupling and proposed a new catalytic cycle where oxidative addition is the rate limiting step (Scheme 61).[108] This major breakthrough made the C–N coupling reaction accessible to a wider range of substrates, including anilines, which did not react very well under the previous conditions. However, despite the improvements achieved with the Buchwald-

Hartwig coupling, limitations such as sensitivity to air and moisture, functional group tolerance and the high cost of palladium, reignited the search for improved methods.

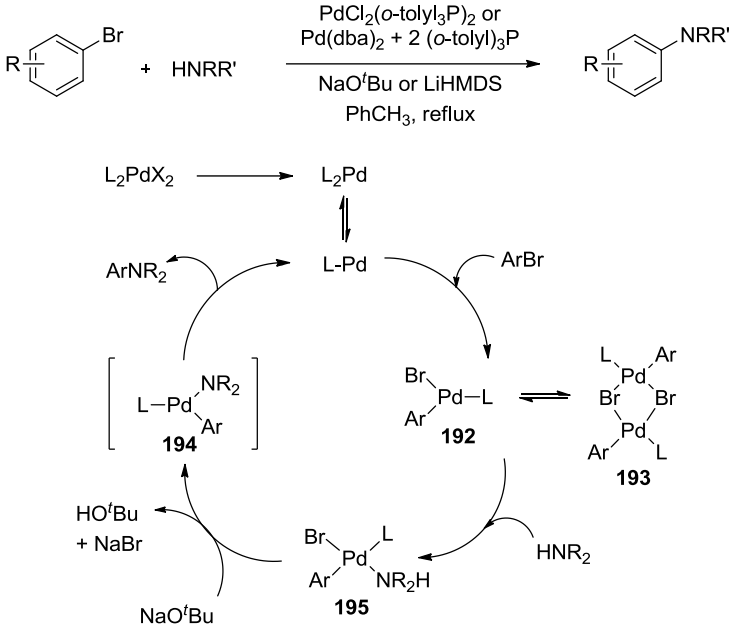

Scheme 61: Proposed mechanism for the tin-free palladium catalysed C−N coupling.

In 1998, the groups of Chan,[109] Evans[110] and Lam[111] independently reported a mild method for the C(aryl)−N and C(aryl)−O coupling reaction. Their method made use of stoichiometric amounts of copper(II) acetate as the catalyst and boronic acids as the aryl donors. In the presence of a base, the C(aryl)−N and C(aryl)−O coupling could be performed at room temperature. This reaction was subsequently shown to work with a large number of different nucleophiles and tolerated a variety of different substrates, making it one of the most efficient ways for the C−N/C−O coupling (Scheme 62).[112] Several modifications of the Chan-Lam reaction have been reported, expanding its scope and it has since been used to synthesise several biologically active compounds (Figure 10).[112]

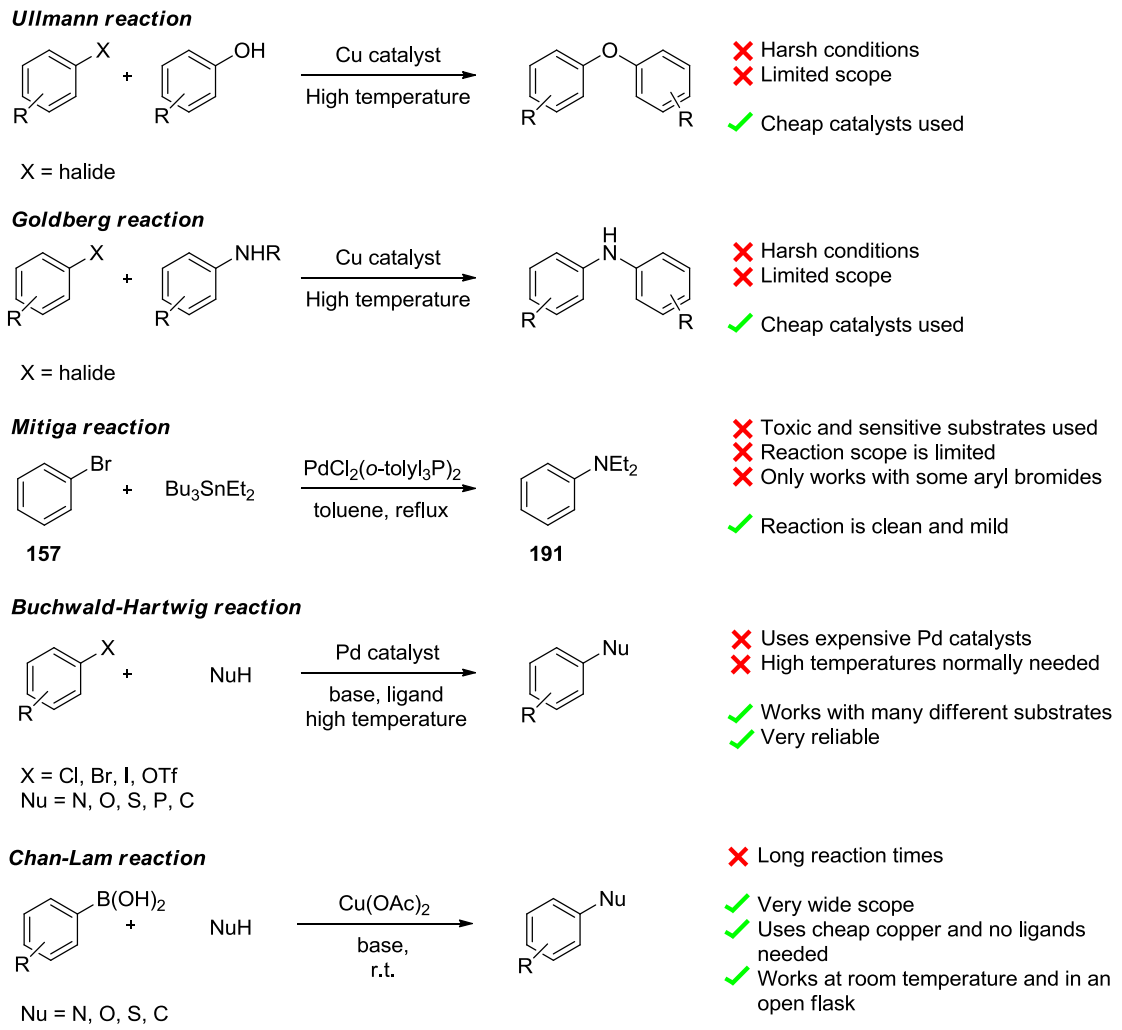

Scheme 62: Comparison of different C–N/ C–O coupling methods.

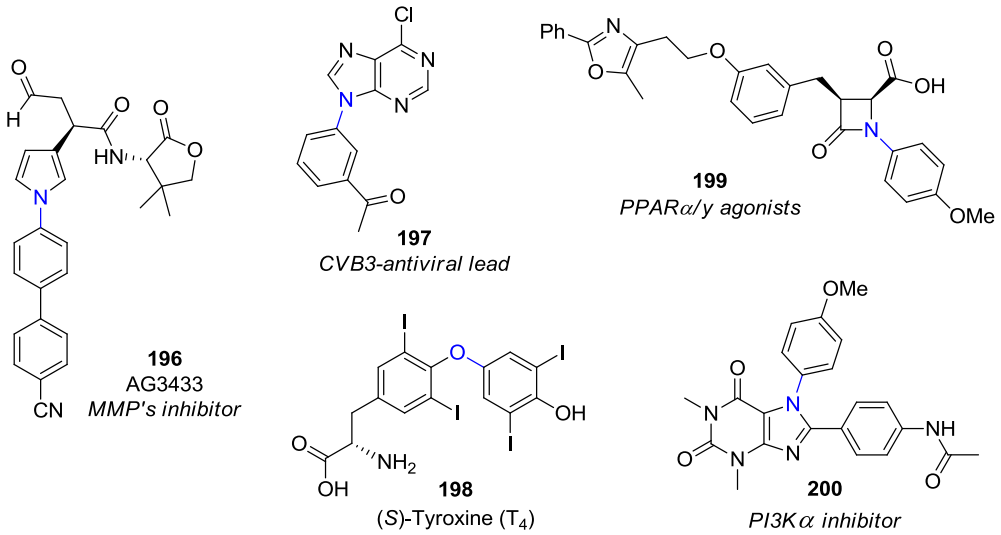

Figure 10: Biologically active compounds synthesised through a Chan-Lam reaction.[113]

Although the catalytic cycle is still somewhat debatable, kinetic and EPR spectroscopy for the methoxylation of tolylboronic acid methylester (Scheme 63) indicates that the

resting state of the catalyst is a Cu(II) with weak anionic ligands such as acetate or methoxide. Transmetalation is considered to be the rate limiting step.[114] Analysis of the reaction stoichiometry suggested that the C−O bond formation, through a reductive elimination step, does not happen from the Cu(II) oxidation state but instead from a Cu(III) species. The oxidation of Cu(II) to Cu(III) occurs from the disproportionation of another Cu(II) to give one equivalent of aryl-Cu(III) and one equivalent of Cu(I). Both the Cu(I) species from the disproportionation reaction and from the C−O reductive elimination step are quickly oxidised to Cu(II) by oxygen in a 4:1 Cu(I)/O_2 ratio.

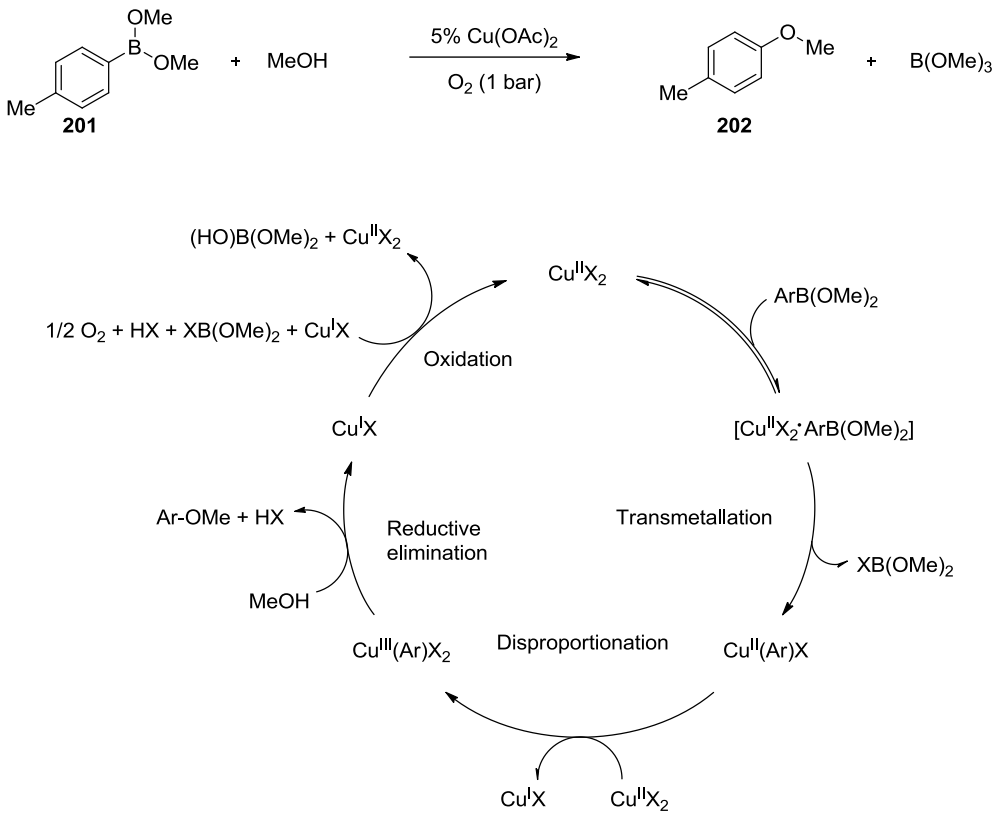

Scheme 63: Proposed catalytic cycle for the methoxylation of tolylboronic acid methylester.

In 2009, the groups of Stevens and van der Eycken reported on the Chan-Lam reaction as a continuous flow protocol using copper acetate (1.0 equiv.), pyridine (2.0 equiv.) and triethylamine (1.0 equiv.) in DCM.[115] Generally, when using anilines (Table 8) or phenols (Table 9) as the nucleophilic partner, moderate to good yields were obtained (56-71% yields, 9 examples).

Table 8: *N*-Arylation of differently substituted anilines.

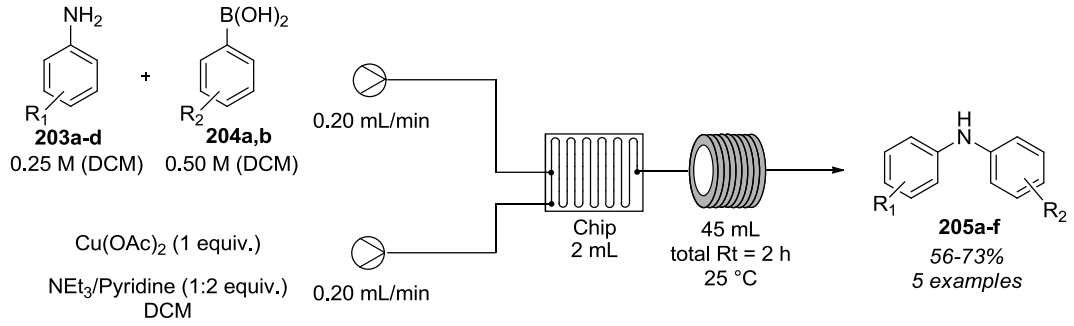

Entry	Product	R_1	R_2	Isolated (g)	Yield[a] (%)
1	**205a**	H (**203a**)	H (**204a**)	1.2	71
2	**205b**	H (**203a**)	3-OEt (**204b**)	1.5	73
3	**205c**	4-Cl (**203b**)	H (**204a**)	1.3	67
4	**205d**	4-Cl (**203b**)	3-OEt (**204b**)	1.7	59
5	**205e**	2,4,6-Cl (**203c**)	3-OEt (**204b**)	No reaction[b]	-
6	**205f**	2,4-NO_2 (**203d**)	3-OEt (**204b**)	1.7	56

[a] 10.0 mmol scale reactions. [b] Only starting material was recovered.

Table 9: *O*-Alkylation of substituted phenols.

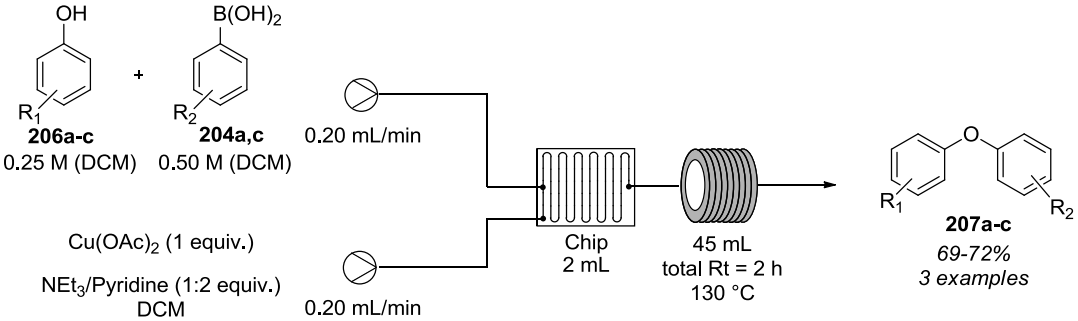

Entry	Product	R_1	R_2	Isolated (g)	Yield[a] (%)
1	**207a**	3-OCH_3 (**206a**)	H (**204a**)	1.44	72
2	**207b**	I (**206b**)	4-OMe (**204c**)	2.25	69
3	**207c**	4-Et (**206c**)	4-OMe (**204c**)	1.59	70

[a] 10.0 mmol scale reactions.

Recently, the Tranmer group reported the use of a copper-filled column as a catalyst with TEMPO as a co-oxidant in MeCN (acetic acid additive) with moderate to good yields of the coupled products being obtained (25-79% yields, 16 examples, Table 10).[116] The use of copper tubing, which serves as both the reactor and the catalyst, with *tert*-butyl peroxybenzoate as the oxidant in MeCN was also described but was outperformed by the copper filled column system.

Table 10: C–N Arylation library using solid copper column.

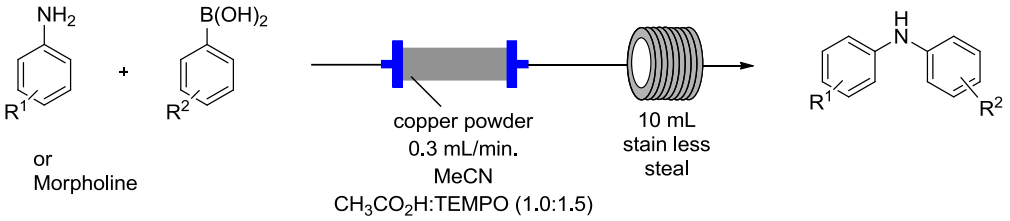

Entry	Aniline (R^1 =)	Boronic acid (R^2 =)	Yield[a] (%)
1	H	H	71/79[b]/72[c]
2	2,4,6-CH_3	H	52[b]/68[c]
3	2-OCH_3	H	66/82[b]
4	4-Cl	H	68/72[b]
5	4-F	H	71[b]
6	2,4-CH_3	H	64/77[b]
7	Morpholine	H	51/57[b]/65[c]
8	H	4-CH_3	71/66[b]
9	2-OCH_3	4-CH_3	45/59[b]
10	4-Cl	4-CH_3	59/57[b]
11	Morpholine	4-CH_3	51[b]
12	H	4-Cl	39/51[b]/52[c]
13	2-CH_3	4-Cl	38/47[b]
14	Morpholine	4-Cl	25[b]
15	2,4-CH_3	4-Cl	37[b]
16	2-CH_3	4-OCH_3	31[b]

[a] Isolated yields (%) with 1 equiv. of acetic acid. [b] 2.0 equiv. of acetic acid. [c] Isolated yields (%) using copper coil, (2.0:1.5) acetic acid:TEMPO.

Although the use of elemental copper is an improvement on the use of stiochiometric copper acetate in continuous flow, the use of TEMPO or *tert*-butyl peroxybenzoate as an oxidant introduces more waste. Employing oxygen gas as an oxidant is preferred as it is cheap, renewable and environmentally benign. We therefore set out to develop a more atom economical way of catalysing the Chan-Lam reaction using a sub-stoichiometric amount of copper and oxygen gas as the oxidant.

2.2.2 Results

2.2.2.1 Synthesis of herbicidal intermediate using the Chan-Lam synthesis in flow

As part of an ongoing study carried out at Syngenta, this investigation was geared towards the synthesis of a pyridazine containing herbicide. The original synthesis (Scheme 64) involved hydrazone formation from a substituted phenylhydrazine such as **208** with 1,1-dimethoxypropan-2-one (**209**) catalysed by $Zn(ClO_4)_2 \cdot 6H_2O$. The resulting aldehyde (**300**) then undergoes a condensation reaction with Meldrum's acid followed by base hydrolysis to give the pyridazine **302** which would then be derivatised to yield various amides (yields not disclosed).

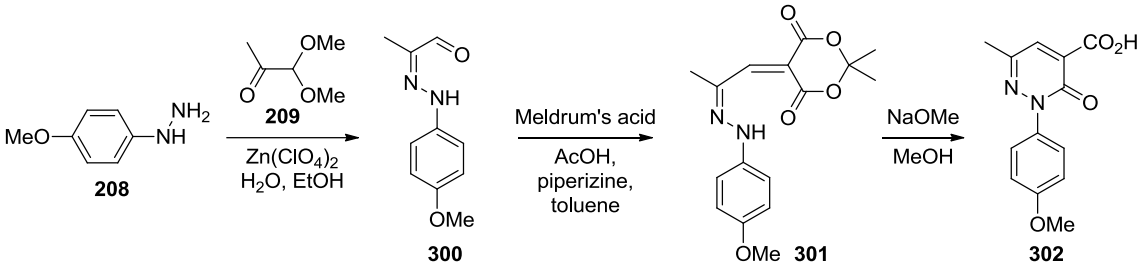

Scheme 64: Original synthesis for pyridazine containing herbicide intermediate **302**.

However, as part of the library synthesis, studying the effect of substituents on the biological activity, some substrates could not be prepared through the original synthesis. Therefore, an alternative route involving C-N coupling through a Chan-Lam synthesis between pyridazine **306** and the appropriate boronic acid **307** was envisaged to yield **305** (Scheme 65). This would be followed by ester hydrolysis to furnish the carboxylic acid **304** which was to be coupled with the appropriate amine to form the active herbicide structure **303**.[117]

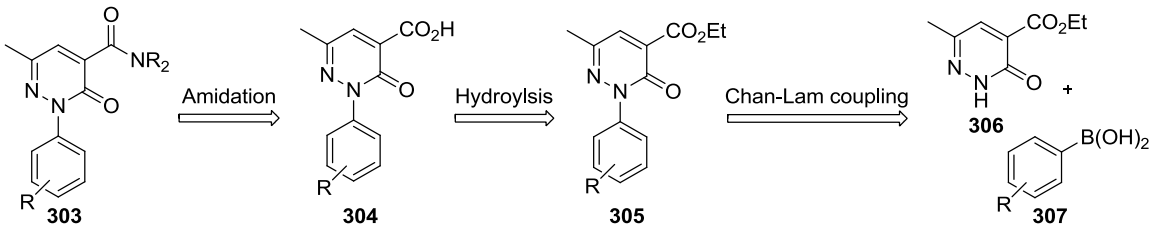

Scheme 65: Synthesis for pyridazine containing herbicide **303** through a Chan-Lam coupling.

The synthesis of the lead compound **309**, containing a 3,4-dimethoxybenzene moiety could only be achieved through the Chan-Lam route. However, it was noticed that the conditions used for this transformation in batch only work well on a small scale (<10 g), when the reaction was scaled up (>10 g) the yield dropped significantly (Scheme 66).

Furthermore, the long reaction times led to hydrolysis of the ester which made the purification harder.

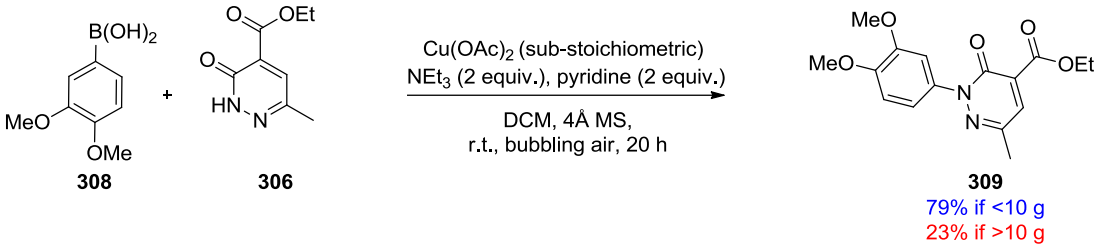

Scheme 66: Chan-Lam synthesis of key building block **309** in batch.

As large quantities of **309** were required for field trials, an improved scale up synthesis of this herbicide intermediate was needed. It is well known that flow chemistry provides reliable means of scaling up of reactions, this prompted us to develop a catalytic flow method for the Chan-Lam synthesis of **309**. The use of oxygen provides the necessary oxidant to reoxidise the Cu(I) that forms after the C−N reductive elimination back to Cu(II), allowing for sub-stoichiometric amounts of copper to be used. Based on our previous experience of using the reverse "tube-in-tube" reactor with other gases, it was decided that the oxygen would be delivered via this reactor type (Scheme 67). Furthermore, a work-up which avoids the use of silica column purification was also required for the scale-up.

From the four different organic solvents investigated (toluene, DCM, MeCN and EtOAc), $Cu(OAc)_2$ only completely dissolved in DCM. Pumping DCM through the HPLC pumps, used as part of the flow system, initially presented some issues. This was mainly due to cavitation just before the pump inlet, attributed to the shear forces present, causing outgassing (air). These bubbles, if left in the system, disturb the flow, resulting in an unstable system. This problem was solved by sonication of the DCM (30 min of sonication per 500 mL of solvent) prior to use, keeping it under positive pressure throughout the experiment (N_2 balloon was used for the positive pressure).

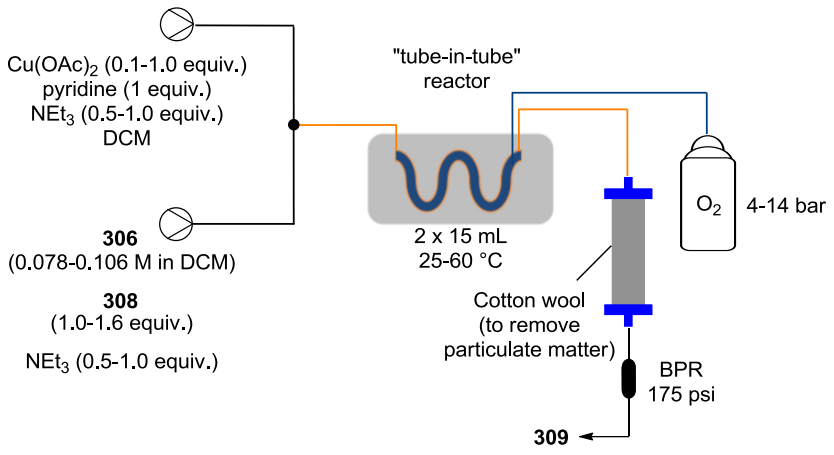

Scheme 67: Setup for the catalytic Chan-Lam reaction of **309** using the "tube-in-tube" reactor.

In an effort to identify the optimum conditions for this reaction, the amount of copper catalyst and the oxygen pressure were studied (Table 11). By starting with one equivalent of $Cu(OAc)_2$ and no oxygen, a 63% yield of **306** to **309** was obtained (Entry 1, Table 11). The yield was reduced to 56% when 0.5 equiv. of $Cu(OAc)_2$ were used (Entry 2, Table 11) fixing the $Cu(OAc)_2$ at 0.5 equiv. an increase in the yield to 83% (Entry 3, Table 11) was observed when 4 bar of oxygen was supplied through the "tube-in-tube" reactor. A further increase in oxygen pressure to 8 bar, 10 bar, 12 bar and 14 bar (Figure 11) indicated that the best yield was obtained at 10 bar (Entries 4-7, Table 11). It is not yet clear as to why there was a slight decrease in yield at 12 bar and 14 bar but this could be due to a slight decrease in residence time associated with an increase in the gas pressure. Lowering the amount of $Cu(OAc)_2$ to 0.25 equiv. and 0.10 equiv., resulted in yields of 88% and 77% respectively (Entries 8-9, Table 11).

Table 11: Optimisation of the amount of copper catalyst and oxygen used.

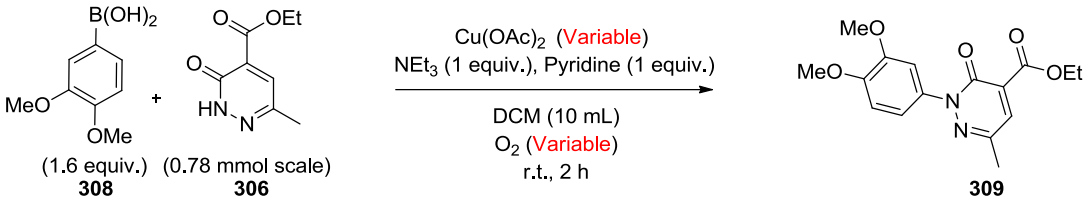

Entry	$Cu(OAc)_2$ (equiv.)	O_2 pressure (bar)	NMR Yield[a] (%)
1	1.00	0	63
2	0.50	0	56
3	0.50	4	83
4	0.50	8	86
5	0.50	10	92
6	0.50	12	86
7	0.50	14	79
8	0.25	10	88
9	0.10	10	77

[a] Yield calculated using 1,3,5-trimethoxybenzene as an internal NMR standard.

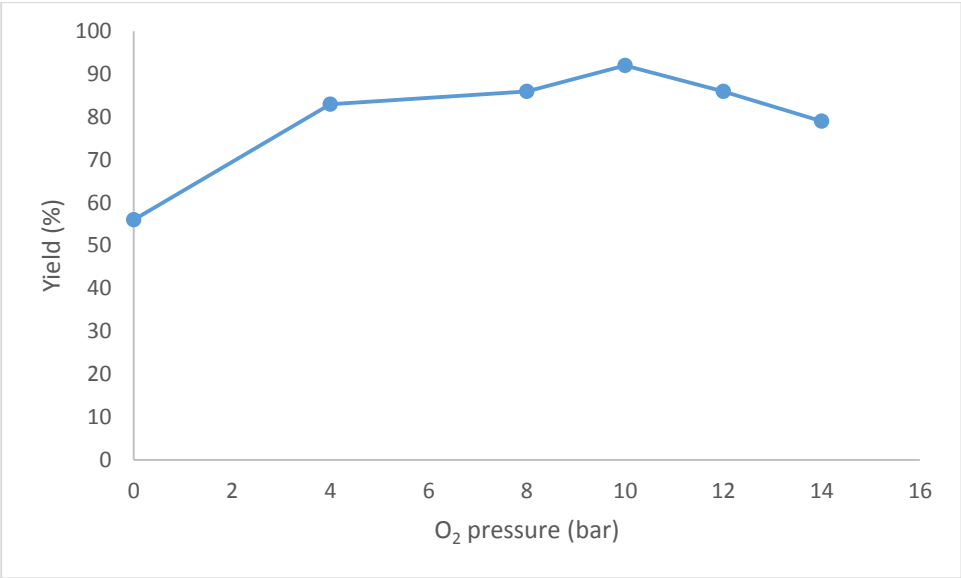

Figure 11: Observed trend for the effect of changing the oxygen pressure on the NMR yield of **309**.

The effect of temperature and residence time on the yield was next studied (Table 12). Increasing the temperature to 40 ºC while maintaining the residence time at 2 h gave a higher yield of 96% (Entry 1, Table 12) and afforded an 83% yield when the residence time was reduced to 1 h (Entry 2, Table 12). Further decreasing the residence time to 0.5 h maintained the yield at 85% (Entry 3, Table 12). The marginally higher yield obtained

with a residence time of 0.5 h compared to 1 h may be due to the better mixing attained at the higher flow rates. A small decrease in yield to 81% was observed when the temperature was increased to 60 ºC while keeping the residence time at 0.5 h (Entry 4, Table 12).

Table 12: Optimisation of residence time and temperature.

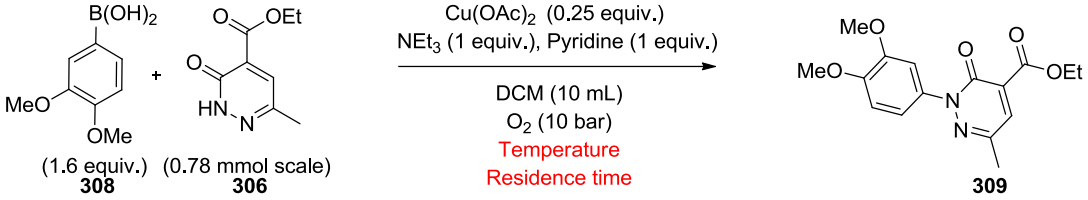

Entry	Residence time (h)	Temperature (ºC)	NMR Yield[a] (%)
1	2	40	96
2	1	40	83
3	0.5	40	85
4	0.5	60	81

[a] Yield calculated using 1,3,5-trimethoxybenzene as an NMR internal standard.

Although the highest yield was obtained at 2 h residence time at a temperature of 40 ºC, it was decided that the best conditions so far were those obtained at 0.5 h with a temperature of 40 ºC as this represents a productivity of 1.27 g h^{-1} when compared to 0.36 g h^{-1} for the 2 h residence time. Productivity was very important for this substrate due to time constraints associated with gaining sufficient material for field trials.

Further optimisation of the process was targeted towards the amount of triethylamine, boronic acid excess and the concentration used (Table 13). An increase in the excess of triethylamine used resulted in an increase in the yield to 92% (Entry 2, Table 13). An attempt to reduce the excess of boronic acid used to 1.4 equiv. and 1.1 equiv. only resulted in lower yields of 83% and 73%, respectively (Entries 3-4, Table 13). Changing the concentration to 0.106 M and 0.142 M resulted in improved yields of 96% and 93% respectively (Entries 5-6, Table 13). An attempt to decrease the boronic excess used to 1.4 equiv. and 1.2 equiv. at 0.106 M concentration proved to be unprofitable as the yields dropped to 83% and 81% respectively (Entries 7-8, Table 13).

Table 13: Optimisation of the amount of boronic acid, triethylamine and concentration used.

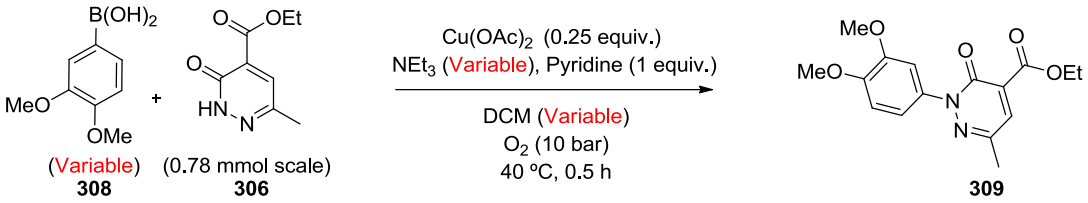

Entry	NEt_3 (equiv.)	Boronic acid (equiv.)	Concentration (M)	NMR Yield[a] (%)
1	1.0	1.6	0.078	85
2	2.0	1.6	0.078	92
3	2.0	1.4	0.078	83
4	2.0	1.1	0.078	73
5	2.0	1.6	0.106	96
6	2.0	1.6	0.142	93
7	2.0	1.4	0.106	83
8	2.0	1.2	0.106	81

[a] Yield calculated using 1,3,5-trimethoxybenzene as an NMR internal standard.

Using the optimised conditions, a scale up of the continuous process was performed (Scheme 68). Using 12.7 mmol of **306** resulted in a 70% isolated yield of pure **309** which represents a productivity of 1.42 g h^{-1}. When the scale was almost doubled to 24.4 mmol of **306** an isolated yield of 71% was obtained with a productivity of 1.44 g h^{-1}. This shows that the flow protocol developed represents a reliable and scalable method for the preparation of **309** through a catalytic Chan-Lam reaction using oxygen gas.

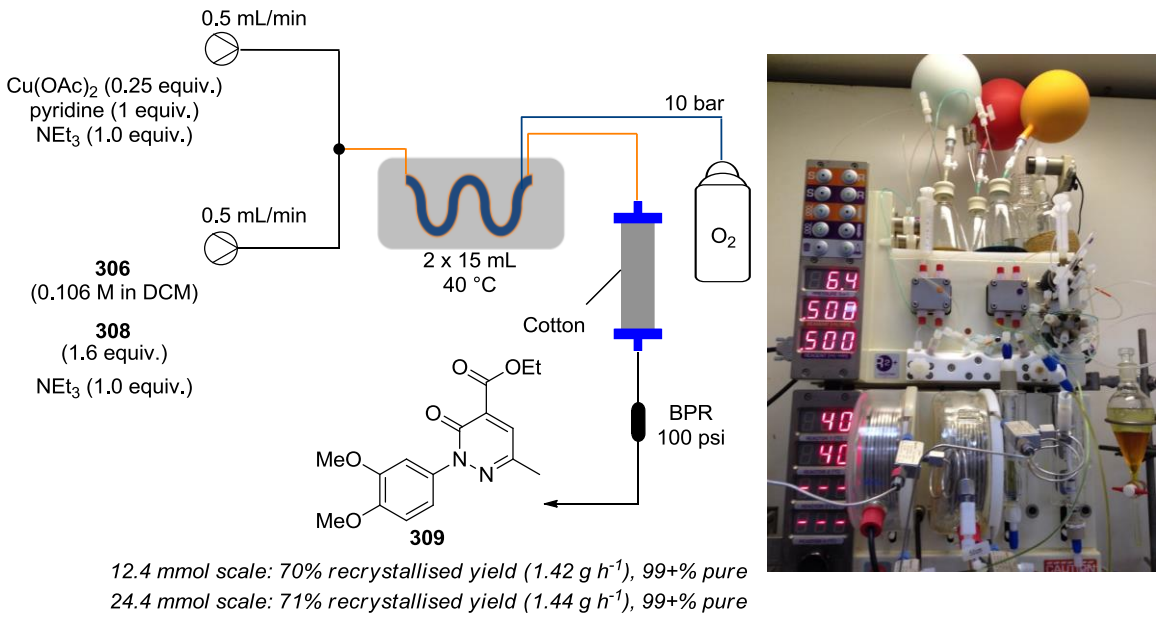

Scheme 68: Optimised process for the synthesis of **309**.

The work up of compound **309** was achieved by washing the crude mixture with diluted HCl aqueous solution (1 M). Purification was then performed through trituration followed by recrystallisation (see experimental), which gave the pure product in 99+% purity (purity measured by ^{1}H NMR spectroscopy with 1,3,5-trimethoxybenzene as an internal standard) for both the 12.4 mmol and 24.4 mmol scale reactions.

2.2.2.2 Scope of Catalytic Chan-Lam Synthesis in Flow

Having identified the optimum conditions for the scale up of herbicidal intermediate **309** through a continuous flow catalytic Chan-Lam synthesis, the scope of this reaction was next evaluated. As the objective was to synthesise a small array of C–N coupled products, a second optimisation using 3-phenyl-1*H*-pyrazole (**310**) as the nucleophilic partner and 4-methoxyphenylboronic acid (**204c**) as the aryl donor was performed (Table 14).

Table 14: Optimisation of the Chan-Lam reaction in continuous flow.

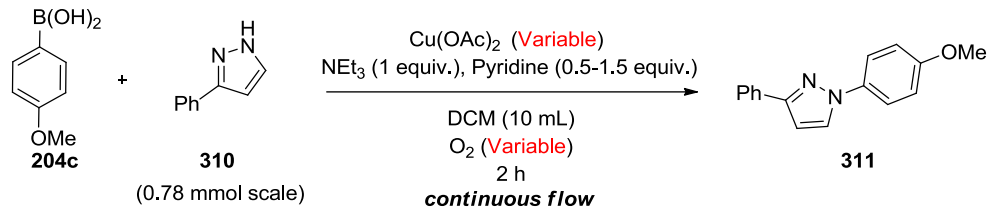

Entry	$Cu(OAc)_2$ (equiv.)	Boronic acid (equiv.)	Temperature (°C)	O_2 pressure (bar)	NMR Yield[a] (%)
1	1.00	1.6	20	0	66
2	0.50	1.6	20	0	48
3	0.25	1.6	20	0	25
4	0.50	1.6	20	4	81
5	0.50	1.6	20	8	85
6	0.50	1.6	20	10	97
7	0.50	1.6	20	12	85
8	0.50	1.6	20	14	83
9	0.25	1.6	20	10	94
10	0.25	1.6	20	12	87
11	0.10	1.6	20	10	50
12	0.25	1.4	20	10	56
13	0.25	1.1	20	10	48
14	0.25	1.6	30	10	87
15	0.25	1.6	40	10	95
16	0.25	1.6	50	10	88
17[b]	0.25	1.6	40	10	93
18[c]	0.25	1.6	40	10	76

[a] Yields calculated using 1,3,5-trimethoxybenzene as an internal NMR standard and represents the average of two runs. [b] 1.5 equiv. of pyridine, [c] 0.5 equiv. of pyridine.

In the first three control experiments no oxygen was supplied to the system and the amount of copper acetate catalyst was varied from 1.0 equiv. to 0.5 equiv. and finally to 0.25 equiv. (entries 1-3, Table 14). As anticipated, with no oxidant to reoxidize the catalyst, the yield dropped in proportion to the amount of catalyst used. Keeping the amount of copper acetate constant (0.5 equiv.), the effect of the oxygen pressure on the yield was investigated (entries 4-8, Table 14). A general increase was again noticeable

on going from 0-10 bar after which a slight decrease in yield was observed at higher pressures (Figure 12). The same trend was also observed during the optimisation of herbicidal intermediate **309** (Figure 11). A decrease in yield was also observed when going from 10 bar to 12 bar of oxygen with 0.25 equiv. of copper acetate (entries 9-10, Table 14)

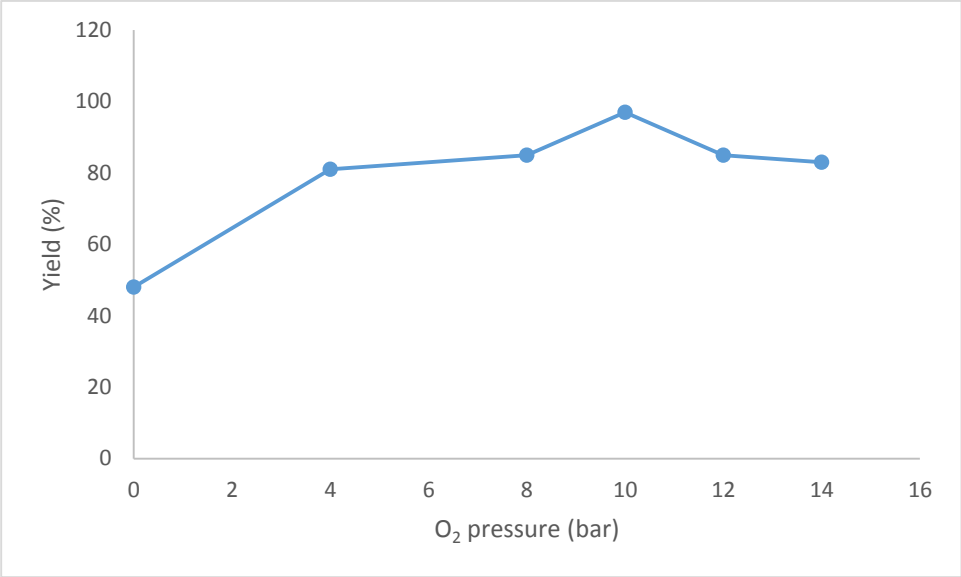

Figure 12: Observed trend for the effect of changing the oxygen pressure on the NMR yield of **311**.

When the amount of copper acetate was further reduced to 0.10 equiv. a drastic decrease in yield was observed indicating that the turnover frequency (TOF) of the catalytic cycle with this amount of copper acetate is not efficient enough to give good yields (entry 11, Table 14). A decrease in yield was also observed when the amount of boronic acid used was decreased to 1.4 equiv. and 1.1 equiv. respectively (entries 12-13, Table 14). Changing the temperature from 20 ºC to 50 ºC did not greatly affect the yields obtained, with 40 ºC giving the most promising result (entries 14-16, Table 14). However, it was observed that less particulate matter was formed in the reactor when higher temperatures were used (40 and 50 ºC), which helps in avoiding possible reactor blockages. Finally, the amount of pyridine added was also studied. Decreasing the amount of pyridine (0.5 equiv.) resulted in a lower yield (76%) while increasing the amount of pyridine (1.5 equiv.) did not show any noticeable change in the yield (93%). This indicates that the pyridine plays an important role in this coupling reaction which could be both due to its effect as a ligand and/or its solubility enhancement of the copper acetate (entries 17-18,

Table 14). The amount of triethylamine was not varied as its quantity was needed to ensure the boronic acid remains soluble in the DCM solvent.

To determine the time needed to reach steady state in the reactor, samples were periodically collected (2 min collection time) and analysed by ^{1}H NMR spectroscopy using 1,3,5-trimethoxybenzene as the internal standard (Figure 13). As expected, the product eluted after 120 min which corresponds with the set residence time. A lower yield was obtained for 120 min (85% yield) which then rapidly increased to 99% and 98% yield at 125 min and 130 min respectively. The yield then stabilised at 96% for the next data points indicating that steady state was achieved at 135 min, which is 15 min after the product first started to elute from the reactor.

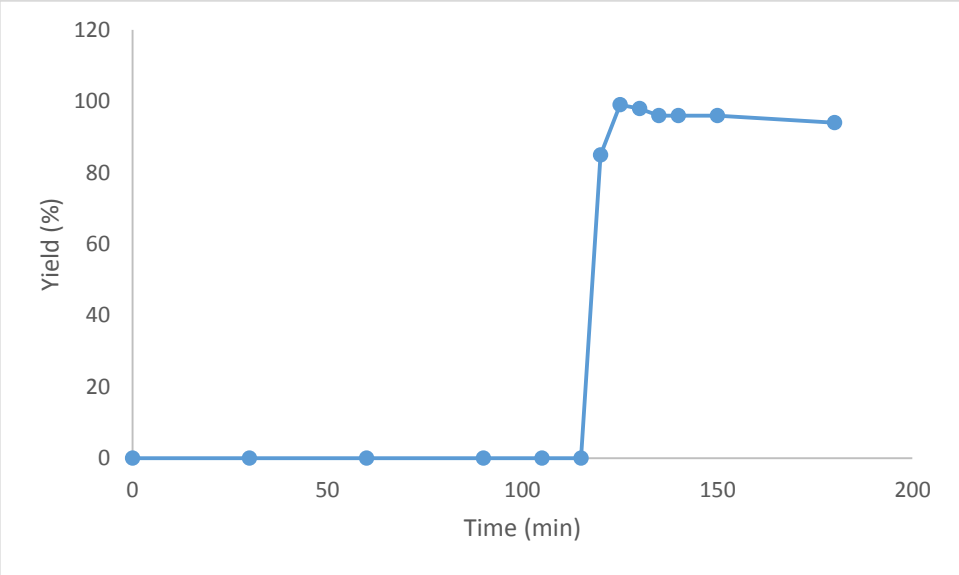

Figure 13: Analysis of the steady state of the reactor.

As it had been determined that the amount of arylboronic acid excess could not be lowered (entries 12-13, Table 14), the use of a polymer supported scavenger was tested in an effort to reduce the amount of excess phenylboronic acid present. The use of QP-DMA, a polymer-supported tertiary amine base, was placed in an Omnifit® column positioned after the "tube-in-tube" reactor, through which the reaction mixture was flowed (Figure 14). It was noticed that this was sufficient to reduce the excess boronic acid present without affecting the yield of the product. The products were still purified using column chromatography, however, the reduction in boronic acid excess made the column chromatography far easier.

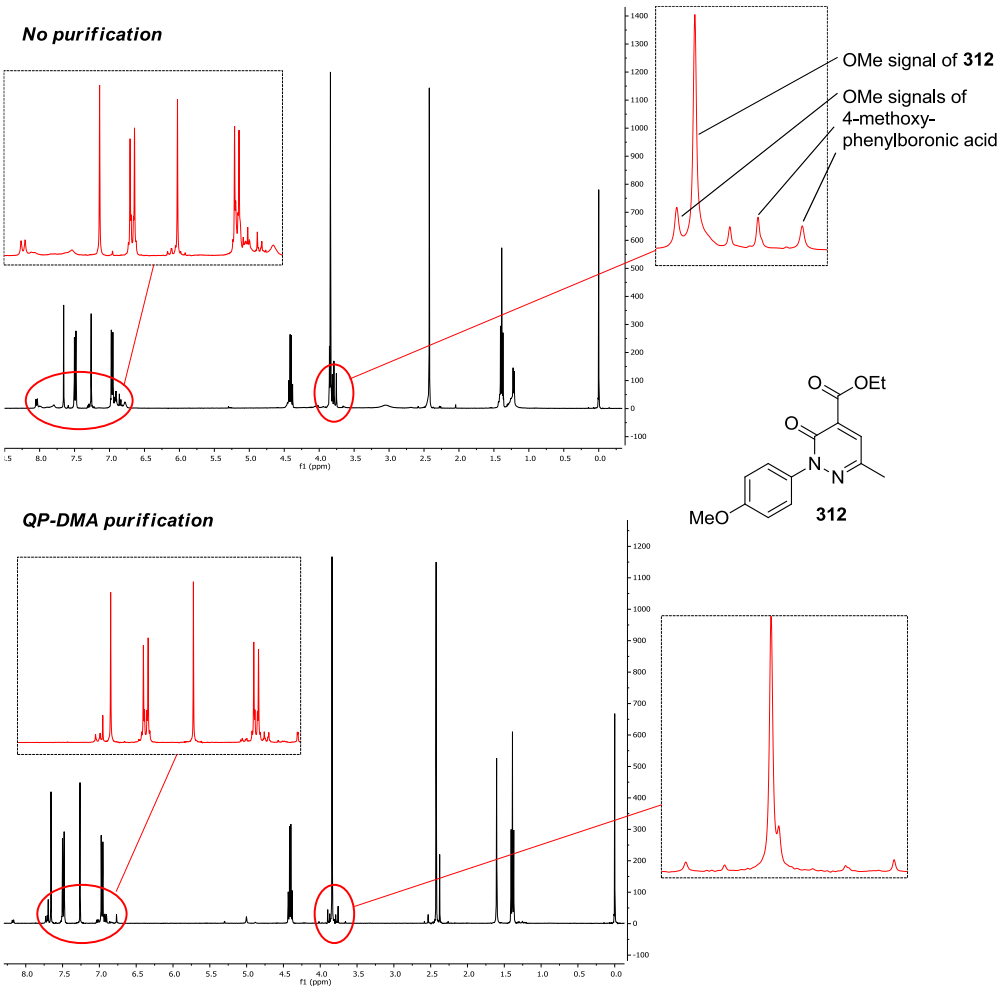

Figure 14: Comparison of ^{1}H NMR spectra of non-purified (top) and QP-DMA purified (bottom) continuous flow synthesis of **312**.

2.2.2.3 Library Formation

Using the optimised conditions for the synthesis of **311**, a small library of compounds was synthesised to demonstrate the scope of the reaction conditions. Excellent isolated yields were obtained when anilines were used as the nucleophilic partner with both phenylboronic acid **204a** (90% yield) and 4-methoxyphenylboronic acid **204c** (92% yield) as the aryl donors (**313** and **205a**, Scheme 69). Phenylboronic acid **204a** also gave a moderate isolated yield when coupled with 2-amino-4-bromopyridine as the nucleophile (50% yield, **314**, Scheme 69) and a good isolated yield with the electron withdrawing 4-chloroaniline (71% yield, **205c**, Scheme 69). Using L-tyrosine methyl ester as the nucleophile with phenylboronic acid **204a**, unfortunately, gave a poor isolated yield of 26% and also exhibited some epimerisation (**315**, 53% *ee* determined by chiral HPLC, Scheme 69). Additionally, a small amount of the product (**315**) reacted further with phenylboronic acid **204a** through the phenol to give **316** in 3% isolated yield. In the case of L-leucine methylester an isolated yield of 60% was realised, which was also

accompanied by partial epimerisation (**317**, 71% *ee* determined by chiral HPLC, Scheme 69).

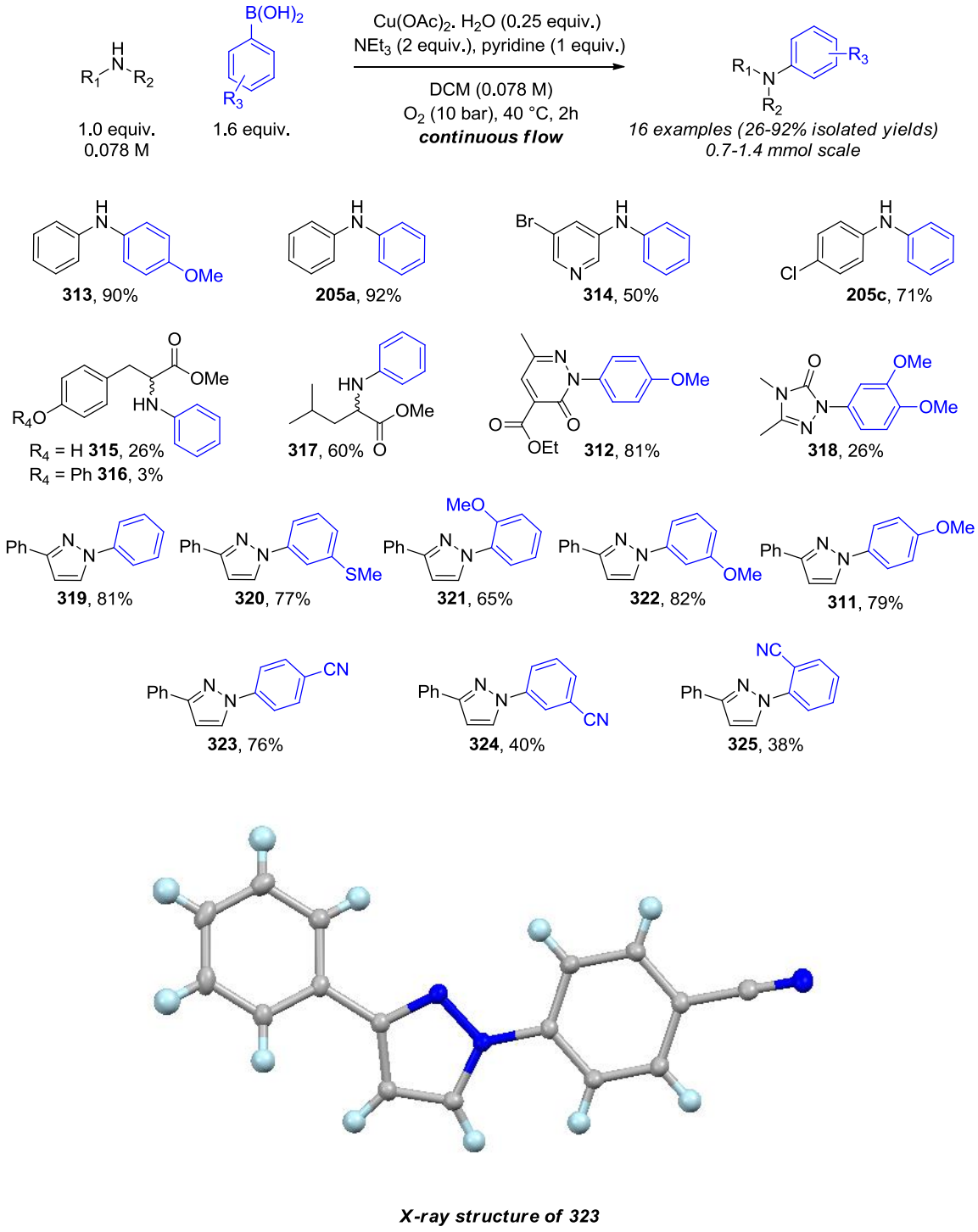

Scheme 69: Scope of the catalytic Chan-Lam reaction in continuous flow.

Using *N*-heterocyclic substrates as the nucleophilic partner with a range of different phenylboronic acids generally gave good isolated yields (**311-312**, **318-325**, Scheme 69).

Compound **306** as the nucleophile with 4-methoxyphenylboronic acid **204c** gave an 81% yield of **312**, which is very close to the yield obtained for the herbicidal intermediate **309**. However, using 3,4-dimethyl-1*H*-1,2,4-triazol-5(4*H*)-one (**329**), which was synthesised using a literature procedure (Scheme 70), with 3,4-dimethoxyphenylboronic acid gave a lower yield of 26% (**318**, Scheme 69). It is not yet clear as to why such a low yield was obtained but the reduced nucleophilicity and higher potential for coordination of the triazole to the copper catalyst might account for this.

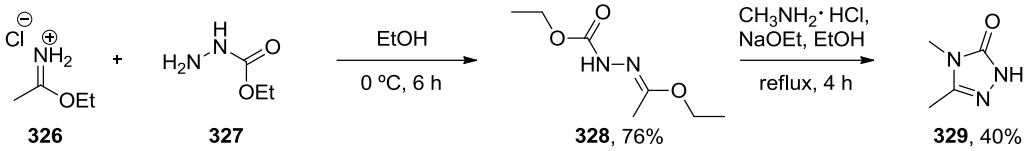

Scheme 70: Syntheses of substrate **329**.

Alternatively, using 3-phenyl-1*H*-pyrazole (**310**) as the nucleophile with a number of different phenylboronic acids gave moderate to good yields (38-82% yields). In general electron-rich phenylboronic acids (**311**, **319-322**, Scheme 69) gave better yields than electron poor ones (**323-325**, Scheme 69). This is probably due to the more favourable thermodynamics with an increase in the electropositivity of boron, which in turn increases the rate of the transmetallation step. Changing the group at the 4-position of the phenylboronic acid gave good yields for both electron rich (**311**, 79% yield) and electron poor (**323**, 76% yield) phenylboronic acids. On the other hand changing the group at the 3-position of the phenylboronic acid gave good yields for electron-rich (**320** and **322**, 77% and 82% yields respectively) but a moderate yield of 40% for electron-poor (**324**) phenylboronic acids. This could be ascribed to both the lower electropositivity of boron associated with the electron-poor phenylboronic acids and also to some chelation of the nitrile group with copper when present at the 3 position. Lower yields for both electron-rich (65% yield) and electron-poor (38% yield) 2-substituted phenylboronic acids were realised, possibly due to steric interactions around the active catalyst and chelation of the nitrile with copper as explained above (**321** and **325** Scheme 69).

It is noteworthy that for all of the 3-phenyl-1*H*-pyrazole couplings, only the 1,3-disubsituted pyrazole products were obtained with no 1,5-disubsituted isomers being detected. For the characterisation of the 1,3-disubsituted pyrazoles, NOESY NMR experiments were used when no published data was available (Figure 15 for **320**, Figure 16 for **323** and Figure 17 for **325**). An X-ray crystal structure for compound **323** was also

obtained, confirming the connectivity. Furthermore, only published data from reactions that can yield only the 1,3-disubstituted pyrazole were considered as it was noted that some of the literature examples were wrongly assigned when both isomers were present. One example is in the formation of **319** through a one-pot oxidation and rearrangement of propargylamine **330** which was reported to form as the main regio-isomer (Scheme 71).[118] However, analysing the ^{1}H and ^{13}C NMR data reported and comparing them with those reported by others, such as that synthesised through a copper-catalysed relay oxidation that can only give the 1,3-disubstituted pyrazole[119] and the NOESY NMR experiments obtained for our sample, it was evident that the wrong assignments were reported by Chen *et al*.[118]

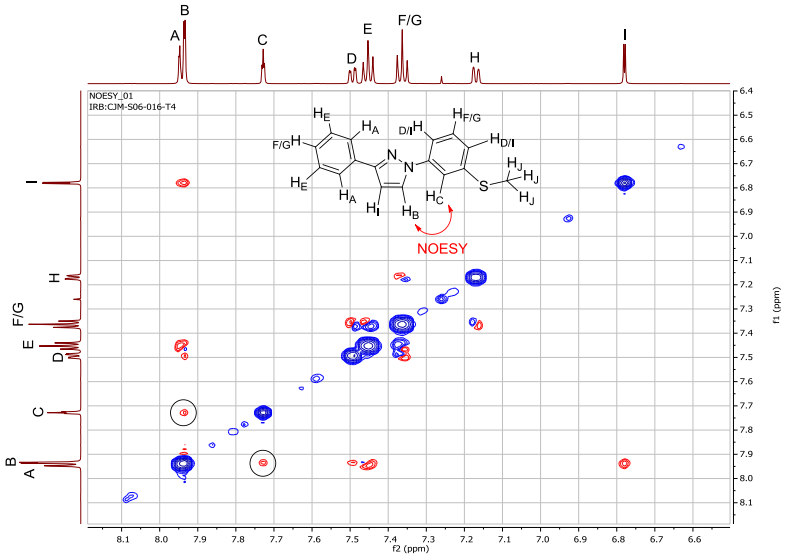

Figure 15: NOESY NMR spectrum for **320** with the characteristic NOESY signal encircled.

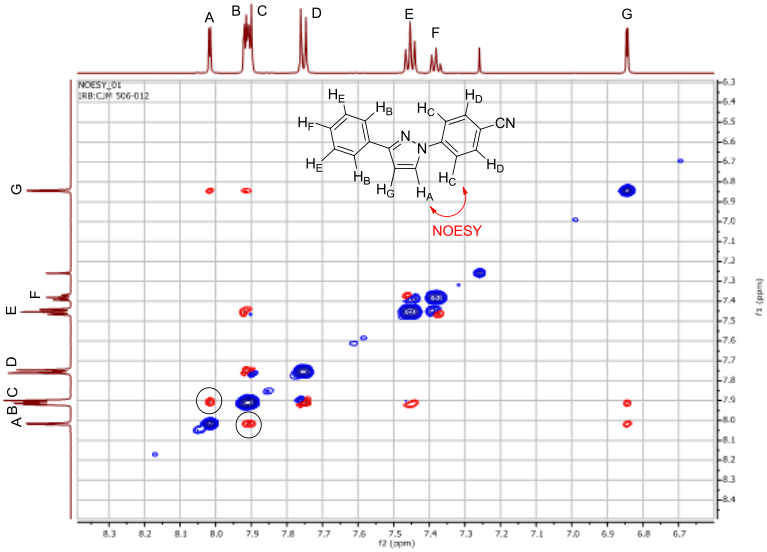

Figure 16: NOESY NMR spectrum for **323** with the characteristic NOESY signal encircled.

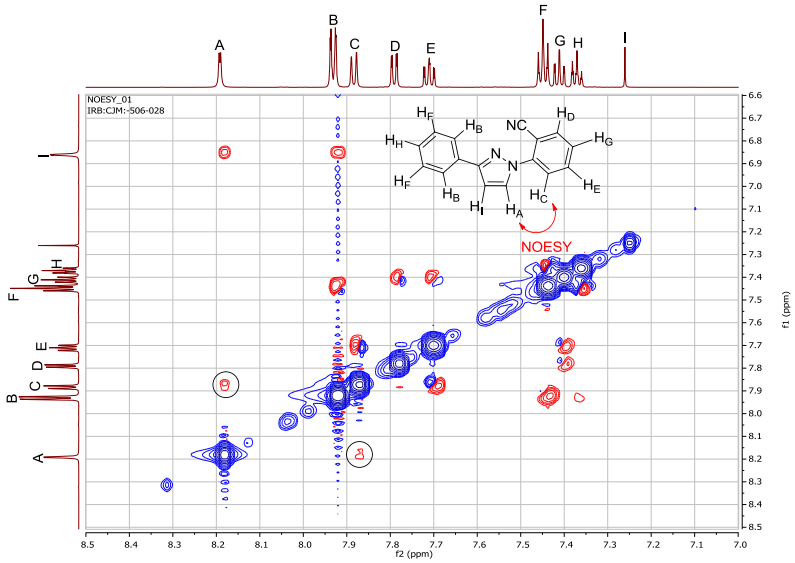

Figure 17: NOESY NMR spectrum for **325** with the characteristic NOESY signal encircled.

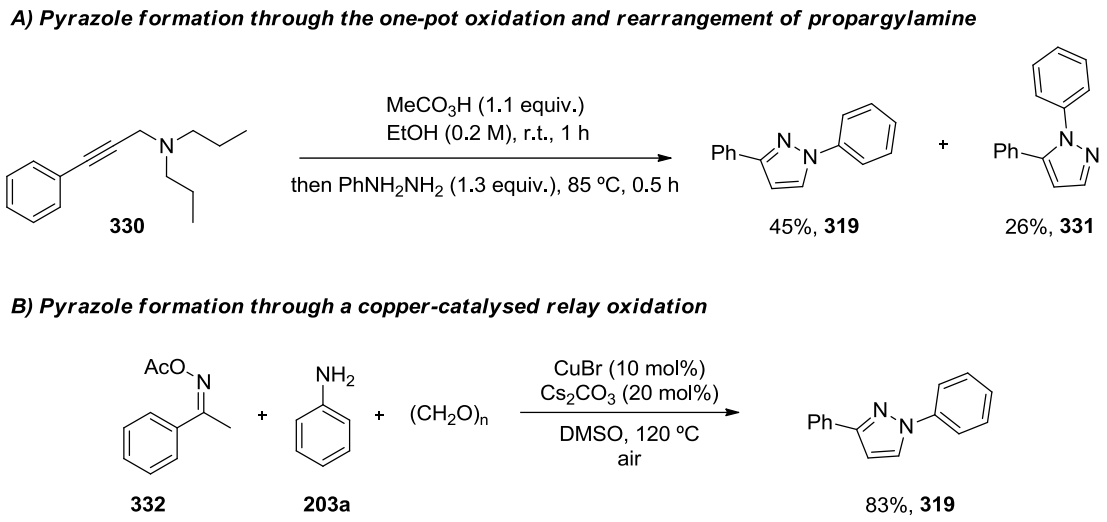

Scheme 71: Reported formation of pyrazole **319** through different routes.

The potential for scalability of these reaction conditions, was demonstrated through the synthesis of **311** at 10 mmol scale, a factor of fourteen times the original 0.7 mmol test reaction (Scheme 72). A slightly improved isolated yield (81%) was obtained for the larger scale experiment when compared to the 79% isolated yield obtained for the smaller scale experiment. The consistency of the yields obtained indicates that the processes is robust and can reliably deliver 0.216 g h^{-1} of **311** at 81% isolated yield.

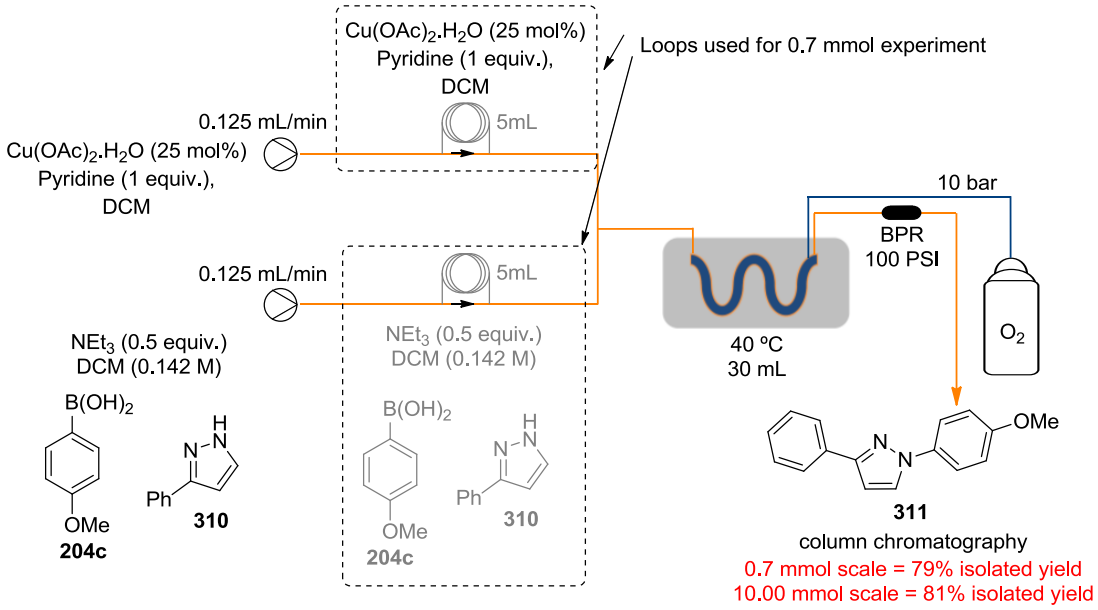

Scheme 72: Scale-up procedure for **311**.

For certain nucleophilic substrates no products were obtained when C-N coupling with 4-methoxyphenylboronic acid (**204c**) was attempted (Figure 18). In the case of **333** precipitation occurred as soon as the two solutions came into contact at the T-piece mixer,

which was probably due to strong coordination to the copper acetate by the imidazole ring. In the case of **334-336** the reduced nucleophilicity of these substrates might account for the 0% conversion. By comparison, all three substrates (**334-336**) also failed to react under batch conditions using 2 equiv. of $Cu(OAc)_2$, 2 equiv. of NEt_3 and 1 equiv. of pyridine at 40 ºC for 48 h confirming their low reactivity.

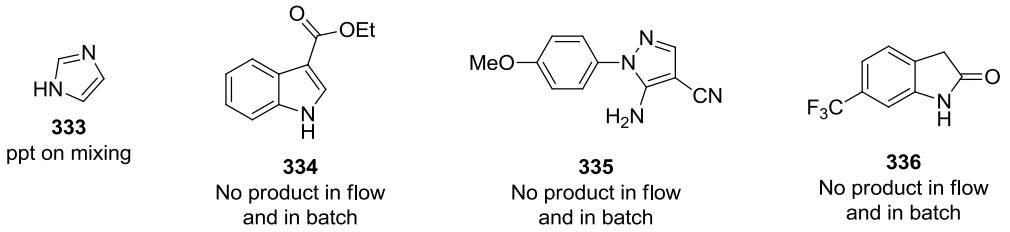

Figure 18: Substrates that gave no products in flow.

2.2.3 Conclusions

The aim of using oxygen as an oxidant for a catalytic Chan-Lam reaction in an effort to reduce the amount of copper catalyst used and increase the rate of the reaction, was the main focus for the synthesis of the herbicidal intermediate **309** via C-N coupling. Making use of flow chemistry not only improved the mixing but also allowed a safe and efficient way of introducing the oxygen through a reverse "tube-in-tube" reactor. Optimisation of the reaction conditions allowed for a scalable and efficient synthesis of **309**. The optimised conditions for the synthesis of **311** were also applied to a number of other substrates to show the scope of the reaction. When using 3-phenyl-1*H*-pyrazole as a nucleophile with a number of different boronic acids, it was noticed that 1,3-disubstituted pyrazoles were selectively obtained over 1,5-disubstituted pyrazoles.

Considering all of these features together, this catalytic flow protocol for the efficient Chan-Lam reactions represents a valuable extension of C(aryl)-N coupling. When compared to current published protocols it is clear that the use of sub-stoichiometric amount of copper catalysts is an advantage over the stoichiometric amount used in studies published by the groups of Stevens and van der Eycken.[115] Additionally, the use of oxygen as the oxidant is clearly advantageous over the use of TEMPO and *tert*-butyl peroxybenzoate as reported by the Tranmer group in terms of atom economy.[116]

2.3 Thiazole Formation Through a Modified Gewald Reaction

2.3.1 Introduction

The synthesis of sulfur-containing heterocycles has long attracted the attention of chemists due to their occurrence as motifs in biologically active compounds, polymers and dyes. Of the sulfur containing heterocycles, thiophenes and thiazoles are especially prevalent in many pharmaceuticals (Figure 19).[120] There are several synthetic routes described for both thiophenes and thiazoles with the Paal-Knorr synthesis[121] being the most common for thiophenes and the Hantzsch synthesis being the current first choice for thiazoles (Scheme 73).[122]

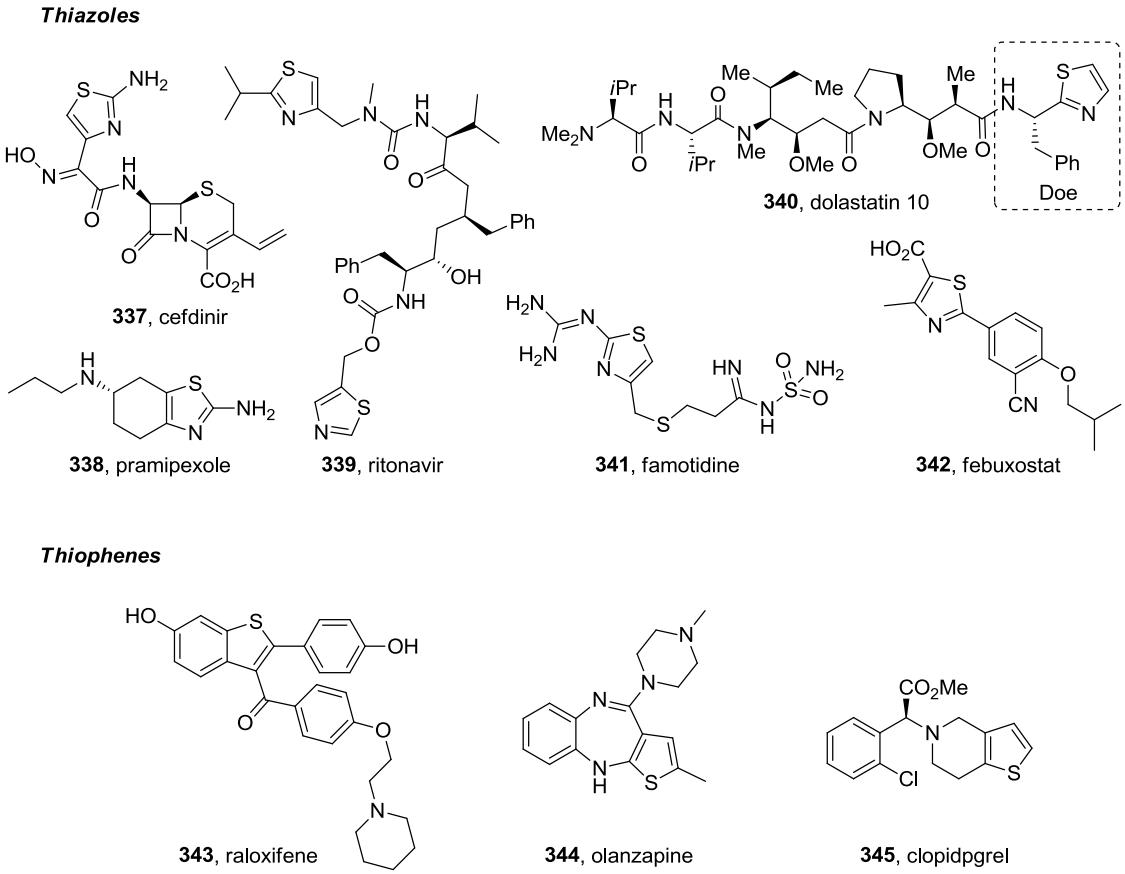

Figure 19: A selection of pharmaceuticals containing thiazoles and thiophenes.

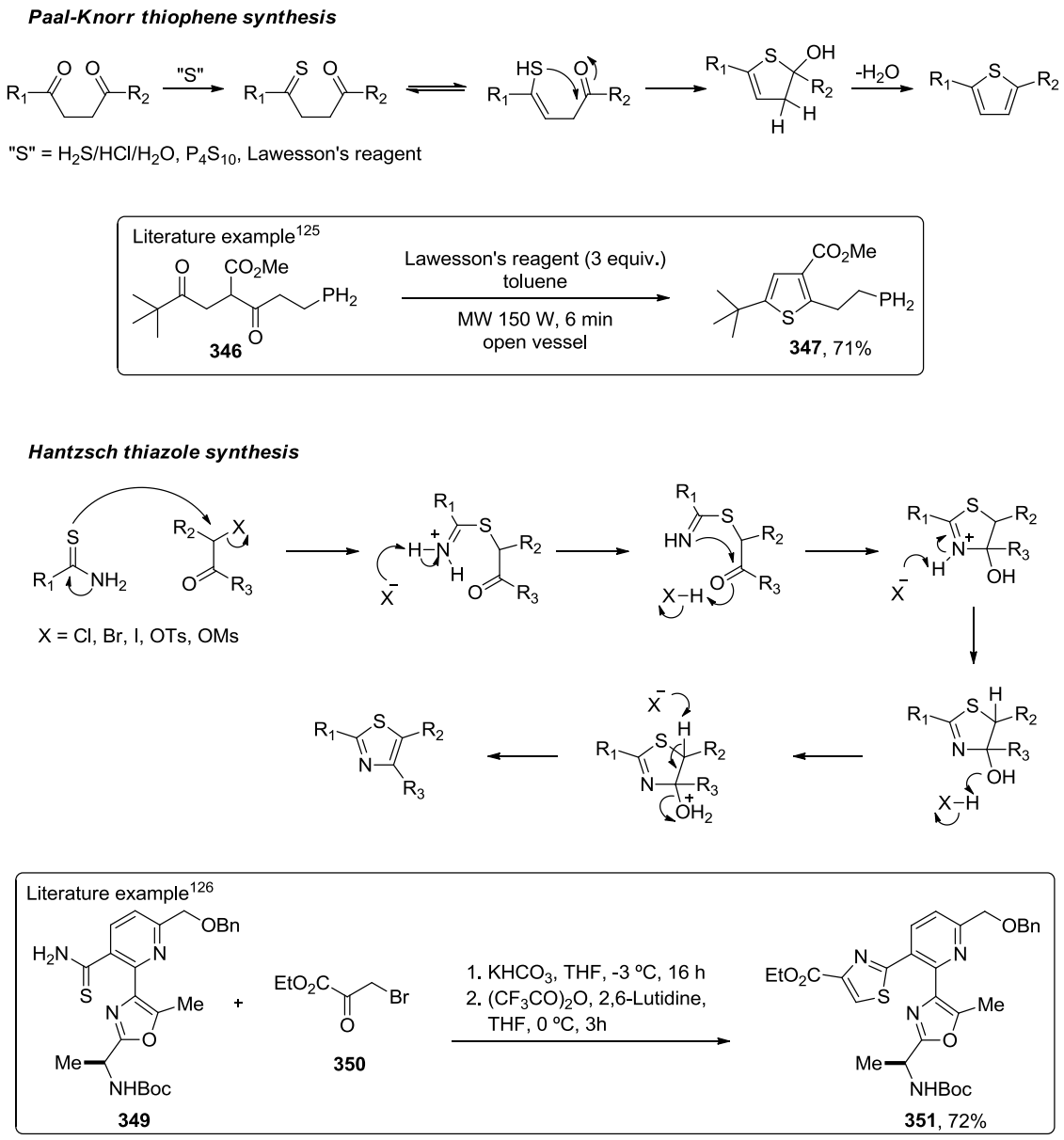

Scheme 73: Paal-Knorr thiophene synthesis[123] and Hantzsch thiazole synthesis.[124]

An alternative strategy is to use the Gewald reaction (Scheme 74),[125] this transformation was first described in 1961. It involves a multi-component condensation between sulfur, an α-methylene carbonyl compound and an α-cyanoester to form 2-aminothiophenes. The mechanism is thought to proceed through an initial Knoevenagel condensation between the α-cyanoester **353** and the carbonyl compound **352**, giving the intermediate **354** which undergoes sulfurisation followed by a 5-exo-dig cyclisation (Baldwin favoured ring closure) to give the 2-aminothiophene product **357** after aromatisation.

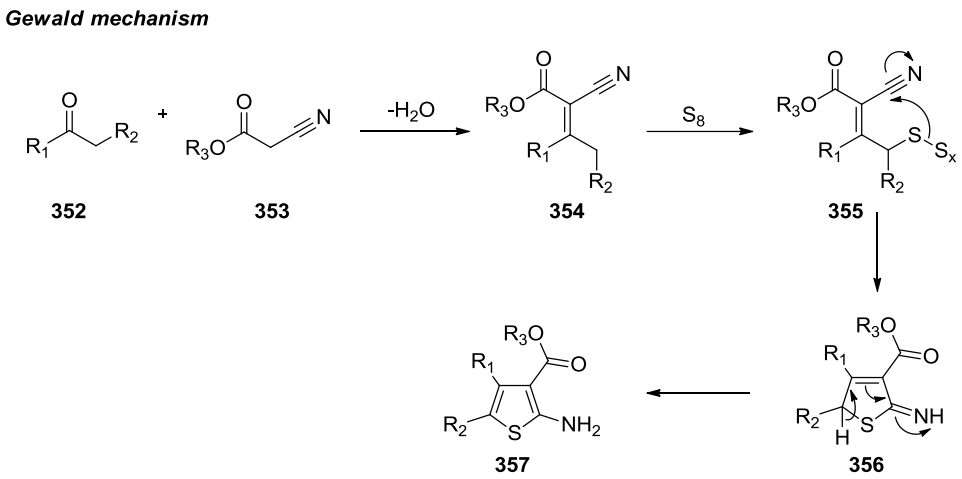

Scheme 74: Gewald reaction mechanism.

Several variations of the Gewald reaction have since been described,[126] however, the use of 1,4-dithian-2,5-diol,[127] which serves as both the sulfur and the α-methylene carbonyl component, sparked our interest as a means of synthesising 3-aryl-2-aminothiophene derivatives. The air stable, readily available 1,4-dithian-2,5-diol is also low cost and does not possess the unpleasant odour that is typically associated with sulfur containing compounds. As well as in the Gewald reaction, 1,4-dithian-2,5-diol has also been used in the synthesis of tetrahydrothiophenes through a Michael/aldol cascade,[128] 2,3-disubstituted thiophenes from alkynones,[129] nitroalkenes,[130] *N*-substituted imides,[131] for the synthesis of 1,3-oxathiolanes[132] and tetrahydrothiopyranols (Scheme 75).[133] In an effort to further expand the scope of this synthetically useful substrate (**358**) and inspired by the Gewald reaction mechanism, other nitrile substrates were targeted with the hope of forming further sulfur containing heterocycles.

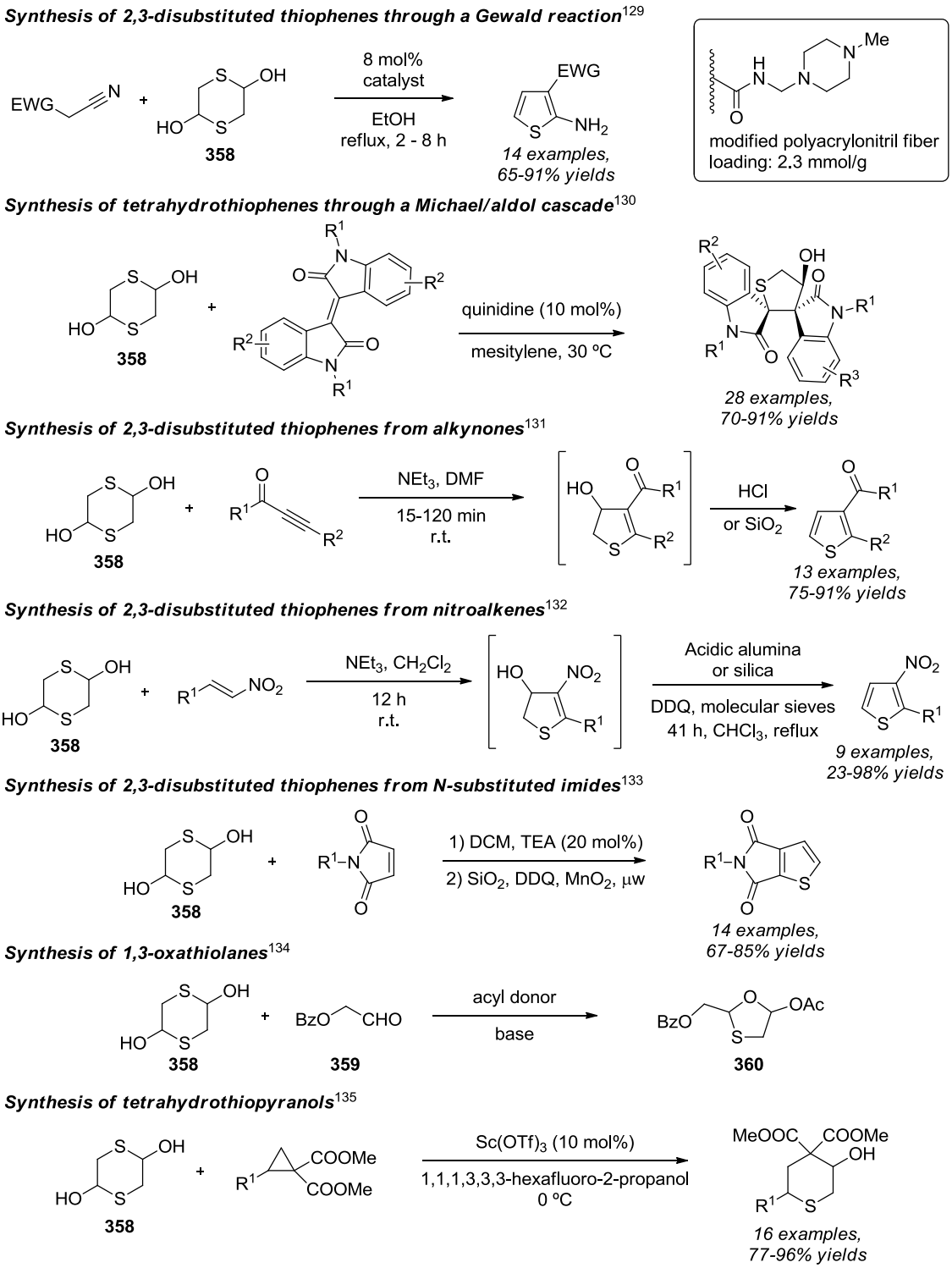

Scheme 75: Use of 1,4-dithian-2,5-diol in different reactions.

2.3.2 Results

With the premise of α-disubstituted nitriles blocking the aromatisation pathway in a Gewald type mechanism, ethyl 2-cyano-2-phenylacetate (**362**) was reacted with 1,4-dithian-2,5-diol (**358**). It was expected that the intermediate (**364**) would be detected (Scheme 76), however, the main product formed showed two sets of new aromatic peaks (two doublets) in the ^{1}H NMR spectrum which were typical of adjacent protons on a five membered aromatic ring (Figure 20). From the ^{1}H NMR spectrum of the crude material it was evident that MeOH driven trans-esterification had occurred with the MeOH (Spectrum A, Figure 20). To aid with the characterisation of the product formed, the crude material was dissolved in 1 mL of MeOH with a stoichiometric amount sodium methoxide in order to transform all of the product to the corresponding methyl ester (Spectrum B, Figure 20). After careful assignment, the structure of the product obtained was assigned as the thiazole, **366**.

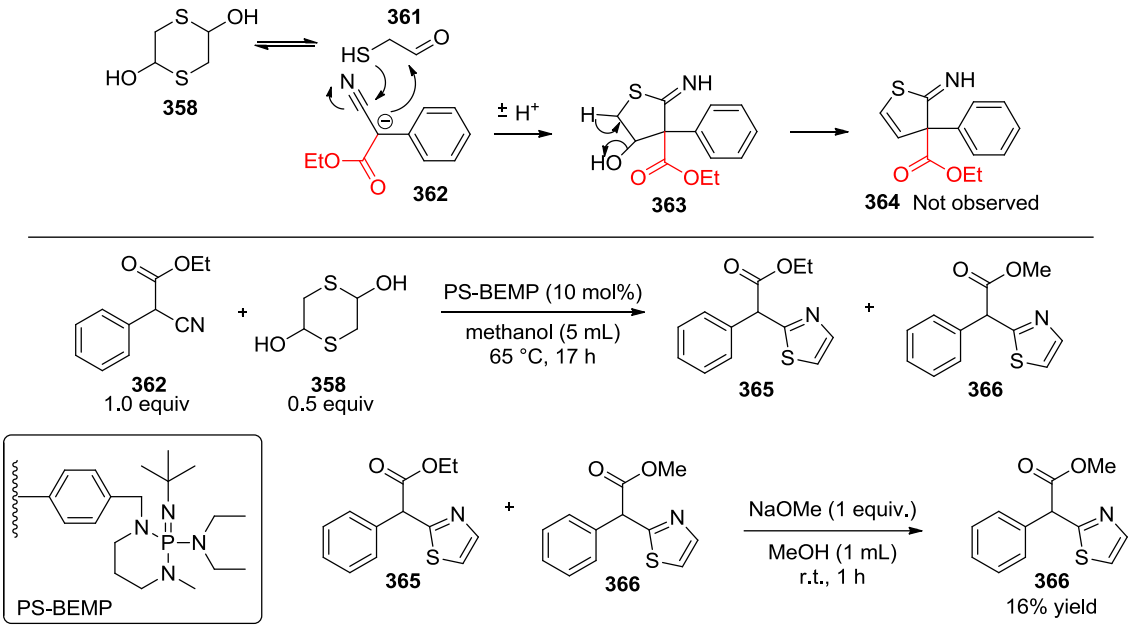

Scheme 76: Attempted synthesis of intermediate **364** through a Gewald type reaction (top). Thiazole formation from the reaction of **362** and **358** (bottom).

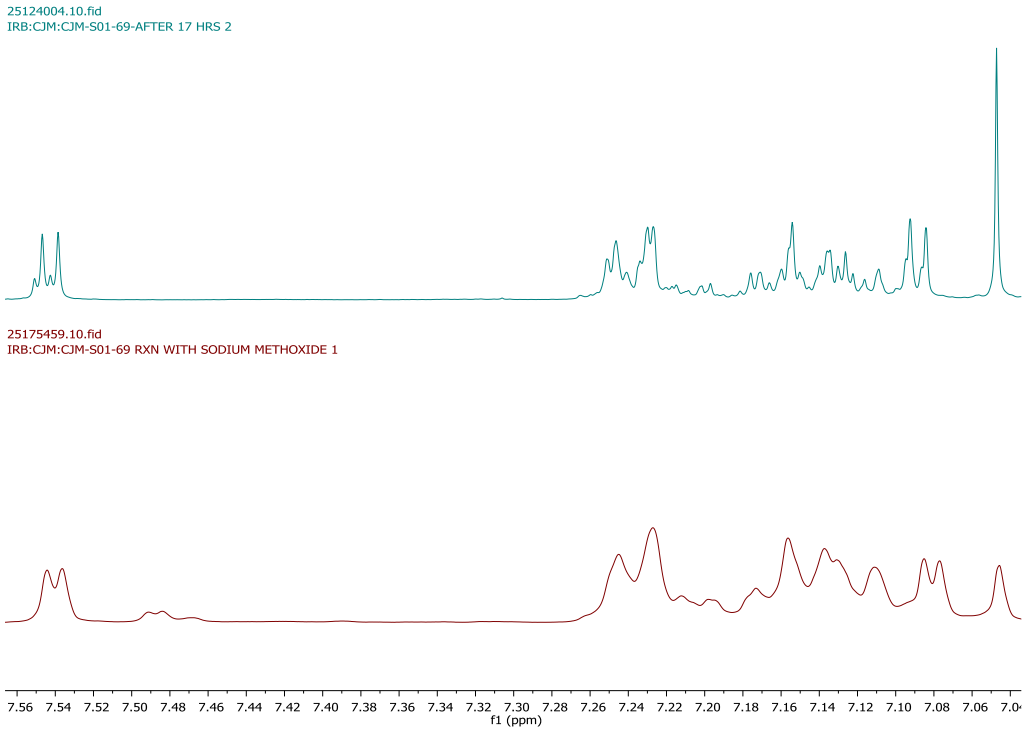

Figure 20: a) ^{1}H NMR of crude reaction after 17 h showing a mixture of two diagnostic doublets at 7.54 ppm and 7.07 ppm (top); b) ^{1}H NMR of crude reaction after adding NaOMe and MeOH to form the methyl ester only showing one set of two diagnostic doublets at 7.54 ppm and 7.07 ppm (bottom).

Although thiazole formation from nitriles has previously been shown to occur with ketones[134] and carboxylic acids,[135] yielding 2,5-disubstituted thiazoles, to our knowledge, aldehydes have only ever been shown to form 2-aminothiophenes.[127] Even though 2-substituted thiazoles are important structures in their own right, further substitution can also easily be achieved through published protocols, in which 2,4-substituted thiazoles, 2,5-substituted thiazoles and also 2,4,5-substituted thiazoles are formed.[136] This further demonstrates the need for a scalable and rapid synthesis of 2-substituted thiazole compounds as core building blocks.

2.3.2.1 Study of the Bifurcation Pathway

From the preliminary results obtained for the reaction of **362** with 1,4-dithian-2,5-diol (Scheme 76) and the published modified Gewald reaction with 1,4-dithian-2,5-diol[127] we hypothesised that substitution at the α-carbon of the nitrile precursor predetermines the reaction outcome, yielding either the thiophene or thiazole product when reacted with 1,4-dithian-2,5-diol. Therefore based on this premise, α-methylene substituted nitriles should result in 2-aminothiophenes and α-methine substituted nitriles would result in 2-substituted thiazoles.

To evaluate our hypothesis, we decided to optimise the conditions for the reaction of ethyl phenylcyanoacetate (**362**) with the aldehyde precursor **358** as a model system. Initially, reactions were performed using conventional heating, however, to allow for a wider temperature range, microwave heating was introduced. This allowed access to higher temperatures above the solvents' atmospheric pressure boiling points.

In the initial screen, the temperature was fixed at 80 °C and the reaction time at 5 h. Variables included the solvent, base and the stoichiometry of **358** (Tab1e 15). Only a small impact upon conversion was observed upon changing the stoichiometry of compound **358** and so it was decided to also maintain this at an equimolar concentration (i.e. 0.5 equiv. of the dimer) as it would simplify the purification later on. All reactions were assessed for conversion of **362** to **365** using ^{1}H NMR analysis of the crude reaction followed by work-up and purification via column chromatography to determine isolated yields.

With regard to solvent selection, trifluroethanol showed by far the best results. This is ascribed to its high polarity (dipole moment at 25 ºC = 2.03) and its slightly acidic nature (pK_a in water at 25 ºC = 12.4) when compared to the other solvents. This is thought to assist in solubilising **358**, subsequently promoting the formation of the aldehyde monomer. MeOH, which was originally used as a solvent, was eliminated from further consideration in order to avoid the undesirably trans-esterification. Results indicated that triethylamine (NEt_3) was the most effective base providing the highest conversion and isolated yield (58%) with tetramethylethylenediamine (TMEDA) also giving a yield of 50% (Table 15, entries 1 and 10). The stronger guanidine base 1,1,3,3-tetramethylguanidine (TMG) and 1,8-diazabicycloundec-7-ene (DBU) both gave full consumption of the nitrile starting material, but generated complicated product mixtures allowing only a moderate isolated yield of 33% in the case of TMG (Table 15, entries 7 and 8). Interestingly, the use of piperidine led to no conversion of the nitrile (**362**) under the standardised reaction conditions (Table 15, entry 9). We believe this is due to its condensation with the aldehyde component (generated from **358**), which inhibits the transformation. In addition, a sulfonic acid bound resin (QP-SA) was also trialled as an additive but showed no conversion, allowing full recovery of the starting nitrile (see later discussion on mechanism). These experiments imply that the deprotonation of the α-methylene adjacent to the nitrile group is an essential step in the mechanism.

Table 15: Scoping experiments using ethyl phenylcyanoacetate (**362**) with different solvents and bases.[a]

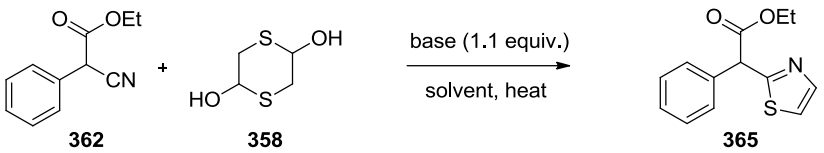

Entry	Base	Solvent	Dithiane (equiv.)	Conversion[b] (%)	Isolated yield (%)
1	NEt_3	trifluoroethanol	0.50	84	58
2			0.55	85	50
3			0.75	94	52
4		ethanol	0.50	25	N/D
5		chlorobenzene		18	
6		1,2-dichloroethane		0	
7	DBU	trifluoroethanol		100	5
8	TMG			100	33
9	piperidine			0	0
10	TMEDA			67	50
11	QP-SA			0	0

[a] The reactions were carried out at 80 °C for 5 h. The reaction scale was 0.22 mmol and a concentration of 0.143 M. [b] Conversion of starting material (**362**) to product (**365**) was measured by ^{1}H NMR spectroscopy. N/D: not determined.

In an attempt to improve the isolated yield of the reaction, a design of experiment analysis (DOE) was performed initially testing three factors; temperature, concentration of **362** and reaction time, while monitoring the response by measuring the isolated yield of **365**. The starting point for the design of the array was the optimum conditions obtained from the initial scoping (Table 15, entry 1). These conditions were used as the centre point for the DOE where "000" refers to the three variables (temperature, time and concentration of **362**) in their middle limits (i.e. temperature = 80 °C, time = 300 min and concentration of **362** = 0.14). We then decided to investigate a maximum limit and minimum limit for each variable. For the temperature, a range of ±40 °C was investigated, while for the time a range of ±120 min was chosen. The concentration of **362** was varied by ±0.07 M. These variations generated the profiles and results as shown in Tables 16 and 17. The cube plot for 1st full factorial screening (Figure 21) makes use of the difference in the middle points (Table 16, entry 3 and 10) as a factor of robustness and applies that factor to the yields of the other entries. Thus the yields shown on the cube plots are "corrected" yields.

Table 16: 1st Full factorial screening for conversion of compound **362**.

Entry	Pattern[a]	Temperature (°C)	Time (min)	Concentration of 362 (M)	Isolated yield (%)
1	-++	40	420	0.21	70
2	++-	120	420	0.07	31
3	000	80	300	0.14	51
4	+++	120	420	0.21	18
5	+--	120	180	0.07	43
6	+-+	120	180	0.21	33
7	--+	40	180	0.21	67
8	---	40	180	0.07	68
9	-+-	40	420	0.07	85
10	000	80	300	0.14	58

[a] Where '+' refers to the maximum limit, '-' refers to the minimum limit and '000' refers to the middle limits.

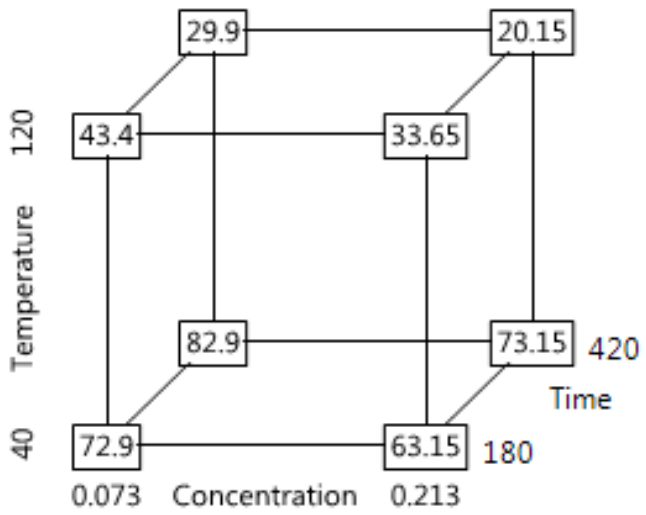

Figure 21: Cube plot for the 1st full factorial screening for **362**.

Having established that a combination of long reaction time, low concentration and low temperature gives the best yield (Table 16, entry 9), we decided to perform a second full factorial screening closer to this point. A temperature of 60 °C, reaction time of 390 min and concentration of **362** of 0.11 were used as the middle limits and a variation of ±20 °C, ±90 min and ±0.07 M for temperature, time and concentration of **362** respectively (Table 17). The cube plot for the second factorial design (Figure 22) again shows the "corrected" yields for the different entries in this series.

Table 17: 2nd Factorial screening for **362**.

Entry	Pattern [a]	Temperature (°C)	Time (min)	Concentration of 362 (M)	Isolated yield (%)
1	++-	80	480	0.04	71
2	---	40	300	0.04	66
3	+++	80	480	0.18	36
4	+-+	80	300	0.18	52
5	-+-	40	480	0.04	76
6	-++	40	480	0.18	56
7	+--	80	300	0.04	66
8	000	60	390	0.11	83
9	000	60	390	0.11	81
10	--+	40	300	0.18	76

[a]Where '+' refers to the maximum limit, '-' refers to the minimum limit and '000' refers to the middle limits.

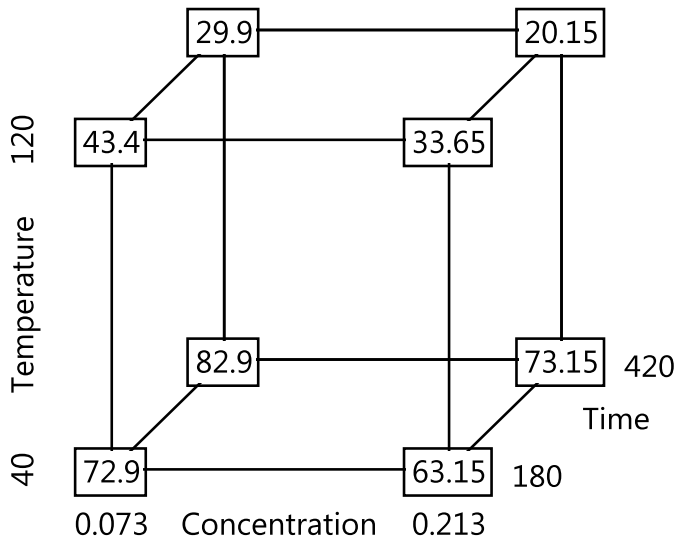

Figure 22: Cube plot for the 2nd factorial screening for **362**.

From the data it was concluded that elevated temperatures resulted in lower isolated yields, most probably due to decomposition of compound **358** or the resulting aldehyde. In general, lower concentration was beneficial but at a consequence of longer reaction times. The best results were entry 9, Table 16 and entries 8 and 9, Table 17 which

produced similar results. The latter conditions were selected to progress due to the increased productivity with regards to the higher concentration and shorter reaction time.

Having established an optimised set of conditions for the formation of thiazole **365**, we next turned our attention to exploring the versatility of the reaction by changing both the aromatic portion and the ester functionality of the substrate.

The majority of the starting materials required as substrates were synthesised according to known procedures (Scheme 77). Transesterification was used to prepare **367** from its corresponding ethyl ester. For compounds **372** and **373** a nucleophilic addition/elimination reaction was used between the corresponding substituted phenylacetonitrile and ethyl chloroformate **369** or diethyl carbonate **372** respectively. A nucleophilic aromatic substitution (S_NAr) reaction was used to generate **377** and **378** while a carbon-carbon coupling reaction catalysed by copper(I) iodide was used to generate **380**. A Knoevenagel condensation[137] between the corresponding benzaldehyde and either methyl cyanoacetate (for **382**), ethyl cyanoacetate (for **383**) or cyanoacetamide (for **389** and **390**) were used. The Knoevenagel condensation product was subsequently reduced to obtain the desired substrates (**384-385**, **391-392**). Finally, compounds **396-399**, were all obtained from the alkylation of either ethyl phenylcyanoacetate **362** or ethyl cyanoacetate **392**.

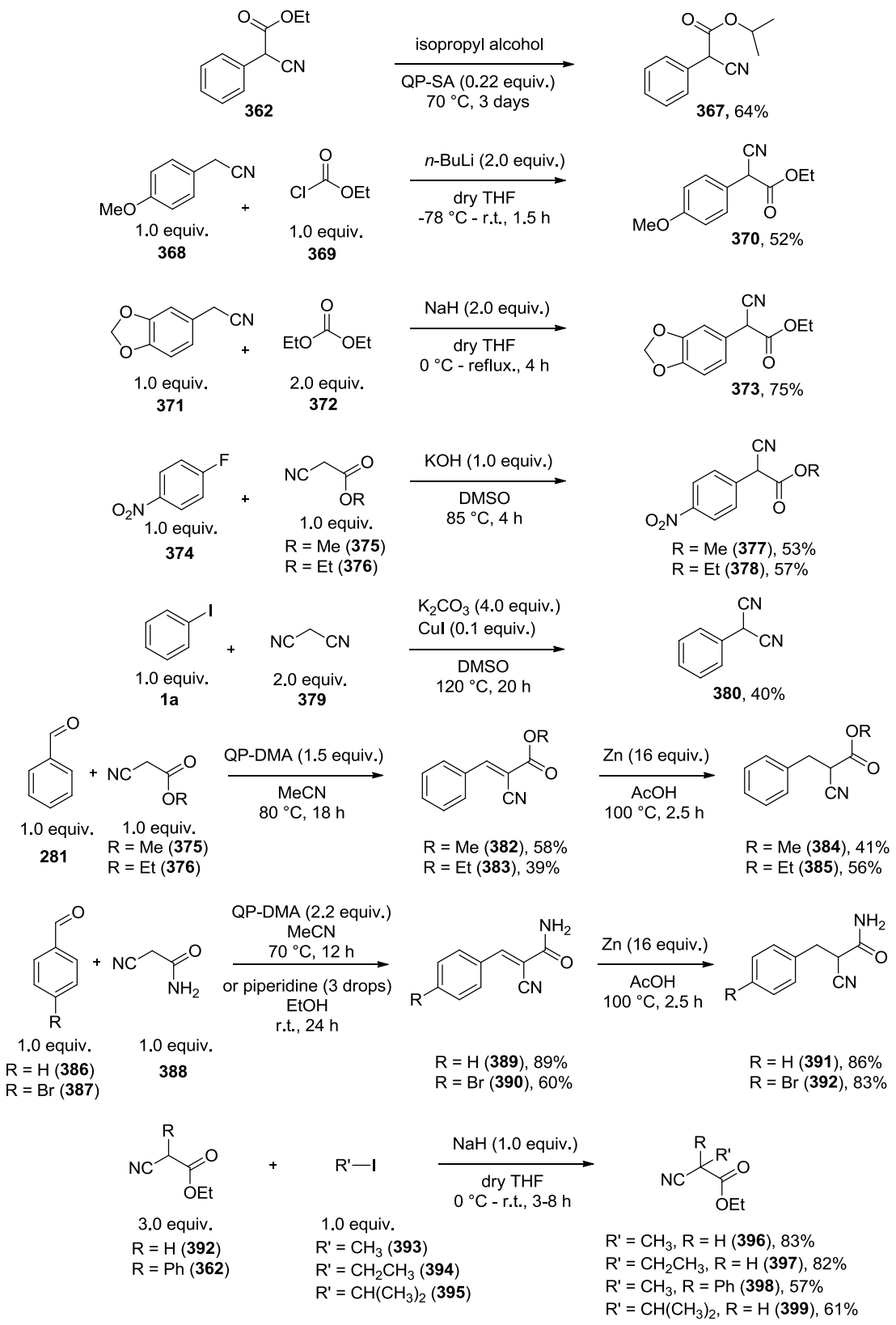

Scheme 77: Synthesis of starting materials.

To allow for direct comparison and evaluation of the influence of substrate variation on the reaction outcome, the optimal reaction conditions generated above were maintained. It should be noted that these reactions are therefore not optimised for each individual case

and that improvements in yield could be achieved as highlighted for substrate **411** (Scheme 78). In general, esters, amides and nitriles are tolerated, with methyl esters giving generally lower yields (hydrolysis occurs from water generated in the reaction) than the corresponding ethyl analogues (compounds **362-363** and **406-407**). The isopropyl ester **367** leads to a lower conversion and isolated yield of **400** presumably as a consequence of additional steric interactions. By changing the electronic character of the aromatic appendage, it was demonstrated that an electron donating group (**401** and **402**) gives rise to superior yields compared to an electron withdrawing group (**403** and **404**). This is presumably due to a subtle balance between the basicity and resulting nucleophilicity of the anion generated, which could, in the case of the more stable (electron withdrawing group) anion, enable a retro-aldol reaction to occur. Substituted malonitrile **380** were also tolerated forming the corresponding cyanothiazole **405** in good yield, with no indication of formation of the di-thiazole product. Benzyl groups can be incorporated (**406-409**) but give low yields (16-37% yields). Changing to an aliphatic group instead of the aromatic moiety (**406-411**) decreases the conversion. Substrates possessing a methyl or an ethyl group react well (**410-411**) but moving to an isopropyl group such as in molecule **399** (Figure 23), reproducibly failed to generate any product, indicating the steric limits of the reaction (A-values for methyl and ethyl substituents are 1.70 and 1.35 kcal mol^{-1} respectively while that of an isopropyl is 2.15 kcal mol^{-1}).[93]

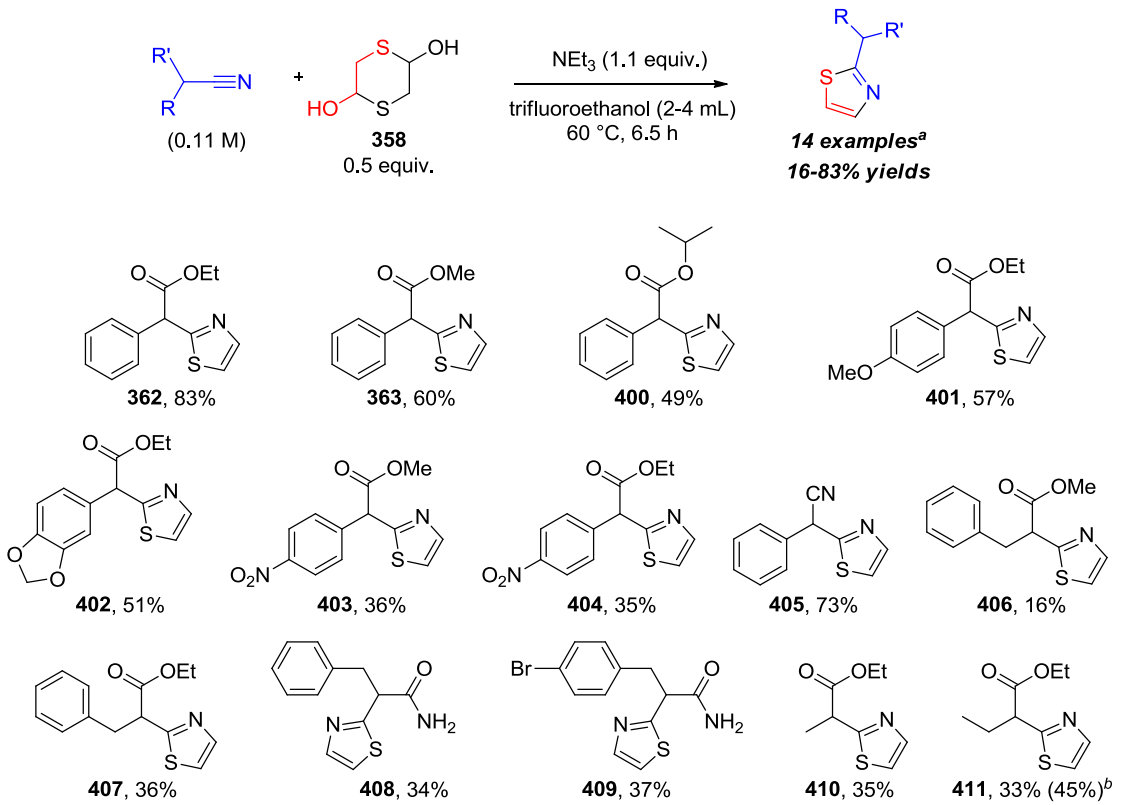

Scheme 78: Scoping of the 2-substituted thiazole formation.
[a] Conditions: 0.22-0.44 mmol scale. [b] 0.50 equiv. 1,4-dithian-2,5-diol (**358**) followed by another 0.50 equiv. of **358** after the first 6.5 h, 0.22 mmol of nitrile, NEt_3 (1.10 equiv.), 2 mL trifluoroethanol, 80 °C, 10.5 h.

Some of the substrates tested failed to generate any product under the standard reaction conditions (Figure 23) which helped to identify certain attributes of the mechanism. For example, phenyl acetonitrile (**412**) failed to react most likely due to the lower acidity of the α-methylene protons. It also failed to form any product when using different bases, namely; polymer supported 2-tert-butylimino-2-diethylamino-1,3-dimethylperhydro-1,3,2-diazaphosphorine (BEMP), 1,8-diazabicyclo[5.4.0]undec-7-ene (DBU) or potassium *tert*-butoxide. Our observations led us to conclude that weaker bases (triethylamine and DBU) were insufficiently strong to deprotonate the benzylic position of **412** (pK_a = 21.9 in DMSO)[138] whereas the stronger bases (BEMP and potassium *tert*-butoxide) were too harsh and led to decomposition of the 1,4-dithian-2,5-diol (**358**).

Diethyl 2-cyanomalonate **413** also proved unreactive, this substrate would be expected to form an extensively delocalised anion which would be a correspondingly poor nucleophile. In addition, substrate **398**, lacking an acidic proton, was recovered quantitatively from the reaction. Finally, compound **399**, as mentioned previously,

possessing a high degree of steric hindrance around the α-carbon adjacent to the cyano group evidenced inhibition of the reaction.

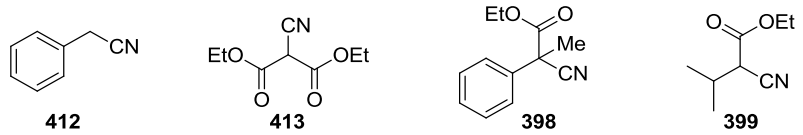

Figure 23: Substrates which did not react under the optimised conditions.

To ascertain that our hypothesis on the origin of selectivity in the synthesis leading to either a thiazole or a thiophene depends on the environment of the carbon adjacent to the nitrile group, the optimised conditions for **362** were used on three substrates (**414**, **376** and **388**). These all possessed an α-methylene adjacent to the nitrile group and upon reaction gave exclusively the 2-aminothiophene products (**415-417**) in good to excellent yields (Scheme 79).

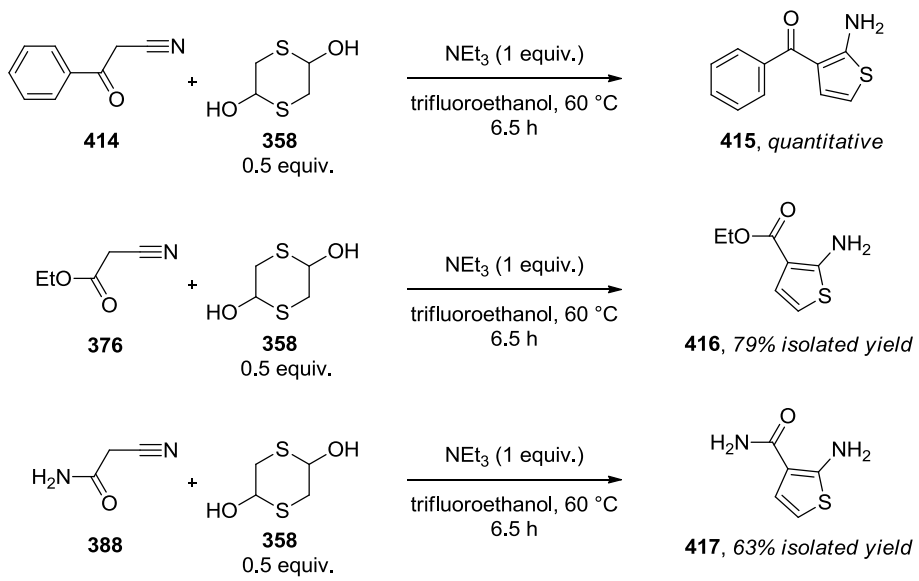

Scheme 79: Illustration of substrates that form thiophenes under Gewald-type conditions.

2.3.2.2 Discussion on the Mechanism

The pathway resulting in thiophene formation (Scheme 80) follows the Gewald mechanism,[126] where the base-promoted deprotonated nitrile precursor (**418**) attacks the aldehyde component **361** (generated from 1,4-dithian-2,5-diol) to give intermediate **419**. This intermediate undergoes a 5-exo-dig cyclisation to form intermediate **420** which after dehydration and proton transfer gives the 2-aminothiophene product **422**. However, the alternative mechanism generating the alternative thiazole had not previously been reported and initially presented some queries. We envisaged two putative mechanisms

for the formation of the thiazole (Scheme 81), which could be involved depending on the specific nitrile substrate involved. Mechanism A is theoretically valid when a methine or methylene group is present in the α-position adjacent to the nitrile group, which is reminiscent of the original Gewald reaction mechanism (Scheme 80). Alternatively, mechanism B would be viable for molecules which possess no protons adjacent to the nitrile group. However, the fact that compounds **398** and **399** did not react implies mechanism A is the predominant pathway. The lack of reactivity encountered with substrate **399** can be attributed to the high degree of steric hindrance inhibiting the nucleophilic attack of the enol formed from **399**. In summary, although the evidence indicates mechanism A is the most likely pathway under the conditions studied in this thesis, it should be noted that several benzonitrile derivatives have been shown to successfully result in thiazole formation when reacted with coupling partners such as 2-mercaptopropionic acid therefore mechanism B may operate under certain conditions.[139]

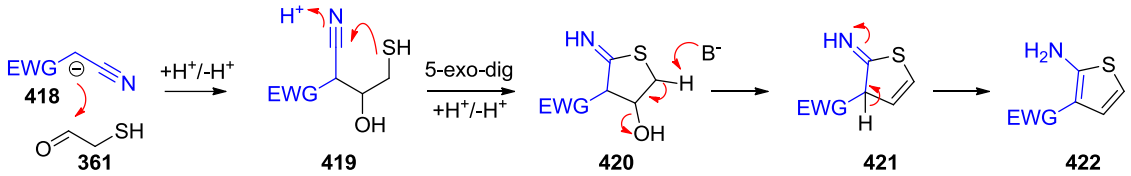

Scheme 80: Gewald mechanism for the synthesis of 2-aminothiophenes.

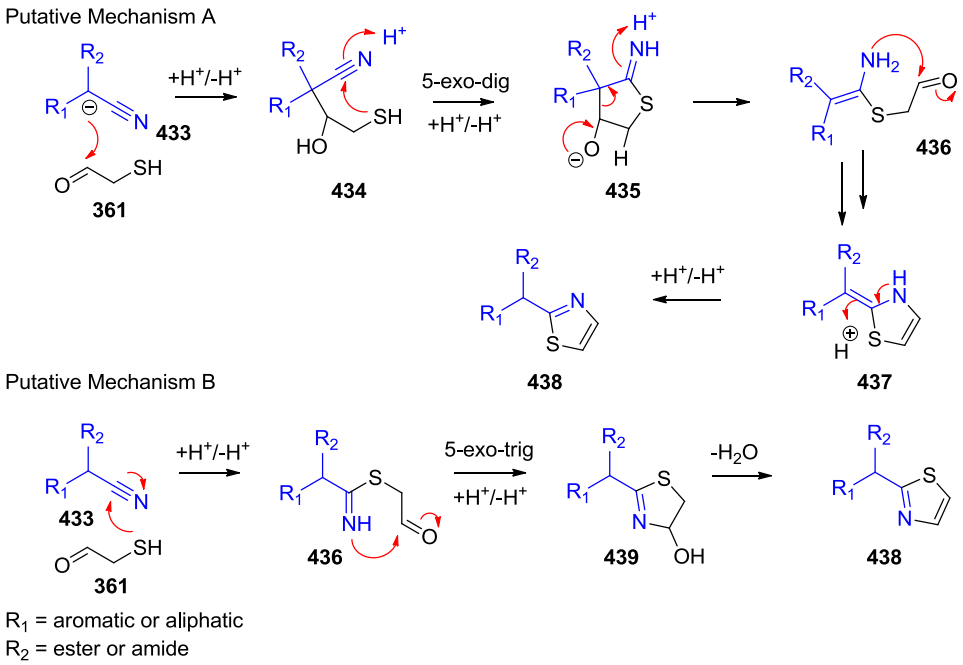

Scheme 81: Proposed mechanisms for the formation of thiazoles.

2.3.2.3 Stability of 2-Substituted Thiazoles

It was noted that ethyl 2-phenyl-2-(thiazol-2-yl)acetate (**362**) changed from a yellow oil to a semi-crystalline material on prolonged standing in air, which when analysed by TLC and ^{1}H NMR spectroscopy showed that the composition had changed. Glycolate **441** was isolated as the main oxidation product through column chromatography. Some related oxidations have previously been described, however, these processes have employed either a palladium catalyst[140] or strong bases such as Cs_2CO_3[141] in the presence of oxygen.

To examine this oxidation in more detail, a fresh batch of **362** was synthesised and then left in a vial exposed to the atmosphere at ambient temperature. After 7 days the ratio of the degradation products was analysed by ^{1}H NMR (71:5:24 for **362**, **440** and **441** respectively). The ratio changed further when left for longer periods (>10 months ratio was 26:7:67 for **362**, **440** and **441** respectively, Scheme 82). Bubbling oxygen through a 0.5 M DMSO-d_6 solution of **362** for 24 h did not show any formation of either **440** or **441**.

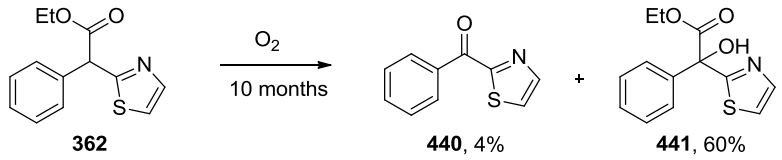

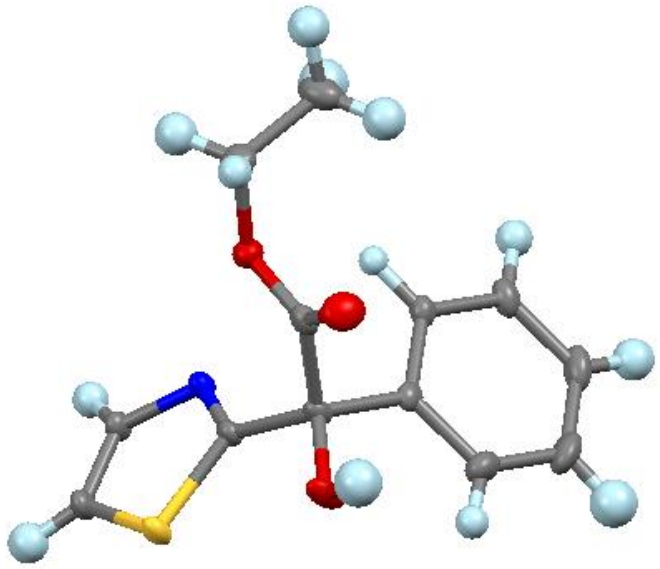

X-Ray structure of 441

Scheme 82: Aerobic oxidation of **362** to give glycolate **441**.

We hypothesise that the two oxidation products (**440** and **441**) are generated through initial enolisation and reactive trapping of oxygen. Even though no base is present for the

deprotonation, the natural enolisation would be sufficient for the reactive trapping of oxygen, albeit slowly. It has previously been reported that hydroperoxides such as **442a-b** cyclise in the presence of a carbonyl moiety to generate a 1,2-dioxetane intermediate **443** that upon decomposition generate carbonyl products **161** and **444** (Scheme 83).[142] It has also been reported that hydroperoxides such as **445** can be reduced with DMSO in the presence of gold nanoclusters stabilized by poly(*N*-vinyl-2-pyrrolidone) (Au:PVP) to form **447** (Scheme 83).[143]

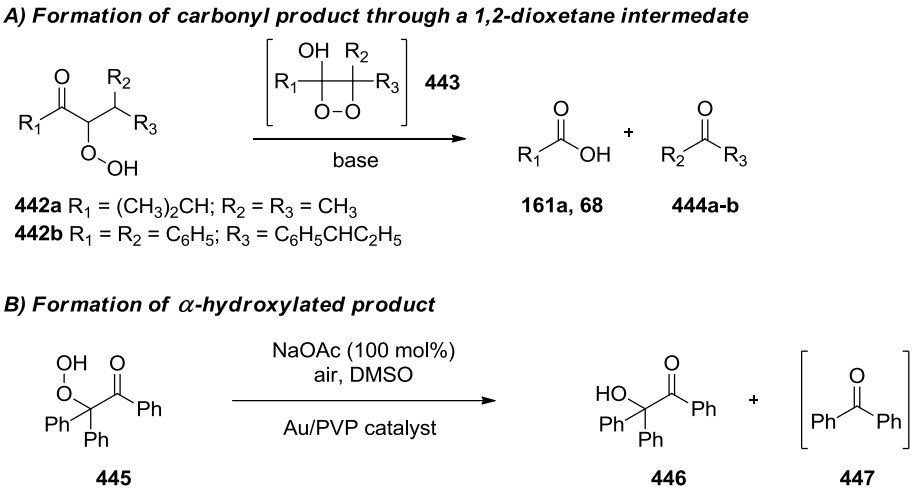

Scheme 83: A) Formation of carbonyl products through 1,2-dioxetane intermediate.[142] B) Formation of α-hydroxylated products with Au/PVP catalyst in DMSO.[143]

Based on these reported reactions, it was hypothesised that the initially formed peroxide intermediate **453** could then potentially cyclise onto the adjacent ester moiety forming a dioxetane intermediate **455** which, after extrusion of CO_2, would furnish product **440** (Scheme 85). Alternatively, the peroxide intermediate **453** could undergo homolytic cleave to form the oxygen-centred radical (**454**) that abstracts a hydrogen atom to form the glycolate **441**. It is also possible that compound **440** is the result of ester hydrolysis (water generated in the formation of **441**), followed by decarboxylation to yield the simple 2-benzyl thiazole. Such compounds are known to oxidise to their corresponding ketones[144] or undergo a 1,2-rearrangement followed by a spontaneous decomposition to form **440**, such as the rearrangement observed with α-hydroperoxy α-alkoxy ketone **448** in the formation of benzoic acid **68** and methyl acetate **450** through the intermediate **449** (Scheme 84).[145]

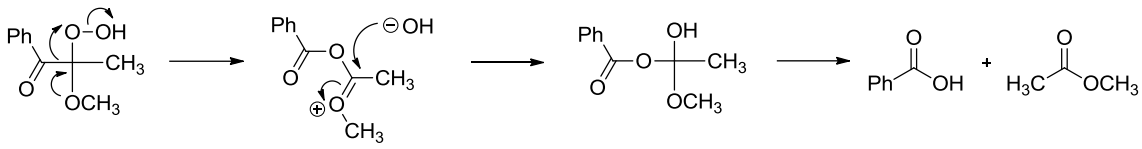

Scheme 84: 1,2- Rearrangement of α-hydroperoxy α-alkoxy ketone **448**.

A further proposed mechanism, not involving the initial enolisation, could be one involving an initial homolytic cleavage of the C-H bond, forming a carbon centred radical **456** which would then go on to react with oxygen to form the peroxo-radical **457** (Scheme 85). The peroxo-radical **457** can then either react with a hydrogen atom to form **453** as part of the formation of **441**, or form the dioxetane intermediate **455** to yield **440**. Similar to mechanism A, there is nothing that induces the initial homolytic cleavage to initiate the reaction, however, we are convinced that considering the long reaction time needed for the transformation, small amounts of **451** or **456** are naturally formed due to the acidic C-H bond present in **362**.

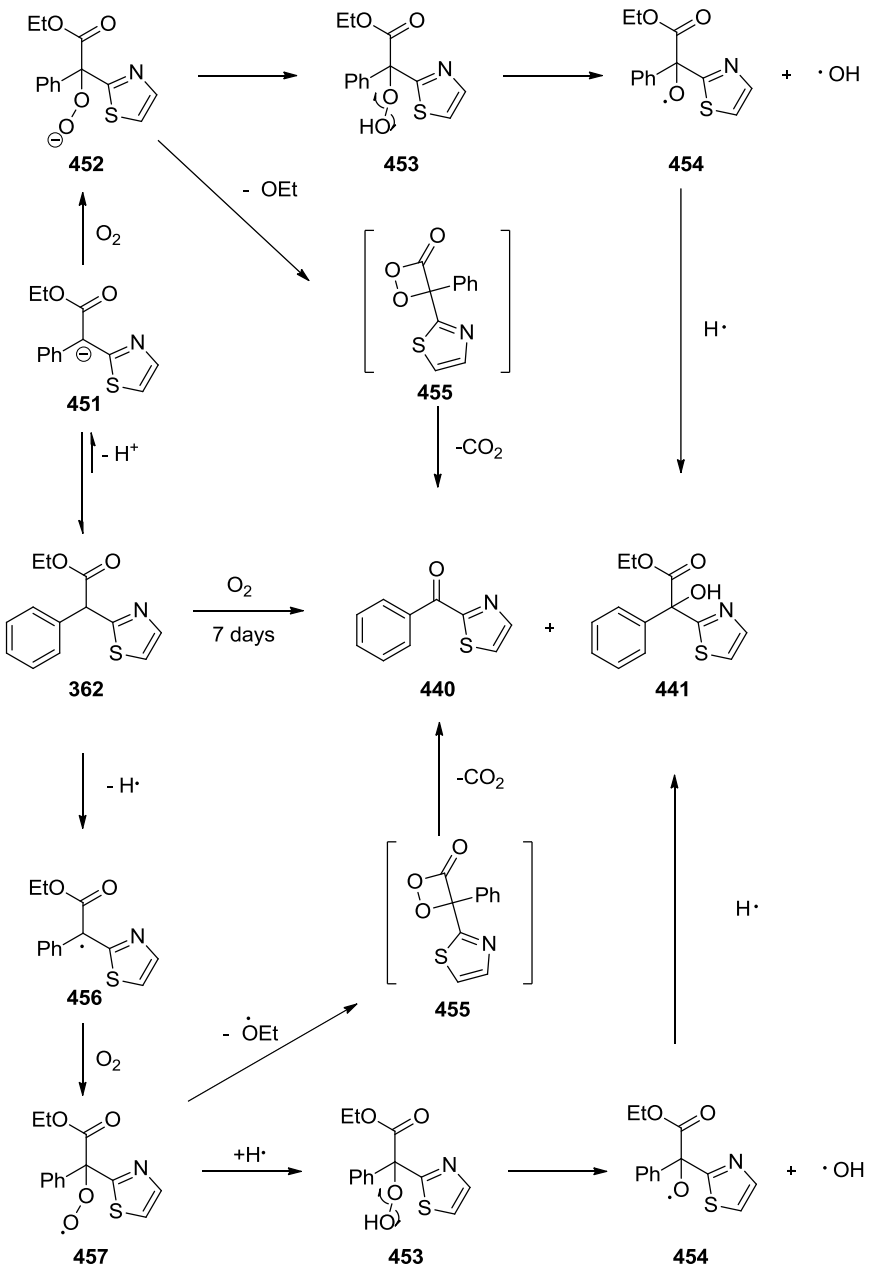

Scheme 85: (Top) putative mechanism A for the formation of **441**, (bottom) putative mechanism A for the formation of **441**.

2.3.4 Conclusions

In an effort to expand the scope of using 1,4-dithian-2,5-diol as a precursor for 2-mercaptoacetaldehyde for the formation of sulfur containing heterocycles, it was successfully shown that α-substitution of the nitrile precursor predetermines the reaction outcome yielding exclusively a thiophene or a thiazole product (Scheme 86).

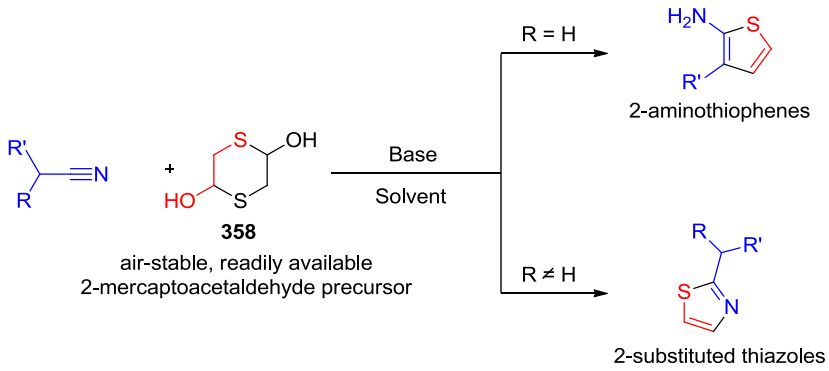

Scheme 86: Bifurcation pathway giving the 2-aminothiophenes or 2-substituted thiazoles accordingly.

The presence of an alkyl or aryl substituent adjacent to the cyano group leads selectively to the thiazole product by blocking the Gewald type reaction mechanism responsible for the formation of the 2-aminothiophene. In the study, the thiazole formation from the appropriately substituted *α*-methine nitrile compounds was evaluated using DOE to determine a general reaction conditions. The DOE derived conditions were used to evaluate the scope of the reaction and demonstrated that most substrates evaluated gave the expected 2-substituted thiazole in a range of yields which was dependant on the substitutents at the *α*-position of the nitrile group.

The synthesis of 2-subsituted thiazoles from readily available, air stable 1,4-dithiane-2,5-diol (**358**) as a precursor for 2-mercaptoacetaldehyde was thus demonstrated to be an effecient tranformation that can be used to functionalise *α*-disubstituted nitriles. One such example being (*S*)-dolaphenine (Doe), a highlighted part of dolastatin 10 (**340** in Figure 19), which could be directly synthesised using this methodology. This was previously synthesised through a multiple-step synthesis in overall low yields (65% yield and 51% both before amine deprotection).[146] Further substitution of 2-substituted thiazoles can also be easily achieved through published protocols to form 2,4-substituted thiazoles, 2,5-substituted thiazoles and also 2,4,5-substituted thiazoles making the synthesised products from this work valuable precursors.[136]

Finally, the natural air oxidation of ethyl 2-phenyl-2-(thiazol-2-yl)acetate **362** to the corresponding glycol was described which is thought to form through the enolisation of the substrate followed by reactive trapping of oxygen, cyclisation and subsequent elimination to form the glycolate **441**.

Experimental Information

Unless specified, reagents were obtained from commercial sources and used without further purification. Solvents were obtained from Fisher scientific, and H_2O was deionised before use.

NMR spectra were recorded on either Bruker Avance-400, Varian VNMRS-600 or Varian VNMRS-700 instrument and was calibrated to the residual solvent according to the literature.[147] Assignments are based on DEPT-135, COSY, NOESY, HSQC and HMBC spectra.

Liquid chromatography-mass spectrometry (LCMS) was performed on an Agilent HP 1100 series chromatograph (Mercury Luna 3µ C18 (2) column) attached to a Waters ZQ2000 mass spectrometer with ESCi ionisation source in ESI mode. Elution was carried out at a flow rate of 0.6 mL/min using a reverse phase gradient of MeCN–water containing 0.1% formic acid. Gradient = 0–1 min: hold MeCN 5%, 1–4 min: ramp MeCN 5–95%, 4–5 min: hold MeCN 95%, 5–7 min: ramp MeCN 95–5%, 7–8 min: hold MeCN 5%. Retention times are reported as Rt. High resolution mass spectra (HRMS) were recorded on a Waters Micromass LCT Premier spectrometer using time of flight with positive electrospray ionisation (ESI+), an ABI/MDS Sciex Q-STAR Pulsar with ESI+ and an ASAP (atmospheric pressure solids analysis probe ionisation), or a Bruker BioApex II 4.7e FTICR utilising either ESI+ or a positive electron ionisation (EI+) source equipped with a direct insertion probe. The mass reported is that containing the most abundant isotopes (^{35}Cl and ^{79}Br). Limit: ± 5 ppm.

IR spectra were recorded neat on a Perkin-Elmer Spectrum Two FT-IR spectrometer using Universal ATR sampling accessories. Letters in parentheses refer to the relative absorbency of the peak: w – weak (<40% of the most intense peak), m – medium (40–75% of the most intense peak), s – strong (>75% of the most intense peak) and br – broad.

Elemental analysis was carried out on an Exeter CE-440 Elemental Analyser with the combustion tube set at an initial 950 ºC which is then elevated at above 1800 ºC.

Melting points were recorded on an Optimelt automated melting point system with a heating rate of 1 °C/min (70% onset point and 10° clear point) and are uncorrected.

X-ray diffraction experiment for **128** was carried out on a D8 Venture 3-circle Bruker AXS diffractometer with a PHOTON 100 CMOS area detector, using graphite-monochromated Mo-K_α radiation ($\bar{\lambda}$=0.71073 Å) from IµS microsource and a Cryostream (Oxford Cryosystems) open-flow N_2 cryostat. The structure was solved by direct methods (SHELXS 2013/1 software[148]) and refined by full-matrix least squares against F^2 of all reflections, using OLEX2[149] and SHELXL 2014/7 software.[150] Crystallographic data for structure **128** have been deposited with the Cambridge Crystallographic Data Centre as supplementary publication CCDC- 1470506.
X-ray diffraction experiment for **323** was carried out on a D8 Venture 3-circle diffractometer (Bruker AXS) with a PHOTON 100 CMOS area detector, using Mo-$K\alpha$ radiation ($\bar{\lambda}$=0.71073 Å) from an IµS microsource with focusing mirrors. The crystal was maintained at T=120 K using a Cryostream (Oxford Cryosystems) open-flow N_2 cryostat. The structure was solved by direct methods and refined by full-matrix least

squares against F^2 of all reflections, using OLEX2,[149] SHELXS 2013/1[148] and SHELXL 2014/7[150] software.

X-ray diffraction experiment for compound **441** have been collected at 120.0(2)K on an Agilent XCalibur 4-circle diffractometer (Sapphire-3 CCD detector, graphite monochromator, λMoKα, λ = 0.71073Å, ω-scan, 1.0°/frame) equipped with a Cryostream (Oxford Cryosystems) open-flow nitrogen cryostat. The structures was solved by direct method and refined by full-matrix least squares on F^2 for all data using Olex2[149] and SHELXTL[148] software. All non-hydrogen atoms were refined anisotropically, hydrogen atoms were found in the difference Fourier maps and refined isotropically. Crystallographic data for structure **441** have been deposited with the Cambridge Crystallographic Data Centre as supplementary publication CCDC-1049429.

General Procedures for Chapter 2.1:

A) Ortho-substituted carbonylation in flow.

For a typical reaction, a Vapourtec R2+ Series was used as the platform with a Vapourtec Gas / Liquid Membrane Reactor to load the carbon monoxide. The HPLC pumps were both set at 0.125 mL/min, the temperature of the reactor at 110 °C, the pressure of CO at 15 bar with a back pressure regulator of 250 psi (17.24 bar). The system was left running for 2 h to reach steady state after which the flow streams were switched to pass from the loops where the substrates and catalysts were loaded. The first loop (5 mL) was filled with a solution of palladium acetate (20 mg, 0.08 mmol), triphenylphosphine (48 mg, 0.168 mmol) in 6 mL of 1,4-dioxane while the second loop (5 mL) was filled with a solution made from the ortho-substituted iodoarene substrate (1.68 mmol), triethylamine (0.272 g, 0.374 mL, 2.69 mmol) and water (0.505 g, 28 mmol) in 5.8 mL of 1,4-dioxane.

An Omnifit® column filled with 1.71 cm^3 (r = 0.33 cm, h = 5.00 cm) of cotton was positioned just before the back pressure regulator to trap any particulate matter. This avoided blocking of the back pressure regulator. After the substrates were passed through the system, the outlet of the flow stream was directed into a receptacle where the excess carbon monoxide gas was vented off into the fume cupboard. The reaction mixture was then evaporated to dryness, EtOAc (25 mL) and sodium carbonate solution (2 M, 10 mL) were added and transferred to a separating funnel. After collecting the aqueous layer, the organic layer was extracted again with sodium carbonate solution (2 M, 2 x 10 mL). The combined aqueous layers were acidified (monitored using pH paper) by the addition of 2 M HCl solution which was then extracted with EtOAc (3 x 25 mL). The organic layer was dried over sodium sulfate, and the solvent evaporated under vacuum to give the crude product. The crude product was then recrystallised from the appropriate solvent to give the pure product.

B) Ortho-substituted carbonylation in batch (Conventional Lab).

A solution of palladium acetate (20 mg, 0.08 mmol) and triphenylphosphine (48 mg, 0.168 mmol) in 11.8 mL of 1,4-dioxane was prepared, to which 2-chloro-iodobenzene (0.401g, 1.68 mmol), triethylamine (0.272 g, 0.374 mL, 2.69 mmol) and water (0.505 g, 28 mmol) were added in a N_2 filled 25 mL flask. A balloon (made from two balloons inside each other) of carbon monoxide was attached to the flask and the flask was emptied through an empty needle. This process was repeated and then the third time the carbon monoxide in the balloon was not emptied by removing the empty needle. The reaction was heated to reflux, cooled after 2 h or 24 h, solvent evaporated and the same extraction/purification for the flow protocol was repeated using MeCN to recrystallise the product.

C) Ortho-substituted carbonylation in batch (High-Pressure Lab).

A solution of palladium acetate (80 mg, 0.32 mmol) and triphenylphosphine (192 mg, 0.672 mmol) in 24 mL of 1,4-dioxane was prepared and stirred for 15 min., to which a solution of 2-chloro-iodobenzene (1.602 g, 6.72 mmol), triethylamine (1.088 g, 1.50 mL, 10.76 mmol) and water (2.02 g, 112 mmol) in 24 mL of 1,4-dioxane was added in the Parr autoclave (stainless steel, 100 mL capacity, 200 bar maximum pressure). The autoclave was tightly sealed and placed in the heating rig. The autoclave was then purged with nitrogen (3 x 10 bar) and with carbon monoxide (3 x 10 bar), keeping 10 bar of

carbon monoxide in the autoclave at which point it was heated to 110 °C over 15 min. The carbon monoxide pressure was adjusted to 15 bar and the reaction was left stirring for 2 h and was then cooled down to 30 °C over 2 h. The autoclave was then purged with nitrogen (4 x 10 bar) and the reaction mixture removed from the autoclave. The same extraction/purification sequence as for the flow protocol was repeated.

Spectroscopic and experimental data for Chapter 2.1:

(4-Bromo-3-iodophenyl)methanol, 121:

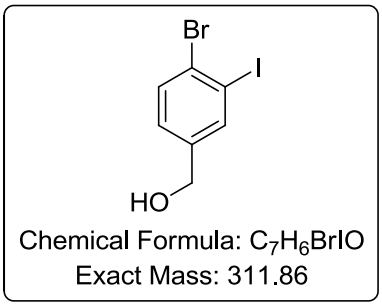

To a suspension of 4-bromo-3-iodobenzaldehyde (1.24 g, 4.0 mmol) in MeOH (6 mL) at 0 ºC was added $NaBH_4$ (0.08 g, 2.0 mmol) in small portions over 10 min. The reaction mixture was allowed to warm to room temperature and left stirring for 1 h. The solvent was then evaporated under vacuum and the residue was dissolved in EtOAc (25 mL) and washed with brine solution (3 x 25 mL). The organic layer was dried over sodium sulfate and the solvent evaporated under reduced pressure to give the desired product as white solid which was used without further purification.

Isolated yield: 1.17 g (93%, 4.00 mmol scale);

White crystals (recrystallised from $CHCl_3$);

^{1}H NMR (400 MHz, $CDCl_3$) δ/ppm δ 7.85 – 7.81 (d, *J* = 4.0 Hz, 1H), 7.55 (d, *J* = 8.2 Hz, 1H), 7.17 – 7.12 (dd, *J* = 4.0, 8.0 Hz 1H), 4.56 (s, 2H), 2.35 (s, br, 1H);

^{13}C NMR (101 MHz, $CDCl_3$) δ/ppm 141.5 (C), 138.6 (CH), 132.7 (CH), 128.7 (C), 128.0 (CH), 101.4 (C), 63.3 (CH_2);

IR (neat) ν = 3293 (br, C-OH), 2921 (w), 1450 (m), 1387 (m), 1195 (w), 1101 (m), 1006 (s), 808 (s) cm^{-1};

LC-MS (MeCN), Rt. 2.14 min, m/z = 295.14 $[M-H_2O]^+$. HR-MS (ESI-TOF) calculated for C_7H_5BrI 294.8619, found 294.8625 (Δ = 2.0 ppm).

M.p. 44-47 °C ($CHCl_3$).

1-Bromo-4-(ethoxymethyl)-2-iodobenzene, 122:

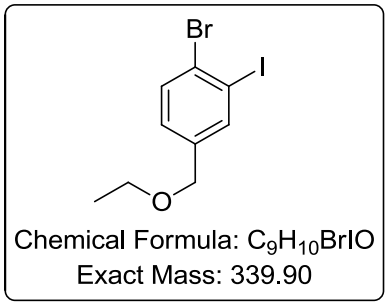

To a solution of (4-bromo-3-iodophenyl)methanol (**121**) (1.15 g, 3.67 mmol) in THF (4 mL) was added NaH (60% in hexane, 0.224 g, 5.5 mmol) in small portions over 5 min while keeping the reaction mixture at 0 ºC. Iodoethane (0.860 g, 0.44 mL, 5.5 mmol) was then added to the reaction mixture after which it was allowed to warm to room temperature and left stirring for 2 h. The reaction solvent was evaporated under vacuum and the residue was dissolved in EtOAc (25 mL) and washed with brine (3 x 25 mL). The organic layer was dried over sodium sulfate and the solvent evaporated under reduced pressure to give the desired product as yellow oil which was purified using flash silica chromatography 0.5:9.5 – 2:3 EtOAc/hexane gradient to give the product as a colourless liquid.

Isolated yield: 0.698 g (56%, 3.67 mmol scale);

Colourless liquid, Rf: 0.32 (2/8, EtOAc/hexane);

^{1}H NMR (400 MHz, $CDCl_3$) δ/ppm 7.87 (dt, *J* = 1.9, 0.7 Hz, 1H), 7.60 (d, *J* = 8.2 Hz, 1H), 7.20 (ddt, *J* = 8.2, 2.0, 0.7 Hz, 1H), 4.43 (d, *J* = 0.8 Hz, 2H), 3.56 (q, *J* = 7.0 Hz, 2H), 1.27 (t, *J* = 7.0 Hz, 3H);

^{13}C NMR (101 MHz, $CDCl_3$) δ/ppm 139.5 (C), 139.2 (CH), 132.5 (CH), 128.6 (CH), 128.5 (C), 101.1 (C), 71.0 (CH_2), 66.1 (CH_2), 15.2 (CH_3);

IR (neat) ν = 2974 (w), 2865 (w), 1454 (m), 1383 (m), 1100 (s), 1009 (m), 811 (m) cm^{-1};

GC-MS (MeCN), Rt. 4.72 min, m/z = 340.0 $[M]^+$. LC-MS (MeCN), Rt. 4.31 min, m/z = 294.86 $[M\text{-}EtOH]^+$, HR-MS (ESI-TOF) calculated for C_7H_5BrI 294.8619, found 294.8611 (Δ = 2.7 ppm), ASAP (MeCN), Rt. 0.51 min, m/z = 335.9 $[M+EtOH+MeCN]^+$. HR-MS ($^+$AP-TOF) calculated for C_9H_8BrIN 335.8885, found 335.8875 (Δ = 3.0 ppm), ASAP (MeCN), Rt. 0.51 min, m/z = 381.9 $[M+H+MeCN]^+$. HR-MS (AP-TOF) calculated for $C_{11}H_{14}BrINO$ 381.9304, found 335.9297 (Δ = 1.8 ppm).

(*Rac*)-(2*S*,4*S*,5*R*)-4-*tert*-butyl 2-ethyl 5-(4-bromo-3-iodophenyl)-4-methylpyrrolidine-2,4-dicarboxylate, 126:

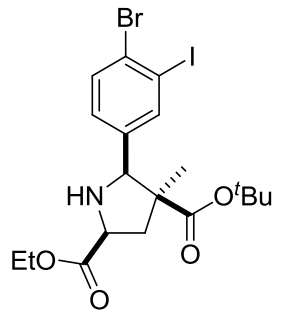

Chemical Formula: $C_{19}H_{25}BrINO_4$
Exact Mass: 537.00

To a suspension of 4-bromo-3-iodobenzaldehyde (1.24 g, 4.0 mmol) and glycine hydrochloride (0.838 g, 6.0 mmol) in MeCN (6 mL), triethylamine (0.836 g, 6.0 mmol) was added and reaction mixture was stirred at room temperature for 4 h. The reaction solvent was evaporated under vacuum and the residue was dissolved in EtOAc (25 mL) and washed with brine solution (3 x 25 mL). The organic layer was dried over sodium sulfate and the solvent evaporated under vacuum to give the desired imine intermediate which was used in the next step without further purification. The imine intermediate was dissolved in THF (6 mL) and *tert*-butyl methacrylate (1.138 g, 8.0 mmol) was added followed by lithium bromide (0.694 g, 8.0 mmol) and triethylamine (1.11 g, 8.0 mmol). The reaction mixture was stirred at room temperature for 2 h after which the reaction solvent was evaporated under reduced pressure and the residue dissolved in EtOAc (25 mL) and washed with brine (3 x 25 mL). The organic layer was dried over sodium sulfate and the solvent evaporated under vacuum to give the desired crude product as a yellow oil which was purified using flash silica chromatography 1:9 EtOAc/hexane.

Isolated yield: 2.00 g (93%, 4.0 mmol scale);

Yellow oil, Rf: 0.15 (2/8, EtOAc/hexane);

^{1}H NMR (600 MHz, $CDCl_3$) δ/ppm; 7.83 (d, *J* = 2.1 Hz, 1H), 7.52 (d, *J* = 8.3 Hz, 1H), 7.22 (dd, *J* = 8.3, 2.2 Hz, 1H), 4.25 (q, *J* = 7.1 Hz, 2H), 3.98 – 3.92 (m, 2H), 2.73 (s, br, 1H), 2.60 (dd, *J* = 13.2, 8.9 Hz, 1H), 2.04 (dd, *J* = 13.2, 8.1 Hz, 1H), 1.42 (s, 3H), 1.31 (t, *J* = 7.1 Hz, 3H), 1.12 (s, 9H).

^{13}C NMR (151 MHz, $CDCl_3$) δ/ppm 173.6 (C), 173.0 (C), 141.5 (C), 139.3 (CH), 132.2 (CH), 128.6 (CH), 128.5 (C), 100.9 (C), 81.2 (C), 71.4 (CH), 61.3 (CH_2), 58.8 (CH), 55.1 (C), 41.3 (CH_2), 27.7 (CH_3), 24.4 (CH_3), 14.4 (CH_3);

IR (neat) ν = 2997 (w), 1933 (w), 1717 (s, C=O), 1449 (m), 1367 (m), 1248 (s), 1149 (s), 1110 (s), 1033 (m), 1009 (m), 847 (m) cm^{-1};

LC-MS (MeCN), Rt. 3.77 min, m/z = 538.4 $[M+H]^+$. HR-MS (ESI-TOF) calculated for $C_{19}H_{25}BrINO_4$ 538.0090, found 538.0073 (Δ = 3.2 ppm).

(*Rac*)-(2*S*,4*S*,5*R*)-4-*tert*-butyl 2-ethyl 5-(4-bromo-3-iodophenyl)-1-ethyl-4-methylpyrrolidine-2,4-dicarboxylate, 128:

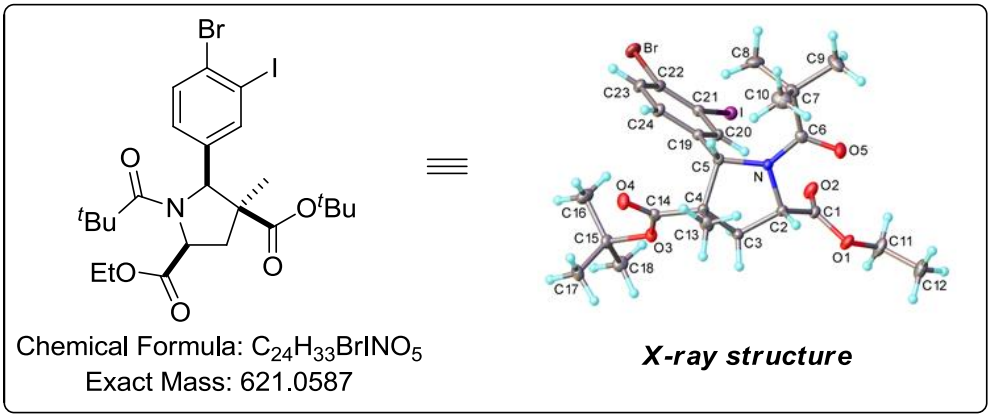

To a solution of compound **126** (2.0 g, 3.72 mmol) in DCM (4 mL) was added pivolyl chloride (0.580 g, 0.594 mL, 4.83 mmol) followed by triethylamine (0.489 g, 0.674 mL, 4.83 mmol) and the reaction was stirred at room temperature for 2 h. The reaction mixture was washed with brine (3 x 25 mL) and the organic layer dried over sodium sulfate and the solvent evaporated under vacuum to give the desired product as a yellow oil which was purified using flash silica chromatography 1:9 EtOAc/hexane.

Isolated yield: 1.49 g (65%, 3.72 mmol scale);

White crystals (recrystallised from CH_3Cl), Rf: 0.24 (2/8, EtOAc/hexane);

^{1}H NMR (600 MHz, $CDCl_3$) δ/ppm 8.04 (s, 1H), 7.83 (d, *J* = 8.3 Hz, 1H), 7.57 (d, *J* = 8.3 Hz, 1H), 4.95 (s, 1H), 4.50 (dd, *J* = 12.0, 7.1 Hz, 1H), 4.29 (q, *J* = 7.1 Hz, 2H), 2.46 (t, *J* = 12.6 Hz, 1H), 1.96 (dd, *J* = 13.1, 7.1 Hz, 1H), 1.42 (s, 3H), 1.33 (t, *J* = 7.1 Hz, 3H), 1.22 (s, 9H), 1.07 (s, 9H);

^{13}C NMR (151 MHz, $CDCl_3$) δ/ppm δ 178.5 (C), 172.2 (C), 170.5 (C), 140.8 (C), 140.1 (CH), 132.4 (CH), 129.5 (CH), 129.0 (C), 100.7 (C), 82.1 (C), 69.0 (CH), 61.2 (CH_2), 60.9 (CH), 56.1 (C), 39.5 (C), 32.6 (CH_2), 28.3 (CH_3), 27.7 (CH_3), 23.5 (CH_3), 14.2 (CH_3);

IR (neat) ν = 2975 (w), 2935 (w), 1743 (s, C=O), 1722 (s, C=O), 1632 (s, amide I band), 1456 (m), 1394 (m), 1251 (m), 1197 (s), 1167 (s), 1129 (s), 730 (s) cm^{-1};

LC-MS (MeCN), Rt. 4.05 min, m/z = 622.5 $[M+H]^+$. HR-MS (ESI-TOF) calculated for $C_{24}H_{34}BrINO_5$ 622.0665, found 622.0662 (Δ = 0.5 ppm).

Crystal data: **128**, $C_{24}H_{33}BrINO_5$, *M*=622.32, *T*=120 K, triclinic, space group $P\bar{1}$ (No. 2), *a*=8.8223(5), *b*=9.7894(5), *c*= 17.1881(9) Å, α= 94.479(2), β= 101.255(2), γ= 116.252(2)º, *V*= 1282.7(1) Å^3, *Z*=2, D_c=1.611 g cm^{-3}, μ=0.74 mm^{-1}, 34192 reflections with 2θ≤71.7º, 10848 unique, R_{int}=0.031, *R(F)*=0.027 [9096 data with *I*≥2σ(*I*)], w*R*(F^2)=0.059 (all data). CCDC-1470506.

2-Chlorobenzoic acid, [CAS Number: 118-91-2], 103:

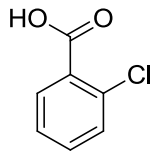

Chemical Formula: $C_7H_5ClO_2$
Exact Mass: 155.9978

Prepared using general procedure A: Isolated yield; 0.183 g (90%, 1.30 mmol scale), prepared using general procedure B after 2 h: Isolated yield; 0.013 g (5%, 1.68 mmol scale) and after 24 h: Isolated yield; 0.024 g (9%, 1.68 mmol scale), prepared using general procedure C: Isolated yield: 0.912 g (87%, 6.72 mmol scale);

Pale yellow crystals (recrystallised from MeCN);

^{1}H NMR (400 MHz, DMSO-d_6) δ/ppm 13.42 (s, br, 1H), 7.78 (d, J = 7.6 Hz, 1H), 7.68 – 7.17 (m, 3H);

^{13}C NMR (151 MHz, DMSO-d_6) δ/ppm 167.2 (C), 133.0 (CH), 132.0 (C), 131.9 (C), 131.2 (CH), 131.1 (CH), 127.7 (CH);

IR (neat) ν = 2820 (w, br), 1683 (s, C=O), 1591 (m), 1473 (m), 1408 (m), 1312 (s), 1267 (s), 1043 (m), 742 (s) cm^{-1};

LC-MS (MeCN), Rt. 2.34 min, m/z = 157.0 $[M+H]^+$. HR-MS (ESI-TOF) calculated for $C_7H_6O_2Cl$ 157.0056, found 157.0063 (Δ = 4.5 ppm).

M.p. 140-141 °C (MeCN) (Literature: 139-140 °C, no solvent specified).[151]

2-Bromobenzoic acid, [CAS Number: 88-65-3], 129:

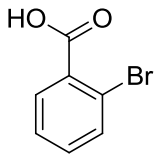

Chemical Formula: $C_7H_5BrO_2$
Exact Mass: 199.9473

Prepared using general procedure A: Isolated yield; 0.185 g (70%, 1.30 mmol scale);

White crystals (recrystallised from MeCN);

^{1}H NMR (400 MHz, DMSO-d_6) δ/ppm 13.39 (s, br, 1H), 7.78 – 7.66 (m, 2H), 7.50 – 7.40 (m, 2H);

^{13}C NMR (151 MHz, DMSO-d_6) δ/ppm 167.4 (C), 133.7 (CH), 132.5 (CH), 130.6 (CH), 127.7 (CH), 127.5 (C), 119.9 (C);

IR (neat) ν = 2646 (w, br), 1675 (s, C=O), 1589 (m), 1473 (m), 1278 (s), 1306 (s). 1265 (s), 1028 (m), 896 (m) cm^{-1};

LC-MS (MeCN), Rt. 2.27 min, m/z = 200.8 $[M+H]^+$. HR-MS (ESI-TOF) calculated for $C_7H_6O_2Br$ 200.9551, found 200.9554 (Δ = 1.49 ppm).

M.p. 147-149 °C (MeCN) (Literature: 147-149 °C, no solvent specified).[151]

2-Fluorobenzoic acid, [CAS Number: 445-29-4], 130:

Chemical Formula: $C_7H_5FO_2$
Exact Mass: 140.0274

Prepared using general procedure A: Isolated yield; 0.152 g (84%, 1.30 mmol scale);

Yellow crystals (recrystallised from MeCN);

^{1}H NMR (400 MHz, DMSO-d_6) δ/ppm 13.23 (s, br, 1H), 7.87 (td, *J* = 7.6, 1.7 Hz, 1H), 7.64 (m, 1H), 7.35 – 7.26 (m, 2H);

^{13}C NMR (151 MHz, DMSO-d_6) δ/ppm 165.5 (d, *J* = 3.0 Hz, C), 161.5 (d, *J* = 256.7 Hz, C), 135.1 (d, *J* = 8.9 Hz, CH), 132.3 (CH), 124.9 (d, *J* = 3.8 Hz, CH), 119.8 (d, *J* = 10.3 Hz, C), 117.4 (d, *J* = 22.1 Hz, CH);

^{19}F NMR (376 MHz, DMSO-d_6) δ/ppm -110.65 (s);

IR (neat) ν = 2820 (w, br), 1685 (s, C=O), 1613 (m), 1465 (m), 1414 (m), 1285 (m), 1271 (m), 1230 (m), 1915 (m), 845 (m), 751 (s) cm^{-1};

LC-MS (MeCN), Rt. 2.06 min, m/z = 139.1 $[M-H]^-$. HR-MS (ESI-TOF) calculated for $C_7H_4O_2F$ 139.0195, found 139.0189 (Δ = 4.3 ppm).

M.p. 122-124 °C (MeCN) (Literature: 123-125 °C, no solvent specified).[152]

2-(Trifluoromethyl)benzoic acid, [CAS Number: 433-97-6], 131:

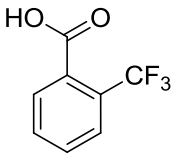

Chemical Formula: $C_8H_5F_3O_2$
Exact Mass: 190.0242

Prepared using general procedure A: Isolated yield; 0. 0.176g (71%, 1.30 mmol scale);

White crystals (recrystallised from MeCN);

^{1}H NMR (400 MHz, $CDCl_3$) δ/ppm 11.23 (s, br, 1H), 8.05 – 7.97 (m, 1H), 7.86 – 7.78 (m, 1H), 7.73 – 7.63 (m, 2H);

^{13}C NMR (151 MHz, $CDCl_3$) δ/ppm 172.2 (C), 132.4 (CH), 132.0 (CH), 131.3 (CH), 129.7 (q, *J* = 2.7 Hz, C), 129.7 (q, *J* = 49.2 Hz, C), 127.2 (q, *J* = 8.5 Hz, CH), 123.3 (q, *J* = 274.6 Hz, C);

^{19}F NMR (376 MHz, DMSO-d_6) δ/ppm -59.32 (s);

IR (neat) ν = 2891 (br), 1700 (s, C=O), 1586 (w), 1416 (w), 1276 (s), 1168 (s), 1127 (s), 1108 (s), 1058 (s), 1038 (s), 893 (m), 765 (s) cm^{-1};

LC-MS (MeCN), Rt. 2.47 min, m/z = 189.4 $[M-H]^-$. HR-MS (ESI-TOF) calculated for $C_8H_5F_3O_2$ 189.0163, found 189.0171 (Δ = 4.2 ppm).

M.p. 108-109 °C (MeCN) (Literature: 108-110 °C, EtOAc/Pet Ether).[153]

2-Methoxybenzoic acid, [CAS Number: 579-75-9], 132:

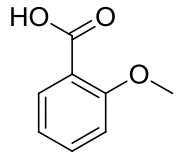

Chemical Formula: $C_8H_8O_3$
Exact Mass: 152.0473

Prepared using general procedure A: Isolated yield; 0.125g (63%, 1.30 mmol scale);

White crystals (recrystallised from MeCN);

^{1}H NMR (400 MHz,$CDCl_3$) δ/ppm 10.76 (s, br, 1H), 8.18 (dd, *J* = 7.8, 1.8 Hz, 1H), 7.58 (ddd, *J* = 8.4, 7.3, 1.8 Hz, 1H), 7.14 (ddd, *J* = 7.8, 7.3, 1.1 Hz, 1H), 7.06 (dd, *J* = 8.4, 1.1 Hz, 1H), 4.08 (s, 3H);

^{13}C NMR (151 MHz, $CDCl_3$) δ/ppm 165.6 (C), 158.2 (C), 135.2 (CH), 133.9 (CH), 122.3 (CH), 117.7 (C), 111.7 (CH), 56.8 (CH_3);

IR (neat) ν = 2950 (w, br), 2648 (w, br), 1668 (s, C=O), 1599 (m), 1578 (m), 1492 (m), 1464 (m), 1314 (m), 1253 (s), 1168 (m), 1088 (m), 1020 (m), 759 (s) cm^{-1};

LC-MS (MeCN), Rt. 2.03 min, m/z = 153.3 $[M+H]^+$. HR-MS (ESI-TOF) calculated for $C_8H_9O_3$ 153.0552, found 153.0554 (Δ = 1.3 ppm).

M.p. 101-102 °C (MeCN) (Literature: 100-102 °C, no solvent specified).[154]

2-Methylbenzoic acid, [CAS Number: 118-90-1], 133:

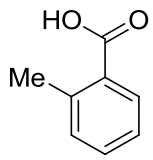

Chemical Formula: $C_8H_8O_2$
Exact Mass: 136.0524

Prepared using general procedure A: Isolated yield; 0.106 g (60%, 1.30 mmol scale);

White crystals (recrystallised from MeCN);

^{1}H NMR (400 MHz, $CDCl_3$) δ/ppm 11.65 (s, br, 1H), 8.13 – 8.05 (m, 1H), 7.47 (td, *J* = 7.5, 1.5 Hz, 1H), 7.30 (t, *J* = 7.4 Hz, 2H), 2.68 (s, 3H);

^{13}C NMR (151 MHz, $CDCl_3$) δ/ppm 173.6 (C). 141.5 (C), 133.1 (CH), 132.1 (CH), 131.7 (CH), 128.4 (C), 126.0 (CH), 22.3 (CH_3);

IR (neat) ν = 2966 (w, br), 2655 (w, br), 1679 (s, C=O), 1577 (m), 1413 (m), 1315 (s), 1276 (s), 1090 (m), 738 (s) cm^{-1};

LC-MS (MeCN), Rt. 2.58 min, m/z = 135.4 $[M-H]^-$. HR-MS ($^-$ESI-TOF) calculated for $C_8H_7O_3$ 135.0446, found 135.0448 (Δ = 1.5 ppm).

M.p. 103-104 °C (MeCN) (Literature: 104-105 °C, no solvent specified).[154]

2-Chloronicotinic acid, [CAS Number: 2942-59-8], 134:

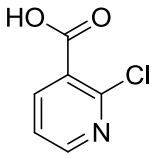

Chemical Formula: $C_6H_4ClNO_2$
Exact Mass: 156.9931

Prepared using general procedure A: Isolated yield; 0.116 g (57%, 1.30 mmol scale);

Yellow crystals (recrystallised from EtOH);

^{1}H NMR (400 MHz, DMSO-d_6) δ/ppm 13.78 (s, br, 1H), 8.56 (dd, *J* = 4.8, 2.0 Hz, 1H), 8.23 (dd, *J* = 7.7, 2.0 Hz, 1H), 7.54 (dd, *J* = 7.7, 4.8 Hz, 1H);

^{13}C NMR (151 MHz, DMSO-d_6) δ/ppm 165.8 (C), 151.7 (CH), 147.8 (C), 140.0 (CH), 128.2 (C), 123.2 (CH);

IR (neat) ν = 2460 (w, br), 1701 (s, C=O), 1577 (s), 1400 (m), 1256 (s), 1231 (s), 1148 (m), 1058 (s), 1066 (s). 819 (m), 769 (s), 715 (s) cm^{-1};

LC-MS (MeCN), Rt. 1.79 min, m/z = 156.0 $[M-H]^-$. HR-MS ($^-$ESI-TOF) calculated for $C_6H_3NO_2Cl$ 155.9852, found 155.9848 (Δ = 2.6 ppm).

M.p. 183 °C (EtOH, decomposed) (Literature: 190-192 °C, no solvent specified).[155]

4-Bromo-2-chlorobenzoic acid, [CAS Number: 59748-90-2], 135:

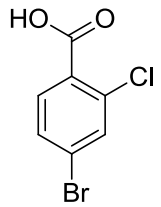

Chemical Formula: $C_7H_4BrClO_2$
Exact Mass: 233.9083

Prepared using general procedure A: Isolated yield; 0.232 g (76%, 1.30 mmol scale);

White crystals (recrystallised from MeCN);

^{1}H NMR (400 MHz, DMSO-d_6) δ/ppm 13.55 (s, br, 1H) 7.86 (d, J = 1.9 Hz, 1H), 7.75 (d, J = 8.3 Hz, 1H), 7.66 (dd, J = 8.3, 1.9 Hz, 1H);

^{13}C NMR (151 MHz, DMSO-d_6) δ/ppm 165.9 (C), 133.0 (C), 132.9 (CH), 132.5 (CH), 130.5 (C), 130.4 (CH), 125.1 (C);

IR (neat) ν = 3089 (w, br), 2562 (w, br), 1676 (s, C=O), 1577 (s), 1430 (m), 1366 (m), 1294 (s), 1254 (s), 1137 (m), 1047 (m), 909 (m), 823 (s) cm^{-1};

LC-MS (MeCN), Rt. 2.56 min, m/z = 232.9 $[M-H]^-$. HR-MS (ESI-TOF) calculated for $C_7H_3O_2ClBr$ 232.9005, found 232.9013 (Δ = 3.43 ppm).

M.p. 171-172°C (MeCN) (Literature: 170-172 °C, no solvent specified).[156]

2-Chloro-4-(trifluoromethyl)benzoic acid, [CAS Number: 23228-45-7], 136:

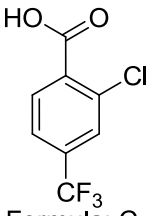

Chemical Formula: $C_8H_4ClF_3O_2$
Exact Mass: 223.9852

Prepared using general procedure A: Isolated yield; 0.128 g (44%, 1.30 mmol scale);

White crystals (recrystallised from MeCN);

^{1}H NMR (400 MHz, DMSO-d_6) δ/ppm 13.85 (s, br, 1H), 8.01 – 7.94 (m, 2H), 7.82 (dd, J = 8.3, 1.7 Hz, 1H);

^{13}C NMR (151 MHz, DMSO-d_6) δ/ppm 165.9 (C), 135.8 (CH), 132.16 (q, J = 32.3 Hz, C), 132.15 (C), 131.4 (C), 127.4 (q, J = 3.8 Hz, CH), 124.2 (q, J = 3.8 Hz, CH), 121.5 (q, J = 274.22 Hz, C);

^{19}F NMR (376 MHz, DMSO-d_6) δ/ppm -61.62 (s);

IR (neat) ν = 2971 (w, br), 1685 (s, C=O), 1299 (m), 1261 (m), 1174 (m), 1161 (s), 1131 (s), 1079 (m), 920 (w), 895 (m), 854 (s) cm^{-1};

LC-MS (MeCN), Rt. 2.68 min, m/z = 223.0 [M-H]$^-$. HR-MS (ESI-TOF) calculated for $C_8H_3O_2F_3Cl$ 222.9774, found 222.9778 (Δ = 1.8 ppm).

M.p. 114-115°C (MeCN) (Literature: 114-116 °C, no solvent specified).[155]

2-Chloro-4-methylbenzoic acid, [CAS Number: 7697-25-8], 137:

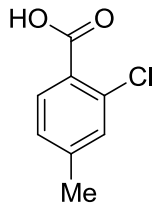

Chemical Formula: $C_8H_7ClO_2$
Exact Mass: 170.0135

Prepared using general procedure A: Isolated yield; 0.152 g (69%, 1.30 mmol scale);

Grey crystals (recrystallised from MeCN);

^{1}H NMR (400 MHz, DMSO-d_6) δ/ppm 13.19 (s, br, 1H), 7.72 (d, J = 7.9 Hz, 1H), 7.38 (dd, J = 1.7, 0.9 Hz, 1H), 7.24 (ddd, J = 7.9, 1.7, 0.9 Hz, 1H), 2.34 (s, 3H);

^{13}C NMR (151 MHz, DMSO-d_6) δ/ppm 166.5 (C), 143.3 (C), 131.9 (C), 131.1 (CH), 131.0 (CH), 128.1 (C), 127.8 (CH), 20.5 (CH_3);

IR (neat) ν = 2542 (w, br), 1675 (s, C=O), 1606 (m), 1490 (w), 1436 (w), 1302 (s), 1268 (s), 1047 (m), 915 (w), 835 (s), 767 (s) cm^{-1};

LC-MS (MeCN), Rt. 2.41 min, m/z = 171.3 [M+H]$^+$. HR-MS (ESI-TOF) calculated for $C_8H_8O_2Cl$ 171.0213, found 171.0207 (Δ = 3.5 ppm).

M.p. 155-156 °C (MeCN) (Literature: 150-152 °C, no solvent specified).[157]

2-Chloro-4-fluorobenzoic acid, [CAS Number: 2252-51-9], 138:

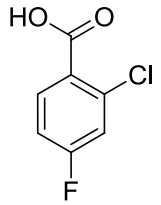

Chemical Formula: $C_7H_4ClFO_2$
Molecular Weight: 174.5569

Prepared using general procedure A: Isolated yield; 0.154 g (89%, 1.30 mmol scale) or 2.372 g (85%, 16.00 mmol scale);

White crystals (recrystallised from MeCN);

^{1}H NMR (400 MHz, DMSO-d_6) δ/ppm 13.45 (s, br, 1H), 7.91 (dd, *J* = 8.7, 6.3 Hz, 1H), 7.56 (dd, *J* = 9.0, 2.6 Hz, 1H), 7.32 (ddd, *J* = 8.8, 8.2, 2.6 Hz, 1H);

^{13}C NMR (151 MHz, DMSO-d_6) δ/ppm 165.7 (s, C), 163.2 (d, *J* = 252.6 Hz, C), 133.7 (d, *J* = 11.1 Hz, C), 133.3 (d, *J* = 9.8 Hz, CH), 127.7 (d, *J* = 3.5 Hz, C), 118.1 (d, *J* = 25.2 Hz, CH), 114.60 (d, *J* = 21.4 Hz, CH);

^{19}F NMR (376 MHz, DMSO-d_6) δ/ppm -106.76 (s);

IR (neat) ν = 3084 (w, br), 2641 (w, br), 1670 (s, C=O), 1577 (s), 1392 (m), 1410 (m), 1310 (m), 1258 (s), 1218 (s), 1048 (m), 912 (s), 870 (s), 770 (s) cm^{-1};

LC-MS (MeCN), Rt. 2.31 min, m/z = 173.1 [M-H]$^-$. HR-MS (ESI-TOF) calculated for $C_7H_3O_2FCl$ 172.9806, found 172.9810 (Δ = 2.3 ppm).

M.p. 185-186 °C (MeCN) (Literature: 180-181 °C, aq. EtOH).[158]

2,4-Dichlorobenzoic acid, [CAS Number: 50-84-0], 139:

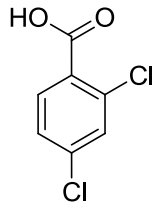

Chemical Formula: $C_7H_4Cl_2O_2$
Exact Mass: 189.9588

Prepared using general procedure A: Isolated yield; 0.171 g (69%, 1.30 mmol scale);

White crystals (recrystallised from MeCN);

^{1}H NMR (400 MHz, DMSO-d_6) δ/ppm 13.56 (s, br, 1H), 7.83 (d, *J* = 8.4 Hz, 1H), 7.74 (d, *J* = 2.1 Hz, 1H), 7.53 (dd, *J* = 8.4, 2.1 Hz, 1H);

^{13}C NMR (151 MHz, DMSO-d_6) δ/ppm 165.8 (C), 136.5 (C), 133.0 (C), 132.4 (CH), 130.2 (CH), 130.1 (C), 127.5 (CH);

IR (neat) ν = 2813 (w, br), 1691 (s, C=O), 1580 (m), 1555 (m), 1474 (w), 1412 (m), 1374 (m), 1302 (s), 1265 (s), 1109 (m), 1052 (s), 914 (m), 872 (s), 837 (s), 771 (s) cm^{-1};

LC-MS (MeCN), Rt. 2.85 min, m/z = 189.0 [M-H]$^-$. HR-MS (ESI-TOF) calculated for $C_7H_3O_2Cl_2$ 188.9510, found 188.9512 (Δ = 1.1 ppm).

M.p. 162-163 °C (MeCN) (Literature: 162 °C, no solvent specified).[159]

1-Naphthoic acid, [CAS Number: 86-55-5], 140:

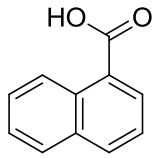

Chemical Formula: $C_{11}H_8O_2$
Exact Mass: 172.0524

Prepared using general procedure A: Isolated yield; 0.100 g (43%, 1.30 mmol scale);

White crystals (recrystallised from MeCN);

^{1}H NMR (400 MHz, DMSO-d_6) δ/ppm 13.16 (s, br, 1H), 8.87 (d, J = 8.5 Hz, 1H), 8.22 – 8.11 (m, 2H), 8.02 (dd, J = 8.0, 1.5 Hz, 1H), 7.71 – 7.55 (m, 3H);

^{13}C NMR (151 MHz, DMSO-d_6) δ/ppm 169.1 (C), 133.9 (C), 133.4 (CH), 131.1 (C), 130.3 (CH), 129.1 (CH), 128.2 (C), 128.0 (CH), 126.7 (CH), 125.9 (CH), 125.4 (CH);

IR (neat) ν = 3046 (br), 1670 (s, C=O), 1593 (m), 1513 (m), 1448 (w), 1413 (m), 1297 (m), 1250 (m), 1204 (m), 1149 (m), 891 (w), 771 (s) cm^{-1};

LC-MS (MeCN), Rt. 2.75 min, m/z = 171.2 [M-H]$^-$. HR-MS (ESI-TOF) calculated for $C_{11}H_7O_2$ 171.0446, found 171.0442 (Δ = 2.3 ppm).

M.p. 165-167 °C (MeCN) (Literature: 166-167, MeCN.[153]

2,5-Dichlorobenzoic acid, [CAS Number: 50-79-3], 141:

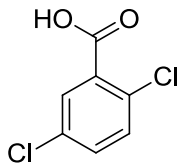

Chemical Formula: $C_7H_4Cl_2O_2$
Exact Mass: 189.9588

Prepared using general procedure A: Isolated yield: 0.118 g (48%, 1.30 mmol scale);

White crystals (recrystallised from MeCN);

^{1}H NMR (400 MHz, DMSO-d_6) δ/ppm 13.73 (s, br, 1H), 7.82 (d, J = 2.4 Hz, 1H), 7.66 – 7.54 (m, 2H);

^{13}C NMR (151 MHz, DMSO-d_6) δ/ppm 165.5 (C), 133.2 (C), 132.34 (CH), 132.25 (CH), 131.8 (C), 130.3 (C), 130.2 (CH);

IR (neat) ν = 2801 (w, br), 1675 (s, C=O), 1583 (w), 1558 (m), 1463 (w), 1436 (m), 1290 (s), 1250 (s), 1107 (m), 1050 (m), 823 (s) cm^{-1};

LC-MS (MeCN), Rt. 2.52 min, m/z = 189.0 [M-H]$^-$. HR-MS (ESI-TOF) calculated for $C_7H_3O_2Cl_2$ 188.9510, found 188.9518 (Δ = 4.2 ppm).

M.p. 153-155 °C (MeCN) (Literature: 155-156 °C, no solvent specified).[160]

2-Chloro-5-(trifluoromethyl)benzoic acid, [CAS Number: 657-06-7], 142:

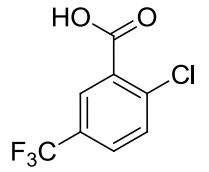

Chemical Formula: $C_8H_4ClF_3O_2$
Exact Mass: 223.9852

Prepared using general procedure A: Isolated yield; 0.136 g (47%, 1.30 mmol scale);

White crystals (recrystallised from $CHCl_3$);

^{1}H NMR (400 MHz, DMSO-d_6) δ/ppm 13.92 (s, br, 1H), 8.09 (d, J = 2.3 Hz, 1H), 7.91 (dd, J = 8.5, 2.3 Hz, 1H), 7.83 – 7.78 (m, 1H);

^{13}C NMR (101 MHz, DMSO-d_6) δ/ppm 166.0 (C), 136.4 (d, J = 1.3 Hz, C), 133.2 (C), 132.4 (CH), 129.4 (q, J = 3.4 Hz, CH), 128.3 (q, J = 33.1 Hz, C), 127.9 (q, J = 3.8 Hz, CH), 123.9 (q, J = 273.5 Hz, C);

^{19}F NMR (376 MHz, DMSO-d_6) δ/ppm -61.34 (s);

IR (neat) ν = 2856 (w, br), 2634 (w, br), 1717 (m), 1690 (s, C=O), 1326 (s), 1304 (m), 1282 (m), 1266 (m), 1248 (m), 1172 (m), 1121 (s), 1080 (s), 1051 (m), 920 (w), 837 (s) cm^{-1};

LC-MS (MeCN), Rt. 2.99 min, m/z = 223.0 [M-H]$^-$. HR-MS (ESI-TOF) calculated for $C_8H_3O_2F_3Cl$ 222.9774, found 222.9766 (Δ = 3.6 ppm).

M.p. 81-83 °C ($CHCl_3$) (Literature: 91-93 °C, no solvent specified).[155]

2-Bromo-5-formylbenzoic acid, [CAS Number: 1289007-84-6], 143:

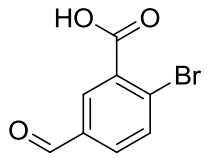

Chemical Formula: $C_8H_5BrO_3$
Molecular Weight: 229.0275

Prepared using general procedure A: Isolated yield; 0.127 g (43%, 1.30 mmol scale),

Amorphous solid;

^{1}H NMR (400 MHz, DMSO-d_6) δ/ppm 13.70 (s, br, 1H), 10.03 (s, 1H), 8.24 (d, J = 2.1 Hz, 1H), 7.98 – 7.86 (m, 2H);

^{13}C NMR (101 MHz, DMSO-d_6) δ/ppm 192.0 (CH), 166.6 (C), 135.2 (C), 135.0 (CH), 134.5 (C), 132.0 (CH), 131.5 (CH), 126.7 (C);

IR (neat) ν = 2945 (w, br), 2785 (w, br), 2638 (w, br), 1663 (s, C=O), 1731 (s, C=O), 1593 (m), 1555 (m), 1368 (m), 1278 (m), 1243 (s), 1190 (s), 1032 (m), 910 (s), 839 (s), 776 (s) cm^{-1};

LC-MS (MeCN), Rt. 2.05 min, m/z = 227.0 [M-H]$^-$. HR-MS (ESI-TOF) calculated for $C_8H_4BrO_3$ 226.9344, found 226.9352 (Δ = 3.5 ppm).

2-Fluoro-5-formylbenzoic acid, [CAS Number: 550363-85-4], 144:

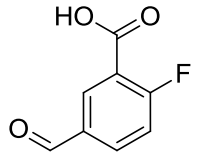

Chemical Formula: $C_8H_5FO_3$
Molecular Weight: 168.1219

Prepared using general procedure A: Isolated yield; 0.102 g (47%, 1.30 mmol scale);

Yellow crystals (recrystallised from MeCN);

^{1}H NMR (400 MHz, DMSO-d_6) δ/ppm 13.66 (s, br, 1H), 10.04 (s, 1H), 8.43 (dd, J = 7.2, 2.3 Hz, 1H), 8.17 (ddd, J = 8.5, 4.7, 2.3 Hz, 1H), 7.56 (dd, J = 10.6, 8.5 Hz, 1H);

^{13}C NMR (151 MHz, DMSO-d_6) δ/ppm 191.8 (s, CH), 164.8 (d, J = 266.0 Hz, C), 164.5 (d, J = 3.1 Hz, C), 135.5 (d, J = 10.9 Hz, CH), 134.5 (d, J = 2.7 Hz, CH), 133.1 (d, J = 3.1 Hz, C), 120.6 (d, J = 11.3 Hz, C), 118.7 (d, J = 23.6 Hz, CH);

^{19}F NMR (376 MHz, DMSO-d_6) δ/ppm -101.25 (s);

IR (neat) ν = 2865 (w, br), 1701 (s, C=O), 1685 (s, C=O), 1610 (m), 1457 (m), 1453 (m), 1437 (m), 1431 (m), 1290 (m), 1245 (s), 1203 (s), 1087 (m), 923 (m), 841 (s) cm^{-1};

LC-MS (MeCN), Rt. 1.93 min, m/z = 167.1 $[M-H]^-$. HR-MS (ESI-TOF) calculated for $C_8H_4FO_3$ 167.0144, found 167.0146 (Δ = 1.2 ppm).

M.p. 162 °C (MeCN, decomposed).

2-Bromo-5-(ethoxymethyl)benzoic acid, 145:

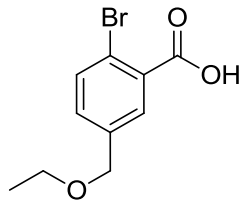

Chemical Formula: $C_{10}H_{11}BrO_3$
Exact Mass: 257.99

Prepared using general procedure A: Isolated yield; 0.156 g (36%, 1.00 mmol scale);

Amorphous solid;

^{1}H NMR (400 MHz, $CDCl_3$) δ/ppm 10.40 (s, br, 1H), 7.96 (d, *J* = 2.2 Hz, 1H), 7.67 (d, *J* = 8.3 Hz, 1H), 7.38 (dd, *J* = 8.2, 2.2 Hz, 1H), 4.51 (s, 2H), 3.57 (q, *J* = 7.0 Hz, 2H), 1.26 (t, *J* = 7.1, 3H);

^{13}C NMR (101 MHz, $CDCl_3$) δ/ppm 170.9 (C), 138.4 (C), 135.0 (CH), 132.7 (CH), 131.5 (CH), 130.5 (C), 121.5 (C), 71.4 (CH_2), 66.3 (CH_2), 15.3 (CH_3);

IR (neat) ν = 2976 (w, br), 2658 (w, br), 1699 (s, C=O), 1471 (w), 1443 (w), 1387 (w), 1295 (m), 1247 (m), 1195 (m), 1099 (s), 1027 (s), 823 (m) cm^{-1};

LC-MS (MeCN), Rt. 2.15 min, m/z = 259.3 $[M+H]^+$. HR-MS (ESI-TOF) calculated for $C_{10}H_{12}BrO_3$ 258.9970, found 258.9965 (Δ = 1.9 ppm).

(*Rac*)-(2-bromo-5-((2*R*,3*S*,5*S*)-3-(*tert*-butoxycarbonyl)-5-(ethoxycarbonyl)-3-methyl-1-pivaloylpyrrolidin-2-yl)benzoic acid, 146:

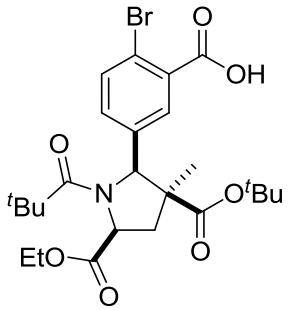

Chemical Formula: $C_{25}H_{34}BrNO_7$
Exact Mass: 539.15

Prepared using general procedure A: Isolated yield; 0.366 g (54%, 1.76 mmol scale);

Colourless crystals (recrystallised from hexane/EtOAc);

^{1}H NMR (700 MHz, $CDCl_3$) δ/ppm 10.02 (s, br, 1H), 8.14 (s, 1H), 8.11 – 8.00 (m, 1H), 7.69 (d, *J* = 8.4 Hz, 1H), 5.09 (s, 1H), 4.55 (dd, *J* = 12.0, 7.1 Hz, 1H), 4.29 (qd, *J* = 7.1, 1.7 Hz, 2H), 2.49 (t, *J* = 12.7 Hz, 1H), 1.99 (dd, *J* = 13.2, 7.1 Hz, 1H), 1.46 (s, 3H), 1.33 (t, *J* = 7.2 Hz, 3H), 1.17 (s, 9H), 1.07 (s, 9H).

^{13}C NMR (176 MHz, $CDCl_3$) δ/ppm 178.9 (C), 172.4 (C), 170.8 (C), 170.2 (C), 139.8 (C), 135.1 (CH), 133.5 (CH), 132.7 (CH), 130.1 (C), 122.0 (C), 82.3 (C), 69.7 (CH), 61.5 (CH_2), 61.2 (CH), 56.3 (C), 39.7 (C), 32.8 (CH_2), 28.4 (CH_3), 27.7 (CH_3), 23.7 (CH_3), 14.3 (CH_3);

IR (neat) ν = 2997 (w, br), 1723 (s, C=O), 1627 (m, amide I band), 1597 (m), 1478 (m), 1369 (m), 1252 (s), 1200 (s), 1130 (s), 1027 (s), 909 (s), 728 (s) cm^{-1};

LC-MS (MeCN), Rt. 3.30 min, m/z = 540.5 $[M+H]^+$. HR-MS ($^+$ESI-TOF) calculated for $C_{25}H_{24}BrNO_7$ 540.1597, found 540.1582 (Δ = 2.8 ppm),

M.p. 162-165 °C (hexane/EtOAc).

2,6-Dimethoxybenzoic acid, [CAS Number: 1466-76-8], 147:

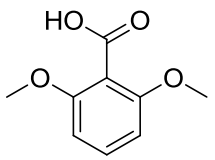

Chemical Formula: $C_9H_{10}O_4$
Molecular Weight: 182.1733

Prepared using general procedure A: Isolated yield; 0.042 g (16%, 1.30 mmol scale);

White crystals (recrystallised from MeCN);

^{1}H NMR (400 MHz, DMSO-d_6) δ/ppm 12.72 (s, br, 1H), 7.32 (t, *J* = 8.4 Hz, 1H), 6.69 (d, *J* = 8.4 Hz, 2H), 3.76 (s, 6H);

^{13}C NMR (101 MHz, DMSO-d_6) δ/ppm 167.2 (C), 156.6 (C), 130.9 (CH), 114.8 (C), 104.6 (CH), 56.2 (CH_3);

IR (neat) ν = 2944 (w, br), 1695 (m, C=O), 1589 (m), 1478 (m), 1476 (m), 1333 (m), 1253 (s), 1110 (s), 1076 (m), 1027 (m), 796 (m) cm^{-1};

LC-MS (MeCN), Rt. 2.07 min, m/z = 181.1 $[M-H]^-$. HR-MS (ESI-TOF) calculated for $C_9H_9O_4$ 181.0501, found 181.0508 (Δ = 3.9 ppm).

M.p. 184-187 °C (MeCN) (Literature: 185-187 °C, hexane).[161]

2-Chloro-6-methylbenzoic acid, [CAS Number: 21327-86-6], 148:

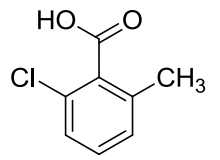

Chemical Formula: $C_8H_7ClO_2$
Exact Mass: 170.0135

Prepared using general procedure A: Isolated yield; 0.054 g (12%, 2.60 mmol scale);

White crystals (recrystallised from hexane);

^{1}H NMR (400 MHz, $CDCl_3$) δ/ppm; 10.07 (s, 2H), 7.29 – 7.22 (m, 2H), 7.14 (dd, *J* = 5.4, 3.4 Hz, 1H), 2.43 (s, 3H).

^{13}C NMR (101 MHz, $CDCl_3$) δ/ppm; 172.7 (C), 137.2 (C), 132.8 (C), 130.8 (C), 130.7 (CH), 128.7 (CH), 127.1 (CH), 19.9 (CH_3).

IR (neat) ν = 2927 (br), 1700 (s, C=O), 1595 (m), 1452 (m), 1282 (m), 1182 (m), 1119 (m), 1071 (w), 870 (m), 774 (s) cm^{-1};

LC-MS (MeCN), Rt. 2.25 min, m/z = 169.5 $[M-H]^-$. HR-MS (ESI-TOF) calculated for $C_8H_6O_2Cl$ 169.0056, found 169.0047 (Δ = 5.3 ppm).

M.p. 100-101 °C (hexane) (Literature: 98-99 °C, hexane).[84b]

2-Naphthoic acid, [CAS Number: 93-09-4], 150:

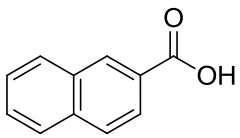

Chemical Formula: $C_{11}H_8O_2$
Exact Mass: 172.0524

Prepared using general procedure A: Isolated yield; 0.125 g (53%, 1.30 mmol scale);

White crystals (recrystallised from *i*PrOH);

^{1}H NMR (400 MHz, DMSO-d_6) δ/ppm; 13.10 (s, br, 1H), 8.62 (s, 1H), 8.17 – 8.09 (m, 1H), 8.06 – 7.94 (m, 3H), 7.64 (m, 2H).

^{13}C NMR (101 MHz, DMSO-d_6) δ/ppm; 167.9 (C), 135.4 (C), 132.6 (C), 131.0 (CH), 129.7 (CH), 128.8 (CH), 128.6 (CH), 128.5 (C), 128.1 (CH), 127.3 (CH), 125.6 (CH).

IR (neat) ν = 2570 (br), 1685 (s, C=O), 1632 (w), 1477 (w), 1424 (m), 1358 (m), 1300 (s), 1239 (m), 1200 (m), 1135 (m), 833 (m), 906 (m), 868 (m), 778 (s), 759 (s) cm^{-1};

LC-MS (MeCN), Rt. 2.23 min, m/z = 171.2 $[M-H]^-$. HR-MS (ESI-TOF) calculated for $C_{11}H_7O_2$ 171.0446, found 171.0444 (Δ = 1.2 ppm).

M.p. 183-186 °C (*i*PrOH) (Literature: 184-185, EtOAc/Ether).[153]

2-(Methylsulfonyl)-4-(trifluoromethyl)benzoic acid, 156:

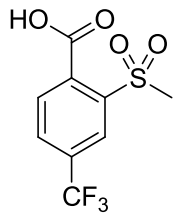

Chemical Formula: $C_9H_7F_3O_4S$
Exact Mass: 268.0017

Procedure 1: To an ice cold solution of 2-(methylsulfonyl)-4-(trifluoromethyl)benzoic acid (**156**, 0.526 g, 2.00 mmol) in MeOH (8 mL) was add Oxone® ($KHSO_5 \cdot 0.5\ KHSO_4 \cdot 0.5\ K_2SO_4$, 0.922 g, 3.00 mmol) in water (7 mL) dropwise. The reaction was left to stir over night and then was diluted with brine solution (30 mL) and extracted with EtOAc (3 x 25 mL). The organic layer was dried over sodium sulfate and the solvent evaporated to give the product.

Procedure 2: A suspension of compound **157** (0.526 g, 2.00 mmol) in acetic acid (8 mL) and acetic anhydride (0.612 g, 6.0 mmol) was prepared and cooled using an ice bath. Hydrogen peroxide (27%, 1.50 g, 6.0 mmol) was added dropwise making sure the temperature did not rise above 5 ºC. The reaction was then warmed up to room temperature and stirred for 30 min. The reaction was heated to 65 °C for 3 h, cooled down, poured over ice and extracted with diethyl ether (3 x 25 mL). The organic layer was washed with brine (9 x 25 mL), dried over sodium sulfate and solvent evaporated under vacuum to give the product as a white powder which was recrystallised from EtOAc to give the pure product.

Procedure 3: To a solution of compound **157** (0.236 g, 1.00 mmol) in acetic acid (5.7 mL) was added QP-SA (0.1 g, 0.22 mmol) and heated at 50 ºC. Hydrogen peroxide solution (27%, 0.40 mL, 0.45 g, 3.53 mmol) was added dropwise and reaction left to stir for 8 h at 50 ºC. The reaction was then cooled to room temperature, diluted with brine (20 mL) and extracted with EtOAc (3 x 25 mL). The organic layer was then washed with brine (5 x 25 mL), dried over sodium sulfate and solvent evaporated under vacuum to give the product as a white powder which was recrystallised from EtOAc to give the pure product.

Procedure 4: A solution of compound **157** (0.236 g, 1.00 mmol) in acetic acid (6.6 mL) was prepared and hydrogen peroxide (27%, 0.40 mL, 0.45 g, 3.53 mmol) was added. The pump was set at 0.1 mL/min. which was connected to an Omnifit® column (0.5 cm radius x 12 cm height, loaded with 12.5 g QP-SA 2.20 mmol/g loading) and maintained at 50 ºC, followed by a variable back pressure regulator set at 5 bar (See Scheme 87). The output solution was collected and diluted with brine (20 mL) and extracted with EtOAc (3 x 25 mL). The organic layer was washed with brine (5 x 25 mL), dried over sodium

sulfate and the solvent evaporated under vacuum to give the product as a white powder which was recrystallised from EtOAc to give the pure product.

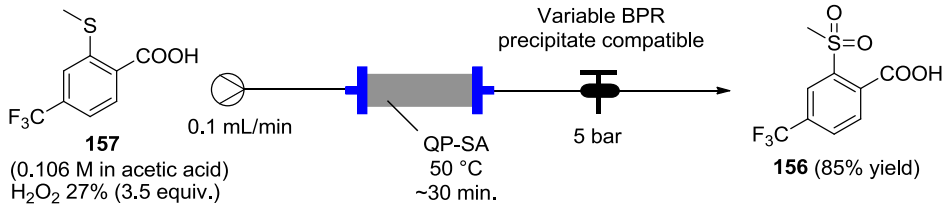

Scheme 87: Oxidation of **156** in flow.

Procedure 5: A mixture of 4:1 MeCN/H_2O (30 mL) was bubbled with F_2/N_2 (1:9, 40 mL/min) for 1 h in a Teflon® lined flask (See Figure 24). A suspension of **157** (0.236 g, 1.00 mmol) in MeCN (10 mL) was added and left stirring for 10 min at room temperature. The reaction was then quenched with K_2CO_3 aqueous solution (1 M, 200 mL) and the organic layer was dried over sodium sulfate and the solvent evaporated under vacuum to give the product as a white powder which was recrystallised from EtOAc to give the pure product.

Figure 24: Fluorination set up including scrubber and mixing tanks.

Using procedure 1: Isolated yield; 0.27 g (5%, 2.0 mmol scale). Using procedure 2: Isolated yield; 0.675 g (63%, 2.0 mmol scale). Using procedure 3: Isolated yield; 0.147 g (55%, 1.0 mmol scale). Using procedure 4: Isolated yield; 0.228 g (85%, 1.0 mmol scale). Using procedure 5: Isolated yield; 0.241 g (90%, 1.0 mmol scale).

White crystals (recrystallised from EtOAc), Rf: 0.06 (9/1, DCM/MeOH);

^{1}H NMR (600 MHz, DMSO-d_6) δ/ppm 14.26 (s, 1H), 8.25-8.19 (m, 2H), 8.01-7.95 (m, 1H), 3.47 (s, 3H);

^{13}C NMR (151 MHz, DMSO-d_6) δ/ppm 168.0 (C), 139.5 (C), 138.6 (C), 131.4 (q, J = 3.28 Hz, CH), 131.1 (q, J = 33.1 Hz, C), 130.8 (CH), 126.7 (q, J = 3.84 Hz, CH), 123.4 (q, J = 272.98 Hz, CF_3), 44.56 (CH_3);

^{19}F NMR (376 MHz, DMSO-d_6) δ/ppm -61.65 (s).

IR (neat) ν = 3236 (w, br), 1749 (m, C=O), 1401 (w), 1378 (w), 1325 (s), 1287 (s), 1226 (s), 1187 (s), 1127 (s), 1113 (s), 1079 (s), 971 (m), 937 (m), 860 (m), 845 (w), 789 (m), 769 (s), 748 (s) cm^{-1};

LC-MS (MeCN), Rt. 2.80 min, m/z = 267.1 [M-H]$^-$. HR-MS (ESI-TOF) calculated for $C_9H_6O_4F_3S$ 266.9939, found 266.9940 (Δ = 0.4 ppm);

Elemental analysis: calculated for $C_9H_7O_4F_3S$ C: 45.76%, H: 2.99%, N: 0.0%; measured C: 45.71% (Δ = 0.05), H: 2.92% (Δ = 0.07), N: 0.01% (Δ = 0.01)

M.p. 154-158 °C (EtOAc).

2-(Methylthio)-4-(trifluoromethyl)benzoic acid, 157:

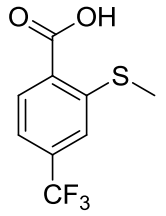

Chemical Formula: $C_9H_7F_3O_2S$
Exact Mass: 236.0119

Procedure 1: A solution of "turbo-Grignard" (*i*PrMgCl.LiCl) (1.3 M in THF, 3.0 mmol, 2.31 mL), was loaded in a 25 mL dry three necked round bottom flask. The (2-bromo-5-(trifluoromethyl)phenyl)(methyl)sulfane (**152**, 0.678 g, 2.5 mmol) was dissolved in 3.5 mL of dry THF and added slowly to the magnesium solution using a syringe. The reaction mixture was left stirring at room temperature for 2 h. A small sample was taken, and checked by GC-MS which shows complete conversion. The reaction mixture was then quenched with 5 pellets of dry ice (solid CO_2) and stirred for 10 min before being quenched by an aqueous solution of HCl (2 M, addition monitored using pH paper). The reaction mixture was diluted with EtOAc (30 mL). The organic layer was extracted with a saturated solution of potassium carbonate (3 x 5 mL). The aqueous layer was made acidic with dropwise addition of HCl (2 M, addition monitored using pH paper) and the solution/suspension extracted with EtOAc (3 x 25 mL). The organic layer was dried over magnesium sulfate, filtered and solvent evaporated to give white crystals of the expected product (0.221 g, 34% yield).

Procedure 2: A solution of compound **152** (0.441 g, 1.63 mmol) was prepared in THF (2.5 mL) and injected in a 2 mL loop on the Vapourtec R2+. "Turbo-Grignard" (*i*PrMgCl.LiCl) (1.3 M in THF) was injected in a separate 2 mL loop. The reactor pumps were set at 0.33 mL/min. with 10 bar CO, 20 mL of PFA reactor set at 70 ºC followed by a 15 mL of "tube-in-tube" reactor at room temperature and BPR of 100 psi (See Scheme 88). The output solution collected was quenched with an aqueous solution of HCl (1 M, addition monitored using pH paper). The mixture was extracted using EtOAc (3 x 25 mL). The organic layer was then extracted with an aqueous solution of NaOH (1 M, 3 x 5 mL). The combined aqueous layers were acidified (monitored using pH paper) by the addition of 2 M HCl solution which was then extracted with EtOAc (3 x 25 mL). The

organic layer was dried over sodium sulfate, and the solvent evaporated under reduced pressure to give the crude product.

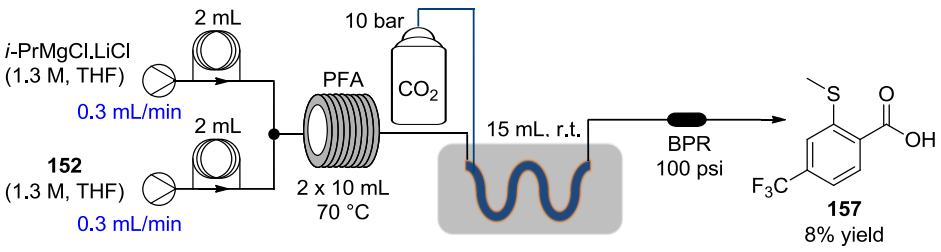

Scheme 88: Grignard hydroxy-carboxylation of **149 u**sing the reverse "tube-in-tube" reactor.

Procedure 3: To a cooled (-78 ºC) solution of compound **152** (1.36g, 5.00 mmol) in THF (25 mL) was added dropwise *n*-BuLi (2.5 M solution in hexane, 2.20 mL, 5.5 mmol) making sure the temperature stays below -70 ºC. After 2 h stirring at -78 ºC, 10 pellets of dry ice (solid CO_2) were added and the mixture stirred for 10 min. The reaction mixture was quenched with an aqueous solution of HCl (1 M, 20 mL, addition monitored using pH paper) and stirred at room temperature for 30 min. The mixture was extracted using EtOAc (3 x 25 mL). The organic layer was then extracted with an aqueous solution of NaOH (1 M, 3 x 5 mL). The combined aqueous layers were acidified (monitored using pH paper) by the addition of 2 M HCl solution which was then extracted with EtOAc (3 x 25 mL). The organic layer was dried over sodium sulfate, and the solvent evaporated under reduced pressure to give the crude product which was recrystallised from MeCN to give the pure product.

Procedure 4: A solution of compound **152** (0.564 g, 2.08 mmol) was prepared in THF (2.1 mL) and injected in a 2 mL loop on the Vapourtec R2+. A separate 2 mL loop was filled with a solution of *n*-BuLi (1.25 M in hexane). The reactor pumps were set at 0.2 mL/min. feeding the loops and 0.4 mL/min. for the pump feeding the "tube-in-tube" reactor with hexane and 10 bar CO at room temperature. After the two injection loops a 2 mL residence time loop was placed after each loop which was immersed in a dry ice/acetone bath (-78 ºC) which then join together through a T-piece which was also immersed in the same cooling bath. After the T-piece the flow stream passed through a PFA reactor (2 mL) also immersed in the same cooling bath then joined with a stream of hexane loaded with CO coming from the "tube-in-tube" reactor at room temperature. The combined stream was passed through another PFA reactor (10 mL) at room temperature and BPR of 75 psi (See Scheme 89). The output solution was collected and quenched with an aqueous solution of HCl (1 M, addition monitored using pH paper). The mixture was extracted using EtOAc (3 x 25 mL). The organic layer was then extracted with an aqueous solution of NaOH (1 M, 3 x 5 mL). The combined aqueous layers were acidified (monitored using pH paper) by the addition of 2 M HCl solution which was then extracted with EtOAc (3 x 25 mL). The organic layer was dried over sodium sulfate, and the solvent evaporated under reduced pressure to give the crude product.

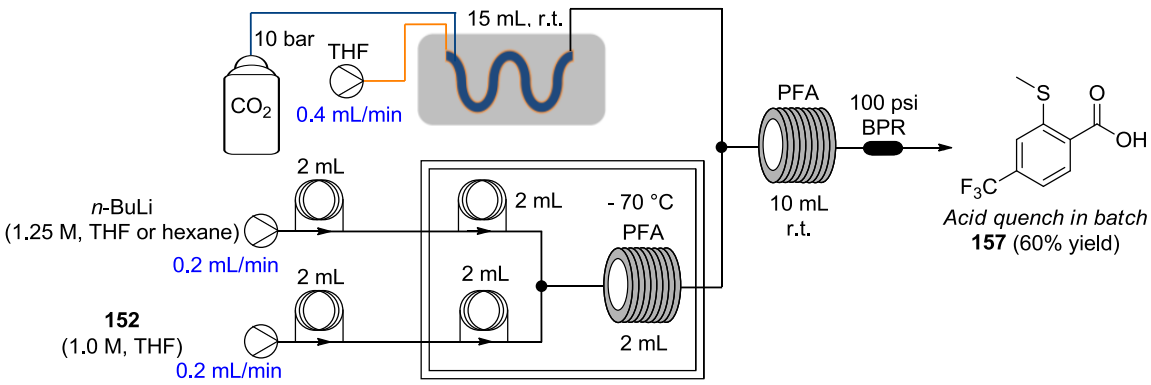

Scheme 89: Lithiation of **152** followed by hydroxy-carbonylation in continuous flow.

Using procedure 1: Isolated yield; 0.201 g (34%, 2.5 mmol scale). Using procedure 2: Isolated yield; 0.025 g (8%, 1.3 mmol scale). Using procedure 3: Isolated yield; 0.985 g (83%, 5.00 mmol scale). Using procedure 4: Isolated yield; 0.280 g (60%, 1.98 mmol scale).

White crystals (recrystallised from MeCN);

^{1}H NMR (400 MHz, DMSO-d_6) δ/ppm 8.06 (d, J = 8.3 Hz, 1H), 7.57-7.52 (m, 2H), 2.49 (s, 3H).

^{13}C NMR (101 MHz, DMSO-d_6) δ/ppm 166.59 (C), 144.08 (C), 132.22 (q, J = 31.9 Hz, C), 131.68 (CH), 131.14 (C), 123.67 (q, J = 273.3 Hz, C), 120.98 (q, J = 3.8 Hz, CH), 120.25 (q, J = 3.6 Hz, CH), 14.76 (CH_3).

^{19}F NMR (376 MHz, DMSO-d_6) δ/ppm -61.69 (s).

IR (neat) ν = 2932 (w, br), 1695 (m, C=O), 1675 (m), 1481 (w), 1419 (w), 1310 (s), 1254 (s), 1185 (s), 1119 (s), 1085 (s), 874 (s), 849 (m), 842 (m), 781 (m), 770 (m) cm^{-1};

LC-MS (MeOH), Rt. 3.21 min, m/z = 235.0 [M-H]$^-$. HR-MS (ESI-TOF) calculated for $C_9H_6O_2F_3S$ 235.0041, found 235.0041 (Δ = 0.0 ppm).

M.p. 192-193 °C (MeCN).

Methyl 2-(methylthio)-4-(trifluoromethyl)benzoate, 158:

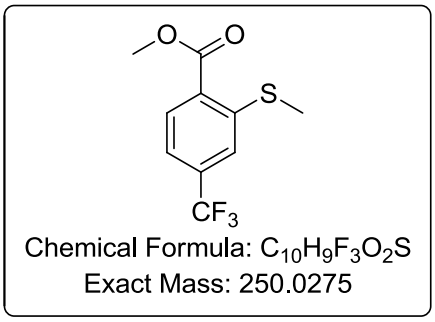

A solution of compound **152** (0.271 g, 1.0 mmol), triethylamine (0.139 mL, 1.1 equiv.) and hydrazine (0.10 mL, 30 mol%) was prepared in 3 mL of a 1:1 mixture of dioxane/ MeOH. Another solution was separately prepared with palladium acetate (11.2 mg, 5 mol%) and Xantphos (34.7 mg, 6 mol%) in 3 mL of dioxane. The respective solutions were injected into 2 mL sample loops on the Vapourtec R2+ reactor and the pumps set at 0.125 mL/min., with 15 bar CO, 30 mL of tube in tube reactor (2 x 15 mL) at 110 °C and BPR of 325 psi (Scheme 90). The solution collected was evaporated down, loaded on silica and purified using flash chromatography with 1:4 EtOAc/hexanes to give 62 mg (22% isolated yield) of pure product as a brown oil.

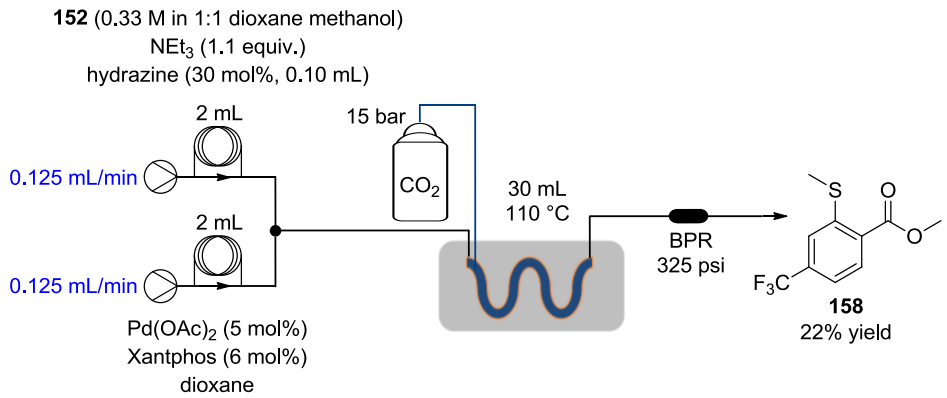

Scheme 90: Alkoxy-carbonylation of **152** in flow.

Isolated yield: 0.062 g (22%, 1.0 mmol scale);

White crystals; Rf: 0.46 (1/4, EtOAc/hexanes);

^{1}H NMR (400 MHz, $CDCl_3$) δ/ppm 8.09 (d, *J* = 7.8 Hz, 1H), 7.47 (s, 1H), 7.39 (d, *J* = 8.2 Hz, 1H), 3.95 (s, 3H), 2.50 (s, 3H).

^{13}C NMR (101 MHz, $CDCl_3$) δ/ppm 165.9 (C), 144.9 (C), 136.6 (q, *J* = 33.0 Hz, C), 131.8 (CH), 129.7 (C), 123.6 (q, *J* = 272.9 Hz, C), 121.1 (q, *J* = 3.7 Hz, CH), 120.1 (q, *J* = 3.7 Hz, CH), 52.5 (CH_3), 15.6 (CH_3).

^{19}F NMR (376 MHz, $CDCl_3$) δ/ppm -63.29 (s).

IR (neat) ν = 2999 (w), 2961 (w), 2926 (w), 1723 (s, C=O), 1478 (w), 1437 (m), 1389 (w), 1314 (s), 1246 (s), 1166 (s), 1110 (s), 1084 (s), 1061 (s), 880 (m), 848 (m), 834 (m), 774 (s), 698 (s) cm^{-1};

ASAP (MeCN), Rt. 0.55 min, m/z = 249.9 $[M+H]^+$. HR-MS (AP-TOF) calculated for $C_{10}H_9O_2F_3S$ 250.0275, found 250.0265 (Δ = 4.0 ppm),

M.p. 45-48 °C (EtOAc/hexanes, 1:1).

General Procedures for Chapter 2.2:

A) Catalytic Chan-Lam in flow:

A solution was prepared from the amine (0.781 mmol) in DCM (5.5 mL) followed by the boronic acid (1.25 mmol) and NEt_3 (0.039 g, 54 µL, 0.391 mmol). Another solution containing $Cu(OAc)_2 \cdot H_2O$ (0.195 mmol, 0.25 equiv.), NEt_3 (0.039 g, 54 µL, 0.391 mmol) and pyridine (0.062 g, 63 µL, 0.781 mmol) in DCM (5.5 mL) was also prepared. The two solutions were separately introduced in 5 mL sample loop as shown in (Scheme 91). The pumps were each set at 0.125 mL/min to achieve a residence time of 2 h. Two reverse "tube-in-tube" reactors were used in series to achieve a combined reactor volume of 30 mL which were heated at 40 ºC. The reaction mixture was then passed through an Omnifit column (r = 0.33 cm, h = 10.00 cm) filled with QP-DMA followed by a back pressure regulator (175 psi). The crude reaction mixture was then passed through a plug of silica to remove most of the excess copper present and the organic solvent from eluent evaporated under reduced pressure. The resultant crude material was then purified using flash chromatography.

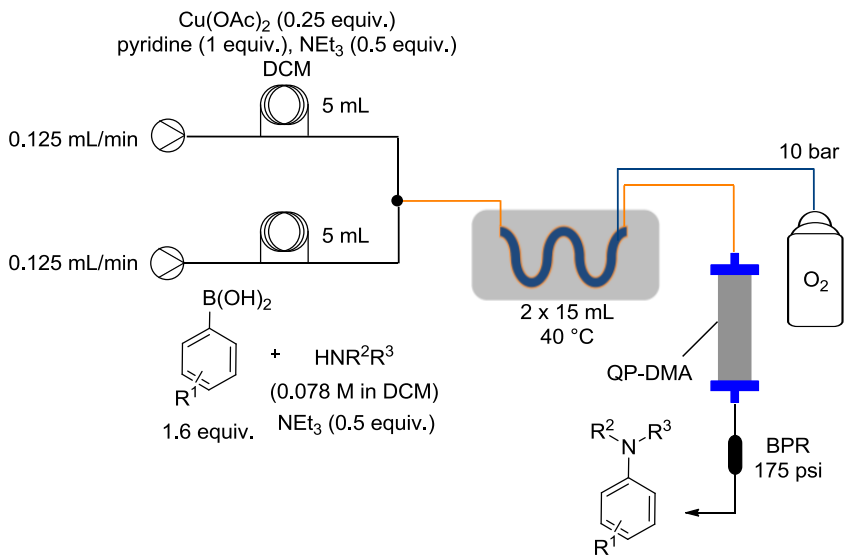

Scheme 91: General flow scheme for catalytical Chan Lam reaction.

Spectroscopic and experimental data for Chapter 2.2:

Ethyl 2-(3,4-dimethoxyphenyl)-6-methyl-3-oxo-2,3-dihydropyridazine-4-carboxylate, 309:

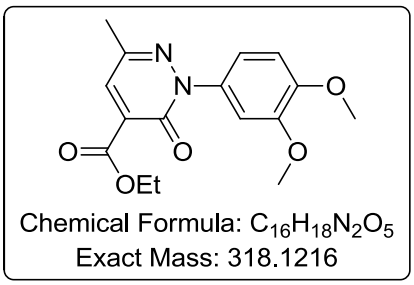

Ethyl 6-methyl-3-oxo-2,3-dihydropyridazine-4-carboxylate (**306**, 7.096 g, 39.0 mmol) and 3,4-dimethoxyphenylboronic acid (4.439 g, 24.4 mmol) were dissolved in DCM (108.1 mL) to which NEt_3 (4.93 g, 6.79 mL, 48.8 mmol) was added. Another solution was made from $Cu(OAc)_2 \cdot H_2O$ (1.219 g, 6.1 mmol) in DCM (105.8 mL) to which NEt_3 (4.93 g, 6.79 mL, 48.8 mmol) and pyridine (1.94 g, 1.97 mL, 24.4 mmol) were added. The stock solutions were separately pumped through two respective HPLC pumps of a Vapourtec flow machine equipped with 2 x 15 mL 'tube in tube' reactors followed by a column reactor filled with cotton as a filter and a 100 psi BPR. The reactors were heated at 40 °C and supplied with oxygen gas at 10 bar of pressure (Scheme 92). The reaction mixture was collected and washed with 1M HCl (2 x 250 mL), organic layer dried over sodium sulfate, filtered and solvent evaporated under reduced pressure. The crude material was purified by trituration (MeOH/diethyl ether/*n*-hexane, 7 mL : 14 mL : 40 mL) and solid obtained recrystallised from *i*-PrOH to give the product as yellow crystals. (5.52 g, 72% yield).

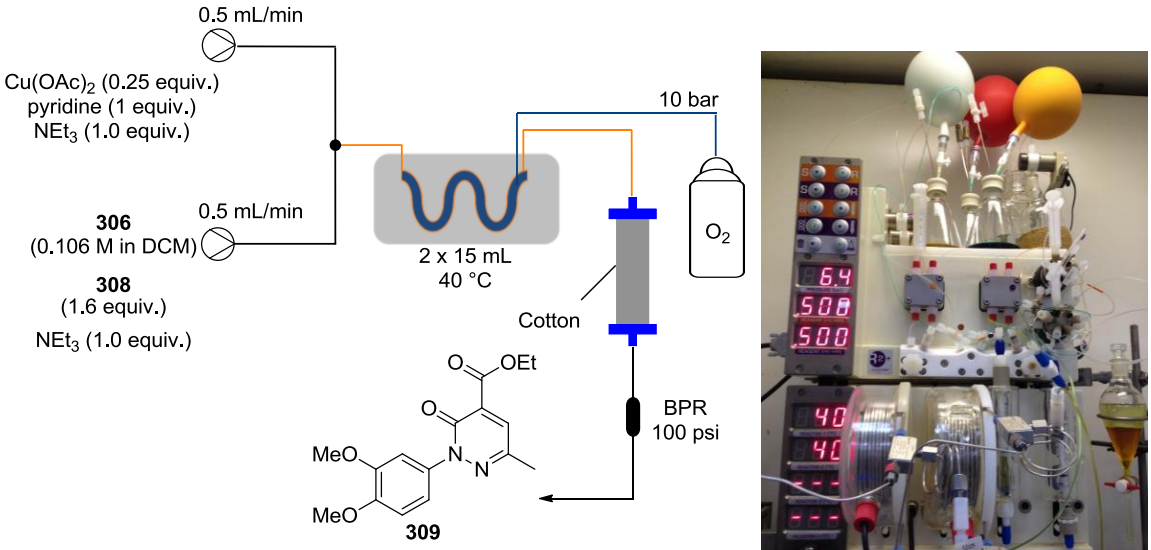

Scheme 92: Optimised process for the synthesis of **309**.

Isolated yield: 5.52 g (72%, 24.4 mmol scale), 99+% purity;

Yellow crystals; Rf: 0.33 (8/2, EtOAc/hexanes);

^{1}H NMR (700 MHz, $CDCl_3$) δ/ppm 7.65 (s, 1H), 7.12 – 7.09 (m, 2H), 6.94 – 6.91 (m, 1H), 4.40 (q, *J* = 7.1 Hz, 2H), 3.91 (s, 3H), 3.89 (s, 3H), 2.43 (s, 3H), 1.39 (t, *J* = 7.1 Hz, 3H);

^{13}C NMR (176 MHz, $CDCl_3$) δ/ppm 163.8 (C), 156.5 (C), 149.2 (C), 149.0 (C), 144.0 (C), 134.8 (C), 134.7 (CH), 131.5 (C), 118.2 (CH), 110.9 (CH), 109.5 (CH), 62.4 (CH_2), 56.3 (CH_3), 56.2 (CH_3), 21.0 (CH_3), 14.3 (CH_3);

IR (neat) ν = 3008 (w), 2992 (w), 1739 (s, C=O), 1656 (m, C=O of lactam), 1609 (s), 1454 (m), 1223 (s), 1174 (m), 1133 (s), 1084 (m), 1026 (s), 950 (m), 852 (m), 804 (s) cm^{-1};

LC-MS (MeCN), Rt. 2.619 min, m/z = 319.2 $[M+H]^+$. HR-MS (ESI-TOF) calculated for $C_{16}H_{19}N_2O_5$ 319.1294, found 319.1287 (Δ = -2.2 ppm);

Elemental analysis: calculated for $C_{16}H_{18}N_2O_5$ C: 60.37%, H: 5.70%, N: 8.80%; measured C: 60.60% (Δ = 0.23), H: 5.70% (Δ = 0.00), N: 8.80% (Δ = 0.01);

M.p. 111-113 °C (*i*PrOH/Toluene, 1:9).

1-(4-Methoxyphenyl)-3-phenyl-1*H*-pyrazole, 311:

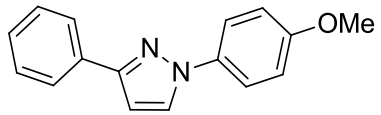

Chemical Formula: $C_{16}H_{14}N_2O$
Exact Mass: 250.1106

Consistent with published data[119]

Prepared using general procedure A: Isolated yield; 0.139 g (79%, 0.70 mmol scale);

Colourless crystals; Rf: 0.36 (8/2, EtOAc/hexanes);

^{1}H NMR (700 MHz, $CDCl_3$) 7.94 – 7.90 (m, 2H), 7.85 (d, *J* = 2.5 Hz, 1H), 7.69 – 7.65 (m, 2H), 7.46 – 7.41 (m, 2H), 7.34 (ddt, *J* = 7.4, 5.6, 1.3 Hz, 1H), 7.01 – 6.97 (m, 2H), 6.75 (d, *J* = 2.4 Hz, 1H), 3.85 (s, 3H);

^{13}C NMR (176 MHz, $CDCl_3$) δ/ppm 158.3 (C), 152.7 (C), 134.2 (C), 133.4 (C), 128.8 (CH), 128.2 (CH), 128.0 (CH), 125.9 (CH), 120.9 (CH), 114.7 (CH), 104.7 (CH), 55.7 (CH_3);

IR (neat) ν = 3003 (w), 1529 (m), 1516 (s), 1458 (m), 1363 (m), 1257 (s), 1234 (m), 1045 (m), 1025 (m), 956 (m) cm^{-1};

LC-MS (MeCN), Rt. 3.63 min, m/z = 251.1 $[M+H]^+$. HR-MS (ESI-TOF) calculated for $C_{16}H_{15}N_2O$ 251.1184, found 251.1192 (Δ = 3.2 ppm);

M.p. 107-108 °C (*i*PrOH) (Literature: 106-107 °C, aq. EtOH).[162]

Ethyl 2-(4-methoxyphenyl)-6-methyl-3-oxo-2,3-dihydropyridazine-4-carboxylate, 312:

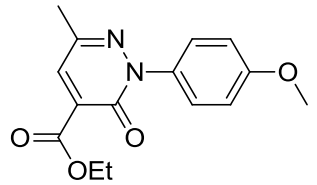

Chemical Formula: $C_{15}H_{16}N_2O_4$
Exact Mass: 288.1110

Prepared using general procedure A: Isolated yield; 0.162 g (81%, 0.697 mmol scale);

Yellow crystals; Rf: 0.24 (1/1, EtOAc/hexanes);

^{1}H NMR (400 MHz, $CDCl_3$) δ/ppm 7.65 (s, 1H), 7.52 – 7.45 (m, 2H), 6.99 – 6.92 (m, 2H), 4.40 (q, *J* = 7.1 Hz, 2H), 3.83 (s, 3H), 2.42 (s, 3H), 1.38 (t, *J* = 7.1 Hz, 3H);

^{13}C NMR (101 MHz, $CDCl_3$) δ/ppm 163.9 (C), 159.5 (C), 156.5 (C), 143.9 (C), 134.74 (CH), 134.66 (C), 131.4 (C), 126.9 (CH), 114.1 (CH), 62.3 (CH_2), 55.7 (CH_3), 21.0 (CH_3), 14.3 (CH_3);

IR (neat) ν = 3022 (w), 2971 (w), 1739 (s, C=O), 1658 (m, C=O of lactam), 1604 (m), 1510 (m), 1314 (m), 1250 (m), 1229 (s), 1150 (m), 1025 (m), 841 (s) cm^{-1};

LC-MS (MeCN), Rt. 2.64 min, m/z = 289.4 $[M+H]^+$. HR-MS (ESI-TOF) calculated for $C_{15}H_{17}N_2O_4$ 289.1188, found 289.1198 (Δ = 3.5 ppm);

Elemental analysis: calculated for $C_{15}H_{16}N_2O_4$ C: 62.49%, H: 5.59%, N: 9.72%; measured C: 62.63% (Δ = 0.14), H: 5.59% (Δ = 0.00), N: 9.73% (Δ = 0.01);

M.p. 80-81 °C (*i*PrOH).

4-Methoxy-*N*-phenylaniline, 313:

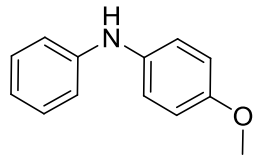

Chemical Formula: $C_{13}H_{13}NO$
Exact Mass: 199.0997

Consistent with published data.[163]

Prepared using general procedure A: Isolated yield; 0.125 g (90%, 0.69 mmol scale);

Colourless crystals; Rf: 0.36 (8/2, EtOAc/hexanes);

^{1}H NMR (400 MHz, $CDCl_3$) δ/ppm 7.28 – 7.22 (m, 2H), 7.14 – 7.08 (m, 2H), 6.98 – 6.83 (m, 5H), 5.54 (s, br, 1H), 3.83 (s, 3H);

^{13}C NMR (101 MHz, $CDCl_3$) δ/ppm 155.4 (C), 145.3 (C), 135.9 (C), 129.4 (CH), 122.4 (CH), 119.7 (CH), 115.8 (CH), 114.8 (CH), 55.7 (CH_3);

IR (neat) ν = 3387 (m), 3010 (w), 2958 (w), 2839 (w), 1595 (m), 1507 (s), 1499 (s), 1462 (w), 1443 (m), 1316 (m), 1298 (m), 1248 (s), 1236 (s), 1182 (m), 1169 (m), 1033 (w), 812 (m), 750 (s), 694 (s) cm^{-1};

LC-MS (MeCN), Rt. 3.15 min, m/z = 200.6 $[M+H]^+$. HR-MS (ESI-TOF) calculated for $C_{13}H_{14}NO$ 200.1075, found 200.1072 (Δ = 1.5 ppm);

M.p. 102-104 °C (MeCN) (Literature: 101-103 °C, no solvent reported).[163]

Diphenylamine, 205a:

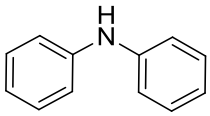

Chemical Formula: $C_{12}H_{11}N$
Exact Mass: 169.0891

Consistent with published data.[164]

Prepared using general procedure A: Isolated yield; 0.108 g (92%, 0.69 mmol scale);

Colourless crystals; Rf: 0.47 (8/2, EtOAc/hexanes);

^{1}H NMR (400 MHz, $CDCl_3$) δ/ppm 7.33 – 7.26 (m, 4H), 7.13 – 7.07 (m, 4H), 6.96 (tt, *J* = 7.3, 1.1 Hz, 2H), 5.82 (s, br, 1H);

^{13}C NMR (101 MHz, $CDCl_3$) δ/ppm 143.2 (C), 129.5 (CH), 121.2 (CH), 118.0 (CH);

IR (neat) ν = 3408 (w), 3384 (m), 3042 (w), 1739 (w, br), 1596 (s), 1519 s), 1496 (s), 1459 (m), 1419 (m), 1319 (m), 1173 (m), 749 (s), 744 (s), 690 (s) cm^{-1};

LC-MS (MeCN), Rt. 3.22 min, m/z = 170.1 $[M+H]^+$. HR-MS (ESI-TOF) calculated for $C_{12}H_{12}N$ 170.0970, found 170.0966 (Δ = 2.4 ppm);

M.p. 53-54 °C (95% EtOH) (Literature: 54-55 °C, no solvent reported).[164]

5-Bromo-*N*-phenylpyridin-3-amine, 314:

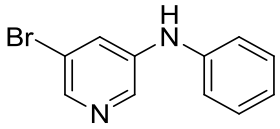

Chemical Formula: $C_{11}H_9BrN_2$
Exact Mass: 247.9949

Prepared using general procedure A: Isolated yield; 0.085 g (50%, 0.69 mmol scale);

Colourless crystals; Rf: 0.20 (8/2, EtOAc/hexanes);

^{1}H NMR (400 MHz, $CDCl_3$) δ/ppm 8.24 (d, *J* = 2.5 Hz, 1H), 8.16 (d, *J* = 2.0 Hz, 1H), 7.52 (t, *J* = 2.2 Hz, 1H), 7.38 – 7.30 (m, 2H), 7.15 – 7.03 (m, 3H), 6.02 (s, br, 1H);

^{13}C NMR (101 MHz, $CDCl_3$) δ/ppm 141.9 (CH), 141.5 (C), 140.7 (C), 137.5 (CH), 130.0 (CH), 124.6 (CH), 123.4 (CH), 121.0 (C), 119.7 (CH);

IR (neat) ν = 3257 (w), 3083 (w), 3047 (w), 2992 (w), 2365 (w), 1739 (w, br), 1614 (w), 1578 (s), 1570 (s), 1497 (s), 1444 (s), 1343 (m), 1331 (m), 1219 (m), 1096 (m), 1005 (m), 854 (s), 750 (s), 693 (s) cm^{-1};

LC-MS (MeCN), Rt. 3.09 min, m/z = 249.0 $[M+H]^+$. HR-MS (ESI-TOF) calculated for $C_{11}H_{10}N_2Br$ 249.0027, found 249.0023 (Δ = 1.6 ppm);

M.p. 160 °C (DCM).

4-Chloro-*N*-phenylaniline, 205c:

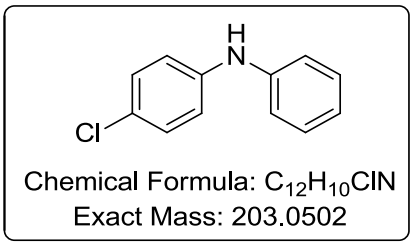

Consistent with published data.[163]

Prepared using general procedure A: Isolated yield; 0.201 g (71%, 1.39 mmol scale);

Yellow oil; Rf: 0.44 (8/2, EtOAc/hexanes);

^{1}H NMR (400 MHz, $CDCl_3$) δ/ppm 7.32 – 7.25 (m, 3H), 7.24 – 7.19 (m, 2H), 7.08 – 7.03 (m, 2H), 7.02 – 6.93 (m, 3H), 5.79 (s, br, 1H);

^{13}C NMR (101 MHz, $CDCl_3$) δ/ppm 142.7 (C), 141.9 (C), 129.6 (CH), 129.4 (CH), 125.7 (C), 121.7 (CH), 119.0 (CH), 118.3 (CH).

IR (neat) ν = 3400 (w, br), 3062 (w), 3029 (w), 1588 (s), 1501 (s), 1499 (s), 1496 (s), 1486 (s), 1310 (s), 1173 (m), 1091 (m), 816 (m), 748 (s), 693 (s) cm^{-1};

LC-MS (MeCN), Rt. 3.29 min, m/z = 204.11 $[M+H]^+$. HR-MS (ESI-TOF) calculated for $C_{12}H_{11}NCl$ 204.0580, found 204.0579 (Δ = 0.5 ppm).

(*Rac*)-methyl 3-(4-hydroxyphenyl)-2-(phenylamino)propanoate, 315:

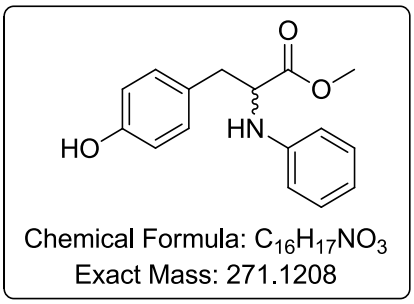

Prepared using general procedure A: Isolated yield; 0.049 g (26%, 0.69 mmol scale);

Colourless crystals; Rf: 0.12 (8/2, EtOAc/hexanes);

^{1}H NMR (400 MHz, $CDCl_3$) δ/ppm 7.18 (dd, *J* = 7.3, Hz, 2H), 7.02 (d, *J* = 8.4 Hz, 2H), 6.76 (t, *J* = 7.3 Hz, 1H), 6.74 (d, *J* = 8,4 Hz, 2H), 6.63 (d, *J* = 7.7 Hz, 2H), 5.08 (s, 1H), 4.33 (t, *J* = 6.1 Hz, 1H), 4.15 (s, br, 1H), 3.68 (s, 3H), 3.14 – 3.00 (m, 2H);

^{13}C NMR (101 MHz, $CDCl_3$) δ/ppm 174.0 (C), 154.8 (C), 146.4 (C), 130.6 (CH), 129.5 (CH), 128.3 (C), 118.7 (CH), 115.6 (CH), 113.8 (CH), 58.0 (CH), 52.3 (CH_3), 37.9 (CH_2);

IR (neat) ν = 3391 (m, br), 3028 (w). 2954 (w), 1727 (m, C=O), 1603 (s), 1515 (s), 1437 (w), 1221 (m, br) cm^{-1};

LC-MS (MeCN), Rt. 2.61 min m/z = 272.4 $[M+H]^+$. HR-MS (ESI-TOF) calculated for $C_{16}H_{18}NO_3$ 272.1287, found 272.1281 (Δ = 2.2 ppm).

(*Rac*)-methyl 3-(4-phenoxyphenyl)-2-(phenylamino)propanoate, 316:

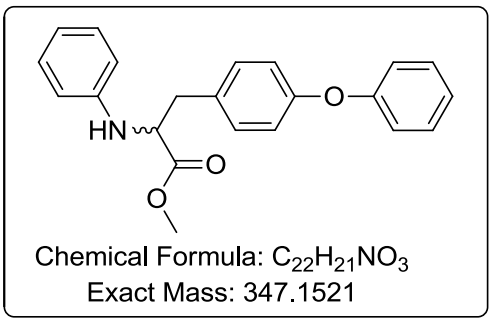

The results from the 2D NMR spectra (2D-NOESY) are consistent with the second alkylation on the phenol rather than the secondary amine. The fact that correlation is present with the ortho-protons on the phenol attached to the amine with the methane and methylene protons but no other correlation of other aromatic protons with the same methane and methylene protons, indicates that the other phenyl ring is not in the same environment. Unfortunately no correlation with the ortho-protons of the phenyl rings separated by the ether bond is present, but this could be due to the conformation of the molecule with the phenyl rings perpendicular to each other.

Prepared using general procedure A: Isolated yield; 8 mg (3%, 0.69 mmol scale);

Colourless crystals; Rf: 0.40 (8/2, EtOAc/hexanes);

^{1}H NMR (700 MHz, $CDCl_3$) δ/ppm 7.35 – 7.31 (m, 2H), 7.20 – 7.16 (m, 2H), 7.14 – 7.08 (m, 3H), 7.00 – 6.97 (m, 2H), 6.95 – 6.92 (m, 2H), 6.76 (tt, *J* = 7.3, 1.1 Hz, 1H), 6.64 – 6.60 (m, 2H), 4.35 (t, *J* = 6.2 Hz, 1H), 3.69 (s, 3H), 3.18 – 3.06 (m, 2H);

^{13}C NMR (176 MHz, $CDCl_3$) δ/ppm 173.6 (C), 157.3 (C), 156.5 (C), 146.3 (C), 131.2 (C), 130.7 (CH), 129.9 (CH), 129.5 (CH), 123.4 (CH), 119.04 (CH), 119.01 (CH), 118.8 (CH), 113.9 (CH), 58.1 (CH), 52.3 (CH_3), 38.1 (CH_2);

IR (neat) ν = 3404 (w), 3030 (w), 2954 (w), 1739 (m, C=O), 1603 (m), 1591 (m), 1506 (s), 1489 (s), 1239 (s) cm^{-1};

LC-MS (MeCN), Rt. 3.67 min, m/z = 348.2 $[M+H]^+$. HR-MS (ESI-TOF) calculated for $C_{22}H_{22}NO_3$ 348.1600, found 348.1609 (Δ = 2.6 ppm).

Methyl 4-methyl-2-(phenylamino)pentanoate, 317:

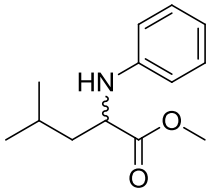

Chemical Formula: $C_{13}H_{19}NO_2$
Exact Mass: 221.1416

Prepared using general procedure A: Isolated yield; 0.153 g (60%, 0.69 mmol scale);

Amorphous solid; Rf: 0.52 (8/2, EtOAc/hexanes);

^{1}H NMR (400 MHz, $CDCl_3$) δ/ppm 7.22 – 7.14 (m, 2H), 6.75 (tt, *J* = 7.4, 1.1 Hz, 1H), 6.65 – 6.60 (m, 2H), 4.11 (dd, *J* = 7.8, 6.6 Hz, 1H), 4.00 (s, br, 1H), 3.71 (s, 3H), 1.81 (dh, *J* = 13.3, 6.6 Hz, 1H), 1.72 – 1.59 (m, 2H), 1.00 (d, *J* = 6.6 Hz, 3H), 0.95 (d, *J* = 6.6 Hz, 3H);

^{13}C NMR (101 MHz, $CDCl_3$) δ/ppm 175.3 (C), 147.1 (C), 129.5 (CH), 118.5 (CH), 113.5 (CH), 55.2 (CH), 52.2 (CH_3), 42.5 (CH_2), 25.0 (CH), 22.9 (CH_3), 22.32 (CH_3);

IR (neat) ν = 3384 (w, br), 3028 (w), 2955 (m), 2870 (w), 1734 (s), 1602 (s), 1507 (m), 1433 (w), 1198 (m), 1155 (s), 748 (s), 691 (s) cm^{-1};

LC-MS (MeCN), Rt. 3.39 min, m/z = 222.2 $[M+H]^+$. HR-MS (ESI-TOF) calculated for $C_{13}H_{20}NO_2$ 222.1494, found 222.1496 (Δ = 0.9 ppm).

1-(3,4-Dimethoxyphenyl)-3,4-dimethyl-1*H*-1,2,4-triazol-5(4*H*)-one, 318:

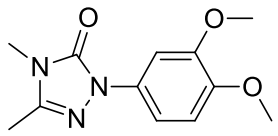

Chemical Formula: $C_{12}H_{15}N_3O_3$
Exact Mass: 249.1113

Prepared using general procedure A: Isolated yield; 0.045g (26%, 0.702 mmol scale);

Off-white crystals (recrystallised using *i*PrOH); Rf: 0.12 (8/2, EtOAc/hexanes);

^{1}H NMR (600 MHz, $CDCl_3$) δ/ppm 7.56 (d, *J* = 2.4 Hz, 1H), 7.45 (dd, *J* = 8.8, 2.4 Hz, 1H), 6.89 (d, *J* = 8.8 Hz, 1H), 3.93 (s, 3H), 3.89 (s, 3H), 3.29 (s, 3H), 2.30 (s, 3H);

^{13}C NMR (151 MHz, $CDCl_3$) δ/ppm 152.3 (C), 149.0 (C), 146.5 (C), 143.8 (C), 131.6 (C), 111.2 (CH), 110.7 (CH), 103.2 (CH), 56.1 (CH_3), 55.9 (CH_3), 27.4 (CH_3), 11.8 (CH_3);

IR (neat) ν = 2943 (w), 2842 (w), 1701 (s), 1604 (w). 1590 (w), 1515 (s), 1466 (m), 1250 (s), 1220 (m), 1027 (m) cm^{-1};

LC-MS (MeCN), Rt. 2.48 min, m/z = 250.1 $[M+H]^+$. HR-MS (ESI-TOF) calculated for $C_{12}H_{16}N_3O_3$ 250.1192, found 250.1196 (Δ = 1.6 ppm);

Elemental analysis: calculated for $C_{12}H_{15}N_3O_3$ C: 57.82%, H: 6.07%, N: 16.86%; measured C: 57.60% (Δ = 0.22), H: 6.08% (Δ = 0.01), N: 16.51% (Δ = 0.35);

M.p. 145-146 °C (*i*PrOH).

1,3-Diphenyl-1*H*-pyrazole, 319:

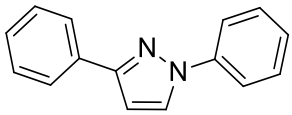

Chemical Formula: $C_{15}H_{12}N_2$
Exact Mass: 220.1000

Consistent with published data[119]

Prepared using general procedure A: Isolated yield; 0.249 g (81%, 0.70 mmol scale);

Colourless crystals (recrystallised using *i*PrOH); Rf: 0.40 (8/2, EtOAc/hexanes);

^{1}H NMR (700 MHz, $CDCl_3$) 7.99 – 7.95 (m, 1H), 7.93 (dd, *J* = 7.8, 1.5 Hz, 2H), 7.80 – 7.76 (m, 2H), 7.50 – 7.46 (m, 2H), 7.44 (t, *J* = 7.6 Hz, 2H), 7.37 – 7.33 (m, 1H), 7.32 – 7.28 (m, 1H), 6.80 – 6.77 (m, 1H);

^{13}C NMR (176 MHz, $CDCl_3$) δ/ppm 153.1 (C), 140.4 (C), 133.2 (C), 129.6 (CH), 128.8 (CH), 128.2 (CH), 128.1 (CH), 126.5 (CH), 126.0 (CH), 119.2 (CH), 105.2 (CH);

IR (neat) ν = 3137 (w), 3065 (w), 1599 (m), 1526 (m), 1506 (m), 1457 (m), 1360 (m), 1303 (w), 1265 (m), 1045 (m), 954 (m), 940 (m) cm^{-1};

LC-MS (MeCN), Rt. 3.53 min, m/z = 221.2 $[M+H]^+$. HR-MS (ESI-TOF) calculated for $C_{15}H_{13}N_2$ 221.1079, found 221.1090 (Δ = 5.0 ppm);

M.p. 84-85 °C (*i*PrOH) (Literature: 83-84 °C, no solvent reported).[165]

1-(3-(Methylthio)phenyl)-3-phenyl-1*H*-pyrazole, 320:

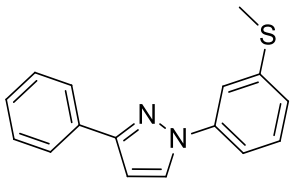

Chemical Formula: $C_{16}H_{14}N_2S$
Exact Mass: 266.0878

Prepared using general procedure A: Isolated yield; 0.286 g (77%, 1.4 mmol scale);

Colourless oil; Rf: 0.50 (8/2, EtOAc/hexanes);

^{1}H NMR (600 MHz, $CDCl_3$) δ/ppm 7.95 (d, *J* = 1.4 Hz, 1H), 7.94 – 7.92 (m, 2H), 7.73 (t, *J* = 2.1 Hz, 1H), 7.49 (ddd, *J* = 8.1, 2.2, 0.9 Hz, 1H), 7.45 (dd, *J* = 8.2, 7.1 Hz, 2H), 7.36 (t, *J* = 7.7 Hz, 2H), 7.19 – 7.15 (m, 1H), 6.78 (d, *J* = 2.4 Hz, 1H), 2.56 (s, 3H);

^{13}C NMR (151 MHz, $CDCl_3$) δ/ppm 153.1 (C), 140.7 (C), 140.5 (C), 133.1 (C), 129.7 (CH), 128.8 (CH), 128.2 (CH), 128.2 (CH), 126.0 (CH), 124.2 (CH), 117.0 (CH), 115.5 (CH), 105.3 (CH), 15.8 (CH_3);

IR (neat) ν = 3062 (w), 2920 (w), 1591 (s), 1583 (s), 1530 (w), 1502 (s), 1479 (m), 1454 (s), 1360 (s), 1045 (s), 963 (m), 945 (m) cm^{-1};

LC-MS (MeCN), Rt. 4.409 min, m/z = 267.1 $[M+H]^+$. HR-MS (ESI-TOF) calculated for 267.0956 $C_{16}H_{15}N_2S$, found 267.0966 (Δ = 3.7 ppm).

1-(2-Methoxyphenyl)-3-phenyl-1*H*-pyrazole, 321:

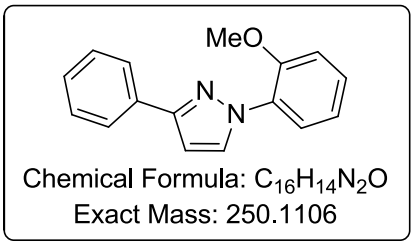

Consistent with published data[119]

Prepared using general procedure A: Isolated yield; 0.227 g (65%, 1.4 mmol scale);

Colourless oil; Rf: 0.43 (8/2, EtOAc/hexanes);

^{1}H NMR (400 MHz, $CDCl_3$) δ/ppm 8.09 (d, *J* = 2.5 Hz, 1H), 7.94 – 7.90 (m, 2H), 7.87 (dd, *J* = 7.9, 1.7 Hz, 1H), 7.44 – 7.40 (m, 2H), 7.35 – 7.29 (m, 2H), 7.09 (td, *J* = 7.7, 1.3 Hz, 1H), 7.06 (dd, *J* = 8.3, 1.2 Hz, 1H), 6.74 (d, *J* = 2.5 Hz, 1H), 3.91 (s, 3H);

^{13}C NMR (151 MHz, $CDCl_3$) δ/ppm 151.8 (C), 151.2 (C), 133.3 (C), 133.0 (CH), 129.8 (C), 128.5 (CH), 127.8 (CH), 127.8 (CH), 125.9 (CH), 125.2 (CH), 121.3 (CH), 112.3 (CH), 103.7 (CH), 56.0 (CH_3);

IR (neat) ν = 3060 (w), 2940 (w), 2839 (w), 1597 (m), 1530 (m), 1508 (s), 1455 (s), 1286 (m), 1259 (m), 1242 (s), 1127 (m), 1022 (s), 954 (m), 942 (m) cm^{-1};

LC-MS (MeCN), Rt. 3.53 min, m/z = 251.2 $[M+H]^+$. HR-MS (ESI-TOF) calculated for 251.14182 $C_{16}H_{15}N_2O$, found 251.1182 (Δ = 0.0 ppm).

1-(3-Methoxyphenyl)-3-phenyl-1*H*-pyrazole, 322:

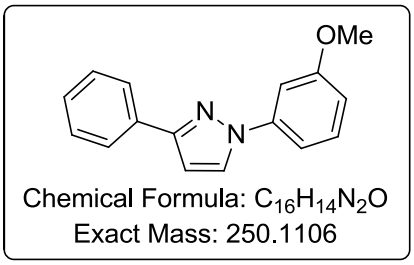

Consistent with published data[119]

Prepared using general procedure A: Isolated yield; 0.287 g (82%, 1.4 mmol scale);

Colourless oil; Rf: 0.36 (8/2, EtOAc/hexanes);

^{1}H NMR (400 MHz, $CDCl_3$) δ/ppm 8.01 – 7.97 (m, 2H), 7.96 (d, *J* = 2.5 Hz, 1H), 7.52 – 7.44 (m, 3H), 7.43 – 7.32 (m, 3H), 6.88 (ddd, *J* = 8.0, 2.5, 1.2 Hz, 1H), 6.80 (d, *J* = 2.5 Hz, 1H), 3.92 (s, 3H);

^{13}C NMR (151 MHz, $CDCl_3$) δ/ppm 160.6 (C), 152.9 (C), 141.4 (C), 133.2 (C), 130.2 (CH), 128.7 (CH), 128.2 (CH), 128.1 (CH), 125.9 (CH), 112.1 (CH), 111.1 (CH), 105.2 (CH), 105.1 (CH), 55.6 (CH_3);

IR (neat) ν = 3065 (w), 2961 (w), 1606 (s), 1593 (s), 1530 (m), 1504 (s), 1362 (m), 1246 (m), 1217 (s), 1170 (m), 1045 (s), 966 (m) cm^{-1};

LC-MS (MeCN), Rt. 3.35 min, m/z = 251.1 $[M+H]^+$. HR-MS (ESI-TOF) calculated for $C_{16}H_{15}N_2O$ 251.1184, found 251.1194 (Δ = 4.0 ppm).

4-(3-Phenyl-1*H*-pyrazol-1-yl)benzonitrile, 323:

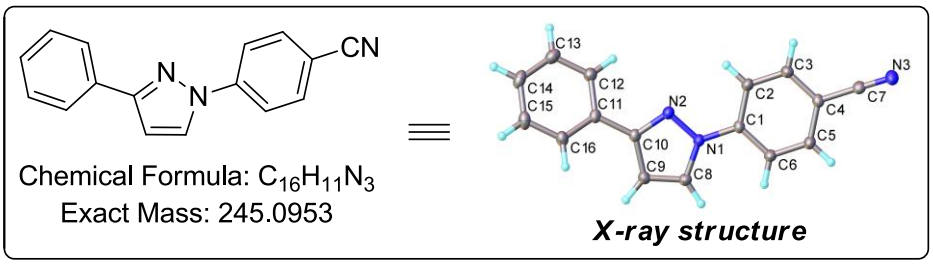

Prepared using general procedure A: Isolated yield; 0.264 g (76%, 1.4 mmol scale);

Colourless crystals (recrystallised using *i*PrOH); Rf: 0.26 (8/2, EtOAc/hexanes);

^{1}H NMR (600 MHz, $CDCl_3$) 8.02 (d, *J* = 2.6 Hz, 1H), 7.94 – 7.88 (m, 4H), 7.78 – 7.73 (m, 2H), 7.45 (dd, *J* = 8.3, 7.0 Hz, 2H), 7.41 – 7.36 (m, 1H), 6.84 (d, *J* = 2.6 Hz, 1H);

^{13}C NMR (151 MHz, $CDCl_3$) δ/ppm 154.2 (C), 142.9 (C), 133.6 (CH), 132.3 (C), 128.8 (CH), 128.6 (CH), 128.0 (CH), 126.0 (CH), 118.7 (CH), 118.5 (CN), 109.3 (C), 106.5 (CH);

IR (neat) ν = 3138 (w), 3123 (w), 2228 (m, CN), 1604 (m), 1533 (m), 1520 (m), 1517 (m), 1457 (m), 1394 (w), 1363 (m), 1183 (m), 953 (m), 939 (m) cm^{-1};

LC-MS (MeCN), Rt. 3.36 min, m/z = 246.1 $[M+H]^+$. HR-MS (ESI-TOF) calculated for $C_{16}H_{12}N_3$ 246.1031, found 246.1032 (Δ = 0.4 ppm);

M.p. 126-131 °C (*i*PrOH).

Crystal Data: **323**, $C_{16}H_{11}N_3$ (*M* =245.28 g/mol): monoclinic, space group $P2_1/c$ (no. 14), *a* = 10.9809(6) Å, *b* = 11.0294(6) Å, *c* = 11.0655(6) Å, *β* = 113.0712(17)°, *V* = 1232.98(12) $Å^3$, *Z* = 4, *T* = 120 K, μ(MoKα) = 0.081 mm^{-1}, *Dcalc* = 1.321 g/cm^3, 26247 reflections measured (5.446° ≤ 2Θ ≤ 60.176°), 3621 unique (R_{int} = 0.0290, R_{sigma} = 0.0186) which were used in all calculations. The final R_1 was 0.0457 (I > 2σ(I)) and wR_2 was 0.1236 (all data).

3-(3-Phenyl-1*H*-pyrazol-1-yl)benzonitrile, 324:

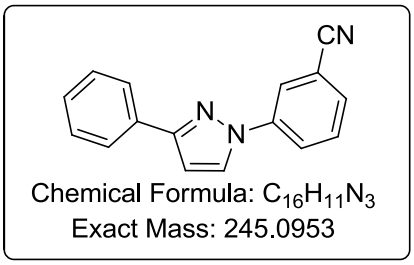

Consistent with published data[119]

Prepared using general procedure A but using 2 equiv. of NEt_3 to aid solubility: Isolated yield; 0.067 g (40%, 0.69 mmol scale);

Colourless oil; Rf: 0.30 (8/2, EtOAc/hexanes);

^{1}H NMR (400 MHz, $CDCl_3$) δ/ppm 8.16 – 8.11 (m, 1H), 8.04 – 7.97 (m, 2H), 7.96 – 7.91 (m, 2H), 7.63 – 7.55 (m, 2H), 7.52 – 7.45 (m, 2H), 7.43 – 7.37 (m, 1H), 6.85 (d, *J* = 2.6 Hz, 1H);

^{13}C NMR (151 MHz, $CDCl_3$) δ/ppm 153.9 (C), 140.7 (C), 132.5 (C), 130.5 (CH), 129.5 (CH), 128.9 (CH), 128.6 (CH), 127.9 (CH), 126.0 (CH), 122.6 (CH), 122.1 (CH), 118.3 (C), 113.7 (C), 106.3 (CH);

IR (neat) ν = 3148 (w), 3064 (w), 2232 (m, CN), 1604 (s), 1587 (s), 1533 (m), 1506 (s), 1455 (s), 1437 (m), 1398 (m), 1368 (s), 1388 (w), 1051 (m), 967 (m) cm^{-1};

LC-MS (MeCN) Rt. 3.18 min, m/z = 246.4 $[M+H]^+$. HR-MS (ESI-TOF) calculated for $C_{16}H_{15}N_2O$ 246.1031, found 246.1040 (Δ = 3.7 ppm).

2-(3-Phenyl-1*H*-pyrazol-1-yl)benzonitrile: 325;

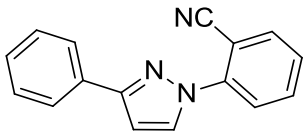

Chemical Formula: $C_{16}H_{11}N_3$
Exact Mass: 245.0953

Consistent with published data[166]

Prepared using general procedure A but using 2 equiv. of NEt_3 to aid solubility: Isolated yield; 0.064 g (38%, 0.69 mmol scale);

Colourless oil; Rf: 0.22 (8/2, EtOAc/hexanes);

^{1}H NMR (700 MHz, $CDCl_3$) δ/ppm 8.19 (d, *J* = 2.6 Hz, 1H), 7.96 – 7.91 (m, 2H), 7.88 (dd, *J* = 8.3, 1.1 Hz, 1H), 7.79 (dd, *J* = 7.8, 1.5 Hz, 1H), 7.71 (ddd, *J* = 8.3, 7.5, 1.5 Hz, 1H), 7.47 – 7.43 (m, 2H), 7.41 (td, *J* = 7.6, 1.1 Hz, 1H), 7.37 (ddt, *J* = 8.0, 6.8, 1.3 Hz, 1H), 6.86 (d, *J* = 2.6 Hz, 1H);

^{13}C NMR (176 MHz, $CDCl_3$) 154.2 (C), 142.0 (C), 134.8 (CH), 134.1 (CH), 132.6 (C), 130.7 (CH), 128.9 (CH), 128.6 (CH), 127.0 (CH), 126.2 (CH), 123.8 (CH), 117.4 (C), 106.2 (CH), 104.9 (C);

IR (neat) ν = 3143 (w), 3065 (w), 2226 (w, CN), 1601 (m), 1580 (m), 1532 (m), 1505 (s), 1455 (s), 1392 (w), 1364 (m), 1310 (w), 1259 (w), 1046 (m), 955 (m), 941 (m) cm^{-1};

LC-MS (MeCN) Rt. 3.11 min, m/z = 246.4 $[M+H]^+$. HR-MS (ESI-TOF) calculated for $C_{16}H_{12}N_3$ 246.1031, found 246.1036 (Δ = 2.0 ppm).

(*E*/*Z*)-ethyl 2-(1-ethoxyethylidene)hydrazinecarboxylate, 328:

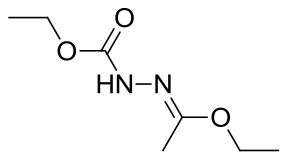

Chemical Formula: $C_7H_{14}N_2O_3$
Exact Mass: 174.1004

Literature procedure.[167]

Ethyl acetimidate hydrochloride (4.96 g, 10 mmol) was dissolved in absolute EtOH (200 mL) and cooled using an ice bath. Ethyl hydrazine carboxylate (4.16 g, 10 mmol) was dissolved in absolute EtOH (80 mL) and added dropwise and reaction left to stir for 6 h at 0 °C. The solvent was evaporated under reduced pressure and the residue was purified using a flash chromatography (9:1, DCM/MeOH) to give the pure product as white crystals (5.27 g, 76% yield) as a mixture of two *E*/*Z* isomers (45:55).

Isolated yield: 5.27 g (76%, 10 mmol scale);

White crystals; Rf: 0.72 (1/9, DCM/MeOH);

Isomer 1: ^{1}NMR (700 MHz, $CDCl_3$) δ/ppm 8.06 (s, br, 1H), 4.08 (q, *J* = 7.0 Hz, 4H), 2.09 (s, 3H), 1.33 (t, *J* = 7 Hz, 6H).

Isomer 2: ^{1}NMR (700 MHz, $CDCl_3$) δ/ppm 6.79 (s, br, 1H), 4.14 (q, *J* = 7.0 Hz, 4H), 1.94 (s, 3H), 1.27 (t, *J* = 7 Hz, 6H).

IR (neat) ν = 3408 (w), 3274 (w, br), 2986 (w), 2938 (w), 1713 (s), 1657 (s), 1500 (br), 1447 (m), 1379 (m), 1338 (w), 1243 (br), 1047 (s), 1017 (w) cm^{-1};

LC-MS (MeCN), Rt. 2.63 min, m/z = 174.8 $[M+H]^+$. HR-MS ($^+$ESI-TOF) calculated for $C_7H_{14}N_2O_3$ 175.1083, found 175.1078 (Δ = 4.6 ppm).

M.p. 60-65 °C (MeOH) (Literature: 68 °C, Pet. Ether).[168]

3,4-Dimethyl-1*H*-1,2,4-triazol-5(4*H*)-one, 329:

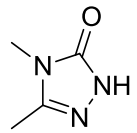

Chemical Formula: $C_4H_7N_3O$
Exact Mass: 113.0589

Literature procedure.[169]

Methylamine hydrochloride (2.70 g, 40 mmol) was dissolved in absolute EtOH (200 mL) to which a suspension of sodium ethoxide (2.72 g, 40 mmol) in absolute EtOH (70 mL) was added and reaction was stirred for 5 min at room temperature. A solution of (*E*)-ethyl 2-(1-ethoxyethylidene)hydrazine carboxylate (**328**, 3.48 g, 20 mmol) in absolute EtOH (50 mL) was added dropwise and reaction refluxed for 4 h. The reaction was then cooled to room temperature and filtered over a celite pad. The eluant was dried under reduced pressure and the resultant residue was recrystallised (through a hot filtration) from EtOAc to give the pure product.

Isolated yield: 0.904 g (40%, 20 mmol scale);

White crystals (recrystallised from EtOAc); Rf: 0.31 (1/9, DCM/MeOH);

^{1}H NMR (600 MHz, DMSO-d_6) δ/ppm 11.28 (s, br, 1H), 3.06 (s, 3H), 2.12 (s, 3H);

^{13}C NMR (151 MHz, DMSO-d_6) δ/ppm 155.1 (C), 144.8 (C), 26.3 (CH_3), 11.4 (CH_3);

IR (neat) ν = 3139 (w, br), 3057 (w, br), 3001 (w, br), 2815 (w, br), 1701 (s), 1663 (s), 1590 (m), 1477 (m), 1474 (m), 1437 (m), 1400 (m), 1376 (m), 976 (m), 797 (m). 736 (s), 609 (s) cm^{-1};

LC-MS (MeCN), Rt. 0.77 min, m/z = 114.4 $[M+H]^+$. HR-MS (ESI-TOF) calculated for $C_4H_7N_3O$ 114.0667, found 114.0647 (Δ = 17.5 ppm or -2.0 mDa).

M.p. 146-149 °C (EtOAc) (Literature: 147 °C, no solvent reported).[169]

General Procedures for Chapter 2.3:

A) Microwave synthesis of thiazoles and 2-aminothiophenes:

In a 2-5 mL microwave vial was placed the nitrile (0.22 mmol, 1 equiv.) and dissolved in trifluoroethanol (2 mL) which was stirred for 2 min at room temperature. Next, 1,4-dithian-2,5-diol (0.11 mmol, 0.5 equiv.) was added and the mixture stirred for 5 min before triethylamine (0.242 mmol, 1.1 equiv.) was added and the mixture further stirred for 2 min. The vial was then sealed and heated in a microwave reactor for 390 min at 60 °C. The solvent was evaporated under reduced pressure and the crude residue was then purified using flash chromatography on silica (EtOAc/hexanes).

Spectroscopic and experimental data for Chapter 2.3:

Ethyl-2-phenyl-2(thiazol-2-yl)acetate, 362:

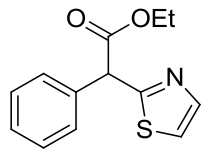

Chemical Formula: $C_{13}H_{13}NO_2S$
Exact Mass: 247.0667

Prepared using general procedure A: Isolated yield; 45 mg (83%, 0.22 mmol scale);

Pale yellow oil; Rf: 0.37 (1:4, EtOAc/hexane);

^{1}H NMR (700 MHz, $CDCl_3$): δ/ppm 7.75 (d, *J* = 3.3 Hz, 1H), 7.45 (d, *J* = 7.4 Hz, 2H), 7.39 – 7.35 (m, 2H), 7.34 – 7.30 (m, 1H), 7.29 (d, *J* = 3.3 Hz, 1H), 5.42 (s, 1H), 4.30 – 4.19 (m, 2H), 1.26 (t, *J* = 7.1 Hz, 3H);

^{13}C NMR (176 MHz, $CDCl_3$) δ/ppm 170.6 (C), 167.6 (C), 142.5 (CH), 136.7 (C), 129.1 (CH), 128.6 (CH), 128.3 (CH), 120.1 (CH), 62.0 (CH_2), 55.6 (CH), 14.2 (CH_3);

IR (neat) ν = 3064 (s), 3031 (s), 2980 (s), 2935 (s), 1730 (w), 1644 (s), 1600 (s), 1494 (m), 1454 (m), 1421 (s), 1390 (s), 1367 (m), 1308 (m), 1231 (m), 1185 (w), 1153 (w), 1130 (m), 1094 (m), 1056 (m), 1021 (w), 916 (s), 863 (m), 789 (m), 724 (w), 698 (w), 644 (s), 610 (m) cm^{-1};

LC-MS (MeCN), Rt. 2.79 min, m/z = 248.8 $[M+H]^+$. HR-MS (ESI-TOF) calculated for $C_{13}H_{14}NO_2S$ 248.0745, found 248.0755 (Δ = 4.0 ppm).

Methyl-2-phenyl-2(thiazol-2-yl)acetate, 363:

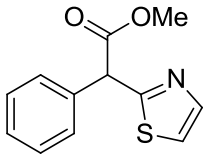

Chemical Formula: $C_{12}H_{11}NO_2S$
Exact Mass: 233.0510

Prepared using general procedure A: Isolated yield; 40 mg (60%, 0.22 mmol scale);

Pale yellow oil; Rf: 0.1 (1/9, EtOAc/hexane);

^{1}H NMR (700 MHz, $CDCl_3$) δ/ppm 7.79–7.75 (m, 1H), 7.46 (d, *J* = 8.3 Hz, 2H), 7.40–7.32 (m, 3H), 7.32–7.29 (m, 1H), 5.46 (s, 1H), 3.79 (s, 3H);

^{13}C NMR (176 MHz, $CDCl_3$) δ/ppm 170.9 (C), 167.5 (C), 142.2 (CH), 136.4 (C), 128.9 (CH), 128.5 (CH), 128.3 (CH), 120.1 (CH), 55.2 (CH), 52.9 (CH_3);

IR (neat) ν = 3088 (w), 2952 (w), 1968 (w), 1732 (s), 1644 (w), 1599 (w), 1494 (w), 1448 (w), 1434 (w), 1388 (w), 1368 (w), 1313 (w), 1241 (m), 1199 (m), 1156 (m), 1133 (m), 1098 (w), 1058 (w), 1005 (m), 892 (w), 863 (w), 795 (w), 728 (s), 697 (s), 654 (w), 612 (m) cm^{-1};

LC-MS (MeCN), Rt. 2.63 min, m/z = 233.9 $[M+H]^+$. HR-MS (ESI-TOF) calculated for $C_{12}H_{12}NO_2S$ 234.0589, found 234.0592 (Δ = 1.3 ppm).

Isopropyl 2-cyano-2-phenylacetate, 367:

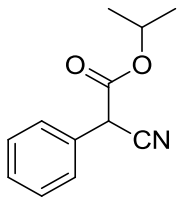

Chemical Formula: $C_{12}H_{13}NO_2$
Exact Mass: 203.0946

Ethyl phenylcyanoacetate (**362**, 0.473 g, 2.5 mmol) was dissolved in *i*PrOH (10 mL) and was stirred for 1 min. Polymer bound sulfonic acid (QP-SA) (200 mg, 2.2 mmol/g loading) was added and reaction was stirred for 3 days at 70 °C. The QP-SA resin was filtered, and the solvent evaporated to give the product as a colourless oil which was used without further purification.

Isolated yield: 0.322 g (64% 2.5 mmol),

Colourless oil; Rf: 0.40 (1/4, EtOAc/hexane);

^{1}H NMR (400 MHz, $CDCl_3$) δ/ppm 7.51 – 7.40 (m, 5H), 5.07 (hept, *J* = 6.3 Hz, 1H), 4.70 (s, 1H), 1.28 (dd, *J* = 7.6, 6.3 Hz, 6H);

^{13}C NMR (101 MHz, $CDCl_3$) δ/ppm 164.6 (C), 130.3 (C), 129.4 (CH), 129.3 (CH), 128.0 (CH), 116.0 (C), 71.6 (CH), 44.2 (CH), 21.6 (CH_3), 21.5 (CH_3);

IR (neat) ν = 3069 (w), 3038 (w), 2986 (w), 2937 (w), 2253 (w), 1739 (s), 1601 (w), 1498 (w), 1467 (w), 1456 (m), 1377(w), 1353 (w), 1256 (m), 1235 (m), 1199 (m), 1101 (s), 1032 (w), 1016 (w), 1004 (w), 956 (w), 917 (w), 901 (w), 83 (w), 732 (m), 695 (s) cm^{-1};

LC-MS (MeCN), Rt. 2.93 min, m/z = 204.0 $[M+H]^+$. HR-MS (ESI-TOF) calculated for $C_{12}H_{14}NO$ 204.1025, found 204.1032 (Δ = 3.4 ppm).

Ethyl 2-cyano-2-(4-methoxyphenyl)-acetate, 370:

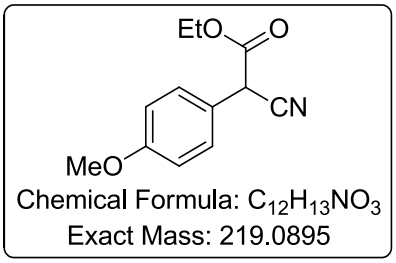

Literature procedure:[170]

A solution of 4-methoxyphenylacetonitrile (0.70 g, 4.76 mmol, 1.00 equiv.) was dissolved in dry THF (4.7 mL) and cooled to -78 °C. To the solution was added drowpwise *n*-butyllithium (6.0 mL, 9.52 mmol, 2.00 equiv.) and the colour of the solution immediately changed to yellow. After stirring for 20 min at -78 °C, a solution of ethyl chloroformate (**369**) (0.52 g, 4.76 mmol, 1.00 equiv.) in THF (1 mL) was added slowly to the stirred solution. The reaction mixture was stirred for 30 min and then allowed to warm to room temperature with stirring for over 1 h. The reaction was quenched with water (10 mL) and EtOAc (25 mL) was added. The layers were separated and the aqueous phase was extracted three times with EtOAc. The combined organic layer was washed with brine (2 x 25 mL), dried over sodium sulfate and the solvent was removed under reduced pressure. The crude material was further purified on a silica column 1:9 – 4:6 EtOAc/hexane gradient to give the product.

Isolated yield: 0.54 g (52%, 4.76 mmol scale);

Colourless oil; Rf: 0.32 (1/4, EtOAc/hexane);

^{1}H NMR (400 MHz, DMSO-d_6) δ/ppm 7.40 – 7.34 (m, 2H), 6.95 – 6.89 (m, 2H), 4.66 (s, 1H), 4.23 (qd, *J* = 7.1, 2.1 Hz, 2H), 3.81 (s, 3H), 1.27 (t, *J* = 7.1 Hz, 3H);

^{13}C NMR (101 MHz, DMSO-d_6) δ/ppm 165.4 (C), 160.3 (C), 129.2 (CH), 122.0 (C), 116.0 (C), 114.8 (CH), 63.3 (CH_2), 55.5 (CH), 43.1 (CH_3), 14.0 (CH_3);

IR (neat) ν = 3744 (w), 2984 (w), 2940 (w), 2910 (w), 2839 (w), 2248 (w), 2001 (w), 1741 (m), 1611 (m), 1586 (w), 1510 (s), 1464 (w), 1443 (w), 1423 (w), 1369 (w), 1304

(m), 1247 (s), 1199 (m), 1179 (m), 1112 (w), 1095 (w), 1027 (m), 942 (w), 833 (m), 811 (m), 793 (w), 753 (w), 634 (w) cm^{-1};

LC-MS (MeCN), Rt. 2.69 min, m/z = 218.2 $[M-H]^-$. HR-MS (ESI-TOF) calculated for $C_{12}H_{14}NO_3$ 220.0974, found 220.0970 (Δ = 1.8 ppm).

Ethyl 2-(benzo[*d*][1,3]dioxol-5-yl)-2-cyanoacetate, 373:

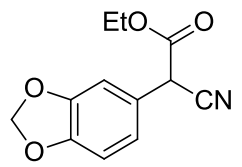

Chemical Formula: $C_{12}H_{11}NO_4$
Exact Mass: 233.0688

Literature procedure:[171]

Sodium hydride (0.799 g, 20.0 mmol) was slowly added to a solution of 3,4-(methylenedioxy)phenylacetonitrile (1.61 g, 10.0 mmol) in THF (20 mL) at 0 °C. Diethyl carbonate (2.36 g, 20.0 mmol) was added dropwise at room temperature and the reaction was refluxed for 4 h. The reaction was quenched with 2 M HCl (20 mL) and most of the THF was removed using a rotatory evaporator. The residue was then extracted with EtOAc (3 × 20 mL), the organic layer was dried over sodium sulfate, filtered and solvent evaporated under reduced pressure to obtain an orange oil which was purified using column chromatography (4:1, hexanes/EtOAc).

Isolated yield: 1.74 g (75%, 10.0 mmol scale);

Colourless oil; Rf: 0.61 (1/1, EtOAc/hexane);

^{1}H NMR (400 MHz, $CDCl_3$) δ/ppm 6.94 – 6.89 (m, 2H), 6.82 (dd, *J* = 7.7, 0.7 Hz, 1H), 6.01 (s, 2H), 4.61 (s, 1H), 4.25 (qd, *J* = 7.1, 2.2 Hz, 2H), 1.29 (t, *J* = 7.1 Hz, 3H);

^{13}C NMR (101 MHz, $CDCl_3$) δ/ppm 165.2 (C), 148.6 (C), 148.6 (C), 123.5 (C), 121.9 (CH), 115.8 (C), 108.9 (CH), 108.4 (CH), 101.8 (CH_2), 63.5 (CH_2), 43.5 (CH), 14.1 (CH_3);

IR (neat) ν = 2986 (w), 2941 (w), 2906 (w), 1744 (s), 1504 (s), 1491 (s), 1447 (m), 1369 (w), 1251 (s), 1105 (w), 1038 (s), 934 (w) cm^{-1};

LC-MS (MeCN), Rt. 2.67 min, m/z = 233.9 $[M+H]^+$. HR-MS (ESI-TOF) calculated for $C_{12}H_{12}NO_4$ 234.0758, found 234.0766 (Δ = 3.4 ppm).

Methyl 2-cyano-2-(4-nitrophenyl)-acetate, 377:

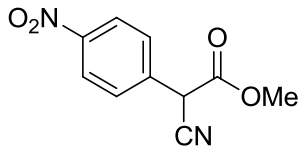

Chemical Formula: $C_{10}H_8N_2O_4$
Exact Mass: 220.0484

Consistent with published data[172]

Potassium hydroxide (0.40 g, 7.09 mmol, 1.00 equiv.) was stirred in DMSO (5 mL) to form a homogeneous solution in a sealed microwave vial. After 10 min of stirring in a water bath at 85 °C, methyl 2-cyanoacetate **375** (1.51 mL, 7.09 mmol, 1.00 equiv.) was added by means of a syringe and the solution stirred for a further 30 min. A solution of 1-fluoro-4-nitrobenzene **374** (2.00 g, 7.09 mmol, 1.00 equiv.) in DMSO (2 mL) was added dropwise at 85 °C. After 4 h the reaction mixture was poured in a beaker filled with ice and HCl (1 M, 5 mL). The vial was washed with EtOAc (20 mL) and the resulting solution was allowed to stir for 2 h. The two layers were separated and the aqueous layer was extracted with EtOAc (3 × 25 mL). The combined organic layers were washed with brine (2 x 25 mL), dried over sodium sulfate and the solvent was removed under reduced pressure. The crude material was purified via a silica column with pure hexanes to elute **374**. Methyl 2-cyanoacetate was removed on a high vacuum.

Isolated yield: 0.834 g (53% 7.09 mmol scale);

Red solid; Rf: 0.05 (2/8, EtOAc/hexane);

^{1}H NMR (700 MHz, $CDCl_3$) δ/ppm 8.28 (d, *J* = 8.8 Hz, 2H), 7.67 (d, *J* = 8.7 Hz, 2H), 4.87 (s, 1H), 3.83 (s, 3H);

^{13}C NMR (176 MHz, $CDCl_3$) δ/ppm 164.2 (C), 148.5 (C), 136.3 (C), 129.2 (CH), 124.5 (CH), 114.4 (C), 54.4 (CH), 43.1 (CH_3);

IR (neat) ν = 3133 (w), 3086 (w), 2973 (w), 2937 (w), 1740 (s), 1735 (s), 1610 (w), 1597 (w), 1523 (s), 1437 (m), 1348 (s), 1313 (m), 1289 (s), 1234 (s), 1165 (m), 1107 (m), 857 (m), 779 (m), 736 (s) cm^{-1};

LC-MS (MeCN), Rt. 2.44 min, m/z = 218.92 $[M-H]^-$. HR-MS (ESI-TOF) calculated for $C_{10}H_7N_2O_4$ 219.0406, found 219.0409 (Δ = 1.4 ppm);

Melting point: 93 – 95 °C.

Ethyl 2-cyano-2-(4-nitrophenyl)-acetate, 378:

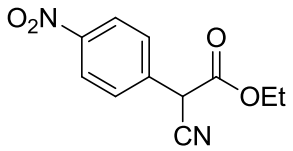

Chemical Formula: $C_{11}H_{10}N_2O_4$
Exact Mass: 234.0641

Consistent with published data[173]

Potassium hydroxide (0.80 g, 14.18 mmol, 1.00 equiv.) was stirred in DMSO (10 mL) to prepare a homogeneous solution in a sealed microwave vial. After 10 min of stirring in a water bath at 85 °C ethyl 2-cyanoacetate **376** (1.51 mL, 14.18 mmol, 1.00 equiv.) was added by means of a syringe and the solution was stirred for further 30 min. Then a solution of 1-fluoro-4-nitrobenzene **374** (2.00 g, 14.18 mmol, 1.00 equiv.) in DMSO (4 mL) was added dropwise at 85 °C. After 4 h the mixture was transferred in a beaker containing ice and HCl (1 M, 10 mL). The vial was washed with EtOAc (40 mL) and the resulting solution was allowed to stir for 2 h. The two layers were separated and the aqueous layer was extracted with EtOAc (3 x 25 mL). The combined organic layers were washed with brine (2 x 25 mL), dried over sodium sulfate and the solvent was removed under reduced pressure. The compound was purified by silica column chromatography with pure hexane to elute **374**. Ethyl 2-cyanoacetate was removed on a high vacuum.

Isolated yield: 1.89 g (57% 14.18 mmol scale);

Red oil; Rf: 0.17 (1/1, EtOAc/hexane);

^{1}H NMR (700 MHz, $CDCl_3$) δ/ppm 8.28 – 8.32 (m, 2H), 7.66 – 7.70 (m, 2H), 4.84 (s, 1H), 4.29 (qd, *J* = 7.1, 1.4 Hz, 2H), 1.31 (t, *J* = 7.1 Hz, 3H);

^{13}C NMR (176 MHz, $CDCl_3$) δ/ppm 163.8 (C), 148.6 (C), 136.6 (C), 129.3 (CH), 124.6 (CH), 114.6 (C), 64.2 (CH_2), 43.5 (CH), 14.0 (CH_3);

IR (neat) ν = 3733 (w), 3588 (w), 2988 (w), 2205 (w), 2059 (w), 2032 (w), 2016 (w), 1999 (w), 1967 (w), 1742 (s), 1608 (w), 1522 (s), 1494 (w), 1468 (w), 1446 (w), 1346 (s), 1318 (m), 1297 (m), 1241 (m), 1199 (m), 1157 (m), 1109 (m), 1016 (m), 855 (m), 828 (m), 770 (w), 734 (m), 692 (m) cm^{-1};

LC-MS (MeCN), Rt. 2.69 min, m/z = 233.2 $[M-H]^-$. HR-MS (ESI-TOF) calculated for $C_{11}H_{11}N_2O_4$ 235.0719, found 235.0725 (Δ = 2.6 ppm).

Ethyl 2-cyano-2-(4-nitrophenyl)acetate, 380:

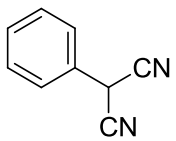

Chemical Formula: $C_9H_6N_2$
Exact Mass: 142.0531

Literature procedure:[174]

Malonitrile **379** (1.06 g, 16.00 mmol, 2.00 equiv.) and iodobenzne **1a** (1.63 g, 8.00 mmol, 1.00 equiv.) were stirred in DMSO (20 mL) with copper iodide (0.152 g, 0.8 mmol, 0.1 equiv.) and potassium carbonate (4.40 g, 32.00 mmol, 4 equiv.). The reaction mixture was heated to 120 °C. After 20 h the reaction mixture was poured in a beaker with HCl (1 M, 15 mL). The resulting mixture was filtered through silica and extracted with EtOAc (50 mL). The two layers were separated and the organic layer was washed with brine (5 x 250 mL). The combined organic layers were dried over sodium sulfate and the solvent was removed under reduced pressure. The crude product was purified by silica column chromatography with EtOAc/hexane (1:9) to give the pure product.

Isolated yield: 0.455 g (40% 8.00 mmol scale);

White solid; Rf: 0.26 (2/8, EtOAc/hexane);

^{1}H NMR (600 MHz, $CDCl_3$) δ/ppm 7.54–7.47 (m, 5H), 5.08 (s, 1H);

^{13}C NMR (151 MHz, $CDCl_3$) δ/ppm 130.4 (CH), 130.0 (CH), 127.2 (CH), 126.2 (C), 111.7 (C), 28.1 (CH);

IR (neat) ν = 3656 (w), 2982 (br), 2889 (br), 2257 (w), 1495 (s), 1455 (m), 1134 (br), 1014 (w), 1004 (w), 752 (m), 734 (s), 694 (s) cm^{-1};

LC-MS (MeOH), Rt. 2.57 min, m/z = 140.1 $[M-H]^-$. HR-MS (ESI-TOF) calculated for $C_9H_5N_2$ 141.0453, found 141.0458 (Δ = 3.5 ppm);

Melting point: 67-68 °C (EtOH).

(*E*)-Methyl-2-cyano-3-phenylacrylate, 382:

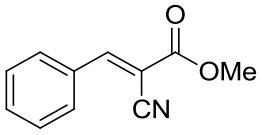

Chemical Formula: $C_{11}H_9NO_2$
Exact Mass: 187.0633

Consistent with published data[175]

Benzaldehyde **281** (1.59 g, 15 mmol, 1.0 equiv.) and methyl-2-cyanoacetate **375** (1.59 g, 16 mmol 1.10 equiv.) were dissolved in MeCN (50 mL) and polymer bound dimethyl benzylamine (QP-DMA, 10 g, 2.2 mmol/g loading) was added. The mixture was stirred under N_2 at 80 °C for 18 h. The solvent was removed under reduced pressure and the crude solid was recrystallised from EtOH to give the product.

Isolated yield: 1.64 g (58%, 15 mmol);

White crystals (recrystallised from EtOH); Rf: 0.33 (2/8, EtOAc/hexane);

^{1}H NMR (700 MHz, $CDCl_3$) δ/ppm 8.27 (s, 1H), 8.01–7.98 (m, 2H), 7.59–7.55 (m, 1H), 7.53–7.49 (m, 2H), 3.94 (s, 3H);

^{13}C NMR (176 MHz, $CDCl_3$) δ/ppm 163.3 (C), 155.6 (CH), 133.7 (CH), 131.7 (C), 131.4 (CH), 129.5 (CH), 115.7 (C), 102.8 (C), 53.7 (CH_3);

IR (neat) ν = 2358 (s), 2341 (s), 1654 (w), 668 (s) cm^{-1};

LC-MS (MeCN), Rt. 2.84 min, m/z = 188.1 $[M+H]^+$. HR-MS (ESI-TOF) calculated for $C_{11}H_{10}NO_2$ 188.0712, found 188.0716 (Δ = 2.1 ppm);

Melting point: 89-90 °C (EtOH). Lit.: 89 °C (EtOH).[176]

Methyl-2-cyano-3-phenylpropanoate, 384:

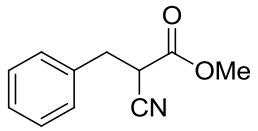

Chemical Formula: $C_{11}H_{11}NO_2$
Exact Mass: 189.0790

Consistent with published data[177]

(*E*)-methyl-2-cyano-3-phenylacrylate **382** (1.40 g, 7.48 mmol, 1.0 equiv.) and zinc powder (7.83 g, 119.7 mmol, 16.0 equiv.) were dissolved in glacial acetic acid (50 mL) and the solution was stirred for 2.5 h at 100 °C. The reaction mixture was filtered through a celite pad and washed with EtOAc (100 mL). The filtrate was neutralised with aqueous $NaHCO_3$ solution and the organic layer was separated, washed with brine (2 × 25 mL), dried over sodium sulfate and the solvent removed under reduced pressure. The crude product was purified via silica column chromatography with a solvent mixture of 1:9 (EtOAc/hexane) with the desired nitrile isolated as a colourless oil.[177]

Isolated yield: 0.583 g (41%, 7.48 mmol);

Colourless oil; Rf: 0.44 (1/9, EtOAc/hexane);

^{1}H NMR (700 MHz, $CDCl_3$) δ/ppm 7.36 – 7.32 (m, 2H), 7.31–7.28 (m, 1H), 7.26 (dd, *J* = 7.0, 1.6 Hz, 2H), 3.78 (s, 3H), 3.73 (ddd, *J* = 8.5, 5.7, 0.9 Hz, 1H), 3.27 (dd, *J* = 13.9, 5.7 Hz, 1H), 3.19 (dd, *J* = 13.9, 8.5 Hz, 1H);

^{13}C NMR (176 MHz, $CDCl_3$) δ/ppm 166.1 (C), 135.3 (C), 129.1 (CH), 128.9 (CH), 127.9 (CH), 116.1 (C), 53.6 (CH_3), 39.6 (CH), 35.8 (CH_2);

IR (neat) ν = 3032 (w), 2956 (w), 2360 (w), 2250 (w), 1743 (s), 1604 (w), 1585 (w), 1497 (m), 1455 (s), 1435 (s), 1340 (m), 1310 (m), 1263 (s), 1210 (s), 1190 (s), 1166 (s), 1081 (m), 1028 (s), 964 (w), 910 (w), 860 (w), 819 (w), 799 (w), 747 (s), 699 (s), 641 (m) cm^{-1};

LC-MS (MeCN), Rt. 2.60 min, m/z = 189.9 $[M+H]^+$. HR-MS (ESI-TOF) calculated for $C_{11}H_{12}NO_2$ 190.0868, found 190.0877 (Δ = 4.7 ppm).

(*E*)-Ethyl-2-cyano-3-phenylacrylate, 383:

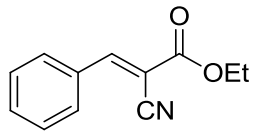

Chemical Formula: $C_{12}H_{11}NO_2$
Exact Mass: 201.0790

Consistent with published data[178]

Freshly distilled benzaldehyde **281** (1.59 g, 15 mmol, 1.0 equiv.) and ethyl 2-cyanoacetate **376** (1.81 g, 16 mmol 1.1 equiv.) were dissolved in MeCN (50 mL) and QP-DMA (10 g, 2.2 mmol/g loading) was added. The mixture was stirred under N_2 at 80 °C for 18 h; the QP-DMA was filtered off and the solvent removed under reduced pressure to give the crude solid which was recrystallised from EtOH.

Isolated yield: 1.166 g (39%, 15 mmol scale);

White crystals (recrystallised from EtOH); Rf: 0.35 (1/9, EtOAc/hexane);

^{1}H NMR (700 MHz, $CDCl_3$) δ/ppm 8.25 (s, 1H), 7.99 (dd, *J* = 7.4, 1.7 Hz, 2H), 7.54 – 7.58 (m, 1H), 7.48 – 7.53 (m, 2H), 4.39 (q, *J* = 7.2 Hz, 2H), 1.40 (t, *J* = 7.2 Hz, 3H);

^{13}C NMR (176 MHz, $CDCl_3$) δ/ppm 162.6 (C), 155.2 (CH), 133.4 (CH), 131.6 (C), 131.2 (CH), 129.4 (CH), 115.6 (C), 103.2 (C), 62.9 (CH_2), 14.3 (CH_3);

IR (neat) ν = 3924 (w), 3869 (w), 3734 (w), 2568 (w), 2366 (s), 2203 (w), 2165 (w), 2033 (w), 1993 (w), 1963 (w) cm^{-1};

LC-MS (MeCN), Rt. 2.88 min, m/z = 202.1 $[M+H]^+$. HR-MS (ESI-TOF) calculated for $C_{12}H_{12}NO_2$ 202.0868, found 202.0865 (Δ = 1.5 ppm);

Melting point: 49–50 °C (EtOH). (Literature: 49-50 °C, EtOH).[178]

Ethyl 2-cyano-3-phenylpropanoate, 385:

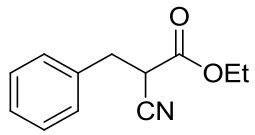

Chemical Formula: $C_{12}H_{13}NO_2$
Exact Mass: 203.0946

Consistent with published data[179]

(*E*)-Ethyl-2-cyano-3-phenylacrylate **382** (0.80 g, 3.98 mmol) and zinc powder (3.98 g, 60.8 mmol, 16.0 equiv.) were dissolved in glacial acetic acid (25 mL) and the solution was stirred for 2.5 h at 100 °C. The reaction mixture was filtered through a celite pad and washed with EtOAc (50 mL). The filtrate was neutralised with aqueous $NaHCO_3$ solution and the organic layer was separated, washed with brine (2 × 25 mL), dried over sodium sulfate and the solvent removed under reduced pressure to obtain the an oil which was purified via short silica column with a solvent mixture of 1:9 (EtOAc/hexane).

Isolated yield: 0.53 g (56%, 3.98 mmol scale);

Pale yellow oil;

^{1}H NMR (700 MHz, $CDCl_3$) δ/ppm 7.32 – 7.37 (m, 2H), 7.30–7.32 (m, 1H), 7.26 – 7.29 (m, 2H), 4.24 (qd, *J* = 7.1, 1.8 Hz, 2H), 3.72 (ddd, *J* = 8.4, 5.8, 1.1 Hz, 1H), 3.28 (dd, *J* = 13.9, 5.8 Hz, 1H), 3.20 (dd, *J* = 13.9, 8.5 Hz, 1H), 1.27 (t, *J* = 7.2 Hz, 3H);

^{13}C NMR (176 MHz, $CDCl_3$) δ/ppm 165.6 (C), 135.4 (C), 129.1 (CH), 128.9 (CH), 127.9 (CH), 116.3 (C), 63.1 (CH_2), 39.8 (CH), 35.9 (CH_2), 14.1 (CH_3);

IR (neat) ν = 3837 (w), 3815 (w), 3768 (w), 2746 (w), 3677 (w), 3648 (w), 2982 (w), 2936 (w), 2248 (w), 1995 (w), 1974 (w), 1739 (s), 1604 (w), 1496 (w), 1454 (w), 1392 (w), 1369 (w), 1256 (m), 1196 (m), 1163 (m), 1095 (w), 1080 (w), 1028 (m), 856 (w), 746 (m), 698 (s) cm^{-1};

LC-MS (MeCN), Rt. 2.78 min, m/z = 204.1 $[M+H]^+$. HR-MS (ESI-TOF) calculated for $C_{12}H_{14}NO_2$ 204.1025, found 204.1019 (Δ = 2.9 ppm).

(*E*)-2-Cyano-3-phenylacrylamide, 389:

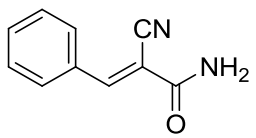

Chemical Formula: $C_{10}H_8N_2O$
Exact Mass: 172.0637

Consistent with published data[180]

Benzaldehyde **386** (1.06 g, 10.0 mmol) and cyanoacetamide (0.84 g, 10.0 mmol) were dissolved in EtOH (28 mL) to which 3 drops of piperidine were added and the solution was stirred for 24 h at room temperature. The solvent was then evaporated under reduced pressure to give a yellow solid which was recrystallised from EtOH.

Isolated yield: 1.54 g (89%, 10.0 mmol scale),

White amorphous solid (recrystallised from EtOH); Rf: 0.53 (1/4, EtOAc/hexane);

^{1}H NMR (400 MHz, DMSO-d_6) δ/ppm 8.19 (s, 1H), 8.02 – 7.86 (m, 3H), 7.79 (s, 1H), 7.62 – 7.52 (m, 3H);

^{13}C NMR (101 MHz, $CDCl_3$) δ/ppm 163.1 (C), 151.0 (CH), 132.8 (CH), 132.4 (C), 130.5 (CH), 129.7 (CH), 116.9 (C), 107.2 (C);

IR (neat) ν = 3395 (w, br), 3315 (w), 3151 (w, br), 2218 (w), 1685 (s), 1595 (m), 1573 (m), 1496 (w), 1494 (w), 1369 (m), 1355 (m), 1314 (w), 1290 (w), 1184 (m), 1104 (w), 765 (m), 741 (m), 683 (s), 677 (s), 595 (s), 582 (s) cm^{-1};

LC-MS (MeOH), Rt. 2.15 min, m/z = 173.0 $[M+H]^+$. HR-MS (ESI-TOF) calculated for $C_{10}H_9N_2O$ 173.0715, found 173.0717 (Δ = 1.2 ppm);

Melting point: 120-121 °C (EtOH). (Literature: 123-124 °C, EtOH).[180]

2-Cyano-3-phenylpropanamide, 391:

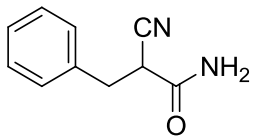

Chemical Formula: $C_{10}H_{10}N_2O$
Exact Mass: 174.0793

Consistent with published data[181]

(*E*)-2-Cyano-3-phenylacrylamide **389** (0.50 g, 2.9 mmol) and zinc powder (3.03 g, 46.4 mmol, 16.0 equiv.) were suspended in glacial acetic acid (12.5 mL) and the suspension was stirred for 2.5 h at 100 °C. The reaction mixture was filtered through a celite pad and washed with EtOAc (50 mL). The filtrate was neutralised with aqueous solution of $NaHCO_3$ and the organic layer was separated, washed with brine (2 × 25 mL), dried over sodium sulfate and the solvent removed under reduced pressure to obtain a white powder which was recrystallised from EtOH to give the product as a white solid.

Isolated yield: 0.432 g (86%, 2.9 mmol scale);

White amorphous solid (recrystallised from EtOH); Rf: 0.53 (1/4, EtOAc/hexane);

^{1}H NMR (400 MHz, DMSO-d_6) δ/ppm 7.79 (s, 1H), 7.50 (s, 1H), 7.40 – 7.20 (m, 5H), 3.95 (dd, J = 8.9, 6.5 Hz, 1H), 3.16 (dd, J = 13.6, 6.5 Hz, 1H), 3.04 (dd, J = 13.7, 8.9 Hz, 1H);

^{13}C NMR (101 MHz, DMSO-d_6) δ/ppm 166.7 (C), 137.3 (C), 129.4 (CH), 128.9 (CH), 127.5 (CH), 118.9 (C), 40.0 (CH), 35.7 (CH_2);

IR (neat) ν = 3379 (w, br), 3314 (w), 3239 (w), 3196 (w, br), 3055 (w), 3032 (w), 2946 (w), 2920 (w), 2257 (w), 1663 (s), 1653 (s), 1622 (m), 1497 (m), 1457 (m), 1415 (m), 1349 (w), 1332 (w), 1283 (m), 1179 (m), 1133 (m), 1081 (w), 775 (m), 711 (s), 630 (s), 617 (s), 593 (s) cm^{-1};

LC-MS (MeCN), Rt. 2.10 min, m/z = 175.2 $[M+H]^+$. HR-MS (ESI-TOF) calculated for $C_{10}H_{11}N_2O$ 175.0871, found 175.0874 (Δ = 1.7 ppm);

Melting point: 129-130 °C (EtOH). (Literature: 130 °C, H_2O).[181]

(*E*)-3-(4-Bromophenyl)-2-cyanoacrylamide, 390:

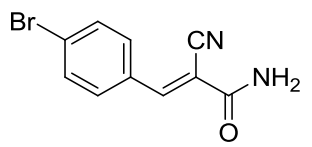

Chemical Formula: $C_{10}H_7BrN_2O$
Exact Mass: 249.9742

To a solution of 4-bromo benzaldehyde **387** (1.85 g, 10 mmol,) and cyanoacetamide **388** (0.81 g, 10 mmol) in MeCN (100 mL), QP-DMA (10 g. 0.22 mmol/g loading) was added. The mixture was stirred under N_2 at 70 °C for 12 h. The QP-DMA was filtered off and the solvent was removed under reduced pressure to give a yellow solid which was recrystallised from *i*PrOH.

Isolated yield: 3.75 g, (60%, 10.0 mmol scale);

Yellow amorphous solid (recrystallised form *i*PrOH); Rf: 0.51 (1/4, EtOAc/hexane);

^{1}H NMR (400 MHz, $CDCl_3$) δ/ppm 8.28 (s, 1H), 7.85 – 7.77 (m, 2H), 7.68 – 7.61 (m, 2H), 6.33 (s, 1H), 5.78 (s, 1H);

^{13}C NMR (101 MHz, $CDCl_3$) δ/ppm 161.5 (C), 152.8 (CH), 132.9 (CH), 132.1 (CH), 130.5 (C), 128.2 (C), 116.9 (C), 103.7 (C);

IR (neat) ν = 3437 (m), 3302 (w), 3142 (m), 3056 (w), 2216 (w), 1696 (s), 1580 (s), 1601 (s), 1559 (m), 1489 (s), 1374 (s), 1309 (s), 1281 (m), 1206 (m), 1186 (m), 1125 (w), 1115 (m), 1006 (m), 828 (s), 809 (s), 777 (m), 697 (m), 577 (s) cm^{-1};

LC-MS (MeCN), Rt. 2.58 min, m/z = 251.0$[M+H]^+$. HR-MS (ESI-TOF) calculated for $C_{10}H_8BrN_2O$ 250.9820, found 250.9826 (Δ = 2.4 ppm);

Melting point: 212-217 °C (decomposed, *i*PrOH).

3-(4-Bromophenyl)-2-cyanopropanamide, 392:

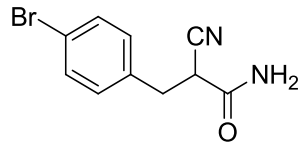

Chemical Formula: $C_{10}H_9BrN_2O$
Exact Mass: 251.9898

A mixture of (*E*)-3-(4-bromophenyl)-2-cyanoacrylamide **390** (0.377 g, 1.50 mmol) and zinc powder (1.56 g, 24.0 mmol, 16.0 equiv.) were suspended in glacial acetic acid (8 mL) and the solution was stirred for 2.5 h at 100 °C. The reaction mixture was filtered through a celite pad and washed with EtOAc (30 mL). The filtrate was neutralised with a saturated aqueous solution of $NaHCO_3$ and the organic layer was separated, washed with brine (2 × 15 mL), dried over sodium sulfate and the solvent removed under reduced pressure to obtain the crude product as an off white solid which was recrystallised from *i*PrOH.

Isolated yield: 0.314 g (83%, 1.5 mmol scale);

White amorphous solid (recrystallised from *i*PrOH); Rf: 0.41 (1/4, EtOAc/hexane);

^{1}H NMR (400 MHz, $CDCl_3$) δ/ppm 7.79 (s, 1H), 7.60 – 7.47 (m, 3H), 7.30 – 7.23 (m, 2H), 3.95 (dd, *J* = 8.7, 6.7 Hz, 1H), 3.13 (dd, *J* = 13.7, 6.7 Hz, 1H), 3.05 (dd, *J* = 13.7, 8.7 Hz, 1H);

^{13}C NMR (101 MHz, $CDCl_3$) δ/ppm 166.5 (C), 136.8 (C), 131.8 (CH), 131.7 (CH), 120.8 (C), 118.7 (C), 39.7 (CH), 34.9 (CH_2);

IR (neat) ν = 3391 (w), 3307 (w), 3192 (w), 2257 (w), 1685 (s), 1619 (w), 1493 (m), 1442 (w), 1401 (m), 1242 (w), 1197 (w), 1179 (w), 1074 (m), 1013 (m), 946 (w), 917 (w), 785 (s), 717 (w), 616 (s), 604 (s) cm^{-1};

LC-MS (MeCN), Rt. 2.72 min, m/z = 252.9 $[M+H]^+$. HR-MS (ESI-TOF) calculated for $C_{10}H_{10}BrN_2O$ 252.9976, found 252.9987 (Δ = 4.4 ppm);

Melting point: 176 °C (decomposed, *i*PrOH).

Ethyl 2-cyanopropanoate, 396:

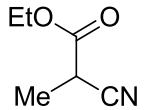

Chemical Formula: $C_6H_9NO_2$
Exact Mass: 127.0633

Literature procedure:[182]

Sodium hydride (58 mg, 1.46 mmol, 0.33 equiv., 60% in paraffin) was suspended in dry THF (1.46 mL) and stirred under N_2 at 0 °C. A solution of ethyl-2-cyano-acetate (500 mg, 4.42 mmol, 1.0 equiv.) in THF (0.74 mL) was added using a syringe. After 15 min stirring at 0 °C, iodomethane (90.8 µL, 207 mg, 1.46 mmol, 0.33 equiv.) was added and the reaction stirred for 3 h. The reaction mixture was quenched with water (10 mL), diethyl ether (10 mL) was added and the separated organic layer was washed with brine (3 × 25 mL). The organic layer was dried over sodium sulfate and the solvent was removed under reduced pressure. The product was purified using silica column chromatography with a solvent mixture of 0.5/9.5 (EtOAc/hexane) and the desired nitrile was recovered as a colourless liquid.

Isolated yield: 51 mg (83%, 1.46 mmol);

Colorless oil; Rf: 0.55 (1/1, EtOAc/hexane).

^{1}H NMR (700 MHz, $CDCl_3$) δ/ppm 4.25 (q, *J* = 7.2 Hz, 2H), 3.52 (q, *J* = 7.4 Hz, 1H), 1.60 – 1.59 (d, *J* = 7.4 Hz, 3H), 1.31 (t, *J* = 7.2 Hz, 3H);

^{13}C NMR (176 MHz, $CDCl_3$) δ/ppm 166.6 (C), 117.5 (C), 62.9 (CH_2), 31.6 (CH), 15.4 (CH_3), 14.1 (CH_3);

IR (neat) ν = 3116 (w), 2983 (w), 2937 (w), 1732 (s), 1499 (w), 1446 (w), 1370 (w), 1254 (m), 1173 (m), 1096 (m), 1047 (m), 1017 (m), 939 (w), 859 (w), 730 (m), 624 (w) cm^{-1};

LC-MS (MeCN), Rt. 1.99 min, m/z = 227.8 $[M+H]^+$. HR-MS (ESI-TOF) calculated for $C_6H_{10}NO_2$ 128.0713, found 128.0713 (Δ = 0.8 ppm).

Ethyl 2-cyanobutanoate, 397:

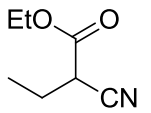

Chemical Formula: $C_7H_{11}NO_2$
Exact Mass: 141.0790

A solution of cyanoethyl acetate (2.172 g, 19.2 mmol) in dry THF (3 mL) was slowly added to a suspension of sodium hydride (0.256 g, 6.4 mmol, 60% in paraffin) and THF (5 mL) under N_2 at 0 °C. After 15 min, a solution of iodoethane (0.998 g, 6.4 mmol) in THF (3 mL) was added dropwise and after stirring the suspension for 15 min at 0 °C, the reaction mixture was allowed to warm to room temperature and stirred for 8 h. The reaction was quenched with HCl solution (1 M, 10 mL) and extracted with EtOAc (2 × 25 mL). The organic layer was dried over sodium sulfate and the solvent evaporated under reduced pressure to give the crude as an orange oil. The crude material was purified via silica column chromatography (1:4, EtOAc/hexanes) to give the desired product.

Isolated yield: 0.740 g (82%, 6.4 mmol);

Colourless oil; Rf: 0.29 (1/1, EtOAc/hexane).

^{1}H NMR (400 MHz, $CDCl_3$) δ/ppm 4.27 (q, *J* = 7.1 Hz, 2H), 3.46 (dd, *J* = 7.4, 6.1 Hz, 1H), 2.07–1.92 (m, 2H), 1.33 (t, *J* = 7.1 Hz, 3H), 1.13 (t, *J* = 7.4 Hz, 3H);

^{13}C NMR (101 MHz, $CDCl_3$) δ/ppm 166.2 (C), 116.6 (C), 62.9 (CH_2), 39.2 (CH), 23.8 (CH_2), 14.2 (CH_3), 11.4 (CH_3);

IR (neat) ν = 2981 (w), 2941 (w), 2884 (w), 2249 (w), 1741 (s), 1462 (w), 1389 (w), 1370 (w), 1247 (m), 1189 (m), 1110 (w), 1021 (m), 955 (w), 854 (w), 811 (w) cm^{-1};

ASAP-MS (MeCN), Rt. 0.41 min, m/z = 142.1 $[M+H]^+$. HR-MS (ASAP) calculated for $C_7H_{12}NO_2$ 141.0862, found 141.0868 (Δ = 4.2 ppm).

Ethyl 2-cyano-2-phenylpropanoate, 398:

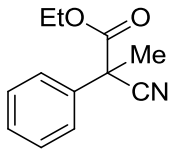

Chemical Formula:
$C_{12}H_{13}NO_2$
Exact Mass: 203.0946

Consistent with published data[182]

Ethyl-2-cyano-2-phenylacetate **362** (300 mg, 1.60 mmol, 1.00 equiv.) was dissolved in dry DMF (1.55 mL) and cooled to 0 °C under a N_2 atmosphere. Sodium hydride (70 mg, 1.76 mmol, 1.1 equiv., 60% in paraffin) was added and mixture stirred for 15 min at 0 °C. After the dropwise addition of iodomethane (227 mg, 1.60 mmol, 1.00 equiv.) the mixture was allowed to warm to room temperature. After 1.5 h, EtOAc amount was added to the solution and the organic layer was washed with brine (3 × 25 mL), dried over sodium sulfate and the solvent was removed under reduced pressure. The crude material was purified using silica column chromatography with a solvent gradient 5:95-20:80 (EtOAc /hexane) to obtain the product as a colourless oil (57% yield).

Isolated yield: 0.186 g (57%, 1.6 mmol);

Colorless oil; Rf: 0.25 (1/9, EtOAc/hexane);

^{1}H NMR (700 MHz, $CDCl_3$) δ/ppm 7.56 – 7.51 (m, 2H), 7.41 (tt, *J* = 6.7, 0.9 Hz, 2H), 7.39 – 7.35 (m, 1H), 4.29 – 4.19 (m, 2H), 1.95 (s, 3H), 1.25 (t, *J* = 7.1, 3H);

^{13}C NMR (176 MHz, $CDCl_3$) δ/ppm 167.9 (C), 135.8 (C), 129.1 (CH), 128.8 (CH), 125.7 (CH), 119.5 (C), 63.2 (CH_2), 48.3 (C), 24.9 (CH_3), 13.8 (CH_3);

IR (neat) ν = 2986 (w), 2942 (w), 2364 (w), 2246 (w), 1962 (w), 1741 (s), 1600 (w), 1991 (w), 1494 (m), 1447 (s), 1380 (m), 1367 (w), 1297 (w), 1235 (s), 1150 (m), 1100 (s), 1077 (m), 1013 (s), 934 (w), 914 (w), 894 (w), 855 (m), 810 (w), 767 (s), 729 (s), 696 (s), 646 (m), 618 (w), 610 (w) cm^{-1};

LC-MS (MeCN), Rt. 3.05 min, m/z = 203.9 $[M+H]^+$. HR-MS (ESI-TOF) calculated for $C_{12}H_{14}NO_2S$ 204.1025, found 204.1027 (Δ = 1.0 ppm).

Ethyl 2-cyano-3-methylbutanoate, 399:

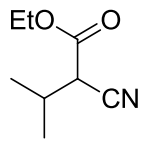

Chemical Formula: $C_8H_{13}NO_2$
Exact Mass: 155.0946

Consistent with published data[183]

A solution of ethyl 2-cyanocetate (1.996 g, 17.64 mmol) in dry THF (3 mL) was slowly added to a suspension of sodium hydride (0.235 g, 5.88 mmol, 60% in paraffin) and THF (5 mL) under a N_2 at 0 °C. After 15 min, a solution of 2-iodopropane (1.00 g, 5.88 mmol) in THF (3 mL) was added dropwise and after stirring the suspension for 15 min at 0 °C, the reaction mixture was allowed to warm to room temperature and stirred for 8 h. The reaction was quenched with HCl (1 M, 10 mL) and extracted using EtOAc (2 × 25 mL). The organic layer was dried over sodium sulfate and the solvent was evaporated under reduced pressure to give the crude as an orange oil. The crude product was purified via silica column chromatography (1:4, EtOAc/hexanes) to give the desired product as a colourless oil.

Isolated yield: 0.557 g (61%, 5.88 mmol scale);

Colourless oil; Rf: 0.27 (1/9, EtOAc/hexane);

^{1}H NMR (400 MHz, $CDCl_3$) δ/ppm 4.27 (qd, *J* = 7.1, 0.8 Hz, 2H), 3.39 (d, *J* = 5.3 Hz, 1H), 2.42 (pd, *J* = 6.8, 5.3 Hz, 1H), 1.32 (t, *J* = 7.1 Hz, 3H), 1.14 (dd, *J* = 12.3, 6.8 Hz, 6H);

^{13}C NMR (101 MHz, $CDCl_3$) δ/ppm 166.1 (C), 115.6 (C), 62.8 (CH_2), 45.5 (CH), 30.1 (CH), 20.8 (CH_3), 19.0 (CH_3), 14.2 (CH_3);

IR (neat) ν = 2972 (m), 2936 (w), 2878 (w), 1743 (s), 1467 (w), 1394 (w), 1370 (w), 1304 (w), 1253 (m), 1192 (m), 1133 (w), 1030 (m), 856 (w) cm^{-1};

LC-MS (MeCN), Rt. 2.55 min, m/z = 156.1 $[M+H]^+$. HR-MS (ESI-TOF) calculated for $C_8H_{14}NO_2$ 156.1021, found 156.1025 (Δ = 2.6 ppm).

Isopropyl 2-phenyl-2-(thiazol-2-yl)acetate, 400:

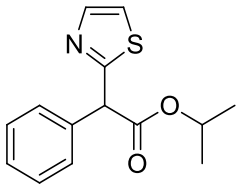

Chemical Formula: $C_{14}H_{15}NO_2S$
Exact Mass: 261.0823

Prepared using general procedure A: Isolated yield; 28 mg (49%, 0.22 mmol scale);

Colourless oil; Rf: 0.23 (1/4, EtOAc/hexane);

^{1}H NMR (400 MHz, $CDCl_3$) δ/ppm 7.75 (d, *J* = 3.3 Hz, 1H), 7.47 – 7.30 (m, 5H), 7.29 (d, *J* = 3.3 Hz, 1H), 5.38 (s, 1H), 5.11 (hept, *J* = 6.3 Hz, 1H), 1.27 (d, *J* = 6.3 Hz, 3H), 1.19 (d, *J* = 6.2 Hz, 3H);

^{13}C NMR (101 MHz, $CDCl_3$) δ/ppm 170.0 (C), 167.6 (C), 142.4 (CH), 136.8 (C), 128.9 (CH), 128.4 (CH), 128.1 (CH), 120.0 (CH), 69.6 (CH), 55.7 (CH), 21.7 (CH_3), 21.5 (CH_3);

IR (neat) ν = 3111 (w), 3088 (w), 3063 (w), 2982 (w), 2936 (w), 1727 (s), 1646 (w), 1599 (w), 1495 (w), 1449 (w), 1387 (w), 1243 (m), 1168 (m), 1100 (s), 1068 (m), 1003 (w), 863 (w), 729 (m), 714 (m), 697 (s);

LC-MS (MeCN), Rt. 3.07 min, m/z = 262.1 $[M+H]^+$. HR-MS (ESI-TOF) calculated for $C_{14}H_{16}NO_2S$ 262.0902, found 262.0900 (Δ = 0.8 ppm).

Ethyl 2-(4-methoxyphenyl)-2-(thiazol-2-yl)acetate, 401:

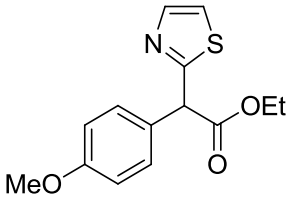

Chemical Formula: $C_{14}H_{15}NO_3S$
Exact Mass: 277.0773

Prepared using general procedure A: Isolated yield; 69 mg (57%, 0.44 mmol scale);

Brown oil; Rf: 0.17 (2/4, EtOAc/hexane);

^{1}H NMR (700 MHz, $CDCl_3$) δ/ppm 7.76 (d, *J* = 3.3 Hz, 1H), 7.37 – 7.40 (m, 2H), 7.30 (d, *J* = 3.3 Hz, 1H), 6.87 – 6.91 (m, 2H), 5.39 (s, 1H), 4.19 – 4.29 (m, 2H), 3.80 (s, 3H), 1.26 (t, *J* = 7.1 Hz, 3H);

^{13}C NMR (176 MHz, $CDCl_3$) δ/ppm 170.8, 168.5, 159.6, 142.1, 129.8, 128.7, 120.2, 114.5, 62.1, 55.4, 54.6, 14.2;

IR (neat) ν = 3849 (w), 3735 (w), 3648 (w), 2982 (w), 2934 (w), 2900 (w), 2836 (w), 2168 (w), 2154 (w), 2130 (w), 2047 (w), 2040 (w), 2024 (w), 1730 (s), 1608 (m), 1509 (s), 1462 (m), 1442 (m), 1421 (w), 1391 (w), 1367 (w), 1302 (m), 1249 (s), 1177 (s), 1156 (s), 1129 (m), 1093 (m), 1055 (w), 1023 (s), 867 (w), 835 (m), 796 (m), 777 (w), 728 (m), 609 (w) cm^{-1};

LC-MS (MeCN), Rt. 2.77 min, m/z = 278.5 $[M+H]^+$. HR-MS (ESI-TOF) calculated for $C_{14}H_{16}NO_3S$ 278.0851, found 278.00853 (Δ = 0.7 ppm).

Ethyl 2-(benzo[*d*][1,3]dioxol-5-yl)-2-(thiazol-2-yl)acetate, 402:

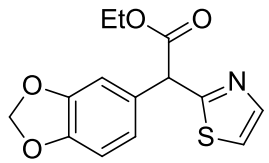

Chemical Formula: $C_{14}H_{13}NO_4S$
Exact Mass: 291.0565

Prepared using general procedure A: Isolated yield; 65 mg (51%, 0.44 mmol scale);

Yellow oil; Rf: 0.07 (1/4, EtOAc/hexane);

^{1}H NMR (400 MHz, $CDCl_3$) δ/ppm 7.75 (d, *J* = 3.3 Hz, 1H), 7.29 (d, *J* = 3.3 Hz, 1H), 6.96 (d, *J* = 1.8 Hz, 1H), 6.90 (ddd, *J* = 8.0, 1.8, 0.5 Hz, 1H), 6.78 (d, *J* = 8.0 Hz, 1H), 5.95 (s, 2H), 5.30 (s, 1H), 4.31 – 4.16 (m, 2H), 1.26 (t, *J* = 7.1 Hz, 3H);

^{13}C NMR (101 MHz, $CDCl_3$) δ/ppm 170.5 (C), 167.7 (C), 148.0 (C), 147.6 (C), 142.5 (CH), 130.2 (C), 122.1 (CH), 120.0 (CH), 109.0 (CH), 108.5 (CH), 101.3 (CH_2), 62.0 (CH_2), 55.0 (CH), 14.01 (CH_3);

IR (neat) ν = 3125 (w), 3082 (w), 2986 (w), 2902 (w), 1732 (s), 1503 (m), 1488 9s), 1444 (m), 1311 (w), 1244 (s), 1186 (s), 1162 (s), 1130 (w), 1099 (w), 1036 (s), 929 (m), 813 (w), 772 (w), 731 (w) cm^{-1};

LC-MS (MeCN), Rt. 2.67 min, m/z = 292.0 $[M+H]^+$. HR-MS (ESI-TOF) calculated for $C_{14}H_{14}NO_4S$ 292.0644, found 292.0641 (Δ = 1.0 ppm).

Methyl 2-(4-nitrophenyl)-2-(thiazol-2-yl)acetate, 403:

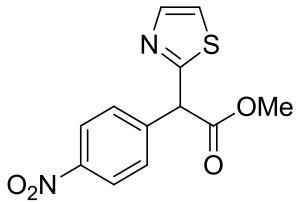

Chemical Formula: $C_{12}H_{10}N_2O_4S$
Exact Mass: 278.0361

Prepared using general procedure A: Isolated yield; 22 mg (36% 0.22 mmol scale);

Pale red oil; Rf: 0.35 (1/1, EtOAc/hexane);

^{1}H NMR (600 MHz, $CDCl_3$) δ/ppm 8.21 – 8.25 (m, 2H), 7.78 (d, *J* = 3.3 Hz, 1H), 7.61 – 7.65 (m, 2H), 7.36 (d, *J* = 3.3 Hz, 1H), 5.54 (s, 1H), 3.68 (s, 3H);

^{13}C NMR (151 MHz, $CDCl_3$) δ/ppm 169.9 (C), 165.1 (C), 147.9 (C), 143.3 (C), 142.9 (CH), 129.9 (CH), 124.2 (CH), 120.7 (CH), 54.8 (CH), 53.4 (CH_3);

LC-MS (MeCN), Rt. 2.77 min, m/z = 279.1 $[M+H]^+$. HR-MS (ESI-TOF) calculated for $C_{12}H_{11}N_2O_4S$ 279.0440, found 279.0439 (Δ = 0.4 ppm).

Ethyl 2-(4-nitrophenyl)-2-(thiazol-2-yl)acetate, 404:

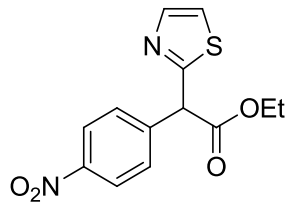

Chemical Formula: $C_{13}H_{12}N_2O_4S$
Exact Mass: 292.0518

Prepared using general procedure A: Isolated yield; 45 mg (35% 0.22 mmol scale);

Pale red oil; Rf: 0.85 (9/1, DCM/MeOH);

^{1}H NMR (400 MHz, $CDCl_3$) δ/ppm 8.27 – 8.20 (m, 2H), 7.80 (d, *J* = 3.3 Hz, 1H), 7.69 – 7.62 (m, 2H), 7.38 (d, *J* = 3.3 Hz, 1H), 5.53 (s, 1H), 4.3 – 4.22 (m, 2H), 1.29 (t, *J* = 7.1 Hz, 3H);

^{13}C NMR (101 MHz, $CDCl_3$) δ/ppm 169.4 (C), 165.1 (C), 147.7 (C), 143.4 (C), 142.8 (CH), 129.7 (CH), 124.1 (CH), 120.5 (CH), 62.5 (CH_2), 54.9 (CH), 14.0 (CH_3);

IR (neat) ν = 3133 (w), 3079 (w), 2988 (w), 2944 (w), 2908 (w), 1733 (s), 1606 (m), 1597 (m), 1519 (s), 1493 (m), 1346 (s), 1322 (m), 1302 (m), 1234 (m), 1185 (s), 1156 (s), 1016 (m), 857 (m), 727 (m) 705 (m) cm^{-1};

LC-MS (MeCN), Rt. 2.77 min, m/z = 291.9 $[M-H]^-$. HR-MS (ESI-TOF) calculated for $C_{13}H_{11}N_2O_4S$ 291.0434, found 291.0440 (Δ = 2.1 ppm).

2-Phenyl-2-(thiazol-2-yl)acetonitrile, 405:

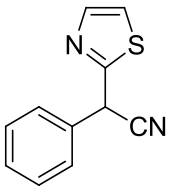

Chemical Formula: $C_{11}H_8N_2S$
Exact Mass: 200.0408

Prepared using general procedure A: Isolated yield; 64 mg (73% 0.44 mmol scale);

Colourless oil; Rf: 0.20 (2/8, EtOAc/hexane);

^{1}H NMR (600 MHz, $CDCl_3$) δ/ppm 7.79 (d, *J* = 3.3 Hz, 1H), 7.53–7.46 (m, 2H), 7.46 – 7.37 (m, 3H), 7.34 (d, *J* = 3.3 Hz, 1H), 5.56 (s, 1H);

^{13}C NMR (151 MHz, $CDCl_3$) δ/ppm 164.3 (C), 143.4 (CH), 133.5 (C), 129.6 (CH), 129.3 (CH), 127.9 (CH), 121.2 (CH), 117.6 (C), 41.2 (CH);

IR (neat) ν = 3119 (w), 3088 (w), 3033 (w), 2982 (w), 2901 (w), 2367 (w), 2250 (w), 1494 (m), 1456 (m), 1129 (w), 1090 (w), 732 (s), 696 (s) cm^{-1};

LC-MS (MeOH), Rt. 2.65 min, m/z = 201.0 $[M+H]^+$. HR-MS (ESI-TOF) calculated for $C_{11}H_8N_2S$ 200.0486, found 200.0496 (Δ = 5.0 ppm).

Methyl 3-phenyl-2-(thiazol-2-yl)propanoate, 406:

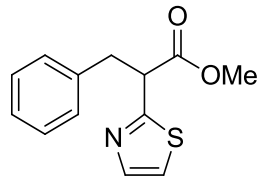

Chemical Formula: $C_{13}H_{13}NO_2S$
Exact Mass: 247.0667

Prepared using general procedure A: Isolated yield; 11 mg (16%, 0.22 mmol scale);

Pale yellow oil; Rf: 0.07 (1/4, EtOAc/hexane);

^{1}H NMR (400 MHz, $CDCl_3$) δ/ppm 7.75 (d, *J* = 3.3 Hz, 1H), 7.29 –7.12 (m, 6H), 4.44 (dd, *J* = 8.5, 7.0 Hz, 1H), 3.67 (s, 3H), 3.47 (dd, *J* = 13.7, 8.5 Hz, 1H), 3.33 (dd, *J* = 13.7, 7.0 Hz, 1H);

^{13}C NMR (101 MHz, $CDCl_3$) δ/ppm 171.6 (C), 166.7 (C), 142.4 (CH), 137.7 (C), 129.0 (CH), 128.7 (CH), 127.0 (CH), 119.8 (CH), 52.7 (CH_3), 51.7 (CH), 39.7 (CH_2);

IR (neat) ν = 3031 (w), 2148 (w), 1983 (w), 1748 (s), 1604 (w), 1496 (w), 1455 (w), 1436 (w), 1283 (m), 1163 (s), 1105 (m), 1082 (m), 1048 (m), 974 (m), 840 (w), 741 (m), 699 (s), 666 (m), 652 (m), 624 (m) cm^{-1};

LC-MS (MeCN), Rt. 0.28 min, m/z = 247.9 $[M+H]^+$, HR-MS (ESI-TOF) calculated for $C_{13}H_{14}NO_2S$ 248.0745, found 248.0749 (Δ = 1.6 ppm).

Ethyl 3-phenyl-2-(thiazol-2-yl)propanoate, 407:

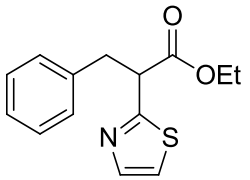

Chemical Formula: $C_{14}H_{15}NO_2S$
Exact Mass: 261.0823

Prepared using general procedure A: Isolated yield; 41 mg (36%, 0.44 mmol scale);

Colorless oil; Rf: 0.12 (1/4, EtOAc/hexane);

^{1}H NMR (400 MHz, $CDCl_3$) δ/ppm 7.83 (d, *J* = 3.2 Hz, 1H), 7.34 (d, *J* = 3.3 Hz, 1H), 7.30 – 7.22 (m, 5H), 4.40 (s, 1H), 4.32 – 4.17 (m, 2H), 3.75 (d, *J* = 13.8 Hz, 1H), 3.42 (d, *J* = 13.8 Hz, 1H), 1.26 (t, *J* = 7.1 Hz, 3H);

^{13}C NMR (101 MHz, $CDCl_3$) δ/ppm 171.91 (C), 171.88 (C), 143.1 (CH), 134.7 (C), 130.5 (CH), 128.1 (CH), 127.2 (CH), 120.4 (CH), 79.2 (CH), 63.4 (CH_2), 45.0 (CH_2), 14.1 (CH_3);

IR (neat) ν = 2978 (w), 2960 (w), 2181 (w), 2034 (w), 1686 (w), 1495 (w), 1453 (m), 1397 (w), 1261 (m), 1179 (m), 1152 (m), 1101 (m), 1030 (m), 860 (w), 732 (m), 698 (m) cm^{-1};

LC-MS (MeCN), Rt. 3.09 min, m/z = 262.1 $[M+H]^+$, HR-MS (ESI-TOF) calculated for $C_{14}H_{16}NO_2S$ 262.0913, found 262.0902 (Δ = 4.2 ppm).

3-Phenyl-2-(thiazol-2-yl)propanamide, 408:

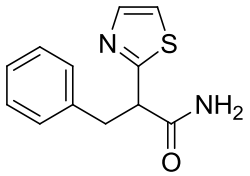

Chemical Formula: $C_{12}H_{12}N_2OS$
Exact Mass: 232.0670

Prepared using general procedure A: Isolated yield; 35 mg (34%, 0.44 mmol scale);

Amorphous white solid (recrystallised from EtOH); Rf: 0.21 (1/4, EtOAc/hexane);

^{1}H NMR (600 MHz, DMSO-d_6) δ/ppm 7.67 (d, *J* = 3.0 Hz, 1H), 7.65 (br, 1H) 7.59 (d, *J* = 3.3 Hz, 1H), 7.27 – 7.19 (m, 2H), 7.16 (m, 3H), 7.06 (br, 1H), 4.30 (dd, *J* = 8.7, 6.7 Hz, 1H), 3.26 (dd, *J* = 13.6, 8.7 Hz, 1H), 3.07 (dd, *J* = 13.6, 6.7 Hz, 1H);

^{13}C NMR (151 MHz, DMSO-d_6) δ/ppm 172.3 (C), 168.7 (C), 142.0 (CH), 139.0 (C), 129.3 (CH), 128.6 (CH), 126.7 (CH), 120.7 (CH), 51.9 (CH), 39.8 (CH_2);

IR (neat) ν = 3291 (w, br), 3117 (w, br), 2918 (w), 1685 (s), 1680 (s), 1676 (s), 1497 (m), 1452 (w), 1428 (w), 1405 (m), 1315 (w), 1286 (w), 1251 (w), 1128 (s), 1061 (m), 835 (m), 745 (m), 728 (s), 695 (s);

LC-MS (MeCN), Rt. 2.13 min, m/z = 233.4 $[M+H]^+$. HR-MS (ESI-TOF) calculated for $C_{12}H_{13}N_2OS$ 233.0749, found 233.0752 (Δ = 1.3 ppm);

Melting point: 145 °C (decomposed, EtOH).

3-(4-Bromophenyl)-2-(thiazol-2-yl)propanamide, 409:

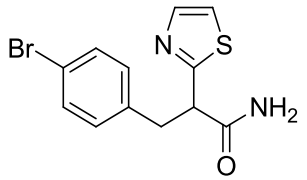

Chemical Formula: $C_{12}H_{11}BrN_2OS$
Exact Mass: 309.9775

Prepared using general procedure A: Isolated yield; 20 mg (37%, 0.176 mmol scale);

White amorphous solid; (recrystallised from MeOH); Rf: 0.18 (1/4, EtOAc/hexane);

^{1}H NMR (600 MHz, DMSO-d_6) δ/ppm 7.67 (d, *J* = 3.0 Hz, 1H), 7.65 (br, 1H), 7.59 (d, *J* = 3.3 Hz, 1H), 7.42 (d, *J* = 8.0 Hz, 2H), 7.12 (d, *J* = 8.0 Hz, 2H), 7.08 (s, 1H), 4.27 (dd, *J* = 8.9, 6.5 Hz, 1H), 3.22 (dd, *J* = 13.6, 8.7 Hz, 1H), 3.06 (dd, *J* = 13.6, 6.8 Hz, 1H);

^{13}C NMR (151 MHz, DMSO-d_6) δ/ppm 172.1 (C), 168.4 (C), 142.1 (CH), 138.4 (C), 131.6 (CH), 131.4 (CH), 120.8 (CH), 119.9 (C), 51.7 (CH), 39.1 (CH_2);

IR (neat) ν = 3303 (br), 3190 (br), 1681 (s), 1498 (m), 1486 (m), 1404 (m), 1284 (w), 1253 (w), 1131 (m), 1065 (m), 1011 (s), 847 (s), 797 (m), 736 (s), 606 (m), 537 (s) cm^{-1};

LC-MS (MeOH), Rt. 2.45 min, m/z = 310.9 $[M+H]^+$. HR-MS (ESI-TOF) calculated for $C_{12}H_{12}BrN_2OS$ 310.9854, found 310.9857 (Δ = 1.0 ppm);

Melting point: 144 °C (decomposed, MeOH).

Ethyl-2-(thiazol-2-yl)propanoate, 410:

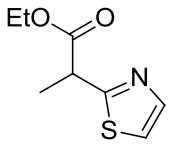

Chemical Formula: $C_8H_{11}NO_2S$
Exact Mass: 185.0510

Prepared using general procedure A: Isolated yield; 14 mg (35%, 0.22 mmol scale);

Pale yellow oil; Rf: 0.46 (1/1, EtOAc/hexane);

^{1}H NMR (700 MHz, $CDCl_3$) δ/ppm 7.73 (d, *J* = 3.3 Hz, 1H), 7.29 (d, *J* = 3.3 Hz, 1H), 4.24 – 4.17 (m, 3H), 1.67 (d, *J* = 7.3 Hz, 3H), 1.26 (t, *J* = 7.1 Hz, 3H);

^{13}C NMR (176 MHz, $CDCl_3$) δ/ppm 172.3 (C), 168.8 (C), 142.3 (CH), 119.4 (CH), 61.6 (CH_2), 44.4 (CH), 18.5 (CH_3), 14.2 (CH_3);

IR (neat) ν = 3116 (w), 2983 (w), 2937 (w), 1732 (s), 1499 (w), 1446 (w), 1370 (w), 1254 (m), 1173 (m), 1138 (m), 1096 (m), 1047 (m), 1017 (m), 939 (w), 859 (w), 730 (m), 624 (w) cm^{-1};

LC-MS (MeCN), Rt. 2.35 min, m/z = 186.9 $[M+H]^+$. HR-MS (ESI-TOF) calculated for $C_8H_{12}NO_2S$ 186.0589, found 186.0588 (Δ = 0.5 ppm).

Ethyl 2-(thiazol-2-yl)butanoate, 411:

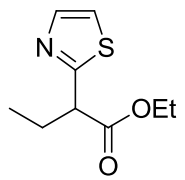

Chemical Formula: $C_9H_{13}NO_2S$
Exact Mass: 199.0667

Prepared using general procedure A: Isolated yield; 15 mg (33%, 0.66 mmol scale);

Colourless oil; Rf: 0.37 (1/1, EtOAc/hexane);

^{1}H NMR (400 MHz, $CDCl_3$) δ/ppm: 7.73 (d, *J* = 3.3 Hz, 1H), 7.29 (dd, *J* = 3.3, 0.5 Hz, 1H), 4.27–4.14 (m, 2H), 4.04 (t, *J* = 7.5 Hz, 1H), 2.25 – 1.97 (m, 2H), 1.26 (t, *J* = 7.1 Hz, 3H), 0.97 (t, *J* = 7.4 Hz, 3H);

^{13}C NMR (101 MHz, $CDCl_3$) δ/ppm: 171.9 (C), 167.7 (C), 142.3 (CH), 119.5 (CH), 61.5 (CH_2), 51.8 (CH), 27.5 (CH_2), 14.3 (CH_3), 11.9 (CH_3);

IR (neat) ν = 3116 (w), 3085 (w), 2972 (w), 2937 (w), 2828 (w), 1733 (s), 1498 (w), 1461 (w), 1370 (w), 1253 (w), 1181 (s), 1138 (w), 1022 (m), 861 (w), 727 (w);

LC-MS (MeCN), Rt. 2.48 min, m/z = 200.8 $[M+H]^+$; HR-MS (ESI-TOF) calculated for $C_9H_{14}NO_2S$ 200.0745, found 200.0751 (Δ = 3.0 ppm).

(2-Aminothiophen-3-yl)(phenyl)methanone, 415:

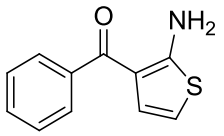

Chemical Formula: $C_{11}H_9NOS$
Exact Mass: 203.0405

Consistent with published data[184]

Prepared using general procedure A: Isolated yield; 45 mg (quantitative, 0.22 mmol scale);

Yellow crystalline product (recrystallised from EtOH);

^{1}H NMR (400 MHz, $CDCl_3$) δ/ppm 7.70 (d, *J* = 7.2 Hz, 2H), 7.42-7.57 (m, 3H), 6.91 (d, *J* = 6.0 Hz, 1H), 6.16 (d, *J* = 6.0 Hz, 1H);

^{13}C NMR (101 MHz, $CDCl_3$) δ/ppm 191.2 (C), 166.1 (C), 140.8 (C), 130.7 (CH), 128.1 (CH), 127.8 (CH), 115.1 (C), 106.1 (CH);

IR (neat) ν = 3359 (m), 3241 (br), 3128 (w), 1600 (m), 1570 (m), 1444 (s), 1420 (s), 1418 (s), 1398 (m), 1325 (m), 1289 (m), 1213 (w), 1078 (w), 946 (w), 833 (s), 698 (s), 672 (s), 664 (m), 654 (m), 587 (m), 494 (s) $cm^{-1;}$

HR-MS (ESI-TOF) calculated 204.0483, found 204.0475 (Δ = 3.9 ppm);

Melting point: 151-153 °C (EtOH). (Literature: 152-153 °C, no solvent reported).[184]

Ethyl 2-aminothiophene-3-carboxylate, 416:

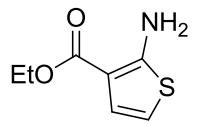

Chemical Formula: $C_7H_9NO_2S$
Exact Mass: 171.0354

Consistent with published data[185]

Prepared using general procedure A: Isolated yield; 30 mg (79%, 0.22 mmol scale);

Colourless oil; Rf: 0.42 (1/9, EtOAc/hexane);

^{1}H NMR (400 MHz, $CDCl_3$) δ/ppm 7.00 (d, *J* = 5.6 Hz, 1H), 6.20 (d, *J* = 5.6 Hz, 1H), 5.93 (s, br, 2H), 4.30 (dd, *J* = 7.0, 14.2 Hz, 2H), 1.36 (t, *J* = 7.0 Hz, 3H);

^{13}C NMR (101 MHz, $CDCl_3$) δ/ppm 165.4 (C), 162.6 (C), 125.9 (CH), 107.3 (C), 106.9 (CH), 59.7 (CH_2), 14.5 (CH_3);

IR (neat) ν = 3435 (w), 3326 (w), 1650 (m), 1582 (m), 1522 (m), 1485 (m), 1400 (m), 1380 (m), 1305 (m), 1261 (m), 1169 (w), 1108 (m), 1070 (w), 1020 (m), 901 (w), 828 (w), 783 (w), 679 (m) cm^{-1};

HR-MS (ESI-TOF) calculated 172.0423, found 172.0424 (Δ = 0.6 ppm).

2-Aminothiophene-3-carboxamide, 417:

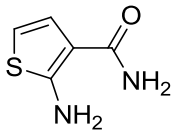

Chemical Formula: $C_5H_6N_2OS$
Exact Mass: 142.0201

Consistent with published data.[127]

Prepared using general procedure A: Isolated yield; 37 mg (63%, 0.44 mmol scale);

Pink amorphous solid; Rf: 0.35 (1/4, EtOAc/hexane);

^{1}H NMR (400 MHz, DMSO-d_6) δ/ppm 7.46 – 7.10 (m, 3H), 7.04 (d, J = 5.8 Hz, 1H), 6.80 (d, J = 50.6 Hz, 1H), 6.22 (d, J = 5.8 Hz, 1H);

^{13}C NMR (101 MHz, $CDCl_3$) δ/ppm 168.0 (C), 162.1 (C), 125.3 (CH), 107.6 (C), 105.8 (CH);

IR (neat) ν = 3438 (w, br), 3409 (w, br), 3321 (w, br), 3261 (w, br), 3208 (w, br), 3119 (w), 3083 (w), 1645 (m), 1594 (s), 1562 (s), 1559 (s), 1520 (s), 1417 (m), 1418 (s), 1348 (m), 1284 (w), 1220 (w), 1101 (m), 895 (w), 872 (w), 785 (m), 690 (m), 664 (m) cm^{-1}.

LC-MS (MeOH), Rt. 1.47 min, m/z = 142.9 $[M+H]^+$. HR-MS (ESI-TOF) calculated for $C_{10}H_9N_2O$ 142.0279, found 142.0278 (Δ = 0.7 ppm);

Melting point: 130 °C (decomposed, EtOH). (Literature: 158-160 °C, no solvent reported).[127]

Phenyl(thiazol-2-yl)methanone, 440:

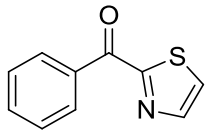

Chemical Formula: $C_{10}H_7NOS$
Exact Mass: 189.02

Consistent with published data[186]

Isolated as an oxidation product of **362** in 12 mg (4% yield).

Pale yellow oil; Rf: 0.47 (1/4, EtOAc/hexane);

^{1}H NMR (700 MHz, $CDCl_3$) δ/ppm 8.49 – 8.45 (m, 2H), 8.10 (d, J = 3.0 Hz, 1H), 7.73 (d, J = 3.0 Hz, 1H), 7.68 – 7.61 (m, 1H), 7.56 – 7.50 (m, 2H).

^{13}C NMR (176 MHz, $CDCl_3$) δ/ppm 184.3 (C), 168.1 (C), 145.0 (CH), 135.4 (C), 133.8 (CH), 131.2 (CH), 128.6 (CH), 126.4 (CH).

LC-MS (MeCN), Rt. 2.35 min, m/z = 186.9 $[M+H]^+$. HR-MS (ESI-TOF) calculated for $C_{10}H_8NOS$ 190.0327, found 190.0323 (Δ = 2.1 ppm).

(Ethyl 2-hydroxy-2-phenyl-2-(thiazol-2-yl)acetate), 441.

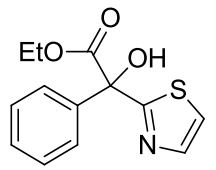

Chemical Formula: $C_{13}H_{13}NO_3S$
Exact Mass: 263.06

≡

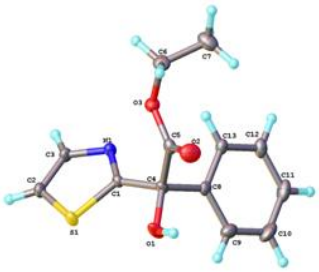

X-Ray structure

Isolated as an oxidation product of **362** in 181 mg (60% yield).

White, crystalline solid; Rf: 0.20 (1/4, EtOAc/hexane);

^{1}H NMR (700 MHz, $CDCl_3$) δ/ppm 7.82 (d, *J* = 3.2 Hz, 1H), 7.73 – 7.70 (m, 2H), 7.40 – 7.33 (m, 4H), 4.92 (s, 1H), 4.35 (q, *J* = 7.1 Hz, 2H), 1.28 (t, *J* = 7.2 Hz, 3H).

^{13}C NMR (176 MHz, $CDCl_3$) δ/ppm 172.3 (C), 171.9 (C), 142.9 (CH), 139.6 (C), 128.8 (CH), 128.3 (CH), 126.7 (CH), 120.7 (CH), 79.5 (C), 63.8 (CH_2), 14.1 (CH_3).

IR (neat) *ν* = 3457 (w, br), 3118 (w), 2982 (w), 1730 (s), 1494 (w), 1449 (w), 1242 (s), 1173 (m), 1097 (m), 1066 (m), 1012 (w), 733 (m), 699 (m) cm^{-1}.

LC-MS (MeCN), Rt. 2.56 min, *m/z* = 263.9 $[M+H]^+$. HR-MS (ESI-TOF) calculated for $C_{13}H_{14}NO_3S$ 264.0694, found 264.0689 (Δ = 1.9 ppm).

Elemental analysis: calculated for $C_{13}H_{13}NO_3S$ C: 59.30%, H: 4.98%, N: 5.32%; measured C: 58.96% (Δ = 0.34), H: 4.95% (Δ = 0.03), N: 5.24% (Δ = 0.08).

Melting point: 95-97 °C (*i*PrOH).

Crystal data for compound **441**: $C_{13}H_{13}NO_3S$, M = 263.30, monoclinic, space group $P2_1/n$ (no. 14), a = 7.5217(2), b = 11.1445(3), c = 14.9519(4) Å, β = 91.003(3)°, V = 1253.16(6) $Å^3$, Z = 4, T = 120.0 K, μ(MoKα) = 0.257 mm^{-1}, D_{calc} = 1.396 g/mm^3, 12888 reflections measured, 3654 unique (R_{int} = 0.0444) were used in all calculations. The final R_1 was 0.0419 (2878 refl. with I > 2σ(I)) and wR_2 was 0.0975 (all data), GOOF = 1.052. CCDC-1049429 (From *i*PrOH).

References

1. Dar, Y. L., *Macromol. Rapid Commun.* **2004**, *25* (1), 34-47.

2. (a) Tierney, J. P.; Lidstrom, P., *Microwave Assisted Organic Synthesis*. Blackwell Publishing: Oxford, 2007; p 1-280; (b) Bogdal, D., Microwave-assisted Organic Synthesis: One Hundred Reaction Procedures. In *Microwave-Assisted Organic Synthesis: One Hundred Reaction Procedures*, Elsevier Science BV: Netherlands, 2005; Vol. 25, pp 1-202.

3. Perreux, L.; Loupy, A., *Tetrahedron* **2001**, *57* (45), 9199-9223.

4. Mallia, C. J.; Baxendale, I. R., *Org. Process. Res. Dev.* **2016**, *20* (2), 327-360.

5. (a) Morimoto, T.; Fuji, K.; Tsutsumi, K.; Kakiuchi, K., *J. Am. Chem. Soc.* **2002**, *124* (15), 3806-3807; (b) Shibata, T.; Toshida, N.; Takagi, K., *Org. Lett.* **2002**, *4* (9), 1619-1621.

6. Ueda, T.; Konishi, H.; Manabe, K., *Angew. Chem. Int. Ed.* **2013**, *52* (33), 8611-8615.

7. Corey, E. J.; Hegedus, L. S., *J. Am. Chem. Soc.* **1969**, *91* (5), 1233-1234.

8. Wieckowska, A.; Fransson, R.; Odell, L. R.; Larhed, M., *J. Org. Chem.* **2011**, *76* (3), 978-981.

9. Lindh, J.; Fardost, A.; Almeida, M.; Nilsson, P., *Tetrahedron Lett.* **2010**, *51* (18), 2470-2472.

10. Ikariya, T.; Murata, K.; Noyori, R., *Org. Biomol. Chem.* **2006**, *4* (3), 393-406.

11. Yang, J. W.; Fonseca, M. T. H.; List, B., *Angew. Chem. Int. Ed.* **2004**, *43* (48), 6660-6662.

12. Banks, R. E.; Mohialdinkhaffaf, S. N.; Lal, G. S.; Sharif, I.; Syvret, R. G., *J. Chem. Soc., Chem. Commun.* **1992**, (8), 595-596.

13. Woolven, H.; Gonzalez-Rodriguez, C.; Marco, I.; Thompson, A. L.; Willis, M. C., *Org. Lett.* **2011**, *13* (18), 4876-4878.

14. Sax, N. I.; Lewis, R. J., *Dangerous properties of industrial materials*. Van Nostrand Reinhold: New York, 1989.

15. Colquhoun, H. M.; Thompson, D. J.; Twigg, M. V., *Carbonylation: Direct Synthesis of Carbonyl Compounds*. Plenum Press: New York, 1991.

16. (a) Baxendale, I. R.; Brocken, L.; Mallia, C. J., *Green Process. Synth.* **2013**, *2* (3), 211-230; (b) McQuade, D. T.; Seeberger, P. H., *J. Org. Chem.* **2013**, *78* (13), 6384-6389; (c) Baxendale, I. R., *J. Chem. Technol. Biotechnol.* **2013**, *88* (4), 519-552; (d) Pastre, J. C.; Browne, D. L.; Ley, S. V., *Chem. Soc. Rev.* **2013**, *42* (23), 8849-8869; (e) Wiles, C.;

Watts, P., *Green Chem.* **2012**, *14* (1), 38-54; (f) Anderson, N. G., *Org. Process. Res. Dev.* **2012**, *16* (5), 852-869; (g) Wegner, J.; Ceylan, S.; Kirschning, A., *Adv. Synth. Catal.* **2012**, *354* (1), 17-57; (h) Malet-Sanz, L.; Susanne, F., *J. Med. Chem.* **2012**, *55* (9), 4062-4098; (i) Wegner, J.; Ceylan, S.; Kirschning, A., *Chem. Commun.* **2011**, *47* (16), 4583-4592.

17. Yue, J.; Chen, G.; Yuan, Q.; Luo, L.; Gonthier, Y., *Chem. Eng. Sci.* **2007**, *62* (7), 2096-2108.

18. (a) Hessel, V.; Angeli, P.; Gavriilidis, A.; Lowe, H., *Ind. Eng. Chem. Res.* **2005**, *44* (25), 9750-9769; (b) Gunther, A.; Jensen, K. F., *Lab Chip* **2006**, *6* (12), 1487-1503; (c) Zanfir, M.; Sun, X.; Gavriilidis, A., *Ind. Eng. Chem. Res.* **2008**, *47* (23), 8995-9005; (d) Kashid, M. N.; Kiwi-Minsker, L., *Ind. Eng. Chem. Res.* **2009**, *48* (14), 6465-6485; (e) Zhao, C.-X.; Middelberg, A. P. J., *Chem. Eng. Sci.* **2011**, *66* (7), 1394-1411; (f) Sobieszuk, P.; Aubin, J.; Pohorecki, R., *Chem. Eng. Technol.* **2012**, *35* (8), 1346-1358.

19. Jahnisch, K.; Baerns, M.; Hessel, V.; Ehrfeld, W.; Haverkamp, V.; Lowe, H.; Wille, C.; Guber, A., *J. Fluorine Chem.* **2000**, *105* (1), 117-128.

20. Wenn, D. A.; Shaw, J. E. A.; Mackenzie, B., *Lab Chip* **2003**, *3* (3), 180-186.

21. (a) Brzozowski, M.; O'Brien, M.; Ley, S. V.; Polyzos, A., *Acc. Chem. Res.* **2015**, *48* (2), 349-362; (b) O'Brien, M.; Baxendale, I. R.; Ley, S. V., *Org. Lett.* **2010**, *12* (7), 1596-1598.

22. Pinnau, I.; Toy, L. G., *J. Membrane Sci.* **1996**, *109* (1), 125-133.

23. Yang, L.; Jensen, K. F., *Org. Process. Res. Dev.* **2013**, *17* (6), 927-933.

24. (a) Kollár, L., Modern Carbonylation Methods. Kollár, L., Ed. Wiley-VCH Verlag GmbH & Co. KGaA: 2008; (b) Fukuyama, T.; Totoki, T.; Ryu, I., *Green Chem.* **2014**, *16* (4), 2042-2050.

25. Fischer, F.; Tropsch, H., *Brennstoff-Chem.* **1926**, *7*, 97-104.

26. Adkins, H.; Krsek, G., *J. Am. Chem. Soc.* **1949**, *71* (9), 3051-3055.

27. Miller, P. W.; Long, N. J.; de Mello, A. J.; Vilar, R.; Passchier, J.; Gee, A., *Chem. Commun.* **2006**, (5), 546-548.

28. Rahman, M. T.; Fukuyama, T.; Kamata, N.; Sato, M.; Ryu, I., *Chem. Commun.* **2006**, (21), 2236-2238.

29. Murphy, E. R.; Martinelli, J. R.; Zaborenko, N.; Buchwald, S. L.; Jensen, K. F., *Angew. Chem. Int. Ed.* **2007**, *46* (10), 1734-1737.

30. Miller, P. W.; Long, N. J.; de Mello, A. J.; Vilar, R.; Audrain, H.; Bender, D.; Passchier, J.; Gee, A., *Angew. Chem. Int. Ed.* **2007**, *46* (16), 2875-2878.

31. Miller, P. W.; Jennings, L. E.; deMello, A. J.; Gee, A. D.; Long, N. J.; Vilar, R., *Adv. Synth. Catal.* **2009**, *351* (18), 3260-3268.

32. Fukuyama, T.; Rahman, T.; Kamata, N.; Ryu, I., *Beilstein J. Org. Chem.* **2009**, *5*, No. 34.

33. Gong, X.; Miller, P. W.; Gee, A. D.; Long, N. J.; de Mello, A. J.; Vilar, R., *Chem.-Eur. J.* **2012**, *18* (10), 2768-2772.

34. Csajagi, C.; Borcsek, B.; Niesz, K.; Kovacs, I.; Szekelyhidi, Z.; Bajko, Z.; Urge, L.; Darvas, F., *Org. Lett.* **2008**, *10* (8), 1589-1592.

35. Koos, P.; Gross, U.; Polyzos, A.; O'Brien, M.; Baxendale, I.; Ley, S. V., *Org. Biomol. Chem.* **2011**, *9* (20), 6903-6908.

36. Mercadante, M. A.; Leadbeater, N. E., *Org. Biomol. Chem.* **2011**, *9* (19), 6575-6578.

37. (a) Kelly, C. B.; Lee, C.; Mercadante, M. A.; Leadbeater, N. E., *Org. Process. Res. Dev.* **2011**, *15* (3), 717-720; (b) Mercadante, M. A.; Leadbeater, N. E., *Green Process. Synth.* **2012**, *1* (6), 499-507.

38. Brancour, C.; Fukuyama, T.; Mukai, Y.; Skrydstrup, T.; Ryu, I., *Org. Lett.* **2013**, *15* (11), 2794-2797.

39. Fukuyama, T.; Mukai, Y.; Ryu, I., *Beilstein J. Org. Chem.* **2011**, *7*, 1288-1293.

40. Gross, U.; Koos, P.; O'Brien, M.; Polyzos, A.; Ley, S. V., *Eur. J. Org. Chem.* **2014**, (29), 6418-6430.

41. Akinaga, H.; Masaoka, N.; Takagi, K.; Ryu, I.; Fukuyama, T., *Chem. Lett.* **2014**, *43* (9), 1456-1458.

42. Fukuyama, T.; Totoki, T.; Ryu, I., *Org. Lett.* **2014**, *16* (21), 5632-5635.

43. Takebayashi, Y.; Sue, K.; Yoda, S.; Furuya, T.; Mae, K., *Chem. Eng. J.* **2012**, *180*, 250-254.

44. Polyzos, A.; O'Brien, M.; Petersen, T. P.; Baxendale, I. R.; Ley, S. V., *Angew. Chem. Int. Ed.* **2011**, *50* (5), 1190-1193.

45. van Gool, J. J. F.; van den Broek, S. A. M. W.; Ripken, R. M.; Nieuwland, P. J.; Koch, K.; Rutjes, F. P. J. T., *Chem. Eng. Technol.* **2013**, *36* (6), 1042-1046.

46. Kupracz, L.; Kirschning, A., *Adv. Synth. Catal.* **2013**, *355* (17), 3375-3380.

47. Nagaki, A.; Takahashi, Y.; Yoshida, J.-i., *Chem.-Eur. J.* **2014**, *20* (26), 7931-7934.

48. Pieber, B.; Glasnov, T.; Kappe, C. O., *RSC Adv.* **2014**, *4* (26), 13430-13433.

49. Wu, J.; Yang, X.; He, Z.; Mao, X.; Hatton, T. A.; Jamison, T. F., *Angew. Chem. Int. Ed.* **2014**, *53* (32), 8416-8420.

50. Kozak, J. A.; Wu, J.; Su, X.; Simeon, F.; Hatton, T. A.; Jamison, T. F., *J. Am. Chem. Soc.* **2013**, *135* (49), 18497-18501.

51. Deng, Q.; Shen, R.; Zhao, Z.; Yan, M.; Zhang, L., *Chem. Eng. J.* **2015**, *262*, 1168-1174.

52. Petersen, T. P.; Polyzos, A.; O'Brien, M.; Ulven, T.; Baxendale, I. R.; Ley, S. V., *Chemsuschem* **2012**, *5* (2), 274-277.

53. Bourne, S. L.; Ley, S. V., *Adv. Synth. Catal.* **2013**, *355* (10), 1905-1910.

54. Pieber, B.; Kappe, C. O., *Green Chem.* **2013**, *15* (2), 320-324.

55. Sipos, G.; Gyollai, V.; Sipocz, T.; Dorman, G.; Kocsis, L.; Jones, R. V.; Darvas, F., *J. Flow Chem.* **2013**, *3* (2), 51-58.

56. Chaudhuri, S. R.; Hartwig, J.; Kupracz, L.; Kodanek, T.; Wegner, J.; Kirschning, A., *Adv. Synth. Catal.* **2014**, *356* (17), 3530-3538.

57. Oliveira, R. L.; Kiyohara, P. K.; Rossi, L. M., *Green Chem.* **2010**, *12* (1), 144-149.

58. Vanoye, L.; Aloui, A.; Pablos, M.; Philippe, R.; Percheron, A.; Favre-Reguillon, A.; de Bellefont, C., *Org. Lett.* **2013**, *15* (23), 5978-5981.

59. Wang, F.; Lei, L. D.; Wu, L. M., *Magn. Reson. Chem.* **2005**, *43* (2), 156-165.

60. He, Z.; Jamison, T. F., *Angew. Chem. Int. Ed.* **2014**, *53* (13), 3353-3357.

61. Gemoets, H. P. L.; Hessel, V.; Noel, T., *Org. Lett.* **2014**, *16* (21), 5800-5803.

62. Park, C. P.; Kim, D.-P., *J. Am. Chem. Soc.* **2010**, *132* (29), 10102-10106.

63. Brzozowski, M.; Forni, J. A.; Savage, G. P.; Polyzos, A., *Chem. Commun.* **2015**, *51* (2), 334-337.

64. Tomaszewski, B.; Schmid, A.; Buehler, K., *Org. Process. Res. Dev.* **2014**, *18* (11), 1516-1526.

65. (a) Knowles, J. P.; Elliott, L. D.; Booker-Milburn, K. I., *Beilstein J. Org. Chem.* **2012**, *8*, 2025-2052; (b) Gilmore, K.; Seeberger, P. H., *Chem. Rec.* **2014**, *14* (3), 410-418.

66. Wootton, R. C. R.; Fortt, R.; de Mello, A. J., *Org. Process. Res. Dev.* **2002**, *6* (2), 187-189.

67. Nagasawa, Y.; Tanba, K.; Tada, N.; Yamaguchi, E.; Itoh, A., *Synlett* **2015**, *26* (3), 412-415.

68. (a) Meyer, S.; Tietze, D.; Rau, S.; Schaefer, B.; Kreisel, G., *J. Photochem. Photobio. A* **2007**, *186* (2-3), 248-253; (b) Kreisel, G.; Meyer, S.; Tietze, D.; Fidler, T.; Gorges, R.; Kirsch, A.; Schaefer, B.; Rau, S., *Chem. Ing. Tech.* **2007**, *79* (1-2), 153-159.

69. Matsushita, Y.; Iwasawa, M.; Suzuki, T.; Ichimura, T., *Chem. Lett.* **2009**, *38* (8), 846-847.

70. Aran, H. C.; Salamon, D.; Rijnaarts, T.; Mul, G.; Wessling, M.; Lammertink, R. G. H., *J. Photochem. Photobio. A* **2011**, *225* (1), 36-41.

71. Carofiglio, T.; Donnola, P.; Maggini, M.; Rossetto, M.; Rossi, E., *Adv. Synth. Catal.* **2008**, *350* (17), 2815-2822.

72. Park, C. P.; Maurya, R. A.; Lee, J. H.; Kim, D.-P., *Lab Chip* **2011**, *11* (11), 1941-1945.

73. Maurya, R. A.; Park, C. P.; Kim, D.-P., *Beilstein J. Org. Chem.* **2011**, *7*, 1158-1163.

74. Bakowski, A.; Dressel, M.; Bauer, A.; Bach, T., *Org. Biomol. Chem.* **2011**, *9* (9), 3516-3529.

75. Mueller, C.; Bauer, A.; Maturi, M. M.; Cuquerella, M. C.; Miranda, M. A.; Bach, T., *J. Am. Chem. Soc.* **2011**, *133* (41), 16689-16697.

76. Bourne, R. A.; Han, X.; Poliakoff, M.; George, M. W., *Angew. Chem. Int. Ed.* **2009**, *48* (29), 5322-5325.

77. Musie, G.; Wei, M.; Subramaniam, B.; Busch, D. H., *Coord. Chem. Rev.* **2001**, *219*, 789-820.

78. Darr, J. A.; Poliakoff, M., *Chem. Rev.* **1999**, *99* (2), 495-541.

79. Levesque, F.; Seeberger, P. H., *Org. Lett.* **2011**, *13* (19), 5008-5011.

80. Levesque, F.; Seeberger, P. H., *Angew. Chem. Int. Ed.* **2012**, *51* (7), 1706-1709.

81. Ushakov, D. B.; Gilmore, K.; Seeberger, P. H., *Chem. Commun.* **2014**, *50* (84), 12649-12651.

82. Ushakov, D. B.; Gilmore, K.; Kopetzki, D.; McQuade, D. T.; Seeberger, P. H., *Angew. Chem. Int. Ed.* **2014**, *53* (2), 557-561.

83. Holmes, N.; Akien, G. R.; Savage, R. J. D.; Stanetty, C.; Baxendale, I. R.; Blacker, A. J.; Taylor, B. A.; Woodward, R. L.; Meadows, R. E.; Bourne, R. A., *React. Chem. Eng.* **2016**, *1* (1), 96-100.

84. (a) Barnard, C. F. J., *Org. Process. Res. Dev.* **2008**, *12* (4), 566-574; (b) Daniewski, A. R.; Liu, W.; Puntener, K.; Scalone, M., *Org. Process. Res. Dev.* **2002**, *6*

(3), 220-224; (c) Ashfield, L.; Barnard, C. F. J., *Org. Process. Res. Dev.* **2007**, *11* (1), 39-43.

85. Cross, R. J.; Kennedy, A. R.; Muir, K. W., *Acta Crystallogr. Sect. C: Cryst. Struct. Commun.* **1995**, *51*, 208-210.

86. (a) Haring, M., *Helv. Chim. Acta* **1960**, *43* (1), 104-113; (b) Comins, D. L.; Brown, J. D., *J. Org. Chem.* **1984**, *49* (6), 1078-1083; (c) Bennetau, B.; Mortier, J.; Moyroud, J.; Guesnet, J. L., *J. Chem. Soc., Perkin Trans. 1* **1995**, (10), 1265-1271.

87. (a) Sanchez, J. P.; Domagala, J. M.; Hagen, S. E.; Heifetz, C. L.; Hutt, M. P.; Nichols, J. B.; Trehan, A. K., *J. Med. Chem.* **1988**, *31* (5), 983-991; (b) Belf, L. J.; Buxton, M. W.; Tilney-Bassett, J. F., *Tetrahedron* **1967**, *23* (12), 4719-4727.

88. Chu, D. T. W.; Nordeen, C. W.; Hardy, D. J.; Swanson, R. N.; Giardina, W. J.; Pernet, A. G.; Plattner, J. J., *J. Med. Chem.* **1991**, *34* (1), 168-174.

89. (a) O'Reilly, N. J.; Derwin, W. S.; Fertel, L. B.; Lin, H. C., *Synlett* **1990**, *1990* (10), 609-610; (b) Fertel, L. B., *Org. Process. Res. Dev.* **1998**, *2* (2), 111-115.

90. (a) Immirzi, A.; Musco, A., *Inorg. Chim. Acta* **1977**, *25*, L41-L42; (b) Clavier, H.; Nolan, S. P., *Chem. Commun.* **2010**, *46* (6), 841-861.

91. van Leeuwen, P.; Kamer, P. C. J.; Reek, J. N. H.; Dierkes, P., *Chem. Rev.* **2000**, *100* (8), 2741-2769.

92. Kaupmees, K.; Trummal, A.; Leito, I., *Croat. Chem. Acta* **2014**, *87* (4), 385-395.

93. Eliel, E. L.; Wilen, S. H.; Mander, L. N., *Stereochemistry of organic compounds*. Wiley & Sons: 1994.

94. Cain, P. A.; Cramp, S. M.; Lambert, C.; Wallis, D. I.; Yarwood, T. D.; Little, G. M.; Morris, J.; Musil, T.; Pettit, S. N.; Smith, P. H. G. Herbicidal 2-cyano-1,3-diones. US 5804532, Sept. 8, 1998.

95. Crowford, K. R.; Hatcher, M.; Jeaon, H.; Jones, G.; Posner, G. H.; Suh, B.-C.; White, J. A.; Yang, H. W. 24-Sulfur-substituted analogs of 1α,25-dihydroxy vitamin D3. WO2003018545 A1, Mar 6, 2003.

96. Rozen, S.; Bareket, Y., *J. Org. Chem.* **1997**, *62* (5), 1457-1462.

97. Montalbetti, C.; Falque, V., *Tetrahedron* **2005**, *61* (46), 10827-10852.

98. Paul, R.; Anderson, G. W., *J. Am. Chem. Soc.* **1960**, *82* (17), 4596-4600.

99. Shioiri, T.; Ninomiya, K.; Yamada, S., *J. Am. Chem. Soc.* **1972**, *94* (17), 6203-6205.

100. Mikoz.xl; lajczyk, M.; Kiez.xl; lbasiński, P., *Tetrahedron* **1981**, *37* (2), 233-284.

101. Ullmann, F.; Bielecki, J., *Berichte Der Deutschen Chemischen Gesellschaft* **1901**, *34*, 2174-2185.

102. (a) Ullmann, F., *Berichte Der Deutschen Chemischen Gesellschaft* **1903**, *36*, 2382-2384; (b) Ullmann, F.; Sponagel, P., *Berichte Der Deutschen Chemischen Gesellschaft* **1905**, *38*, 2211-2212.

103. Goldberg, I., *Berichte Der Deutschen Chemischen Gesellschaft* **1906**, *39*, 1691-1692.

104. Hurtley, W. R. H., *J. Chem. Soc.* **1929**, 1870-1873.

105. (a) Wang, S.; Dong, Y.; Wang, X.; Hu, X.; Liu, J. O.; Hu, Y., *Org. Biomol. Chem.* **2005**, *3* (5), 911-916; (b) Liu, Y.; Bai, Y.; Zhang, J.; Li, Y.; Jiao, J.; Qi, X., *Eur. J. Org. Chem.* **2007**, *2007* (36), 6084-6088.

106. Kosugi, M.; Kameyama, M.; Migita, T., *Chem. Lett.* **1983**, (6), 927-928.

107. Paul, F.; Patt, J.; Hartwig, J. F., *J. Am. Chem. Soc.* **1994**, *116* (13), 5969-5970.

108. (a) Guram, A. S.; Rennels, R. A.; Buchwald, S. L., *Angew. Chem. Int. Ed.* **1995**, *34* (12), 1348-1350; (b) Louie, J.; Hartwig, J. F., *Tetrahedron Lett.* **1995**, *36* (21), 3609-3612.

109. Chan, D. M. T.; Monaco, K. L.; Wang, R. P.; Winters, M. P., *Tetrahedron Lett.* **1998**, *39* (19), 2933-2936.

110. Evans, D. A.; Katz, J. L.; West, T. R., *Tetrahedron Lett.* **1998**, *39* (19), 2937-2940.

111. Lam, P. Y. S.; Clark, C. G.; Saubern, S.; Adams, J.; Winters, M. P.; Chan, D. M. T.; Combs, A., *Tetrahedron Lett.* **1998**, *39* (19), 2941-2944.

112. Rao, K. S.; Wu, T.-S., *Tetrahedron* **2012**, *68* (38), 7735-7754.

113. Fischer, C.; Koenig, B., *Beilstein J. Org. Chem.* **2011**, *7*, 59-74.

114. (a) King, A. E.; Brunold, T. C.; Stahl, S. S., *J. Am. Chem. Soc.* **2009**, *131* (14), 5044-5045; (b) King, A. E.; Huffman, L. M.; Casitas, A.; Costas, M.; Ribas, X.; Stahl, S. S., *J. Am. Chem. Soc.* **2010**, *132* (34), 12068-12073.

115. Singh, B. K.; Stevens, C. V.; Acke, D. R. J.; Parmar, V. S.; Van der Eycken, E. V., *Tetrahedron Lett.* **2009**, *50* (1), 15-18.

116. Bao, J.; Tranmer, G. K., *Tetrahedron Lett.* **2016**, *57* (6), 654-657.

117. Mitchell, G. Herbicidal compounds. US 2015/0072860 A1, 12, March, 2015.

118. Chen, J.; Properzi, R.; Uccello, D. P.; Young, J. A.; Dushin, R. G.; Starr, J. T., *Org. Lett.* **2014**, *16* (16), 4146-4149.

119. Tang, X.; Huang, L.; Yang, J.; Xu, Y.; Wu, W.; Jiang, H., *Chem. Commun.* **2014**, *50* (94), 14793-14796.

120. Baumann, M.; Baxendale, I. R.; Ley, S. V.; Nikbin, N., *Beilstein J. Org. Chem.* **2011**, *7*, 442-495.

121. (a) Paal, C., *Berichte der deutschen chemischen Gesellschaft* **1884**, *17* (2), 2756-2767; (b) Knorr, L., *Berichte der deutschen chemischen Gesellschaft* **1884**, *17* (2), 2863-2870.

122. Wang, Z., Hantzsch Thiazole Synthesis. In *Comprehensive Organic Name Reactions and Reagents*, John Wiley & Sons, Inc.: 2010.

123. Minetto, G.; Raveglia, L. F.; Sega, A.; Taddei, M., *Eur. J. Org. Chem.* **2005**, (24), 5277-5288.

124. (a) C. Bagley, M.; T. Buck, R.; Lucy Hind, S.; J. Moody, C., *J. Chem. Soc., Perkin Trans. 1* **1998**, (3), 591-600; (b) Bagley, M. C.; Bashford, K. E.; Hesketh, C. L.; Moody, C. J., *J. Am. Chem. Soc.* **2000**, *122* (14), 3301-3313.

125. Gewald, K., *Angew. Chem. Int. Ed.* **1961**, *73* (3), 114-&.

126. Sabnis, R. W.; Rangnekar, D. W.; Sonawane, N. D., *J. Heterocycl. Chem.* **1999**, *36* (2), 333-345.

127. Ma, L.; Yuan, L.; Xu, C.; Li, G.; Tao, M.; Zhang, W., *Synthesis-Stuttgart* **2013**, *45* (1), 45-52.

128. (a) Gui, Y.-Y.; Yang, J.; Qi, L.-W.; Wang, X.; Tian, F.; Li, X.-N.; Peng, L.; Wang, L.-X., *Org. Biomol. Chem.* **2015**, *13* (22), 6371-6379; (b) Zhou, P.; Cai, Y.; Lin, L.; Lian, X.; Xia, Y.; Liu, X.; Feng, X., *Adv. Synth. Catal.* **2015**, *357* (4), 695-700.

129. Vatansever, E. C.; Kilic, K.; Ozer, M. S.; Koza, G.; Menges, N.; Balci, M., *Tetrahedron Lett.* **2015**, *56* (40), 5386-5389.

130. (a) McNabola, N.; O'Connor, C. J.; Roydhouse, M. D.; Wall, M. D.; Southern, J. M., *Tetrahedron* **2015**, *71* (28), 4598-4603; (b) O'Connor, C. J.; Roydhouse, M. D.; Przybyl, A. M.; Wall, M. D.; Southern, J. M., *J. Org. Chem.* **2010**, *75* (8), 2534-2538.

131. (a) Shi, W.; Sun, S.; Hu, Y.; Gao, T.; Peng, Y.; Wu, M.; Guo, H.; Wang, J., *Tetrahedron Lett.* **2015**, *56* (25), 3861-3863; (b) Shi, W.; Wan, L.; Hu, Y.; Sun, S.; Li, W.; Peng, Y.; Wu, M.; Guo, H.; Wang, J., *Tetrahedron Lett.* **2015**, *56* (16), 2083-2085.

132. Hu, L.; Ren, Y.; Ramström, O., *J. Org. Chem.* **2015**, *80* (16), 8478-8481.

133. Wang, H.-P.; Zhang, H.-H.; Hu, X.-Q.; Xu, P.-F.; Luo, Y.-C., *Eur. J. Org. Chem.* **2015**, *2015* (16), 3486-3494.

134. (a) Brown, M. D.; Gillon, D. W.; Meakins, G. D.; Whitham, G. H., *J. Chem. Soc., Perkin Trans. 1* **1985**, (8), 1623-1626; (b) Sadek, K. U.; Mourad, A. F. E.; Abdelhafeez, A. E.; Elnagdi, M. H., *Synthesis-Stuttgart* **1983**, (9), 739-741; (c) Asinger, F.; Fabian, K.; Vossen, H.; Hentschel, K., *Justus Liebigs Annalen der Chemie* **1975**, *1975* (3), 410-414; (d) El Rady, E. A., *Synth. Commun.* **2006**, *36* (1), 37-49.

135. (a) Elnagdi, M. H.; Khalifa, M. A. E.; Ibraheim, M. K. A.; Elmoghayar, M. R. H., *J. Heterocycl. Chem.* **1981**, *18* (5), 877-879; (b) Elagamey, A. G. A.; Eltaweel, F. A.; Amer, F. A.; Zoorob, H. H., *Arch. Pharm.* **1987**, *320* (3), 246-252.

136. Tani, S.; Uehara, T. N.; Yamaguchi, J.; Itami, K., *Chem. Sci.* **2014**, *5* (1), 123-135.

137. Knoevenagel, E., *Berichte der deutschen chemischen Gesellschaft* **1898**, *31* (3), 2596-2619.

138. Bordwell, F. G.; Bares, J. E.; Bartmess, J. E.; McCollum, G. J.; Vanderpuy, M.; Vanier, N. R.; Matthews, W. S., *J. Org. Chem.* **1977**, *42* (2), 321-325.

139. Zhou, G.-L.; Tams, D. M.; Marder, T. B.; Valentine, R.; Whiting, A.; Przyborski, S. A., *Org. Biomol. Chem.* **2013**, *11* (14), 2323-2334.

140. Chuang, G. J.; Wang, W.; Lee, E.; Ritter, T., *J. Am. Chem. Soc.* **2011**, *133* (6), 1760-1762.

141. Liang, Y.-F.; Jiao, N., *Angew. Chem. Int. Ed.* **2014**, *53* (2), 548-552.

142. Richards.Wh; Hodge, V. F.; Stiggall, D. L.; Yelvingt.Mb; Montgome.Fc, *J. Am. Chem. Soc.* **1974**, *96* (21), 6652-6657.

143. Sakurai, H.; Kamiya, I.; Kitahara, H.; Tsunoyama, H.; Tsukuda, T., *Synlett* **2009**, (2), 245-248.

144. Dos Santos, A.; El Kaim, L.; Grimaud, L., *Org. Biomol. Chem.* **2013**, *11* (20), 3282-3287.

145. Sawaki, Y.; Ogata, Y., *J. Am. Chem. Soc.* **1975**, *97* (24), 6983-6989.

146. (a) García-Reynaga, P.; VanNieuwenhze, M. S., *Tetrahedron Lett.* **2012**, *53* (37), 4989-4993; (b) Irako, N.; Hamada, Y.; Shioiri, T., *Tetrahedron* **1992**, *48* (35), 7251-7264.

147. Gottlieb, H. E.; Kotlyar, V.; Nudelman, A., *J. Org. Chem.* **1997**, *62* (21), 7512-7515.

148. Sheldrick, G., *Acta Crystallographica Section A* **2008**, *64* (1), 112-122.

149. Dolomanov, O. V.; Bourhis, L. J.; Gildea, R. J.; Howard, J. A. K.; Puschmann, H., *J. Appl. Crystallogr.* **2009**, *42* (2), 339-341.

150. Sheldrick, G., *Acta Crystallographica Section A* **2015**, *71* (1), 3-8.

151. Shaikh, T. M.; Hong, F.-E., *Tetrahedron* **2013**, *69* (42), 8929-8935.

152. Durka, K.; Lulinski, S.; Dabrowski, M.; Serwatowski, J., *Eur. J. Org. Chem.* **2014**, (21), 4562-4570.

153. Yonemoto-Kobayashi, M.; Inamoto, K.; Kondo, Y., *Chem. Lett.* **2014**, *43* (4), 477-479.

154. Sathyanarayana, P.; Ravi, O.; Muktapuram, P. R.; Bathula, S. R., *Org. Biomol. Chem.* **2015**, *13* (37), 9681-9685.

155. Mongin, F.; Desponds, O.; Schlosser, M., *Tetrahedron Lett.* **1996**, *37* (16), 2767-2770.

156. Chi-Chung Choy, J.; Jaime-Figueroa, S. Deprotection of BOC-Protected Compounds. US 2010/0311968 A1, 2010.

157. Thirumamagal, B. T. S.; Narayanasamy, S.; Venkatesan, R., *Synth. Commun.* **2008**, *38* (16), 2820-2825.

158. Sturm, K.; Siedel, W.; Weyer, R.; Ruschig, H., *Chem. Ber. Recl.* **1966**, *99* (1), 328-&.

159. Ley, C. P.; Yates, M. H., *Org. Process. Res. Dev.* **2008**, *12* (1), 120-124.

160. Tong, L. K. J.; Kenyon, W. O., *J. Am. Chem. Soc.* **1947**, *69* (6), 1402-1405.

161. Phillion, D. P.; Pratt, J. K., *Synth. Commun.* **1992**, *22* (1), 13-22.

162. Alper, H.; Prickett, J. E.; Wollowitz, S., *J. Am. Chem. Soc.* **1977**, *99* (13), 4330-4333.

163. Jadhav, R. R.; Huddar, S. N.; Akamanchi, K. G., *Eur. J. Org. Chem.* **2013**, *2013* (30), 6779-6783.

164. Zhu, X.; Su, L.; Huang, L.; Chen, G.; Wang, J.; Song, H.; Wan, Y., *Eur. J. Org. Chem.* **2009**, *2009* (5), 635-642.

165. Dissanayake, A. A.; Odom, A. L., *Chem. Commun.* **2012**, *48* (3), 440-442.

166. Patra, T.; Agasti, S.; Akanksha; Maiti, D., *Chem. Commun.* **2013**, *49* (1), 69-71.

167. Kahveci, B., *Molecules* **2005**, *10* (2), 376-382.

168. Kahveci, B.; Yılmaz, F.; Menteşe, E.; Ülker, S., *Chemistry of Heterocyclic Compounds* **2015**, *51* (5), 447-456.

169. Ün, R.; Îkizler, A., *Chimica Acta Turcica* **1975**, *3*, 113-132.

170. Doraswamy, K.; Venkata Ramana, P., *Chem. Sci. Trans.* **2013**, *2* (2), 649-655.

171. Nappi, M.; Bergonzini, G.; Melchiorre, P., *Angew. Chem. Int. Ed.* **2014**, *53* (19), 4921-4925.

172. Bunegar, M. J.; Dyer, U. C.; Evans, G. R.; Hewitt, R. P.; Jones, S. W.; Henderson, N.; Richards, C. J.; Sivaprasad, S.; Skead, B. M.; Stark, M. A.; Teale, E., *Org. Process. Res. Dev.* **1999**, *3* (6), 442-450.

173. Hammond, G. B.; Plevey, R. G.; Sampson, P.; Tatlow, J. C., *J. Fluorine Chem.* **1988**, *40* (2), 81-98.

174. Okuro, K.; Furuune, M.; Miura, M.; Nomura, M., *J. Org. Chem.* **1993**, *58* (26), 7606-7607.

175. Ghislieri, D.; Gilmore, K.; Seeberger, P. H., *Angew. Chem. Int. Ed.* **2015**, *54* (2), 678-682.

176. Balalaie, S.; Bararjanian, M.; Hekmat, S.; Salehi, P., *Synth. Commun.* **2006**, *36* (17), 2549-2557.

177. Nath, D.; Skilbeck, M. C.; Coldham, I.; Fleming, F. F., *Org. Lett.* **2014**, *16* (1), 62-65.

178. Gupta, M.; Gupta, R.; Anand, M., *Beilstein J. Org. Chem.* **2009**, *5*, 68.

179. Doni, E.; Mondal, B.; O'Sullivan, S.; Tuttle, T.; Murphy, J. A., *J. Am. Chem. Soc.* **2013**, *135* (30), 10934-10937.

180. Wang, D.-Y.; Xi, G.-H.; Ma, J.-J.; Wang, C.; Zhang, X.-C.; Wang, Q.-Q., *Synth. Commun.* **2011**, *41* (20), 3060-3065.

181. Hessler, J. C., *J. Am. Chem. Soc.* **1913**, *35* (8), 990-994.

182. Yin, L.; Kanai, M.; Shibasaki, M., *Tetrahedron* **2012**, *68* (17), 3497-3506.

183. Ramachary, D. B.; Kishor, M.; Reddy, Y. V., *Eur. J. Org. Chem.* **2008**, *2008* (6), 975-993.

184. Hirohashi, T.; Inaba, S.; Yamamoto, H., *Bull. Chem. Soc. Jpn.* **1975**, *48* (1), 147-156.

185. Nakhi, A.; Adepu, R.; Rambabu, D.; Kishore, R.; Vanaja, G. R.; Kalle, A. M.; Pal, M., *Bioorg. Med. Chem. Lett.* **2012**, *22* (13), 4418-4427.

186. Ghorai, P.; Kraus, A.; Keller, M.; Götte, C.; Igel, P.; Schneider, E.; Schnell, D.; Bernhardt, G.; Dove, S.; Zabel, M.; Elz, S.; Seifert, R.; Buschauer, A., *J. Med. Chem.* **2008**, *51* (22), 7193-7204.